

AGE RESOLUTION OF PEAK METAMORPHISM WITHIN THE
CALEDONIDES OF NORTHERN SCOTLAND AND SHETLAND

Anna Frances Bird

Royal Holloway University of London

A thesis submitted for the degree of Doctor of Philosophy

December 2011

ABSTRACT

This project aims to define the timing(s) of peak metamorphism using Lu-Hf and Sm-Nd geochronology of garnets. The thesis focuses on the poly-metamorphic Northern Highland Terrane of Scotland and attempts to constrain the age of the many crustal deformation events. The project also uses Rb-Sr geochronology to date cooling. LA ICP MS and EPMA have been used to establish garnet compositions to determine if the ages yielded represent growth ages or cooling ages.

The research has shown that the currently understood model for the Caledonian orogeny in the Northern Highlands is over simplistic. Mid-Ordovician (Grampian) garnet growth ages have been recorded throughout the Moine Supergroup, including the Morar Group which indicates that the Northern Highlands shares the Grampian event recorded in the Dalradian Supergroup in Scotland and Ireland. Several samples provide evidence of a later garnet growth episode at ~450 Ma recorded within the Morar Group and part of the Glenfinnan. This study also demonstrates that the Neoproterozoic metamorphic events happened earlier than originally thought, with garnet growth recorded at ~950 Ma. This early garnet growth event recorded within the Morar Group also shows that deposition of these sediments must have ceased prior to 950 Ma. The Neoproterozoic metamorphic events can be split into several discrete episodes, with the Morar and Glenfinnan groups recording different events suggesting that they were tectonically distinct during the majority of the Neoproterozoic. This study also dated garnets within the basement inliers of the Moine Supergroup. The ages from the inliers show that there was an early Mesoproterozoic garnet growth event at ~1650 Ma which was recorded in an inlier in Sutherland and in Glenelg. Eclogite metamorphism within the Eastern Unit of the Glenelg-Attadale inlier has been dated at ~1200 Ma, which is significantly older than previous results.

"It just shows what can be done by taking a little trouble," said Eeyore. "Do you see, Pooh? Do you see, Piglet? Brains first and then Hard Work."

A.A. Milne, *Winnie the Pooh, The House at Pooh Corner*



TABLE OF CONTENTS

ABSTRACT	1
TABLE OF CONTENTS	3
LIST OF FIGURES	8
LIST OF TABLES	22
ACKNOWLEDGEMENTS	24
CHAPTER 1 : Introduction to the geology of the Scottish Calidonides	25
1.1 Introduction	25
1.2 General geology	26
1.3 Tectonostratigraphy of the Moine Supergroup.....	28
1.3.1 Inverness-shire, Argyll and Easter-Ross	29
1.3.2 Sutherland and the Fannichs	31
1.4 Age and Depositional Setting of the Moine Supergroup.....	33
1.4.1 Age of deposition	33
1.4.2 Setting of deposition	34
1.5 Regional Metamorphism and fabrics.....	36
1.6 Tectonic setting of the Moine deformation events	40
1.6.1 Neoproterozoic	40
1.6.2 Cambrian to Silurian	41
1.7 Timings of faulting and thrusting	41
1.7.1 The Moine Thrust.....	41
1.7.2 Sgurr Beag Thrust	42
1.7.3 The Great Glen Fault.....	43
1.8 Orogenic activity within the Moine.....	44
1.9 The Grampian Terrane	46
1.9.1 Tectonostratigraphy of the Dalradian.....	47
1.9.2 Dalradian sedimentation.....	48
1.9.3 Regional metamorphism and associated structures.....	49
1.10 The metasedimentary rocks of Shetland.....	51
1.11 Correlations between the Scottish Highlands and Scandinavia, East Greenland and Irish Caledonides	53
1.11.1 East Greenland	53
1.11.2 Scandinavia	56

1.12	Project Aims	57
CHAPTER 2 : Methodology Literature Review		59
2.1	Chemical properties of Sm-Nd and Lu-Hf	59
2.2	Sm-Nd and Lu-Hf geochronology in garnets	59
2.3	¹⁷⁶ Lu decay constant and CHUR parameters	60
2.4	The effect of inclusions on garnet geochronology	63
2.4.1	The effect of zircon within this study	64
2.5	Closure temperature (T _C) in garnet	67
2.5.1	Previous T _C estimates.....	69
2.6	Method of Sm-Nd and Lu-Hf dating	70
2.6.1	Age Calculation.....	70
2.6.2	Two point isochrons.....	71
2.6.3	Garnet core and rim dating.....	71
2.7	Analytical techniques	73
2.7.1	Sampling methodology	73
2.7.2	Rock crushing	73
2.7.3	Mineral separation (Lu-Hf, Sm-Nd and Rb-Sr analyses).....	74
2.7.4	X-ray fluorescence spectrometry – major and trace element analysis	74
	Fused glass disc preparation	74
	Pressed pellet preparation	75
	XRF Analysis.....	75
2.7.5	Mineral chemistry – major and trace element analysis.....	76
	Sample preparation.....	76
	Major element mineral analyses by electron probe.....	77
	Mineral analyses by LA-ICP-MS.....	77
2.7.6	Preparation for Lu-Hf and Sm-Nd analyses.....	78
	Sample leaching and dissolution.....	78
	Separation chemistry	79
	Column Calibration.....	80
2.7.7	Lu, Hf, Sm and Nd Mass spectrometry.....	81
2.7.8	Rb-Sr analysis	84
	Sample dissolution and column chemistry.....	84
	Bead making and loading procedures	85
2.7.9	Rb and Sr Mass spectrometry	85

CHAPTER 3 : THE BASEMENT INLIERS	87
3.1 Synopsis.....	87
3.2 Introduction	87
3.3 Regional Geology	88
3.4 Regional basement (pre-1 Ga) geology of NW Scotland and related areas	90
3.4.1 The Lewisian Gneiss Complex	91
3.5 The Rhinns Complex and Annagh Gneiss Complex	94
3.5.1 East Greenland	98
3.5.2 The Grenville Belt.....	100
3.5.3 The Fennoscandian Nordic basement	103
3.6 The Glenelg-Attadale Inlier.....	104
3.6.1 AB07-09 – Streaky Eclogite	106
3.6.2 AB07-10 – Beinn Fhada Eclogite	108
3.6.3 AB07-12 – Garnet-kyanite-pelite.....	110
3.7 The Borgie Inlier	112
3.7.1 AB07-18 – Borgie Granulite.....	113
3.8 Results and interpretation	115
3.9 Discussion	121
3.9.1 1750 - 1600 Ma events	121
3.9.2 1250 - 1200 Ma events.....	122
3.9.3 1020 - 900 Ma events	122
3.10 Conclusions	124
CHAPTER 4 : NEOPROTEROZOIC METAMORPHIC EVENTS.....	125
4.1 Synopsis.....	125
4.2 Introduction	125
4.3 Previous Geochronology	126
4.4 Sample descriptions.....	132
AB07-02 – Polish Pelite.....	132
AB07-03 – Glenuig Pelite.....	135
AB07-04 - Loch Eilt Semi-pelitic Gneiss	136
AB07-28 – Glenborrowdale Pelite.....	137
AB07-29- Shiaba Pelite.....	138
AB07-31- Meadie Pelite	139
AB08-01 – Glenfinnan Group Garnet Gneiss	140

AB09-05 – Glenborrodale Pelitic Gneiss.....	142
IA1- Creag Mhor Pelite.....	143
4.5 Results and interpretation.....	144
4.5.1 Morar Group.....	144
4.5.2 Glenfinnan Group.....	149
4.6 Discussion	154
4.6.1 Morar Group.....	154
4.6.2 Glenfinnan Group.....	156
4.6.3 Tectonic implications of the new data	156
4.7 Conclusions	157
CHAPTER 5 : The Caledonian Orogeny	159
5.1 Synopsis.....	159
5.2 Introduction	160
5.3 Models for the Caledonian Orogeny	162
5.3.1 Grampian.....	162
5.3.2 Scandian Orogeny	163
5.4 Previous Geochronology	167
5.4.1 Evidence for Mid-Ordovician deformation and deformation	167
5.4.2 Evidence for Silurian deformation and metamorphism	168
5.5 Sample descriptions.....	170
AB07-05 – Loch Quioch Amphibolite.....	170
AB07-08 – Basal Pelite.....	172
AB07-11- Armadale Pelite.....	174
AB07-13 – Drumnadrochit Migmatite.....	175
AB07-14 – Drumnadrochit Amphibolite	177
AB07-15 - Talmine Pelite	179
AB07/17 - Ben Hope Sill suite amphibolite	181
AB07/21 – Strathy Complex Amphibolite.....	183
AB07/22 - Naver nappe garnetiferous gneiss	184
AB07/23 – Dava Succession Amphibolite.....	186
AB07/27 – Leven Schist	187
AB07-30 – Mull Amphibolite.....	188
AB08-02 – Vaich Amphibolite	189
5.5.1 Summary	190

5.6	Results and interpretation	191
5.6.1	The Morar Group	191
5.6.2	The Glenfinnan Group	195
5.6.3	The Strathy Complex and the Naver Nappe	197
5.6.4	The Dava Succession and the Dalradian Supergroup	198
5.7	Discussion	203
5.7.1	Timing of the Mid-Ordovician event	203
	Sgurr Beag and Naver Nappes	203
	Morar Group.....	204
	The Dava Succession and the Grampian terrane.....	204
5.7.2	Implications of Late Ordovician garnet growth	205
5.7.3	Scandian garnet growth.....	207
5.7.4	Textural relations within the Moine Supergroup	207
5.7.5	Relationship between Northern Highland and Grampian terranes during the Silurian	209
5.8	Conclusions	210
CHAPTER 6 : SHETLAND		212
6.1	Synopsis.....	212
6.2	Introduction	212
6.3	Geological setting and previous geochronology	213
6.4	Sample Descriptions	217
	AB08-04 – Yell Sound Group Pelitic Gneiss	217
	AB08-06 – Migga Ness.....	218
	AB08-08 – Kirkrabister Amphibolite	220
	AB08-13 – North Roe Schist	221
6.5	Results and interpretation	222
6.6	Discussion	224
6.7	Conclusions	226
CHAPTER 7 : The Uplift of the Moine Supergroup		227
7.1	Synopsis.....	227
7.2	Introduction	227
7.3	Previous Geochronology	228
7.4	Sample descriptions.....	231
	AB07-02 – Polish Pelite [NM 7445 8392].....	233

AB07-03 – Glenuig Pelite [NM 6707 7756].....	233
AB07-04 – Loch Eilt Semi-pelitic Gneiss [NM 8511 8174]	234
AB07-08 - Basal Pelite [NG 7689 1491]	235
AB07-11 – Armadale Pelite [NG 6409 0353].....	236
AB07-12 – Eastern Unit Pelite [NG 9049 2330]	237
AB07-13 – Drumnadrochit Migmatite [NH 4888 3233]	238
AB07-15 – Talmine Pelite [NC 5735 6324]	239
AB07-27 – Leven Schist [NN 2611 8032].....	240
AB07-29 – Shiaba Pelite [NM 4438 1890].....	241
AB07-31 – Meadie Pelite [NC 5231 4022].....	242
7.5 Results and interpretation	243
7.6 Discussion	245
7.7 Conclusions	248
CHAPTER 8 : Timing of Peak metamorphism.....	250
8.1 Introduction	250
8.2 Garnet size and age.....	250
8.3 Difference between Lu-Hf and Sm-Nd ages	251
8.4 Summary of conclusions from the previous chapters.....	252
8.4.1 The basement inliers	252
8.4.2 Neoproterozoic garnet growth.....	254
8.4.3 Ordovician garnet growth	256
8.4.4 Summary Table	257
8.5 Future work	259
REFERENCES	260
APPENDIX 1: XRF Data	295
APPENDIX 2: LA ICPMS Data	on accompanying CD

LIST OF FIGURES

Figure 1-1, simplified geological map of the Northern Highland and Grampian terranes, Abbreviations are; AGG – Ardgour Granitic Gneiss; BHT – Ben Hope Thrust; C – Cairngorms; CCG – Carn Chuinneag Granite; GD – Glen Doe; GS – Glen Shiel; K – Knoydart; KLH – Kinlochourn; LBC – Loch Borrolan Complex; MT – Moine Thrust; NT – Naver Thrust; SBT – Sgurr Beag Thrust; SC – Strathy Complex; SoT – Sole Thrust. 27

Figure 1-2, adapted from Holdsworth et al. 1994. Detailed Tectonostratigraphy of the Moine Supergroup within the Northern Highlands, suspected Moine equivalents from Shetland and the Grampian terrane are not included. The Moine type sections are shown in columns 1 and 2. The locations of the columns are shown on the map. The columns show general lithologies, thrusts, basement and amphibolite content. Abbreviations are; MT – Moine Thrust; SBT – Sgurr Beag Thrust; KT – Knoydart Thrust. Sections are not drawn to scale. 29

Figure 1-3, from Cawood et al. (2010) showing the Neoproterozoic reconstruction of eastern Laurentia, Baltica and northern Amazonia. Baltica is shown in pre and post 1265 Ma position. The rotation of Baltica opened the Asgard Sea. Brown blocks correlate to units associated with the Renlandian orogenic cycle and blue blocks relate to Knoydartian influenced units. The abbreviations are; GT – Grampian Terrane; M – Moine Supergroup; Hf – Hebridean Foreland; K – Krummedal succession; Rb – Rockall Bank; Sa/So – Sværholt and Sørøy successions; Sh – Shetland; Sn – Sveconorwegian orogeny; Ss – Sunas orogen; Se – Eastern terrane of Svalbard; Sc – Central terrane of Svalbard; Sw – Western terrane of Svalbard. 36

Figure 1-4, metamorphic zonal map of the Northern Highlands adapted from Winchester, 1974. 37

Figure 1-5, from Prave et al. (2009), extremely simplified composite stratigraphic column focusing on the main carbonate rock units of the Dalradian Supergroup in the British–Irish isles. (Note that the glaciogenic rocks are shown in upper case in the stratigraphic column.) 47

Figure 1-6, from Jones & Blake (2003) showing the metamorphic zones of the Grampian Highlands. All zones are shown apart from the staurolite zone which is a thin band between the garnet and kyanite zones. 51

Figure 1-7, simplified geological map of Shetland showing the main units, faults and thrusts, adapted from Flinn (1988). 52

Figure 1-8, simplified geological map of the East Greenland Caledonides from Higgins et al. (2004). The western limit of deformation is largely concealed by Inland Ice. Abbreviations A – Ardencaple Fjord; Am – Ammassalik; K – Ketilidian orogen. 53

Figure 1-9, latest Neoproterozoic arrangement for the Laurentian margin from Leslie et al. 2008. The suggested position of Baltica, Barentsia and Siberia along with the line of Iapetan separation are shown. The inset shows the location of Scottish ‘Promontory’ (S) within a wider global continental plate reconstruction. Abbreviations are GGF – Great Glen Fault; HB – Highland Border; MT – Moine Thrust; OIT – Outer Isles Thrust; SBT – Sgurr Beag Thrust; Sh – Shetland. 55

Figure 1-10, Simplified tectonostratigraphy of the Scandinavian Caledonides, from Roberts 2002. 56

Figure 2-1, Simplified isochron, showing the effect of a zircon inclusion within a garnet on a Lu-Hf age. The True Age and Measured Age isochrons are labelled on the diagram. The whole rock field is shown, where in this field the measured whole rock fraction lies depends on the amount of older zircon inclusions that were dissolved during digestion. The field of older zircons is shown in the diagram. The common reservoir is what the garnet grew from. The measured garnet, pure garnet and the mix are also indicated within the figure. 64

Figure 2-2, zircon U-Pb age against $^{176}\text{Hf}/^{177}\text{Hf}$ ratio using data from Kemp et al. (2006); Corfu & Noble (1992); Goodge et al. (2008) and Goodge & Vervoort (2006). 66

Figure 2-3, from Pollington & Baxter (2011) showing models of garnet age, total growth is equal to 1 fractional radius and total time is equal to fractional age. a) constant volumetric growth rate resulting in total growth in total time, b) decelerating growth rate; decelerating by 5% of the previous value every 0.1 mm, c) accelerating growth rate, accelerating by 5% of the previous value every 0.1 mm, d) pulsed growth rate. 72

Figure 2-4, standard JMC 475 97ppb over the period of use. It should give a value of 0.282165. The solid line shows the long term mean and the dashed lines mark the 2sd on the long term mean. 76

Figure 2-5, $^{143}\text{Nd}/^{144}\text{Nd}$ for 200 ppb Aldrich Nd and 200 ppb Aldrich Nd Ce standards should be 0.511407, the area between the dashed lines shows the long term mean. 83

Figure 2-6, $^{143}\text{Nd}/^{144}\text{Nd}$ values from 200 ppb Aldrich Nd and 200 ppb Aldrich Nd Ce plotted against $^{142}\text{Nd}/^{144}\text{Nd}$. The gradient is used to calculate the $^{143}\text{Nd}/^{144}\text{Nd}$ values in the samples. 84

Figure 2-7 Exponential and tail corrected $^{87}\text{Sr}/^{86}\text{Sr}$ for SRM run throughout the period of study. The area between the dashed lines is the long term mean. 86

Figure 3-1 sketch map of the Northern Highland Terrane showing the relationship with the basement inliers and the Moine Supergroup. BHT – Ben Hope Thrust; MT – Moine Thrust; NT – Naver Thrust; SBT – Sgurr Beag Thrust; SoT – Sole Thrust. Inliers are: A – Attadale; B – Borgie; F – Fannich; Fa – Farr; G – Glenelg; LS – Loch Shin; R – Ribigill; S – Glen Strathfarrar; SC – Scardroy; St – Strathan. 89

Figure 3-2, from Park 1985, reconstruction of eastern Laurentia and Baltic between 1900-1500 Ma. Abbreviations Lew – Lewisian; HBF – Highland Boundary Fault; NAC – North Atlantic Craton (Nain) ; SUP – Superior craton; Mak – Makkovik belt; Ket – Ketilidian belt; Lap-Kola – Lapland-Kola belt; TIB – Trans-Scandinavian igneous belt; W Nag – W Nagssugtoqidian belt; E Nag – E Nagssugtoqidian (or Ammassalik) belt; B – BABEL deep seismic reflection line. 90

Figure 3-3. Adapted from Wheeler et al. 2010. Rock types, protolith and metamorphic ages from the Caledonian Foreland. Protolith ages are shown in normal text and metamorphic ages are shown in grey italics. Ages are mainly U-Pb zircon ages and are detailed in Table 3-1. 91

Figure 3-4 map showing the location of Precambrian rocks in Ireland and SW Scotland. Abbreviations: AGC – Annagh Gneiss Complex; CWI – Colonsay West Islay block; GGF – Great Glen Fault; LF – Leannan Fault (Daly 2009). 95

Figure 3-5 sketch map of the Annagh Gneiss Complex within the North Mayo Inlier showing the subdivisions of the Annagh Gneiss Complex (Daly 2009). 97

Figure 3-6 simplified geological map of the East Greenland Caledonides from Higgins et al. (2004). The western limit of deformation is largely concealed by Inland Ice. Abbreviations A – Ardencaple Fjord; Am – Ammassalik; K – Ketilidian orogen. 98

Figure 3-7 Geology of Laurentia (Buchan et al. 2000). Greenland, Rockall Bank and northern British Isles are shown in a pre-Mesozoic reconstruction with respect to the

rest of Laurentia. NAC – North Atlantic craton, comprising the Nian Province of eastern North America and its equivalent in southern Greenland. 100

Figure 3-8. Sketch map of the Grenville orogenic belt of America and Canada (adapted from Corriveau et al. 2007 and Rivers 2009). The Archaean crustal blocks, Superior, Churchill and Nain are indicated as is the Grenville front, ABT is the Allochthon Boundary Thrust between the allochthonous and parautochthonous belts. 102

Figure 3-9. Adapted from Bingen et al. 2008. Sketch map of Fennoscandian crust showing main age areas. 103

Figure 3-10. Simplified geological map of the Glenelg-Attadale Inlier from Storey et al. 2010. The numbers indicate the sample localities; 9 – AB07-09, 10 – AB07-10, and 12 – AB07-12. BSZ – Barnhill Shear Zone; ISZ – Inverinate Shear Zone. 106

Figure 3-11, AB07-09 in thin section, A shows one of the veins/ streaks consisting of quartz, plagioclase and kyanite and an amphibolised area of the sample. B shows the same view in XP. C shows a fresher part of the sample and D shows the same view in XP. 107

Figure 3-12, MgO, CaO, Lu, Hf, Sm and Nd profile across a garnet from AB07-09 undertaken on the LA ICPMS at Royal Holloway, University of London. The sample was normalised internally to 39.30% SiO₂ obtained from the electron microprobe at the Natural History museum and externally to SRM 612. 108

Figure 3-13, shows AB07-10 in thin section, A shows one of the euhedral garnets with omphacite and opaque inclusions, B shows the same view in XP. C and D shows the symplectitic texture which dominates this sample and a large amphibolite. 109

Figure 3-14, MgO, CaO, Lu, Sm and Nd profile across a garnet from AB07-10, undertaken on the LA ICPMS at Royal Holloway, University of London. The sample was normalised internally to 39.30% SiO₂ obtained from the electron microprobe at the Natural History museum and externally to SRM 612. Hf profile is not included for this sample as its concentration was less than the detection limit on the LA ICP MS. 110

Figure 3-15, AB07-12 in thin section, A and B highlight the fabric which wraps the garnets. C and D shows a similar view with kyanite present associated with biotite. 111

Figure 3-16, MgO, CaO, Lu and Sm profile across a garnet from AB07-12, undertaken on the LA ICPMS at Royal Holloway, University of London. The sample was

normalised internally to 38.41% SiO₂ obtained from the electron microprobe at the Natural History museum and externally to SRM 612. Hf and Nd profiles are not included for this sample as their concentrations were less than the detection limit on the LA ICP MS. 111

Figure 3-17. Adapted from Strachan et al. (2010). Simplified geology map of north Scotland, circled number 1 is the location of sample AB07-18. BHT – Ben Hope Thrust; MT – Moine Thrust; NT – Naver Thrust; TT – Torrisdale Thrust; ST – Swordly Thrust; SHG – Strath Halladale Granite; LL – Loch Loyal. 112

Figure 3-18 shows AB07-18 in thin section, A and B highlight the granulitic texture. Clinopyroxene and garnet are often seen with a rim of amphibole. 114

Figure 3-19 MgO, CaO, Lu, Sm and Nd profile across a garnet from AB07-18, undertaken on the LA ICPMS at Royal Holloway, University of London. The sample was normalised internally to 38.27% SiO₂ obtained from the electron microprobe at the Natural History museum and externally to SRM 612. Hf profile is not included for this sample as its concentration was less than the detection limit on the LA ICP MS. 114

Figure 3-20, initial ¹⁴³Nd/¹⁴⁴Nd ratios for AB07-18. 117

Figure 3-21 showing isochron diagrams for all samples which gave three point or more Lu-Hf ages. The different garnet fractions are labelled and the whole rock is indicated by WR. Error bars are included on the diagram but in most cases they are smaller than the symbol. 118

Figure 3-22 showing isochron diagrams for all samples which gave three point or more Sm-Nd ages. The different garnet fractions are labelled and the whole rock is indicated by WR. Error bars are included on the diagram but in most cases they are smaller than the symbol. 119

Figure 3-23. From Temperley & Windley 1997, schematic section based on exposures along the NE and SE shores of Loch Duich. A – deflection of earlier fabrics, B – secondary shear foliations, C – vergence of shear folds, and D – low angle asymmetric boudins. Structures demonstrate top-to-east shear, which is also observed within the overlying Moine. 123

Figure 4-1, abbreviations 1 – AB08-01; 2 – AB07-02; 3 – AB07-03; 4 – AB07-04; 5 – AB09-05; 28 – AB07-28; 29 – AB07-29; 31 – AB07-31; IA1 – IA1; BHT – Ben Hope

Thrust; K – Knoydart mica mine; MT – Moine Thrust; SBc – Sgurr Breac; SBT – Sgurr Beag Thrust; SoT – Sole Thrust. 137

Figure 4-2, A and B shows AB07-02 in thin section. A shows three different textural zones within the garnet. The S_2 fabric, made up of quartz, white mica and biotite can be seen to be wrapping the garnets. 133

Figure 4-3, LA ICPMS element zonation across AB07-02 going from garnet rim to core to rim. 134

Figure 4-4, thin section photos for AB07-03, A shows garnets with zoning and S_1 planar inclusions. The S_2 fabric made up of biotite, muscovite, feldspar and quartz is wrapping the garnets. 135

Figure 4-5, thin section photos showing the relation of garnet and the surrounding fabric. A shows the sample in PP and B shows the sample in XP. 136

Figure 4-6, LA ICPMS trace for AB07-04. 137

Figure 4-7, A shows AB07-28 in PP and B shows the sample in XP. The garnets can be seen to be complexly zoned and surrounded by chlorite. The matrix is crenulated and is made up of quartz, biotite, white mica and feldspar. 138

Figure 4-8, A shows AB07-29 in PP and B shows the sample in XP. The fabric can be seen to have been crenulated and consists of muscovite, feldspar, biotite and quartz. 138

Figure 4-9, A shows one of the garnets from AB07-31 in PP, showing the curved inclusion trails which join up with the fabric. Chlorite is present round the edges of the garnets. B shows the same view in XP. C shows two of the large staurolites within the sample in PP, D shows the same view in XP. 139

Figure 4-10, LA ICPMS profiles for AB07-31 across one garnet. 140

Figure 4-11, A shows one of the garnets from AB08-01 in PP, showing the clear distinction between the garnet core and rim. B shows the same view in XP and clearly shows the biotite wrapping the garnet. C shows the fabric consisting of biotite, feldspar and quartz, and one of the large sphenes present within this sample. D shows the same view but in XP. 141

Figure 4-12, LA ICPMS profiles for AB08-01 from garnet rim to garnet core. 142

Figure 4-13, A shows AB09-05 in PP showing the fabric wrapping the garnets. B shows the same view in XP. 143

Figure 4-14, shows IA1 in thin section. A shows the fabric dominated by white mica wrapping the garnet. Chlorite is also surrounding the garnets; B shows the same view in XP. C shows a large garnet with an inclusion poor core and an inclusion rich rim; D shows the same view in XP, the mica rich and quartz rich layers in the fabric can be seen clearly. 143

Figure 4-15 $^{176}\text{Lu}/^{177}\text{Hf}$ vs $^{176}\text{Hf}/^{177}\text{Hf}$; $^{176}\text{Lu}/^{177}\text{Hf}$ vs $1/\text{Hf}$; $^{147}\text{Sm}/^{144}\text{Nd}$ vs $^{143}\text{Nd}/^{144}\text{Nd}$ and $^{147}\text{Sm}/^{144}\text{Nd}$ vs $1/\text{Nd}$ for AB07-31. The filled black squares are the measured garnet core fractions, the empty black squares are the garnet rim fractions, the grey squares are the measured whole rock fractions, the filled black circles are the old calculated end members and the empty circles are the Caledonian end members. The end members were 950 Ma and 430 Ma. 146

Figure 4-16 $^{176}\text{Lu}/^{177}\text{Hf}$ vs $^{176}\text{Hf}/^{177}\text{Hf}$; $^{176}\text{Lu}/^{177}\text{Hf}$ vs $1/\text{Hf}$; $^{147}\text{Sm}/^{144}\text{Nd}$ vs $^{143}\text{Nd}/^{144}\text{Nd}$ and $^{147}\text{Sm}/^{144}\text{Nd}$ vs $1/\text{Nd}$ for AB07-02. The filled black squares are the measured garnet core fractions, the empty black squares are the garnet rim fractions, the grey squares are the measured whole rock fractions, the filled black circles are the old calculated end members and the empty circles are the Caledonian end members. The end members were 950 Ma and 460 Ma. 148

Figure 4-17 $^{176}\text{Lu}/^{177}\text{Hf}$ vs $^{176}\text{Hf}/^{177}\text{Hf}$; $^{176}\text{Lu}/^{177}\text{Hf}$ vs $1/\text{Hf}$; $^{147}\text{Sm}/^{144}\text{Nd}$ vs $^{143}\text{Nd}/^{144}\text{Nd}$ and $^{147}\text{Sm}/^{144}\text{Nd}$ vs $1/\text{Nd}$ for AB08-01. The filled black squares are the measured garnet core fractions, the empty black squares are the garnet rim fractions, the grey squares are the measured whole rock fractions, the filled black circles are the old calculated end members and the empty circles are the Caledonian end members. The end members were 780 Ma and 460 Ma. 150

Figure 4-18 $^{176}\text{Lu}/^{177}\text{Hf}$ vs $^{176}\text{Hf}/^{177}\text{Hf}$; $^{176}\text{Lu}/^{177}\text{Hf}$ vs $1/\text{Hf}$; $^{147}\text{Sm}/^{144}\text{Nd}$ vs $^{143}\text{Nd}/^{144}\text{Nd}$ and $^{147}\text{Sm}/^{144}\text{Nd}$ vs $1/\text{Nd}$ for AB07-04. The filled black squares are the measured garnet core fractions, the empty black squares are the garnet rim fractions, the grey squares are the measured whole rock fractions, the filled black circles are the old calculated end members and the empty circles are the Caledonian end members. The end members were 780 Ma and 460 Ma. 151

Figure 5-1, Adapted from Dewey & Strachan (2003) and Roberts (2003). Simplified tectonic map of the Caledonides in the Mid- Late Silurian, showing the main structures

and areas affected by Caledonian deformation. Major faults and thrusts; GGF – Great Glen Fault; HBF – Highland Boundary Fault; SUF – Southern Upland Fault; IS – Iapetus Suture; MTZ – Moine Thrust Zone. NHT – Northern Highland Terrane. 161

Figure 5-2. Adapted from Leslie et al. (2009). Diagram 1 shows a pre-Grampian stage showing south directed subduction forming an island arc complex. Diagram 2 shows the initial collision of the arc and the trench leading to the obduction of ophiolites and crustal thickening, deformation and metamorphism on the Laurentian margin. Diagram 3 shows continued collision resulting in folding and underthrusting of the Laurentian margin and a north dipping subduction zone. 163

Figure 5-3, Adapted from Strachan et al. (2010). The top diagram shows how continued subduction was achieved by the reversal of polarity of subduction at the end of the Grampian developing an active margin and creating the Southern Uplands accretionary prism. The bottom diagram shows the underthrusting of Baltica beneath Laurentia and the development of E and W directed thrust systems. This was followed by strike-slip displacement along the Great Glen Fault. 164

Figure 5-4 is a schematic plate tectonic diagram for the Silurian at ~430 Ma. The position of the Northern Highlands is shown in the box. It shows one way of explaining the lack of Scandian deformation in the Grampian Highlands by invoking ~700 km of sinistral displacement along the GFF (Dewey & Strachan 2003; Kinny et al. 2003). 165

Figure 5-5 shows what are presumed to be Scandian lineations across the western Moine with an indication that Grampian events are apparently confined to the eastern Moines (Kinny et al. 2003). Abbreviations BHT – Ben Hope Thrust; MT – Moine Thrust; NT – Naver Thrust; SBT – Sgurr Beag Thrust; SoT – Sole Thrust; ST – Swordly Thrust. 167

Figure 5-6 thin section photos for AB07-05 (Loch Quioch Amphibolite). A shows AB07-05 in PP and the fabric dominated by hornblende, biotite and quartz wrapping the garnets. B shows the same view in XP. All abbreviations are from Kretz (1983). 170

Figure 5-6, simplified geological map of the Northern Highland and the Grampian terranes, the numbers within circles represent sample numbers; 2 – AB08-02; 5 – AB07-05; 8 – AB07-08; 13 – AB07-13; 14 – AB07-14; 15 – AB07-15; 17 – AB07-17; 21 – AB07-21; 22 – AB07-22; 23 – AB07-23; 27 – AB07-27; 30 – AB07-30. Abbreviations; AGG – Ardour Granitic Gneiss; GDS – Glen Dessary Syenite; GD – Glen Doe; GS –

Glen Scaddle; SBT – Sgurr Beag Thrust; K – Knoydart; MT – Moine Thrust; SoT – Sole Thrust; NT – Naver Thrust; BHT – Ben Hope Thrust. 171

Figure 5-8, A shows a garnet from AB07-08 with curved inclusion trails which often meet up with the surrounding fabric, this garnet also shows an inclusion rich core. B shows the same view in XP, showing a large biotite which appears to be sheared. C shows several garnets with the inclusion trails joining up with the fabric, D shows the same view in XP. 172

Figure 5-9, LA ICPMS data from a garnet from AB07-08 normalised to a SiO₂ value of 37.2%. 173

Figure 5-10, A and B show AB07-11 in thin section. The garnets show continuous inclusion trails from core to rim, pronounced pressure tails and are wrapped by the fabric. 174

Figure 5-11, LA ICPMS data from a garnet from AB07-11 normalised to a SiO₂ value of 37.2%. 175

Figure 5-12, A shows one of the small euhedral garnets next to one of the large garnets. Kyanite is also shown with its reaction rim. B shows the same view in XP, highlighting the reaction rim. 176

Figure 5-13, LA ICPMS data from a garnet from AB07-13 normalised to 37.6% SiO₂. 177

Figure 5-14, A shows the granoblastic texture made up of garnet, amphibolite, epidote, quartz and plagioclase. The same view is shown in B in XP. 178

Figure 5-15, LA ICPMS data from a garnet from AB07-14 normalised to a SiO₂ value of 38.2%. 179

Figure 5-16, A and B show the curved inclusion trails within the garnets. C and D show the fabric with biotite dominated layers and quartz dominated layers, which wraps garnet. The garnet in C and D has a reaction rim. 180

Figure 5-17, LA ICPMS data from a garnet from AB07-15 normalised to a SiO₂ value of 37.0%. 181

Figure 5-18, A and B show the fabric, dominated by amphibole, biotite, feldspar and quartz, wrapping garnets. C and D show one of the large garnets with inclusion trails that are oblique to the main fabric. 182

Figure 5-19, LA ICPMS data from a garnet from AB07-17 normalised to a SiO₂ value of 37.0%. 183

Figure 5-20 thin section photos for AB07-21 (Strathy Complex Amphibolite). A and B show amphibole that is in equilibrium next to amphibole which is clearly not in equilibrium. C and D show the large quartz inclusions within the large garnets. All of the pictures show the weak fabric. 184

Figure 5-21 thin section photos for AB07-22 (Naver nappe garnetiferous gneiss). A and B show the fabric defined by amphibolite, biotite, quartz and feldspar. C and D show the small garnets within this sample surrounded by amphibolite and biotite. 185

Figure 5-22, LA ICPMS data from a garnet from AB07-22 normalised to a SiO₂ value of 37.5%. 185

Figure 5-23, A and B show the granoblastic texture made up of amphibolite, epidote, quartz, garnet and sphene. C shows a euhedral garnet surrounded by amphibole. 186

Figure 5-24 thin section photos for AB07-27 (Leven Schist). A and B show the inclusion trails within the garnet continuing into the surrounding matrix showing that the garnets are post-kinematic. The fabric is slightly crenulated. A biotite porphyroblasts can also be seen in the top part of each picture which has been deformed. 187

Figure 5-25, LA ICPMS data from a garnet from AB07-27 normalised to a SiO₂ value of 39.3%. 188

Figure 5-26 thin section photos for AB07-30 (Mull Amphibolite). A and B show one of the large garnets which is very inclusion rich. The inclusions are dominated by quartz. The surrounding fabric is made up of amphibole, epidote, feldspar and quartz. C and D show smaller garnets with sieve-like textures. 189

Figure 5-27 thin section photos of AB08-02 (Vaich Amphibolite). A and B show a garnet from AB08-02 which has planar inclusion trails. The garnet is strongly wrapped by the fabric dominated by amphibole. The garnet has pressure shadows with biotite and quartz. 190

Figure 5-28, $^{176}\text{Lu}/^{177}\text{Hf}$ vs $^{176}\text{Hf}/^{177}\text{Hf}$, $^{176}\text{Lu}/^{177}\text{Hf}$ vs $1/\text{Hf}$, $^{147}\text{Sm}/^{144}\text{Nd}$ vs $^{143}\text{Nd}/^{144}\text{Nd}$ and $^{147}\text{Sm}/^{144}\text{Nd}$ vs $1/\text{Nd}$ for AB07-08. The filled black squares are the measured garnet core fraction, the empty black squares are the garnet rim fraction, the grey squares are

the measured whole rock fractions, the filled black circles are a 840 Ma end member and the empty circles are a 430 Ma end member. 192

Figure 5-29, $^{147}\text{Sm}/^{144}\text{Nd}$ vs $^{143}\text{Nd}/^{144}\text{Nd}$ and $^{147}\text{Sm}/^{144}\text{Nd}$ vs $1/\text{Nd}$ for AB07-13. The filled black square is the measured garnet core fraction, the empty black square is the garnet rim fraction, the grey square is the measured whole rock fraction, the filled black circle is a 780 Ma end member and the empty circle is a 465 Ma end member. The end members are based on the ages of monazite inclusions within a garnet from close to this sample (Cutts et al. 2010). 195

Figure 5-30 showing isochron diagrams for all samples which gave a three point or more Lu-Hf age. The garnet fractions are labelled and the whole rock is indicated by WR. Error bars are included on the diagram but in most cases they are smaller than the symbol. 199

Figure 5-29 showing isochron diagrams for all samples which gave three point or more Sm-Nd ages. The garnet fractions are labelled and the whole rock is indicated by WR. Error bars are included on the diagram but in most cases they are smaller than the symbol. 200

Figure 6-1, simplified geological map of Shetland showing the main units, faults and thrusts, adapted from Flinn (1988). 215

Figure 6-2, a – photo of AB08-04 in the field prior to sampling showing the main fabric; b – shows folded pegmatites cutting through AB08-04; c thin section photo of AB08-04 in plane polarised light showing the main foliation defined by the biotites and the plentiful small garnets; d showing the same view as c in cross polars. 217

Figure 6-3, a – photo of AB08-06 in the field prior to sampling showing the main fabric; b – shows the undulating fabric caused by the large boudins; c thin section photo of AB08-04 in plane polarised light showing mineral relations, especially pyroxene surrounded by amphiboles; d showing the same view as c in cross polars. 219

Figure 6-4, LA ICPMS profile for AB08-06 using a SiO₂ value of 37.1% . 219

Figure 6-5, a – photo of AB08-08 in the field prior to sampling showing the amphibolite body; b – shows the large garnets wrapped by the fabric; c thin section photo of AB08-04 in plane polarised light showing the amphibole rich fabric wrapping the garnets, and the slightly curved inclusion trails within the garnet; d showing the same view as c in cross polars 220

Figure 6-6 a – photo of AB08-13 in the field prior to sampling showing the amphibolite body; b – shows the large garnets wrapped by the fabric; c thin section photo of AB08-04 in plane polarised light showing the amphibole rich fabric wrapping the garnets, and the slightly curved inclusion trails within the garnet; d showing the same view as c in cross polars 221

Figure 7-1, previously published Rb-Sr, Ar-Ar and K-Ar ages plotted against distance along strike of the Moine Thrust Zone, a shows all the data and b shows just the data between 500 – 350 Ma. Data from Giletti et al., 1961; Freeman et al., 1998; and Dallmeyer et al., 2001. 231

Figure 7-2 abbreviations; 2 – AB07-02; 3 – AB07-03; 4 – AB07-04; 8 – AB07-08; 11 – AB07-11; 12 – AB07-12; 13 – AB07-13; 15 – AB07-15; 27 – AB07-27; 29 – AB07-29; 31 – AB07-31; BHT – Ben Hope Thrust; K – Knoydart mica mine; MT – Moine Thrust; SBc – Sgurr Breac; SBT – Sgurr Beag Thrust; SoT – Sole Thrust. 232

Figure 7-3 AB07-02 in thin section showing the white mica and biotite dominated matrix wrapping the garnets. 233

Figure 7-4 AB07-03 in thin section showing the crenulated matrix dominated by white mica and biotite with quartz rich layers. 234

Figure 7-5 AB07-04 in thin section showing the coarser nature of this sample compared with AB07-02 and AB07-03. The thin section also shows plentiful biotite. 235

Figure 7-6 AB07-08 in thin section showing large biotite porphyroblasts with a fine grained matrix surrounding them consisting of quartz, biotite and white mica. 236

Figure 7-7 AB07-11 in thin section showing the crenulated matrix with quartz rich and mica rich domains. 237

Figure 7-8 AB07-12 in thin section showing the plentiful biotite wrapping the garnets with white mica and opaque minerals. 238

Figure 7-9 AB07-13 in thin section showing kyanite surrounded by fine grained white mica and the gneissic fabric of the sample. 239

Figure 7-10 AB07-15 in thin section showing large garnets wrapped by the mica and quartz rich fabric. C and D show the biotite and quartz dominated layers. 240

Figure 7-11 AB07-27 in thin section showing the crenulated fine grained matrix consisting of quartz, white mica and biotite. 241

Figure 7-12 AB07-29 in thin section showing the strongly crenulated cleavage made up of white mica and biotite. 241

Figure 7-13 AB07-31 in thin section showing biotite that has been converted to chlorite with white mica which make up the fabric that joins up with inclusions in the garnet porphyroblasts. 222

Figure 7-14, data from this study plotted with all previously published ages against distance along the Moine Thrust Zone, a shows all the dates and b shows the ages between 550 – 350 Ma. These graphs exclude sample AB07-27 (Leven Schist) as it is not part of the Moine Supergroup but part of the Dalradian Supergroup. 245

Figure 7-15 a simplified geological map of the Northern Highlands. The samples that do not give Caledonian garnet or white mica ages are circled. 248

Figure 8-1 garnet size versus Lu-Hf and Sm-Nd age. 250

Figure 8-2 graph showing Lu-hf ages versus Sm-Nd ages on all garnets which gave reliable ages. The empty symbols give ages from pelites and the filled symbols from eclogites, amphibolites and granulites. 251

Figure 8-3, simplified geological map of the Northern Highland and Grampian terranes, Abbreviations are; AGG – Ardour Granitic Gneiss; BHT – Ben Hope Thrust; C – Cairngorms; CCG – Carn Chuinneag Granite; GD – Glen Doe; GS – Glen Shiel; K – Knoydart; KLH – Kinlochourn; LBC – Loch Borrolan Complex; MT – Moine Thrust; NT – Naver Thrust; SBT – Sgurr Beag Thrust; SC – Strathy Complex; SoT – Sole Thrust. Sample numbers are 2 – AB07-02; 3 – AB07-03; 4 – AB07-04; 5 – AB07-05; 8 – AB07-08; 9 – AB07-09; 10 – AB07-10; 11 – AB07-11; 12 – AB07-12; 13 – AB07-13; 14 – AB07-14; 15 – AB07-15; 17 – AB07-17; 18 – AB07-18; 21 – AB07-21; 22 – AB07-22; 23 – AB07-23; 27 – AB07-27; 28 – AB07-28; 29 – AB07-29; 31 – AB07-31; 81 – AB08-01; 82 – AB08-02; 95 – AB09-05; IA – IA1. 253

Figure 8-4, from Cawood et al. (2010) showing the Neoproterozoic reconstruction of eastern Laurentia, Baltica and northern Amazonia. Baltica is shown in pre and post 1265 Ma position. The rotation of Baltica opened the Asgard Sea. Red blocks correlate to units associated with the Renlandian orogenic cycle and yellow blocks relate to Knoydartian influenced units. The abbreviations are; GT – Grampian Terrane; M – Moine Supergroup; Hf – Hebridean Foreland; K – Krummedal succession; Rb – Rockall Bank; Sa/So – Sværholt and Sørøy successions; Sh – Shetland; Sn – Sveconorwegian

orogeny; Ss – Sunsas orogen; Se – Eastern terrane of Svalbard; Sc – Central terrane of Svalbard; Sw – Western terrane of Svalbard. 255

LIST OF TABLES

Table 1-1 deformation phases in the Northern Highland Terrane. Adapted from Kocks 2002 & Emery 2005. Abbreviations; AGG – Ardgour Granitic Gneiss; GDS – Glen Dessary Syenite; MT – Moine Thrust; SBT – Sgurr Beag Thrust.	39
Table 2-1 summary of previously published ^{176}Lu decay constants.	60
Table 2-2 XRF parameters for each element analysed. Abbreviations; C – coarse collimator; F – fine collimator; FL – flow counter; FS – flow and scintillation counters. Crystal numbers; 1 – Lithium fluoride 220 (LiF 220); 2 – Lithium fluoride 200 (LiF 200); 3 – Germanium; 4 – Pentaerythritol; 5 – Thallium acid phthalate; 6 – Indium antimonide.	75
Table 2-3 major element XRF results for the sample that was replicated 6 times.	76
Table 2-4 trace element XRF results from the sample repeated 6 times.	76
Table 2-5 standards ran during EPMA analysis.	77
Table 2-6 comparison between CaO and MgO concentrations obtained from EPMA and LA ICPMS for several of the garnets analysed within this study.	78
Table 2-7 targeted isotopic ratios for spiking.	79
Table 2-8 columns used for mineral separation.	79
Table 2-9 Lu column calibration testing columns 1, 3, 4 and 8. The fractions are arranged in the order they came off the columns, the first fraction should have LREE and MREE, in the second fraction some Yb may be seen, the third fraction is where the majority of the Yb comes off and the last fraction is where Lu is found. The voltage was corrected for the amplifier offset.	80
Table 2-10, MC ICPMS collector configurations for Hf, Lu, Nd and Sm analysis.	82
Table 3-1 summary of geochronology from basement rocks of NHT and the Lewisian Gneiss Complex, adapted from Wheeler et al. 2010.	92
Table 3-2 summarising the Lu-Hf results from the basement inliers.	120
Table 3-3 summarising the Sm-Nd results from the basement inliers.	120

Table 3-4 summarising the Rb-Sr results from the basement inliers.	120
Table 4-1 summary of previous Neoproterozoic geochronology. Mineral references use Kretz 1983.	128
Table 4-2; Results of Lu-Hf garnet analyses for samples which give Neoproterozoic ages.	201
Table 4-3; Results of Sm-Nd analyses for samples which give Neoproterozoic ages.	202
Table 5-1 Lu-Hf Garnet Analyses Results for samples which gave Caledonian ages.	159
Table 5-2 Sm-Nd Garnet Analyses Results for samples which gave Caledonian ages.	189
Table 6-1 Lu-Hf garnet results from Shetland samples.	223
Table 6-2 Sm-Nd garnet results from Shetland samples.	223
Table 7-1 summary of all published Rb-Sr, Ar-Ar and K-Ar dates from the Moine Supergroup and inliers.	228
Table 7-2; Rb-Sr Mica Analyses Results, (Bird & McDermott, Nuffield bursary, RHUL). The dates marked with an asterisk are samples that were not radiogenic enough to provide a meaningful age.	244
Table 8-1, summary of deformational events the Moine Supergroup has been subjected to. References used for the published ages are set out in the bottom of the table.	258

ACKNOWLEDGEMENTS

First of all I would like to thank my family; Mum, Dad, Maggie, Granny B and my brother Pete. My mum and dad have supported me through every decision I have made, and along with Maggie, encouraged an interest in science and the outdoors which has lead me on the route to where I am now. I would like to dedicate this thesis to Maggie; I know she would have been tickled pink to have a doctor as a granddaughter, even if it wasn't a "*real*" one. I hope to one day be as strong and independent as she was.

I would like to thank my supervisors Matthew Thirlwall and Rob Strachan. Matthew has spent countless hours helping and guiding me, teaching me about accuracy and precision and the importance of good data. Rob introduced me to the beautiful Northern Highlands and kindly undertook almost all of the rock bashing. I also would like to thank Rob for giving me an appreciation of good ale.

Thanks to the Edinburgh Geo Ladies who made my time at Edinburgh unforgettable. While at Royal Holloway I have met and worked alongside many great people. Special thanks has to go to Paul, Vicky, Pete, Hammertime, Clare, Inga and JPF for many cups of tea, always being there when I needed cheering up and for being such great friends. I would also like to thank Kev for helping to keep me sane (and fit) by taking me running and to the Beehive for well deserved pints and many post-work moans.

Another person who has helped me massively in the putting together of this thesis and deserves a special mention is Christina, from cheering me up after many lab related disasters to being my running partner and drinking buddy. I have no doubt that without Christina's help and support that I would be submitting a different thesis. Also thanks to Toby who I suspect has had many an evening ruined by Christina and I trying to do some work or generally have a long (and perhaps boring) discussion about isotopic geochemistry.

And finally, the biggest (and bestest) thanks has to go to Andy, who has always been there when I needed him.

CHAPTER 1: INTRODUCTION TO GEOLOGY OF THE SCOTTISH CALEDONIDES

1.1 Introduction

The identification of the timing(s) of peak metamorphism is extremely important in poly-metamorphic terranes in order to establish when deformation events occurred and the geographical extent of these events. A classic example of this is provided by the Moine Supergroup within the Northern Highland Terrane, Scotland, which is the focus of this study. The Northern Highland Terrane makes up part of the Caledonide mountain system which spans Scotland, Ireland, Scandinavia, Svalbard, eastern Greenland, north-east America and parts of north-central Europe. The Caledonides were formed in Ordovician to early Devonian time from the closure of the Iapetus Ocean which lay between Laurentia, Baltica and Avalonia (e.g. Jones & Blake 2003). The Caledonides of mainland Scotland make up a series of fault-bounded terranes, the Southern Uplands which consist of sedimentary rocks interpreted to represent part of an accretionary wedge, and the Grampian and Northern Highland terranes which are made up of metasedimentary rocks. The Grampian and Northern Highland terranes are found north of the Highland Boundary Fault, which is exposed between Arran and Stonehaven (Figure 1-1). This area mostly consists of Cambrian and Precambrian rocks and later igneous intrusions, the remnants of which have formed mountain massifs such as the Cairngorms and the Cuillins on Skye. This area is split into two terranes, the Northern Highland Terrane and the Grampian Terrane. The Northern Highland Terrane consists of Neoproterozoic metasedimentary rocks of the Moine Supergroup which are thrust onto the Cambro-Ordovician sedimentary rocks and the Lewisian Gneiss Complex of the Hebridean Terrane. Across the Great Glen Fault, the Grampian Terrane consists of a variety of meta-sediments and igneous intrusives. Rocks similar to those found in the Grampian and Northern Highland terranes of mainland Scotland are also thought to occur on Shetland. The Caledonides of the Northern Highland Terrane of mainland Scotland and Shetland is the main focus of this study.

1.2 General geology

The Moine Supergroup outcrops within the Northern Highland Terrane and consists of a series of Neoproterozoic metasediments, igneous intrusives of various ages, and basement inliers which have been correlated with the Archaean Lewisian Gneiss Complex of the Hebridean terrane (Holdsworth et al. 1994) (Figure 1-1). Research on the Moine has been undertaken since the late 1800s, it represents a classical area in the history of structural geology where some of the fundamental concepts of basement-cover relationships were understood for the first time (e.g. Ramsay 1958; Rathbone & Harris 1979). The published geochronology indicates that the Moine Supergroup has undergone at least three metamorphic events, the Knoydartian (~840 Ma) and two related to the Caledonian Orogeny (Grampian and Scandian events). The Moine Supergroup has a long and complex metamorphic history making it ideal for a geochronological study using modern techniques.

The Moine Supergroup is separated from the Hebridean terrane by the Moine Thrust Zone to the northwest. The oldest part of the northern Highlands is the Lewisian Gneiss Complex which has yielded isotopic ages as old as 3.13 Ga (Gibbons & Harris, 1994; Whitehouse et al. 1996, 1997; Kinny & Friend 1997; Friend & Kinny 2001). These gneisses are a small part of a very extensive region of Archaean crust separated from the Laurentian shield of Greenland and North America by the Atlantic Ocean and from Scandinavia by Caledonian structures and rift structures associated with the formation of the North Sea (e.g. Jones & Blake 2003; Higgins & Leslie 2008). The main outcrops of the Lewisian Gneiss Complex in Scotland occur on the islands of the Outer Hebrides and on a coastal belt of the mainland between Cape Wrath in the north to Loch Torridon in the south. Units that can be correlated with the Lewisian also outcrop in the Inner Hebrides and in Shetland where they are within the Caledonian orogenic belt (Flinn 1988).

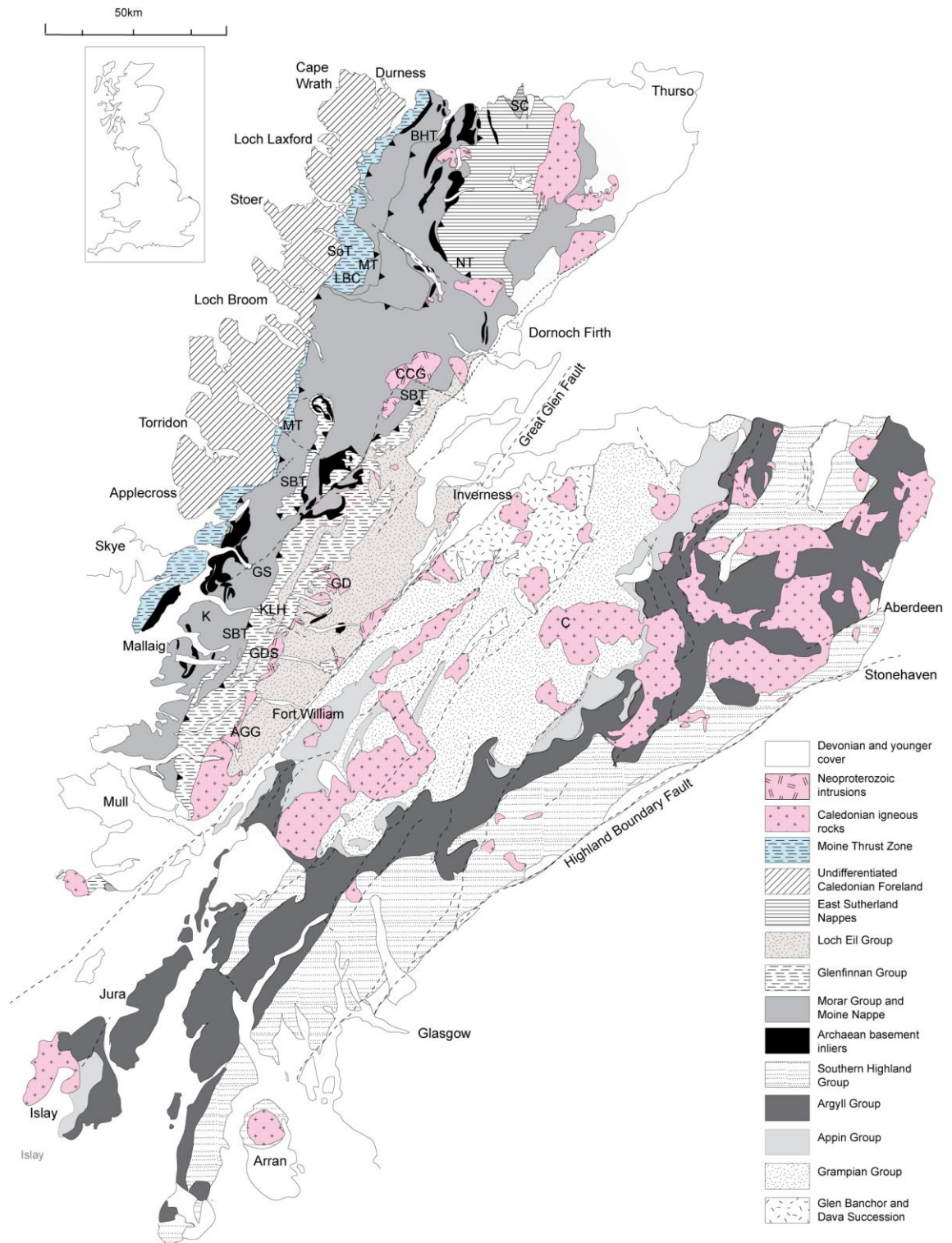


Figure 1-1, simplified geological map of the Northern Highland and Grampian terranes, Abbreviations are; AGG – Ardour Granitic Gneiss; BHT – Ben Hope Thrust; C – Cairngorms; CCG – Carn Chuinneag Granite; GD – Glen Doe; GS – Glen Shiel; K – Knoydart; KLH – Kinlochourn; LBC – Loch Borrolan Complex; MT – Moine Thrust; NT – Naver Thrust; SBT – Sgurr Beag Thrust; SC – Strathy Complex; SoT – Sole Thrust.

The Lewisian Gneiss Complex consists of a crystalline, mainly gneissose basement of granulite and amphibolite facies metamorphic grade with metasedimentary rocks, pegmatites and ultramafics. The basement is overlain unconformably by a gently tilted sedimentary cover which is known as the Torridonian Supergroup. The Torridonian Supergroup consists of the Stoer, Sleat and Torridon groups (e.g. Park et al. 2003; Kinnaird et al. 2007) and mainly consists of sandstone but also has shale, and mudstone, and fills palaeovalleys in the underlying Lewisian. It is overstepped by a Cambrian-Ordovician shelf sequence which consists of quartz arenites, limestones and dolomites (Park et al. 1994). At Assynt, within the Moine Thrust Zone, the cover and basement rocks are imbricated, folded and stacked up in a complex sequence of thrusts (Strachan et al. 2010). The Moine rocks rest on the roof thrust to this belt. The Torridonian Supergroup crops out extensively from Cape Wrath to Sleat in Skye.

The Moine Supergroup is limited to the southeast by the Great Glen Fault. The Grampian terrane to the south east is dominated by the Dalradian Supergroup which comprises the Grampian, Appin, Argyll and Southern Highland groups which are made up of metasediments and mafic metavolcanic rocks (e.g. Harris et al. 1994). Also within the Grampian Highlands are possible equivalents of the Moine Supergroup which are known as the Dava and Glen Banchor succession. These are of generally higher metamorphic grade and greater structural complexity than the overlying metasedimentary rocks of the Dalradian, although the inferred unconformity between the two has been largely obscured by tectonism (e.g. Piasecki & van Breemen 1979; Highton et al. 1992).

1.3 Tectonostratigraphy of the Moine Supergroup

The Moine Supergroup is made up of Neoproterozoic psammites, semi-pelites and pelites, with various suites of igneous intrusives (Strachan et al. 2010 and references therein). All of these rocks occur in thick formations as well as in striped or banded units which are characterized by rapid alterations of lithology at centimetre to metre scales. The units are divided into a series of thrust nappes, separated by regional ductile thrusts (e.g. Holdsworth et al. 1994). Sedimentary structures are often present in areas of low tectonic strain and provide evidence on the original way-up of local successions. The distribution of the various units is shown on Figure 1-2.

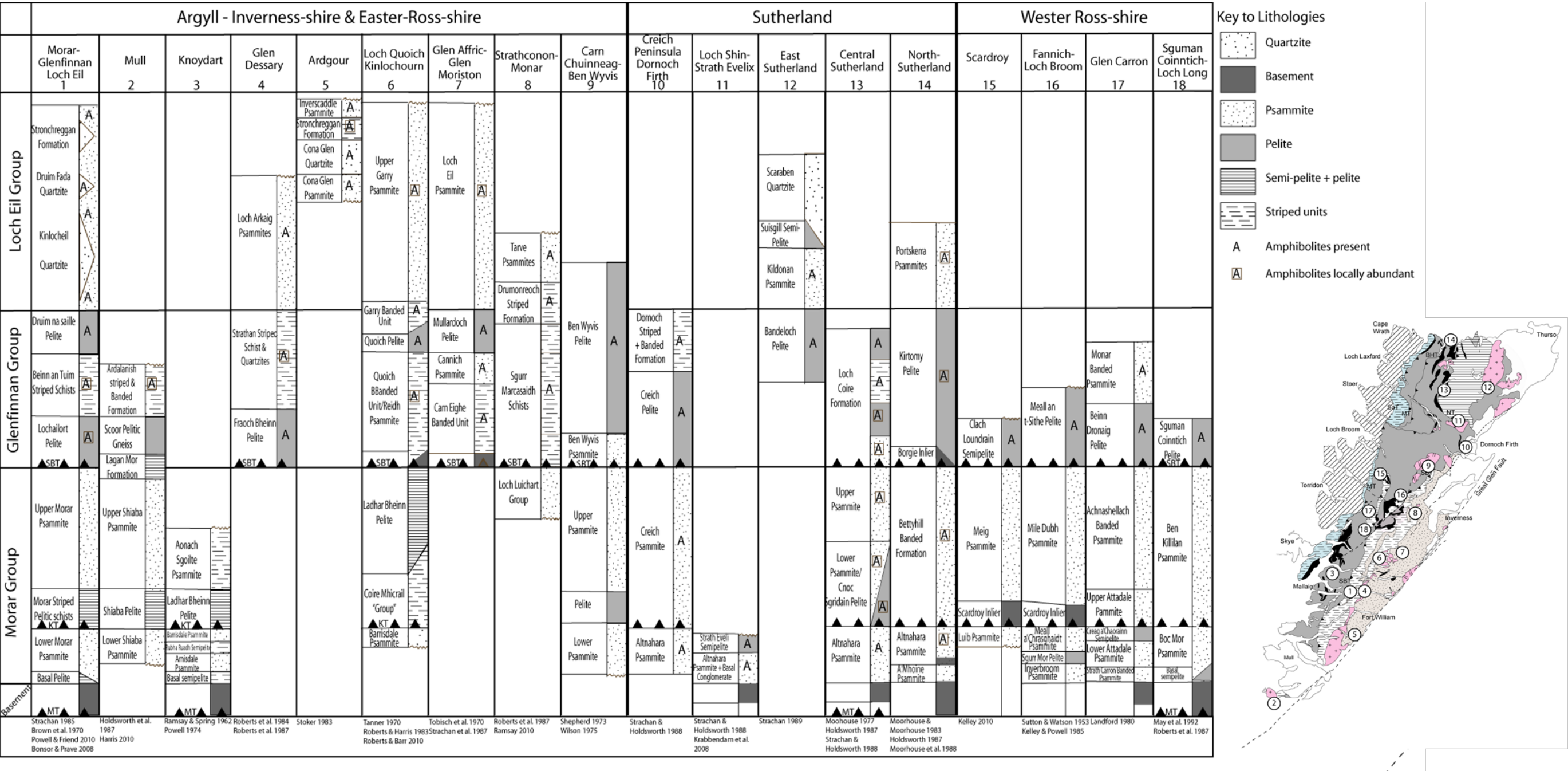


Figure 1-2, adapted from Holdsworth et al. 1994. Detailed Tectonostratigraphy of the Moine Supergroup within the Northern Highlands, suspected Moine equivalents from Shetland and the Grampian terrane are not included. The Moine type sections are shown in columns 1 and 2. The locations of the columns are shown on the map. The columns show general lithologies, thrusts, basement and amphibolite content. Abbreviations are; MT – Moine Thrust; SBT – Sgurr Beag Thrust; KT – Knoydart Thrust. Sections are not drawn to scale.

1.3.1 Inverness-shire, Argyll and Easter-Ross

The Moine rocks in Inverness-shire, Argyll and Easter-Ross comprise three lithostratigraphic units, the Morar, Glenfinnan and Loch Eil groups. The Morar Group forms the Moine Nappe and is thought to represent the oldest parts of the Moine (Holdsworth et al. 1987, 1994; Roberts et al. 1987; Harris & Johnstone 1991). The type area for the Morar Group stratigraphy displays four formations; in ascending order these are the Basal Pelite, Lower Morar Psammite, Morar Pelite and Upper Morar Psammite (Richey & Kennedy 1939; Ramsay & Spring 1962; Johnstone et al. 1969; Brown et al. 1970; Holdsworth et al. 1994). Basement inliers are found at the bottom of the Morar Group lithological succession once the successions have been structurally restored and the effects of deformation the Morar has undergone have been removed. The basement inliers are found in the cores of major early isoclinal folds (Powell 1974; Tanner 1970), and often have the Basal Pelite overlying them. The Basal Pelite comprises a tectonic melange of Moine semi-pelite and retrogressed gneissic blocks derived from the underlying basement (Ramsay & Spring 1962). The Knoydart thrust is the only structure that appreciably disrupts the sequence and is only seen on the eastern limb of the Morar Antiform, though a common succession is recognized in its footwall and its hangingwall (Holdsworth et al. 1994). The thick psammities within the Morar Group are commonly weakly strained and therefore preserve sedimentary structures, which means an original way-up and palaeocurrent information can be determined from cross-bedding within the psammities (e.g. Wilson et al. 1953; Glendinning 1988; Bonsor & Prave 2008).

The Glenfinnan Group overlies the Morar Group and mainly comprises striped units of thinly interbedded psammities, semi-pelites, quartzites and pelites. Tectonic strain is commonly high and sedimentary structures are therefore rare. Estimates of original thickness vary from 1-4 km. On the mainland, the Morar and Glenfinnan Groups are separated by the Sgurr Beag Thrust; however Holdsworth et al. (1987) recognized that the boundary between the Morar and Glenfinnan Groups may be transitional on the Ross of Mull. Allochthonous slices of Lewisianoid basement are also present along the Sgurr Beag Thrust and are interfolded with the base of the Glenfinnan Group, thus are assumed to lie at the stratigraphic base of the Group (Tanner 1970). Glenfinnan Group rocks also appear as migmatitic gneisses next to the Great Glen Fault at Achnacarry and

at Invermoriston (British Geological Survey 2007). The Glenfinnan and the western Loch Eil Group rocks within Inverness-shire, Argyll and Easter-Ross have been affected by major NNE-SSW trending folds which are referred to as the 'Northern Highland Steep Belt' (Strachan et al. 2010).

The Loch Eil Group occurs as synformal infolds within the Glenfinnan Group (Roberts et al. 1984) (Strachan et al. 2010). It consists of a monotonous sequence of psammites up to 5 km, with local quartzites; sedimentary structures are common locally. It stratigraphically overlies the Glenfinnan Group and according to Roberts & Harris (1983) and Strachan (1985) the contact is sedimentary. The folds of the Northern Highland Steep Belt have little influence on the Loch Eil Group, as the majority of it lies to the east of this belt (Roberts et al. 1987).

1.3.2 Sutherland and the Fannichs

The Moine rocks of north Sutherland comprise two major structural units, the Moine and Naver nappes, separated by the Naver Thrust (Kinny et al. 2003). Both the Moine and Naver nappes are imbricated internally by subordinate ductile thrusts, including the Ben Hope and Swordly thrusts (Moorhouse 1977; Holdsworth & Strachan 1988; Moorhouse & Moorhouse 1988; Moorhouse et al. 1988; Strachan & Holdsworth 1988; Holdsworth et al. 2001). The Sgurr Beag Thrust extends northwards into Ross-shire (Wilson & Shepherd, 1979; Kelley & Powell, 1985) and is thought to correlate with either the Naver or Swordly thrusts in central Sutherland (Barr et al. 1986; Strachan & Holdsworth, 1988), although there are major differences between the metamorphic grades of the Loch Coire migmatites that occur above the Naver Thrust in Sutherland and the Glenfinnan Group rocks to the south. It could be that the Skinsdale Thrust is a more likely correlative of the Sgurr Beag Thrust, as the rocks above the thrust are generally unmigmatized psammites, semi-pelites and quartzites similar to the types of lithologies seen in the Glenfinnan Group (Kocks et al. 2006). The Moine rocks within the structurally lower Moine Nappe are unmigmatized psammites of the Morar Group that locally preserve sedimentary structures and are less than 500 m thick once the effects of deformation have been removed, which is substantially thinner than the 5 km thick Morar Group to the south (Holdsworth 1989; Holdsworth et al. 1994). Basement inliers which have generally been correlated with the Lewisian are widely exposed within the Moine Nappe in fold cores and in the hangingwalls of thrusts. In contrast,

the Naver nappe is made up of strongly deformed and migmatised psammites and pelitic paragneisses. Concordant amphibolite sheets are interpreted as deformed and metamorphosed basic intrusions (Holdworth 1989; Friend et al. 2000; Kinny et al. 2003).

Also within the Moine Supergroup of north Sutherland is a unique fault-bounded unit made up of an association of amphibolites and siliceous grey gneisses called the Strathy Complex, shown on Figure 1-1. It outcrops within the Naver nappe and comprises of meta-igneous rocks and is different lithologically and chemically from the surrounding Moine and basement inliers (Moorhouse & Moorhouse 1983). The complex has been described as being bounded by brittle faults and to have been faulted into the Moine (Burns et al. 2004), although subsequent interpretations depicted the west margin of the complex as a major ductile thrust and suggest that it structurally underlies the Moine (Moorhouse & Moorhouse 1988). It is linked to a prominent magnetic anomaly that is terminated 9 km offshore, possibly by an ENE trending fault (Moorhouse & Moorhouse 1983; Burns et al. 2004). Both the amphibolites and the siliceous gneisses were interpreted to have been derived from a depleted mantle source, and are thought to be cogenetic. The complex seems to have recorded Caledonian deformation; it is unknown whether it records older events (Burns et al. 2004).

The Morar Group in the Fannichs, south west of the Assynt culmination, occurs as a single thrust sheet, known as the Achness Thrust Sheet which is over 70 km long, 20 km wide and 10 km thick (Krabbendam et al. 2008). This sheet is split into four formations, Altnaharra, Glascarnoch, Vaich Crom and Diebidale. The Altnaharra Formation crops out over 1500 km² and comprises of more than three kilometres thickness of psammite. Further southeast, in Wester-Ross there are large outcrops of basement at Scardroy and Glenelg. The possible relationship between the basement inliers and the Lewisian Gneisses is controversial, as there is little evidence seen within the inliers for the metamorphic events recorded within the Lewisian Gneisses. The inliers show evidence for Mesoproterozoic metamorphism (Sanders et al. 1984) and the associated literature will be discussed in depth in Chapter 3.

1.4 Age and Depositional Setting of the Moine Supergroup

1.4.1 Age of deposition

The Moine Supergroup is completely unfossiliferous; therefore its age is constrained mainly by isotopic data. Age ranges from detrital zircon data vary with the different nappes within the Supergroup. The oldest detrital zircon age range is from the Naver Nappe giving a range between 2940-926 Ma, with dominant clusters at 1650 Ma, 1400 and 1050 Ma (Friend et al. 2003). The Morar Group gives an age range between 2707 Ma and 947 Ma with clusters at 1650 and 1400 Ma (Friend et al. 2004; Kirkland et al. 2008). The Glenfinnan and Loch Eil Groups show a similar age range to the Morar Group between 1889-908 Ma, however they show a greater proportion of Grenville detritus (950-1100 Ma) than the Morar Group (Cawood et al. 2004). The Glenfinnan and Loch Eil Groups also record age clusters at 1500 and 1100 Ma, which is different from the clusters recorded by the Naver Nappe rocks, suggesting these nappes may have had different depositional sources (Cawood et al. 2004; Friend et al. 2003). There are very few Archaean or late Palaeoproterozoic grains indicating that the sedimentary precursors were not derived from the Hebridean terrane, thus it has been suggested by some authors (Emery 2005; Cawood et al. 2004) that it is unlikely that the Moine had the same source as the Torridon Group. The data suggest that Moine sedimentation must have commenced after 1100-1000 Ma and show an increase of Proterozoic detritus (Grenville) material up sequence, which is consistent with Moine deposition happening during the later stages of Grenville exhumation. There is a general south to north or west to east direction recorded in palaeocurrent features within the Moine Supergroup which is consistent with a Laurentian source for the Moine (Friend et al. 2003; Kinny et al. 1999, 2003; Cawood et al. 2004; Kirkland et al. 2008). The youngest published detrital zircon age found within the Morar Group is 980 ± 4 Ma (Cawood et al. 2007), a younger U-Pb (SIMS) age of 908 ± 8 Ma was obtained from a detrital zircon from the Achnaconeran Formation near Drumnadrochit (Emery 2005; Cutts et al. 2010), interpreted to be part of the Glenfinnan Group (Strachan et al. 1988).

A lower limit of Moine sedimentation is provided by ages of igneous intrusions and by an age from a zircon overgrowth from the Lower Psammite of the Morar Group of 842 ± 20 Ma, which has been interpreted to date magmatic crystallization of this overgrowth related to the Knoydartian orogeny (Kirkland et al. 2008). The igneous intrusions give

U-Pb zircon ages close to 870 Ma (Friend et al. 1997; Millar 1999; Rogers et al. 2001). Dyke or sill-like metabasic bodies are common within the Glenfinnan and Loch Eil Groups but rare within the Morar Group, except in west Sutherland (Holdsworth 1989; Millar 1999). The intrusions are usually foliated amphibolites with some metagabbros present locally, and display tholeiitic chemistry similar to modern mid-ocean ridge type basalts (Millar 1999; Dalziel & Soper 2001). Millar (1999) obtained a U-Pb zircon age of 873 ± 6 Ma from a metagabbro that intrudes the Glen Doe body of the West Highland Granitic Gneiss (WHGG) which is thought to represent its age of magmatic crystallization. It is assumed the rest of the suite is of a similar age and was intruded during crustal extension, as the tholeiitic-type basalt chemistry is consistent with intrusion through a thinned continental crust. The West Highland Granitic Gneiss (WHGG) is a series of separate bodies that outcrop near the boundary between the Glenfinnan and Loch Eil groups (Barr et al. 1985). The granitic gneiss is thought to have been formed by the anatexis of the Moine rocks at a deeper level (Barr et al. 1985). Friend et al. (1997) dated zircons from the granitic protolith of the Ardgour body and obtained an age of 873 ± 7 Ma; Rogers et al. (2001) achieved a similar age of 870 ± 30 Ma. This is similar to the age Millar (1999) determined, which is interpreted to be associated with crustal thinning. However if these intrusions were emplaced during rifting, then these ages do not need to give a younger limit to deposition as sedimentation could have gone on for longer. In contrast the Ardgour Gneiss is likely to have formed during crustal melting which suggests that ~ 870 Ma is an upper limit on sedimentation, but it is likely to have ceased prior to this (Friend et al. 1997, 2003; Millar 1999; Cawood et al. 2004, 2007; Kirkland et al. 2008). The Moine rocks were therefore probably derived partly from the erosion of the 1.1-1.0 Ga Grenville orogenic belt that formed during the assembly of the supercontinent Rodinia, as well as other basement sources located along the eastern margin of Laurentia (Cawood et al. 2007).

1.4.2 Setting of deposition

Sedimentary structures within the Moine, especially within the Glenfinnan Group and the north coast migmatites, are often deformed, obscured or obliterated completely due to high strain rates and metamorphic recrystallisation. The Morar Group provides the best area for study of the depositional processes that formed the Moine as sedimentary structures are often well preserved. Glendinning (1988) studied the sedimentary

structures within the Upper Morar Psammite, and found tabular and trough cross-bedding in co-sets up to 0.5 m thick. Coarse-grained to gravelly psammite locally displays cross-beds >0.5 m thick. Most palaeocurrents are unidirectional to the north or north east, but bipolar cross-stratification and dunes and ripples with mudstone drapes are present locally. The Upper Morar Psammite was interpreted as a tidal shallow marine deposit, although later work by Bonsor & Prave (2008) interpreted the Upper Morar Psammite as a retrogradational alluvial braidplain due to the lack of evidence for flow reversals and lack of variability within the trough crossbedded sections. A fluvial origin can also not be discounted on the grounds of the arkosic nature of the rocks when compared with other tidal shallow marine deposits. The Loch Eil Group was also interpreted as shallow marine on the grounds of unidirectional and bipolar cross-bedding and wave ripples (Strachan 1986). Krabbendam et al. (2008) studied the sedimentology of the Morar Group (Altnaharra Formation) by examining the low strain areas that show relatively undeformed sedimentary structures. The structures seen include isolated channels, nested channels, planar and trough cross-bedding, planar stratification and abundant soft-sediment deformation. The variety of grain sizes seen suggests high flow velocities in channels deep enough to form metre-scale bedforms, and the arrangement of these channels suggests a braided fluvial environment, in agreement with Bonsor & Prave (2008). Thus a correlation between the Torridonian and the Morar Group could be a possibility as it is well known that the Torridonian was deposited in a fluvial environment (e.g. Park et al. 1994). Krabbendam et al. (2008) suggest a correlation between the Applecross-Aultbea and Altnaharra formations.

The general consensus was that the Moine sedimentary basins were located within the Rodinia supercontinent, near to the junction between three major continental blocks, Laurentia, Baltica and Amazonia (Daziell & Soper, 2001). More recent work from Cawood et al. (2010) suggest that the Moine Supergroup was deposited along the margin of the Asgard Sea which opened when Baltica rotated away from East Greenland at ~1265 Ma, shown in Figure 1-3.

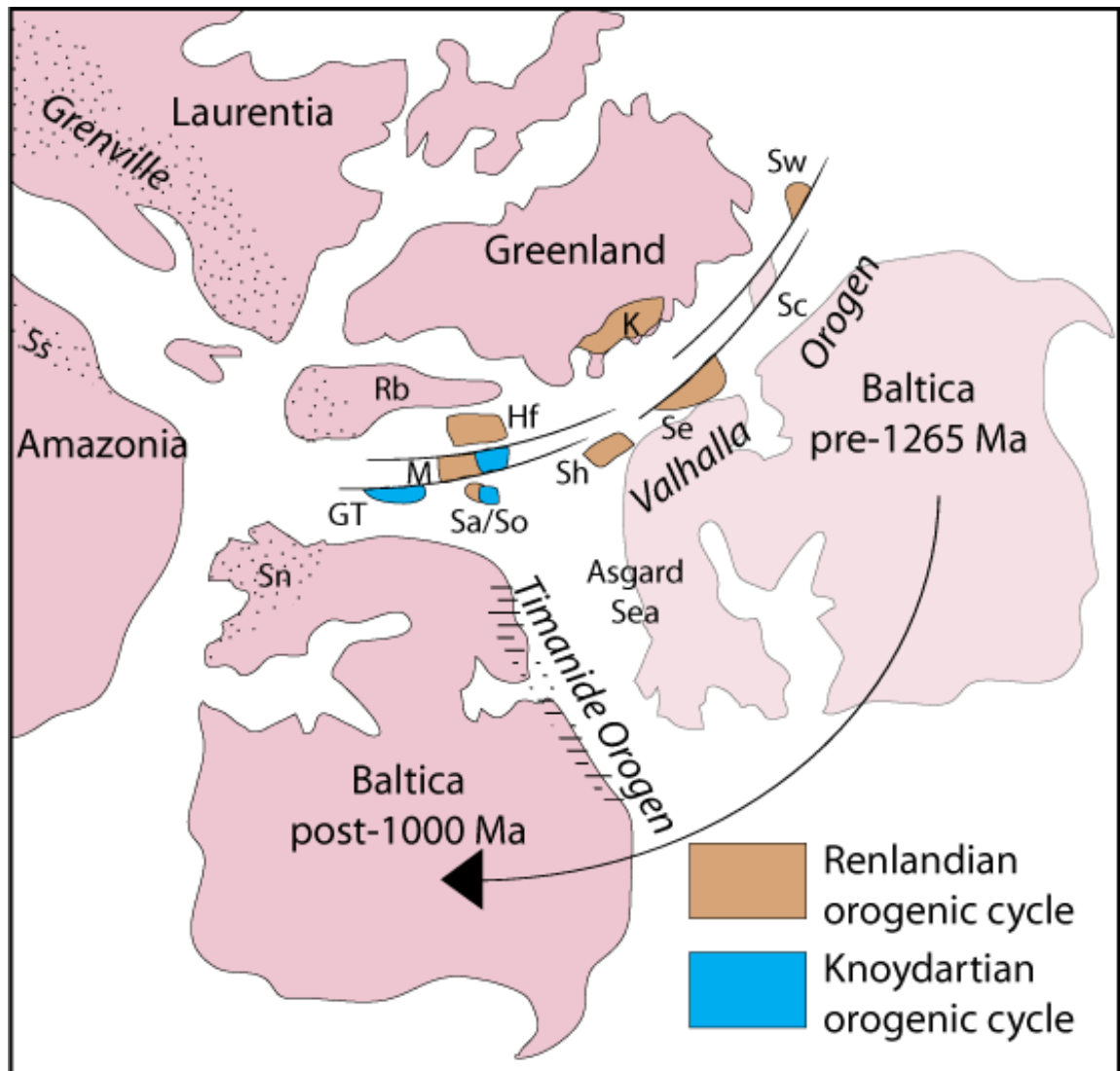


Figure 1-3, from Cawood et al. (2010) showing the Neoproterozoic reconstruction of eastern Laurentia, Baltica and northern Amazonia. Baltica is shown in pre and post 1265 Ma position. The rotation of Baltica opened the Asgard Sea. Brown blocks correlate to units associated with the Renlandian orogenic cycle and blue blocks relate to Knoydartian influenced units. The abbreviations are; GT – Grampian Terrane; M – Moine Supergroup; Hf – Hebridean Foreland; K – Krummedal succession; Rb – Rockall Bank; Sa/So – Sværholt and Sørøy successions; Sh – Shetland; Sn – Sveconorwegian orogeny; Ss – Sunsas orogen; Se – Eastern terrane of Svalbard; Sc – Central terrane of Svalbard; Sw – Western terrane of Svalbard.

1.5 Regional Metamorphism and fabrics

Metamorphic grade within much of the Moine Supergroup is hard to determine because of the scarcity of aluminium silicate minerals, it has therefore been defined in terms of minerals assemblages in calc-silicates (Johnstone et al. 1969; Winchester 1974; Tanner 1976; Powell et al. 1981). Metamorphic grade within the Moine Supergroup appears simple as it generally increases from greenschist facies in the west, through epidote-amphibolite facies into low amphibolite facies in the eastern part of the group, where

kyanite occasionally appears in pelites and calc-silicates show hornblende \pm plagioclase assemblages. This is shown in Figure 1-4, which shows the lower amphibolite area in the west (garnet and biotite zones) next to an area of higher grade migmatitic rocks assigned to the sillimanite zone. The sillimanite zone broadly correlates with the outcrop of the Glenfinnan Group and the boundary between this high grade belt and the Morar Group is coincident with the Sgurr Beag and Naver thrusts (Powell et al. 1981; Strachan & Holdsworth 1988).

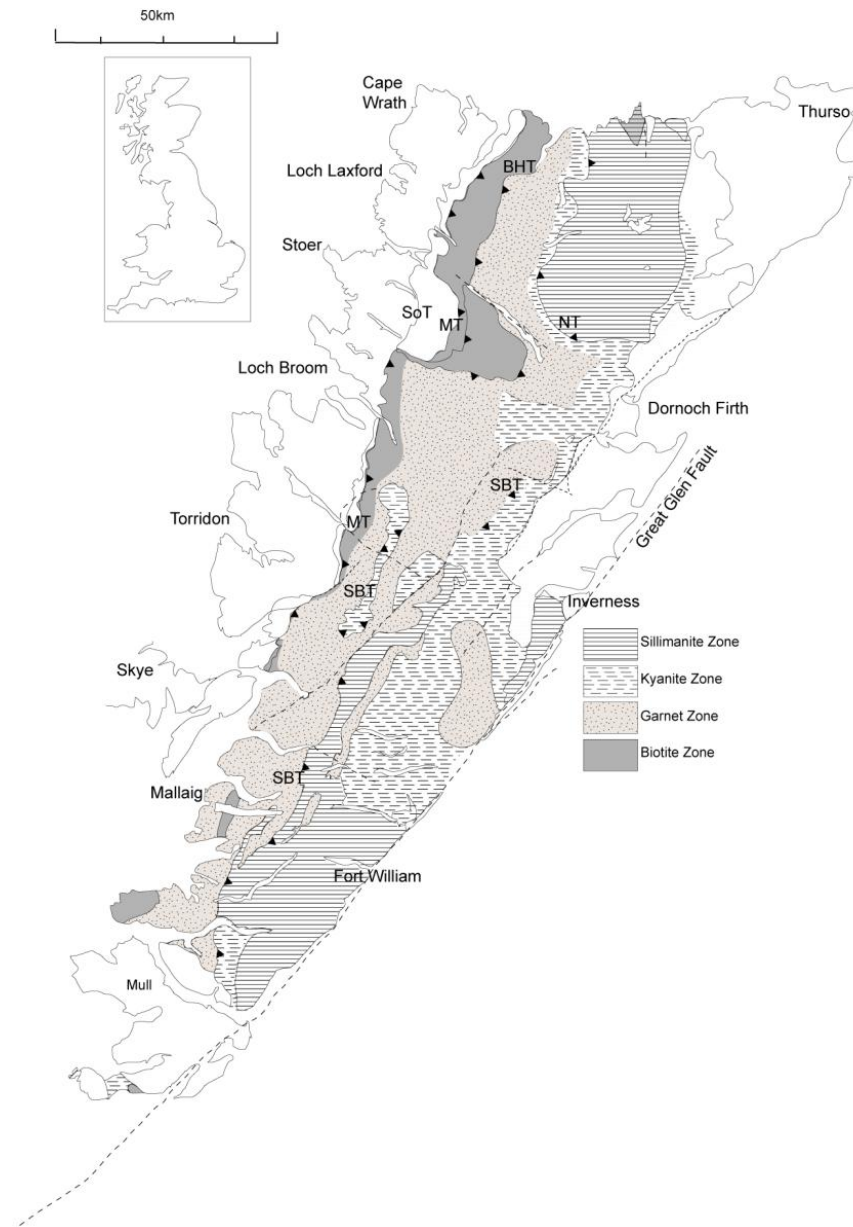


Figure 1-4, metamorphic zonal map of the Northern Highlands adapted from Winchester, 1974.

On the eastern side of the high grade Glenfinnan Group is the lower amphibolite facies Loch Eil Group; the high grade Glenfinnan Group rocks re-appear locally adjacent to the Great Glen Fault. This apparently simple appearance of metamorphic grade across the Moine is further complicated when considering that the Moine Supergroup has been metamorphosed and deformed more than once. Establishing which deformation event is responsible for peak metamorphism is difficult due to the poly-metamorphosed nature of these rocks. The metamorphism phases were each accompanied by folding and deformation, and were not recorded throughout the entire Moine Supergroup, making correlations more difficult (Strachan 1985), current interpretations are summarised in Table 1-1. This is the main focus of this project and will be discussed in more detail within the following chapters.

Table 1-1, deformation phases in the Northern Highland Terrane. Adapted from Kocks 2002 & Emery 2005. Abbreviations; AG G – Ardgour Granitic Gneiss; GDS – Glen Dessary Syenite; MT – Moine Thrust; SBT – Sgurr Beag Thrust.

	NORTH				SOUTH					Knoidartian	
	Moine Nappe	Naver Nappe			Ross-shire	Inverness-shire				Grampian	
		Western Belt	Central Belt	Eastern Belt		Moine Thrust Zone	Glenfinnan Group	Morar Group	Loch Eil Group	Scandian	
D1	Locally S0/S1 refolded by D2 (1, 2)	Locally S0/S1 refolded by D3 (6, 8, 9, 29)		Migmatites crenulated by D2 (11, 29)	Local S0/S1 commonly crenulated by D2 (24)					Migmatitic layering reworked by D2 (10, 14)	
	Associated with Grt grade metamorphism (1, 2)	Migmatisation dated at 467 ± 10 Ma (8)		High pressure melt (Grt in leucosome) (12)						Prograde garnet growth dated at 724 ± 6 Ma associated with amphibolite facies metamorphism (30)	
	Intrusion of alkaline Loch A'Mhoid Metagabbro suite during Late Neoproterozoic (29)			Interpreted to correspond to the 461 ± 13 Ma event observed in west (9)						U-Pb titanite age of 737 ± 5 Ma from calc-silicate pod dates prograde event (27)	
Post D1					Prograde Grt growth (24)						
D2	Tight to isoclinal F2 folds, sheath folds, ductile thrusts (1, 2, 3)		Composite S0/S1/S2 foliation, N-S trending L2 (10, 11)		Isoclinal and reclined F2-folds and NW trending L2 (14, 15)	Youngest part of the foreland propagating Scandian thrust system. MT movement dated at 431.1 ± 1.2 Ma finishing at 429.2 ± 0.5 Ma (28)	Structures that relate to D2 are traceable from flat belt to steep belt where they pre-date GDS dated at 447.9 ± 2.9 Ma (28)	Tight to isoclinal D2 folding during NW directed ductile thrusting, NW trending lineation (10, 20, 21, 22)	Recumbent sheath folds developed by low angle simple shear parallel to N-S trending lineation (16)		
	Late syn-D2 metagranites date fabric to c. 429 ± 11 Ma (7)		Tight to isoclinal F2 folding, sill-grade metamorphism and migmatisation at 461 ± 13 Ma (9)	Tight to isoclinal folds (13)	NW directed thrusting along the SBT (10)		Metamorphism reflected by a 455 ± 5 Ma U-Pb monazite age obtained from the AGG (25)	Amphibolite facies metamorphism dated by Rb-Sr WR age of 467 ± 20 Ma from Morar Pelite (26)	S-C fabrics indicating top to N sense of shear parallel to N-S trending lineation (10)		
	L2 lineation indicates changing transport direction from early NNW to late WNW (5)		L2 plunges ESE-SE (6)		S-C fabrics, NW trending L2, top to NW shear, sill grade metamorphism (12)				Amphibolite facies metamorphism at 470 ± 2 Ma at Fort Augustus (17)		
	Syn D2 Grt-St-grade metamorphism (2, 4, 6)										
Post D2	Brittle imbrication in the MT footwall - Assynt culmination		431 ± 10 Monazite age may reflect heating during renewed crustal thickening (9)								
	Brittle folds show ESE extension (2)										
D3		F3-cross folds (5)		Large scale open F3 folds, trending Ne-SW, no pervasive fabric associated (11, 13)		Widespread upright folding to the W of the Loch Quoich Line, formation of the NHSB. F3 folds trend N-S to NNE-SSW. Post dates the emplacement of the Glen Dessary Syenite. (10, 28)					
D4	Formation of Torrisdale Steep Belt (6, 29)			Kinking of F3 folds (11, 13)							

1 - Barr et al. 1986; 2 - Holdsworth 1989; 3 - Moorhouse & Moorhouse 1988; 4 - Strachan & Holdsworth 1988; 5 - Alsop et al. 1996; 6 - Burns 1994; 7 - Kinny et al. 2003; 8 - Friend et al. 2001; 9 - Kinny et al. 1999; 10 - Strachan & Evans 2006; 11 - McCourt 1980; 12 - Kocks 2002; 13 - Strachan 1988; 14 - Kelley & Powell 1985; 15 - Wilson & Shepherd 1979; 16 - Holdsworth & Roberts 1984; 17 - Rogers et al. 2001; 18 - Van Breeman et al. 1979; 19 - Roberts et al. 1984; 20 - May et al. 1993; 21 - Ramsay 1958; 22 - Powell 1966; 23 - Freeman et al. 1988; 24 - Vance et al. 1998; 25 - Aftalion & Van Breeman 1980; 26 - Brewer et al. 1979; 27 - Tanner & Evans 2003; Goodenough et al. 2011; 29 - Strachan et al. 2010; 30 - Cutts et al. 2010

1.6 Tectonic setting of the Moine deformation events

1.6.1 Neoproterozoic

The palaeotectonic setting of the Moine basins is uncertain, thus the setting of Neoproterozoic tectonothermal events is problematical. Relating the Knoydartian to a subduction zone is hard as the Moine is lacking in any proven Neoproterozoic calc-alkaline rocks or ophiolites, the only rocks in the region of this age with calc-alkaline characteristics are found in the Sørøy Succession in Norway (Cawood et al. 2010). The most recent analysis of the palaeomagnetic and geological constraints suggests that the western Scandinavian margin of Baltica faced the eastern Greenland margin of Laurentia in its right way orientation (Cawood & Pisarevsky, 2006). On this basis Scotland lies on a corner of the Laurentian margin and potentially in the vicinity of a RRR triple junction between Laurentian, Baltica and Amazonian. It has been suggested (e.g. Vance et al. 1998; Cawood et al. 2004; Daziel & Soper 2001) that the Moine rocks may have been deposited in an aborted zone of crustal extension and rifting that developed at the same time as east Gondwana separated from west Laurentia to form the Pacific Ocean, and that the Knoydartian deformation resulted from closure of this localized rift. However more recent studies by Cawood et al. (2010) suggest that the Knoydartian was part of the Valhalla Orogen, which was initiated by a 95° clockwise rotation of Baltica with respect to Laurentia at the end of the Mesoproterozoic. This opened the Asgard Sea and the Moine Supergroup was then deposited on the Laurentian side. Cawood et al. (2010) suspect there were at least two tectonothermal episodes, the Renlandian (980-910 Ma) and the Knoydartian. The Knoydartian orogeny is thought to include three episodes of crustal thickening at 830-820 Ma, 800-790 Ma and 730-710 Ma (Cawood et al. 2010), suggesting ~100 Ma of crustal thickening. Renlandian deformation has so far not been recorded within the Moine Supergroup, which could suggest it was located some distance away from the zone of deformation. The Renlandian orogenic event is thought to have resulted from the development of a subduction zone along the edge of the Laurentian margin shortly after the opening of the Asgard Sea. Evidence for a subduction zone at this time is provided from calc-alkaline igneous suites within the Norwegian Svaerholt succession (Kirkland et al. 2007) and Eastern Svalbard (Johansson et al. 2000). Cutts et al. (2009a) show from the Westing

Group in Shetland that the Renlandian orogenic event was characterised by PT conditions of ~650°C and 8-9 kbar at around 950-930 Ma.

1.6.2 Cambrian to Silurian

During the Cambrian and into the early Ordovician, the Moine Supergroup is thought to have been located on the Laurentian margin and was probably overlain by shelf sediments that pass SE into the upper Dalradian (e.g. Jones & Blake 2003). Sedimentation was terminated in the early to Mid-Ordovician by the Grampian orogenic event. One possible model for the Grampian orogenic event is the Laurentian margin colliding with an intra oceanic subduction zone and an island arc causing an ophiolite to over thrust the Laurentian margin (e.g. Lambert & McKerrow 1976; Soper et al. 1999). The Grampian orogeny is also thought to have caused nappe stacking and regional deformation of the Moine Supergroup and the Dalradian Supergroup (Harris et al. 1994). Remnants of this ophiolite may be represented by the ophiolitic rocks found on Unst in Shetland and intermittently along the Highland Boundary Fault. The later Scandian event represents the final closure of Laurentia and Baltica and has only been interpreted to have been recorded within the Northern Highlands, suggesting that the Northern Highland and Grampian terranes were not adjacent at this time (Dewey & Strachan 2003). This will be discussed in more detail in Chapter 5.

1.7 Timings of faulting and thrusting

Many of the faults within the Moine Supergroup have been described as ‘slides’ in the older literature, the term describes a tectonic break of uncertain geometry (Strachan et al. 2010). These breaks must have occurred during or before regional metamorphism as there is often no evidence of brittle textures or cataclastic rocks (Tanner 1970).

1.7.1 The Moine Thrust

The Moine Thrust is interpreted as the youngest of the Scandian structures within the Northern Highlands and forms the NW margin to the Caledonian orogenic belt. The Moine Thrust Zone, close to Loch Eriboll, is one of the most intensely studied areas of the Northern Highlands (e.g. Peach et al. 1907; Soper & Wilkinson 1975; McClay & Coward 1981), with the whole of Assynt now making up Scotland’s first European Geopark. The Moine Thrust Zone is over 190 km in length (Figure 1-1) and varies from

0-11 km in width. It is exposed between Loch Eriboll in western Sutherland and the Sound of Sleat on Skye in the south west. The thrust separates the over-thrust Moine Supergroup from the Caledonian Foreland; within the thrust zone are slices of Lewisian, Torridonian, Cambrian and Ordovician units that are separated by sharp, brittle thrusts. The thrust zone is bound by the Sole Thrust to the west and the Moine Thrust to the east (Figure 1-1). Above this is a belt of mylonites, made up of recrystallised Moine metasediments, Lewisian gneisses and Cambrian sediments, which show signs of intense deformation (Holdsworth et al. 2007). As the fabric within this mylonitic belt is parallel to the regional lineation within the Moine Nappe, which is interpreted to be Scandian in age, it is thought the Moine Thrust is also a Scandian feature. Geochronology from this area is predominantly Rb-Sr, K-Ar or ^{39}Ar - ^{40}Ar on feldspars and muscovites and has resulted in ages between 408-449 Ma (Kelley 1988; Dallmeyer et al. 2001; Freeman et al. 1998). These ages are likely to be cooling ages as Rb-Sr and ^{39}Ar - ^{40}Ar have blocking temperatures in the range of 300-500°C for muscovites and feldspars. U-Pb zircon ages of 431.1 ± 1.2 Ma and 429.2 ± 0.5 Ma were obtained from the Loch Borrolan early and late suites which provide syn- and post- movement constraints on the movement of the Moine Thrust (Goodenough et al. 2011). As displacement on the thrust is thought to be in the region of 50-100km (Butler & Coward 1984) it is likely that the ages from Loch Borrolan Complex correspond to the termination of thrusting. This will be discussed in more depth in Chapter 5.

1.7.2 Sgurr Beag Thrust

The Sgurr Beag Thrust was first referred to as the Sgurr Beag slide (Tanner 1970) as the nature of the structure was unclear, as it appears essentially concordant and is syn-metamorphic. It was identified by a disrupted sheet of 'Lewisian' which marks a separation of two different lithological successions (the Morar and Glenfinnan Groups), as seen at Glen Shiel and Kinlochourn, (Tanner 1970; Rathbone & Harris 1979). However where 'Lewisian' is not present the slide is difficult to identify and recognition of it depends on distinguishing between the Morar and Glenfinnan Groups, assuming that the slide should separate these units everywhere. Later it became acknowledged that the Sgurr Beag Slide and the other 'slides' that had been recognised within the Moine Supergroup represent major, mid-crustal ductile thrusts (Kelley & Powell 1985). The Sgurr Beag Thrust has a complex refolded geometry due to having been refolded

(Tanner 1970; Johnson et al. 1979), in contrast to the thrusts of the northern Moines (Naver and Swordly) which are fairly simple curved ductile thrust zones (Soper & Barber, 1982). Tanner (1970) and Tanner et al. (1970) concluded that the thrust was a regional structure and could be traced for at least 25 km, dividing the Moine Supergroup into two distinct nappes and suggested that movement occurred before folding related to D_3 and during folding related to D_2 , prior to the peak of regional metamorphism. Powell (1974) and Powell et al. (1981) also concluded that thrusting occurred during D_2 which they suggest is related to the Caledonian orogeny and to peak metamorphism. They also suggested that the thrust was coeval with the formation of mylonites within the Moine Thrust zone, reinforcing the relationship to the Caledonian orogeny. This was supported by the U-Pb zircon age of ~555 Ma from the Carn Chuinneag granite and a 750 Ma age (Rb-Sr muscovite) from a pegmatite, both of which have later shearing overprinting related to the Sgurr Beag Thrust (Pidgeon & Johnson, 1974; Long & Lambert, 1963; Wilson, 1975).

More recent work from Tanner & Evans (2003) disputes Caledonian-aged movement along the Sgurr Beag Thrust. A U-Pb titanite age from a calc-silicate pod within the Morar Pelite close to the Sgurr Beag Thrust gives an age of 737 ± 5 Ma, which was suggested to date the main regional metamorphic event within the Morar Group (D_2), thus suggesting that this is also when the main movement on the Sgurr Beag Thrust occurred. A consequence of this theory is that it suggests that the Morar and Glenfinnan Groups share a similar metamorphic history. One aim of this study is to establish whether there is a shared aspect and, if so, how much is shared between the two groups.

1.7.3 The Great Glen Fault

Movement on the Great Glen Fault is thought to have occurred during the very late stages of collision between Laurentia, Baltica and Avalonia, after the main phase of Scandian deformation (Dewey & Strachan, 2003). The fault is made up of a 3 km wide belt of fracturing of Moine and Dalradian rocks (Stewart et al. 2000; Strachan et al. 2010). The Great Glen Fault has been linked to the Walls Boundary Fault on Shetland (Flinn, 1961; McBride, 1994) and to the Loch Gruinart-Leannan Fault in Islay and Ireland (Alsop, 1992). Dewey & Strachan (2003) suggest that there was approximately 500-700 km of sinistral movement along the Great Glen Fault during the Silurian to early Devonian. This is due to the lack of evidence within the Grampian terrane for

regionally significant Silurian metamorphism and ductile deformation, thus suggesting that during the Silurian it was far removed from the location of the Scandian collision between Baltica and the sector of the Laurentian margin that contained the Northern Highland terrane (Coward 1990; Dallmeyer et al. 2001; Dewey & Strachan 2003; Kinny et al. 2003). This would also explain the lack of Grampian metamorphic ages found within the Northern Highland terrane. However, Thirlwall (1989) argued that there was limited (~100 km) of movement along the Great Glen Fault. The reason for this is from geochemical data from plutons and volcanic rocks within the Grampians and the Northern Highlands which have distinct high Sr and Ba and depleted Nb. These igneous rocks lie on a northerly trend across the Great Glen Fault and have an eastern boundary to their unique chemistry. Thirlwall (1989) demonstrated using Nd, Sr and Pb isotopes that these rocks were sourced from a part of mantle that had been separate from the rest of the mantle for approximately 1000 Ma. As these high Sr rocks are present on both sides of the Great Glen Fault, it was suggested that there cannot have been 100s of kilometres of movement on the fault. Another view comes from Briden et al. (1984), who suggested that the displacement along the Great Glen is unlikely to have been more than 200-300 km; this is in contrast to palaeomagnetic data from Middle to Upper Devonian rocks from North America and Europe which indicate 2000 km of sinistral displacement (Van der Voo & Scotese 1981).

1.8 Orogenic activity within the Moine Supergroup

The orogenic activity will be covered in more detail in Chapter 3-7. The metamorphic events that have affected the Moine Supergroup are known as the Knoydartian, the Grampian and the Scandian. There is an argument from some authors (e.g. Barr et al. 1985; Vance et al. 1998) that there was also an earlier orogenic event at ~870 Ma related to the West Highland Granite Gneiss, the suggestion is that the WHGG is syn-orogenic in origin related to D₁ folding of the Moine. This is in contrast to Soper & Harris (1997), Millar (1999) and Dalziel & Soper (2001) who propose that the WHGG was formed during crustal extension of the Moine sedimentary basin and emplacement of the metabasic suite. The Knoydartian event is thought to be one of the earliest metamorphic events to have affected the Moine Supergroup and is thought to have been recorded as D₂ isoclinal interfolding of basement inliers and the overlying Moine, as

seen between Glenelg and the Morar Group in Inverness-shire. The Knoydartian has been dated by Sm-Nd on post-D₁ garnets from the Morar Group, which give ages between 820-790 Ma (Vance et al. 1998). This is thought to date prograde metamorphism due to crustal thickening (Vance et al. 1998). There are also U-Pb titanite and zircon ages from pegmatites ranging between 827 Ma and 737 Ma (Tanner & Evans, 2003; Rogers et al. 1998) which suggests that there may have been more than one phase of Neoproterozoic metamorphism. Rogers et al. (1998) suggest that the Knoydartian pegmatite generation was due to localised high temperature shearing and metamorphism within the Moine sequence during crustal thickening.

The Grampian and Scandian events make up the Caledonian orogeny. The Grampian event is thought to have occurred between 480-465 Ma and the Scandian event at 435-425 Ma (e.g. Kinny et al. 2003; Dewey & Strachan 2003). The Grampian event is best developed within the Dalradian rocks of the Grampian Terrane. There is no published isotopic evidence for Grampian deformation within the Morar Group, apart from a Rb-Sr whole rock isochron of 467 ± 20 Ma (Brewer et al. 1979). Dallmeyer et al. (2001) suggest this could be due to a western “front” to Grampian deformation, which could perhaps be buried underneath younger thrusts, for example the Naver or Swordly thrusts. Grampian deformation is recorded within the Naver Nappe and has been dated using U-Pb on zircons, giving ages of 467 ± 10 Ma and 461 ± 13 Ma (Kinny et al. 1999); it is also seen and has been dated close to the Great Glen Fault in Inverness-shire (Roberts et al. 2001; Cutts et al. 2010).

Scandian deformation and metamorphism is interpreted as being widespread within the Morar Group, and is thought to be represented by the D₂ fabrics (Barr et al. 1986; Holdsworth 1989; Moorhouse & Moorhouse 1988). D₃ is represented by widespread, minor tight to isoclinal folds and a penetrative schistosity. Displacements along the Swordly, Naver, Ben Hope and perhaps the Sgurr Beag thrusts are also thought to be related to the Scandian event (Strachan & Holdsworth 1988). The Scandian deformation is thought to be responsible for the major folds within the Morar Group, which often have basement inliers within their cores, and for the basement inliers which are present as thin allochthonous slices along the Naver, Swordly and Ben Hope thrusts (Holdsworth 1989). D₄ was associated with extensive upright folding along north-south axes; this is mostly likely associated with the formation of Northern Highland Steep

Belt which is thought to be Scandian in age (Roberts et al. 1984; Strachan & Evans 2008).

1.9 The Grampian Terrane

The Dalradian Supergroup outcrops within the Grampian Terrane of mainland Scotland and is bounded to the north by the Great Glen Fault and to the south by the Highland Boundary Fault. Dalradian rocks also occur in Jura, Islay, Ireland and Shetland (e.g. Harris et al. 1994; Strachan et al. 2002). The Supergroup was deposited during the mid- to late Neoproterozoic, during the post-Pan African rifting of eastern Rodinia and the formation of the Iapetus Ocean (Cawood et al. 2001; 2003; 2004). The rift and rift-drift events are recorded within the Dalradian which comprises a progradational passive margin sedimentary sequence along the Laurentian margin (Anderton 1985; Glover & McKie 1996). It is dominated by marine meta-sandstones, siltstones, mudstones and carbonate rocks intruded by granites and volcanics of Precambrian and Lower Palaeozoic age (Halliday et al. 1989). They reveal a history of repeated uplift, rifting and complex internal basin architecture.

The Dalradian Supergroup is separated into the Grampian, Appin, Argyll and Southern Highland Groups (Harris et al. 1978, 1994), (Figure 1-5). Underlying the Dalradian is the Glen Banchor and Dava succession which makes up the oldest group within the Grampian Terrane. They comprise mainly gneissose to locally migmatitic psammites and semi-pelites. They are intensely recrystallised and do not preserve sedimentary structures; they appear to have been more intensely deformed than the overlying Grampian Group rocks (Highton et al. 1999). The contact between the Grampian Group and the Glen Banchor and Dava succession is marked by the Grampian Shear Zone and its nature is contentious. Smith & Robertson (1999) believe that the contact is a sheared unconformity, and that the Glen Banchor and Dava successions are equivalent to the Moine Supergroup. This suggested that the rocks were migmatised at ~840 Ma and the migmatisation event was related to the Knoydartian and was overprinted by Caledonian metamorphism. In this scenario, 840 Ma would give a maximum age of deposition of the Dalradian. An alternative view held by Highton et al. (1999) and Phillips et al. (1999) is that the Appin, Grampian and Glen Banchor and Dava successions all shared the same Knoydartian (~840 Ma) deformation, and then were overprinted by the

Caledonian orogeny. In this case the onset of sedimentation of the Dalradian could be older than ~800 Ma. However, there is no evidence for Knoydartian metamorphism within the undisputed Dalradian rocks and there is evidence of progressive overstep of younger lithologies onto older ones (Robertson & Smith 1999). Geochronology from this area includes U-Pb analyses from pegmatites within the Grampian Shear Zone that give ages of 808 ± 11 Ma, 806 ± 3 Ma and 804 ± 13 Ma (Noble et al. 1996); and U-Pb zircon analysis from a kyanite-bearing migmatite of 840 ± 11 Ma (Highton et al. 1999). These ages appear to support the theory that the Glen Banchor and Dava successions were deformed by the Knoydartian orogeny.

1.9.1 Tectonostratigraphy of the Dalradian

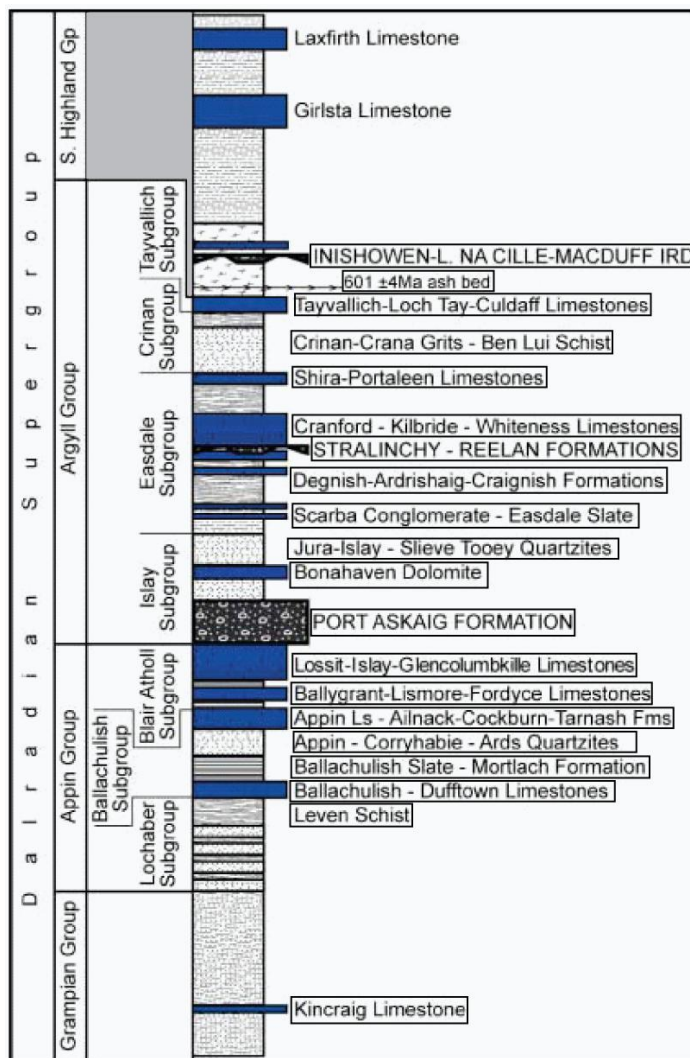


Figure 1-5, from Prave et al. (2009), extremely simplified composite stratigraphic column focusing on the main carbonate rock units of the Dalradian Supergroup in the British–Irish isles. (Note that the glacial rocks are shown in upper case in the stratigraphic column.)

The Grampian Group crops out in the north of the Grampian Terrane and is approximately 8 km thick. The lower part of the group is dominated by psammites and the upper part consists of semipelites and psammites. In low strain areas sedimentary structures are preserved which suggest that the group was deposited in a sand-dominated deep water and shelf environment (Hickman 1975; Banks & Winchester 2004; Banks 2007). The contact between the Grampian and Appin groups is transitional and the Appin Group consists of sandstones, limestones, shales and quartzites and represents shelf deepening (Johnson 1991). Above the Appin Group is the Argyll Group, which records further shelf deepening; at the base of this group is the Port Askaig Tillite, which can be traced into western Ireland. The Port Askaig Tillite is the oldest of the recognised glacial deposits within the Dalradian, associated with the Sturtian glaciation; the other glacial layer within the Highlands of SE Scotland is comprised of the Loch na Cille and MacDuff Boulder bed within the Southern Highland Group (Prave et al. 2009). Also within the Argyll Group is the Tayvallich subgroup which includes the Tayvallich Volcanic formation made up of lavas and tuff and has MORB-type chemistry (Dempster et al. 2002; Halliday et al. 1981). Above the Argyll Group is the Southern Highland Group which is made up of deep water turbidites (Johnson 1991).

1.9.2 Dalradian sedimentation

The Dalradian Supergroup was likely deposited in half grabens due to the rifting of the Laurentian passive margin to form the Iapetus Ocean (Anderton 1985). The age of the Dalradian is given by sparse fossils and isotopic analysis, however, the Supergroup must span 200 Ma of depositional history (Jones & Blake 2003). Deposition is thought to have occurred between 730-470 Ma and the sediments have an apparent thickness of 25 km; however it is unlikely to represent one continuous succession. Only two depositional ages are known for the Dalradian; U-Pb ages of 595 ± 4 Ma for a feldspar-rich dyke (Halliday et al. 1989) and 601 ± 4 Ma for an ash bed (Dempster et al., 2002) both from the Tayvallich Volcanic Formation within the Southern Highland Group. Detrital zircons within the supergroup range from 900-3200 Ma in age, with peaks at around 1800 Ma, 1750-1700 Ma, 1650-1600 Ma, 1550-1500 Ma and 1100-900 Ma (Cawood et al. 2003). The zircon ages are consistent with a Laurentian provenance and

are similar to those obtained from the Moine Supergroup and the Torridonian Supergroup. The youngest detrital zircon is 900 ± 17 Ma and the $^{87}\text{Sr}/^{86}\text{Sr}$ whole rock isotope data from the lowermost meta-carbonate rocks of the Grampian Group are consistent with a global late-Neoproterozoic strontium sea-water signature younger than 800 Ma, perhaps as young as 670 Ma (Thomas et al. 2004). This is in contrast to recent $\delta^{13}\text{C}$ data by Prave et al. (2009), which show possible correlations between the Ballachulish limestone and the 800 Ma Bitter Springs anomaly, seen in the worldwide $\delta^{13}\text{C}$ curve. Another correlation that can be used to constrain age of deposition is seen between the 635 Ma pre-Marinoan Trezona anomaly and the Easdale and Bonahaven glacial deposits in Ireland. Also the anomaly recorded within the Girdsta limestone of the Southern Highland Group (Shetland) correlates with the Shuram-Wonoka anomaly which is between 600-551 Ma (Figure 1-5) (Prave 1999). The youngest preserved glacial interval is within the Southern Highland Group and consists of boulder beds found in Donegal, Ireland and the MacDuff Boulder Beds in south-west and north-east Scotland which can be reasonably linked with the 582 Ma Gaskiers glaciation in Newfoundland (Bowring et al. 2007; Prave et al. 2009). Within the MacDuff slate are acritarch fossils which are thought to be Ordovician in age (Molyneux 1998), which is younger than the age suggested from the MacDuff Boulder Beds. Thus the timing of onset of sedimentation within the Dalradian is still contentious.

Robust biostratigraphic information is only found within the upper parts of the Southern Highland Group within the Leny Limestone which has Lower Cambrian *Pagetia* trilobites indicating an approximate age of 515 Ma (Pringle 1940; Tanner 1995). A lower limit of sedimentation is set by the Grampian orogeny between 470-460 Ma.

1.9.3 Regional metamorphism and associated structures

Ordovician deformation and metamorphism of the Dalradian is thought to have resulted from the collision between Laurentia and an intra-oceanic subduction zone and magmatic arc complex (Lambert & McKerrow 1976; Dewey & Ryan 1980). On a large scale the structures are simple tight to isoclinal folds that trend NE-SW across the region and can be traced for hundreds of kilometres along strike. At least four major phases of regional significant deformation are recognised. D_1 produced a set of upright folds which resulted from initial crustal shortening, the shape of these folds was controlled by the pre-deformation shape of the Dalradian rift basins (Robertson & Smith

1999). Continued crustal thickening lead to the deep burial and metamorphism of the Dalradian and the formation of nappe and slide structures associated with D₂. The D₂ folds were generally recumbent and isoclinal in style. The Tay Nappe was formed at this time and faces towards the south-east, in contrast to the other major folds associated with D₂ (Jones & Blake 2003). A set of NE-SW trending open folds formed during D₃ and D₄, probably from continued crustal shortening that led to the steepening of D₂ folds and produced steep belts. The fabrics associated with D₁ and D₂ are preserved throughout the whole Dalradian, D₃ and D₄ fabrics are not preserved throughout the region but are still widespread (Dempster 1985; Jones & Blake 2003).

The Dalradian Supergroup contains the type outcrops for Barrovian and Buchan metamorphism, and the pelites show an increase in grade from chlorite zone pelites in the south-west to sillimanite zone in the north-east, Figure 1-6. Metamorphism is thought to have occurred during burial associated with D₂ (Johnson 1991; Jones & Blake 2003); however there appears to be a lack of correlation between temperature and pressure suggesting that burial was not the sole cause of metamorphism, this is seen clearly in the Buchan region. The Buchan and Barrovian metamorphic events coeval but have been subjected to different pressures. Dempster (1985) and Dempster et al. (1995) obtained maximum K-Ar muscovite and biotite ages of 484 ± 10 Ma and 474 ± 9 Ma respectively. Rb-Sr ages from muscovite and biotite of 482 ± 5 Ma and 468 ± 5 Ma complement these ages (Evans and Soper 1997).

The Aberdeenshire Gabbros have yielded ages that are predominantly in the range of 465-475 Ma (Brown et al. 1965; Bell 1968; Pankhurst 1970; van Breeman & Boyde 1972; Dempster et al. 2002; Fettes 1970; Friedrich et al. 1999; Kneller & Aftalion 1987; Oliver et al. 2000; Pankhurst 1974) with a few younger ages ~445 Ma which are Rb-Sr or K-Ar ages so represent cooling and uplift; and a few much older ages from inherited zircons of ~850 Ma which are similar in age to the older intrusions in the Northern Highland terrane. Sm-Nd garnet geochronology has been undertaken on samples from the Argyll Group and give ages of 467 ± 2.5 Ma and 472 ± 2 Ma which are interpreted to represent garnet grade and kyanite grade peak metamorphism, respectively (Oliver et al. 2000). Almost all of the ages reflect the Grampian Orogeny.

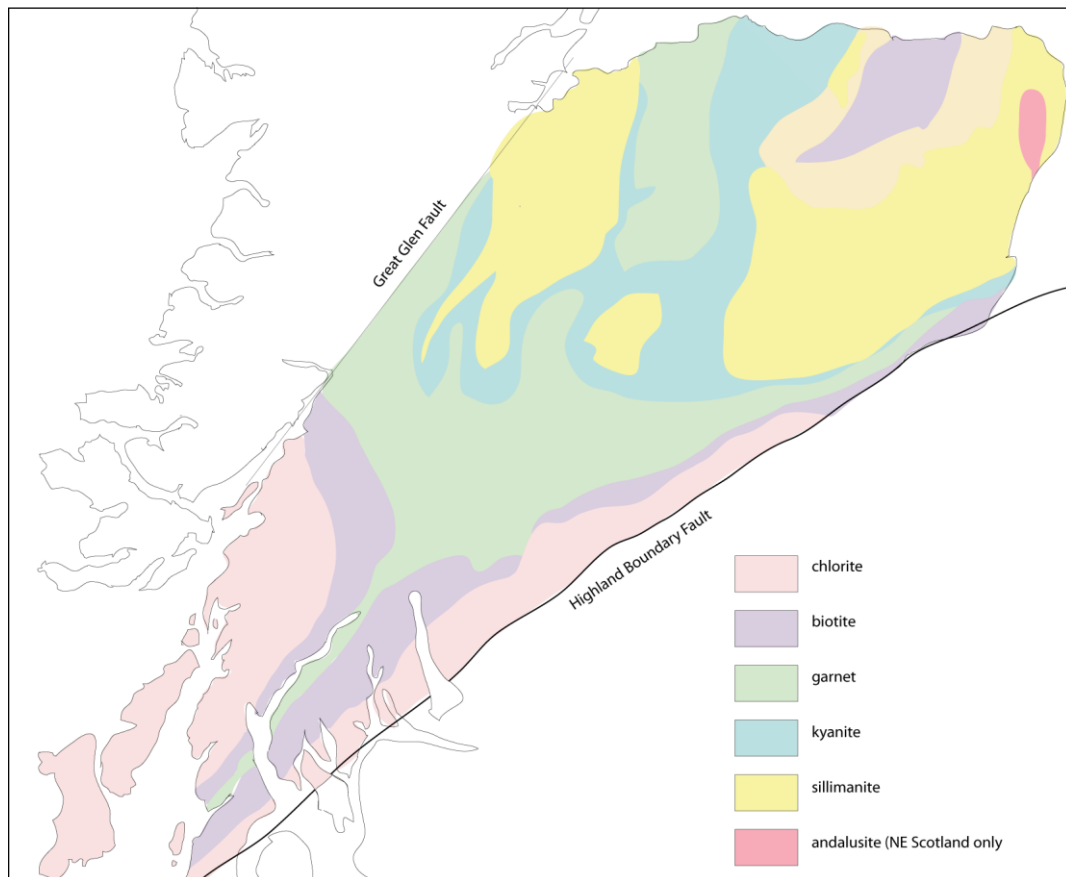


Figure 1-6, from Jones & Blake (2003) showing the metamorphic zones of the Grampian Highlands. All zones are shown apart from the staurolite zone which is a thin band between the garnet and kyanite zones.

1.10 The metasedimentary rocks of Shetland

Some metasedimentary rocks in Shetland are similar to the Moine Supergroup, but a precise correlation is uncertain (Flinn 1988; Strachan & Holdsworth 1988). Moine-like rocks are found on both sides of the Walls Boundary Fault; on the east of the fault, the Moine rocks make up most of Yell and part of Lunna Ness. They are known as the Yell Sound Group (Flinn 2007) and are dominated by psammites with basement inliers. The sequence is disrupted by the Nesting Fault and bound to the east by the Hascosay Slide.

West of the Walls Boundary Fault the Moine rocks are found close to North Roe and consist of psammitic metasediments with pelites and quartzites which are interleaved with tectonically banded slices of basement gneisses, these gneisses are referred to as the Eastern Gneisses (Flinn 1988), shown in Figure 1-7. The psammites are bound to the west by basement gneisses which Flinn (1988) referred to as the Western Gneisses. The Moine-like psammites are bound to the east by the Virdibreck Shear Zone; on the

other side lie rocks that have been correlated with the Dalradian Supergroup (Flinn 1988). Together the psammites, Lewisian inliers and garnet mica schist comprise the generally east-dipping, NNE-striking Sand Voe Schuppen Zone, which is bound to the west by the Wester Keolka shear, isolated occurrences of which form Hillswick Ness and two other isolated and tectonically bounded slivers lying immediately to the west of the Walls Boundary Fault (Flinn 1988). Dalradian equivalent units make up much of Mainland and Whalsey. Shetland will be discussed in detail in Chapter 6

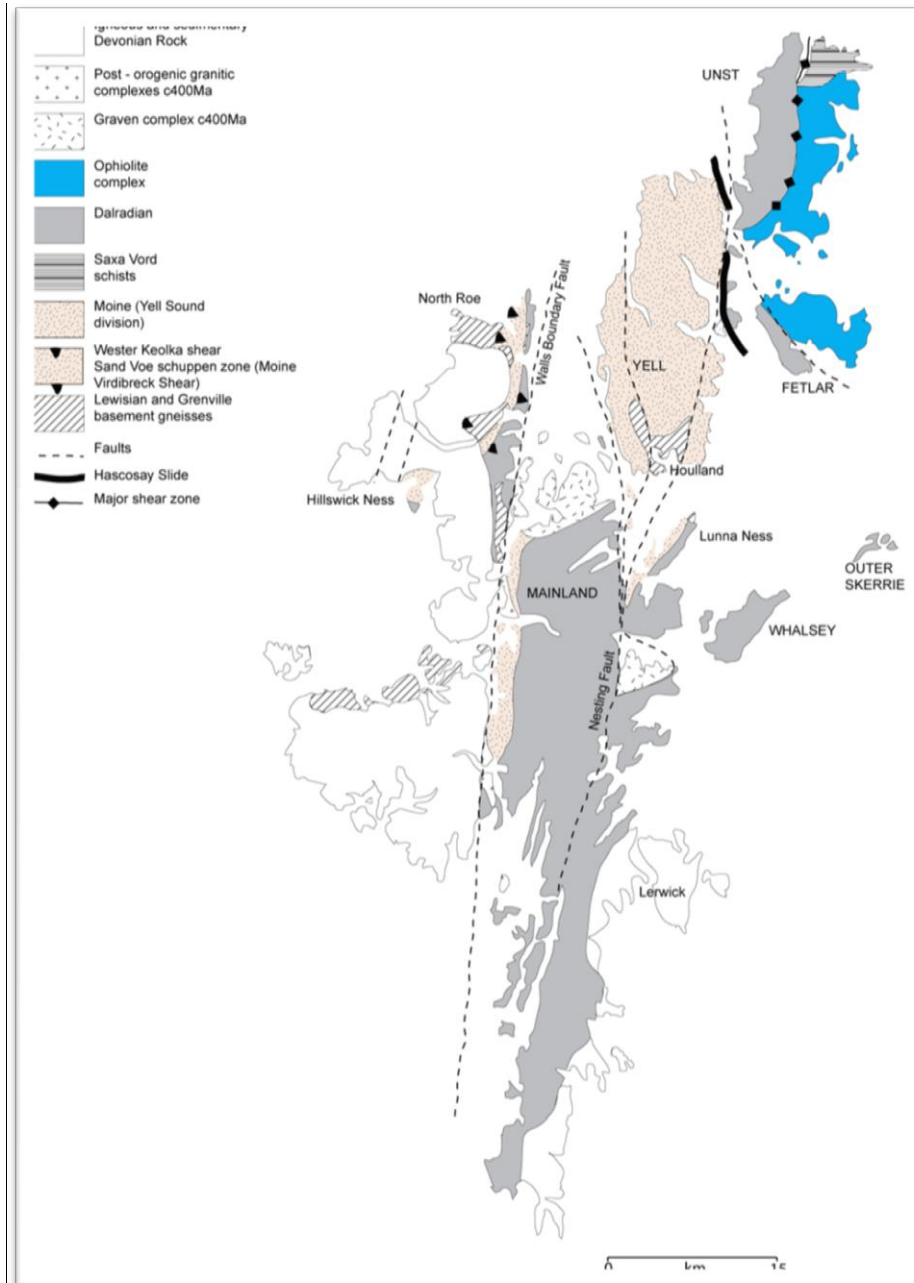


Figure 1-7, simplified geological map of Shetland showing the main units, faults and thrusts, adapted from Flinn (1988).

1.11 Correlations between the Scottish Highlands and Scandinavia, East Greenland and Irish Caledonides

1.11.1 East Greenland

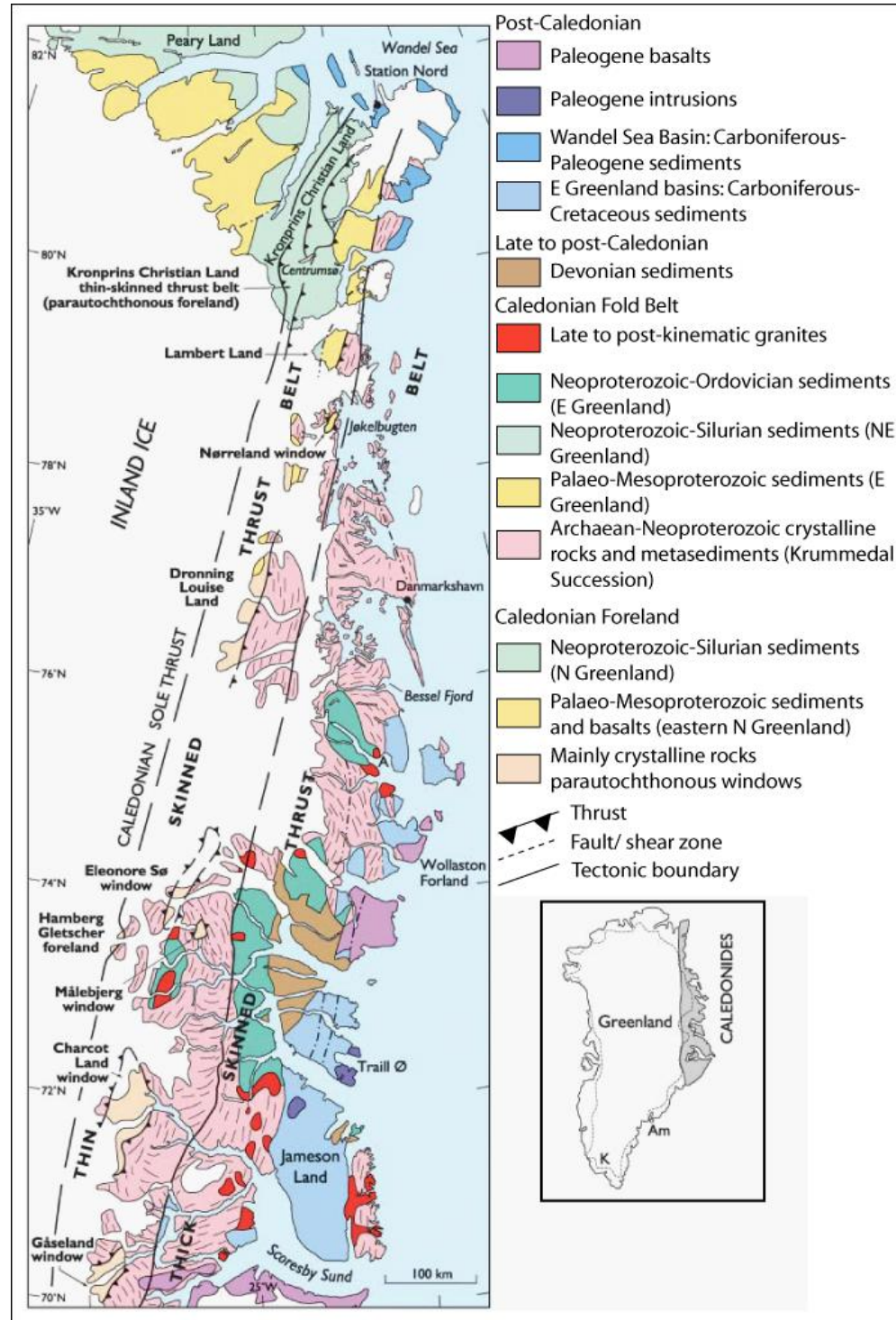


Figure 1-8, simplified geological map of the East Greenland Caledonides from Higgins et al. (2004). The western limit of deformation is largely concealed by Inland Ice. Abbreviations A – Ardencaple Fjord; Am – Ammassalik; K – Ketilidian orogen.

The Caledonides of East Greenland are approximately 1300 km in length and share a Neoproterozoic to lower Paleozoic geological history with the Scottish Highlands. The areas of East Greenland that can be correlated with the Laurentian foreland succession of the north-west Scottish Highlands consist of Kronprins Christian Land in eastern North Greenland and parautochthonous successions that are exposed in tectonic windows in the East Greenland Caledonides (Leslie et al. 2008), Figure 1-8. Areas which may be correlated to the Northern Highland and Grampian terranes include parts of Kronprins Christian Land, the Franz Joseph allochthon and Niggli Spids and Hagar Bjerg thrust sheets. The comparable sequence of Moine meta-sediments in East Greenland are represented by the Krummedal succession (Higgins, 1988), widely distributed in both the Niggli Spids and the Hagar Bjerg thrust sheets. Deposition of the Krummedal succession occurred after 1050 Ma, and appears to have shared a similar provenance with the Moine Supergroup (Friend et al. 2003). Archaean and mid-Palaeoproterozoic detrital zircons are rare, indicating that the Grenville belt was likely to have been a significant source (Leslie et al. 2008; Watt et al. 2000). This indicates that late- Mesoproterozoic sedimentary basins extended over a very large area ($>1000 \text{ km}^2$), and the Krummedal succession may represent a northward continuation of marine dispersal of parts of the Moine Supergroup (Leslie et al. 2008). Both the Moine Supergroup and the Krummedal succession record evidence for high pressure and high temperature metamorphism. The Krummedal succession was affected by one high grade metamorphic event during the Neoproterozoic which culminated in the generation of large volumes of S-type granites at 910-930 Ma (Leslie & Nutman; 2003; Leslie et al. 2008). This is of significance to this study as it shows that the Krummedal succession was metamorphosed earlier than at least the Glenfinnan and Loch Eil groups (Cawood et al. 2010).

The Dalradian Supergroup is of a similar age to the Eleonore Bay Supergroup, the overlying Tillite Group and the Kong Oscar Fjord Group within the Franz Joseph Allochthon (Higgins & Phillips 1979; Higgins et al. 2004) (Figure 1-8). Like the Dalradian of Scotland, these units are not as well constrained chronologically as the corresponding units in the Scottish mainland, but are estimated to have been deposited between 940-460 Ma (Friedrich et al. 1999; S nderholm et al. 2008). Unlike the Dalradian they show no evidence of contemporaneous volcanic activity (Leslie et al. 2008). Leslie et al. (2008) describe the relationship between the Eleonore Bay

Supergroup and the underlying Krummedal as cover and basement and suggest a similar relationship to the Dalradian and the Dava and Glen Banchor succession rocks. As both groups seem to have been deposited during rifting, a general correlation could be proposed. Figure 1-9 shows the inferred Neoproterozoic disposition of Baltic, East Greenland, Shetland and Scotland.

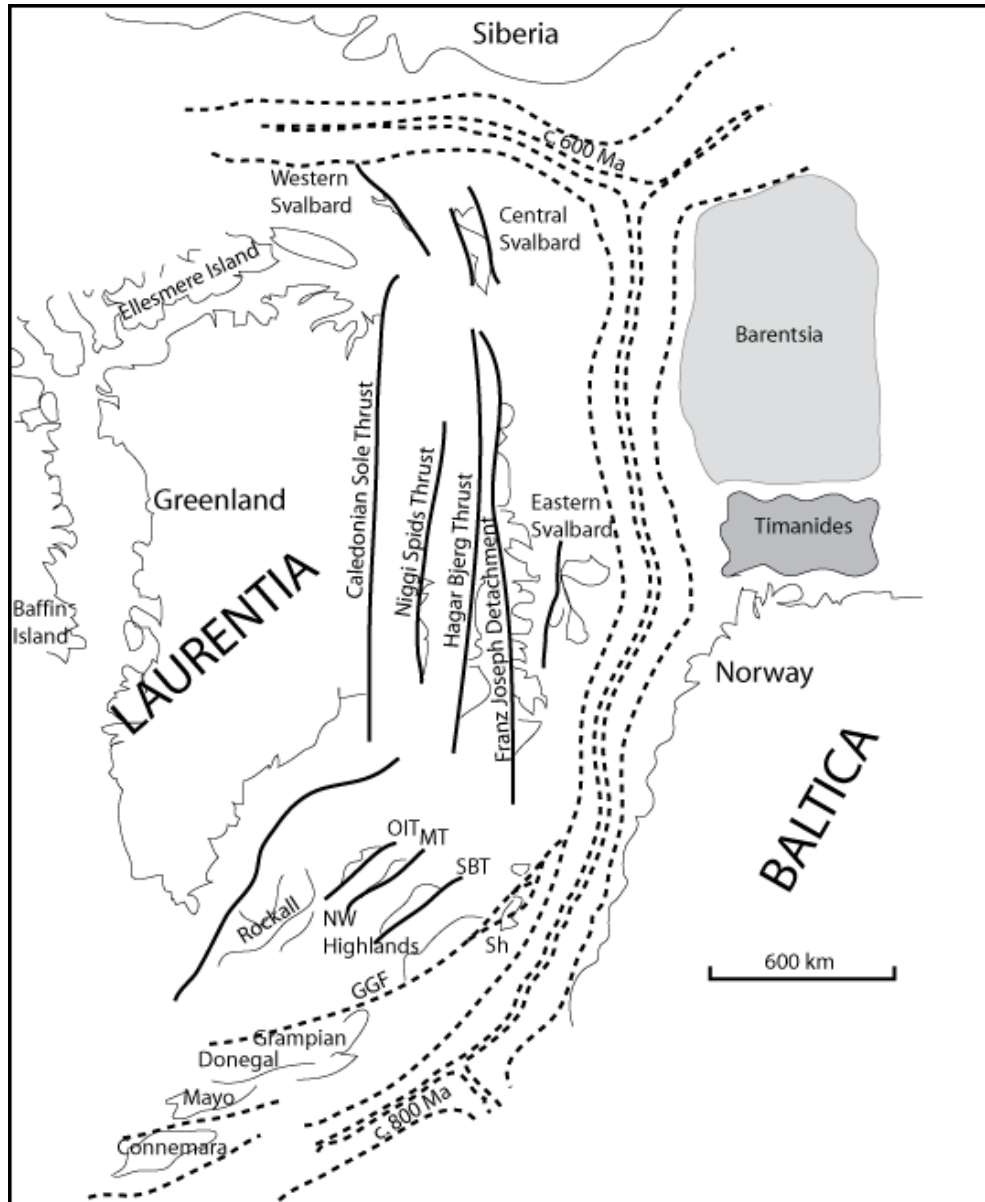


Figure 1-9, latest Neoproterozoic arrangement for the Laurentian margin from Leslie et al. 2008. The suggested position of Baltica, Barentsia and Siberia along with the line of Iapetus separation are shown. The inset shows the location of Scottish 'Promontory' (S) within a wider global continental plate reconstruction. Abbreviations are GGF – Great Glen Fault; HB – Highland Border; MT – Moine Thrust; OIT – Outer Isles Thrust; SBT – Sgurr Beag Thrust; Sh – Shetland.

There is little evidence within the East Greenland Caledonides of arc-collisional events associated with the Grampian event or any other short-lived marginal arc or basin collision with the margin. This suggests that the collision was accommodated by the later Scandian event (Leslie et al. 2008; Roberts et al. 2001).

1.11.2 Scandinavia

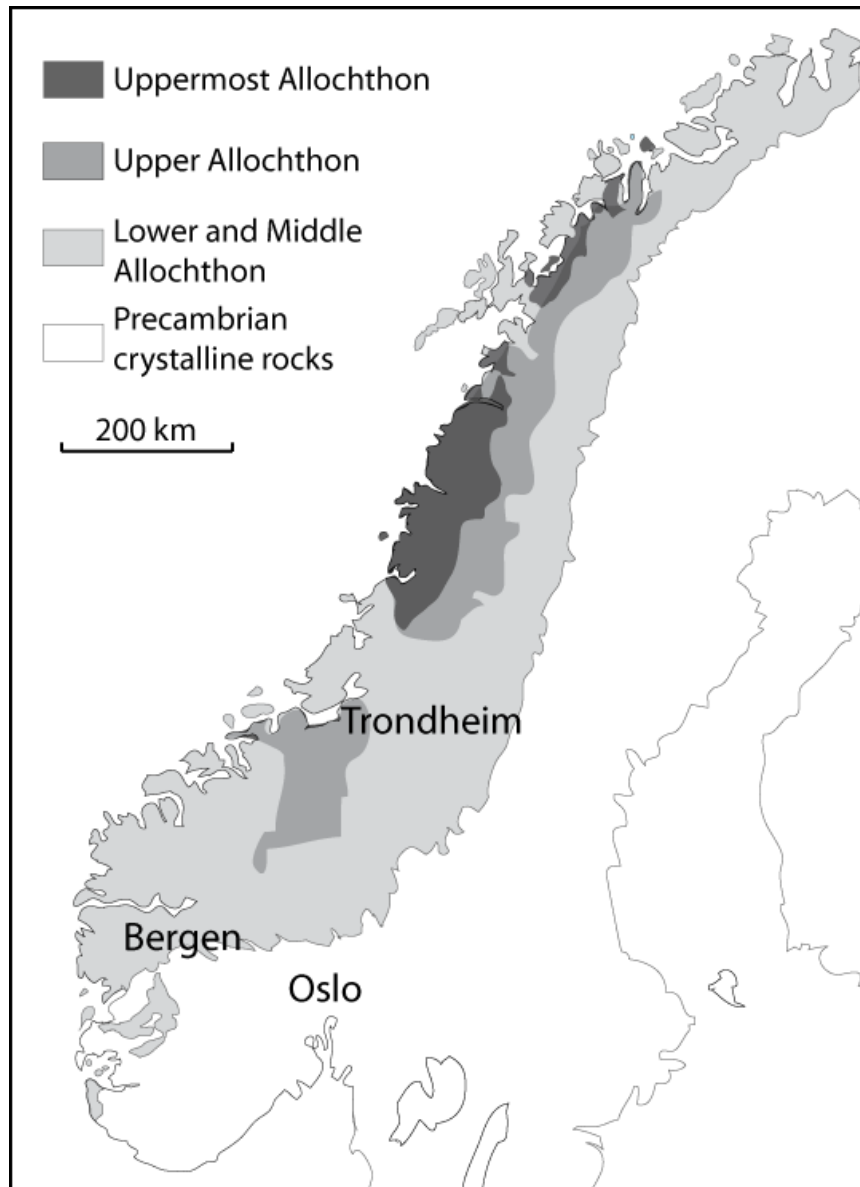


Figure 1-10, Simplified tectonostratigraphy of the Scandinavian Caledonides, from Roberts 2002.

The Caledonides of Scandinavia are divided into the Autochthon, Parautochthon, Lower, Middle, Upper and Uppermost Allochthons (Roberts & Gee 1985) (Figure 1-10). The Autochthon, Parautochthon, Lower and Middle Allochthons are Balto-

Scandian derived, whereas the Upper Allochthon is Iapetus-derived and the Uppermost Allochthon is Laurentian-derived (Gee 1975; Kirkland et al. 2005, 2006).

They have been affected by two Caledonian events, the Finnmarkian (540-490 Ma) and the Scandian (425-400 Ma) (Roberts 2001). The Porsanger Orogeny (840-820 Ma) is recorded within the Upper Allochthon and the Uppermost Allochthon and may be related to the Knoydartian (Daly et al. 1991). Within the Uppermost Allochthon ~710 Ma deformation has been recorded and assigned to the Snøfjord event (Kirkland et al. 2006), this is similar to the 730 Ma age from Loch Eilt close to the Sgurr Beag Thrust (Tanner & Evans 2003).

1.12 Project Aims

Despite many publications and years of research into the perplexing metamorphic history and architecture of the Scottish Caledonides, there still remain several fundamental problems. As mentioned in section 1.5, the timings of peak metamorphism are poorly understood as previous work has focused on several small areas and no regional correlations have been drawn. Linkage of various structures and deformation fabrics with orogenic events is also problematic in many areas. This study aims to carry out the first regional study to determine the timing(s) of peak metamorphism within the Scottish Caledonides. Some of the issues that this study hopes to address include:

- Evaluate the current Grenville metamorphic ages from the basement inliers.
- Determine the cause and spatial extent of the Knoydartian tectonothermal event (or events).
- Date peak metamorphism in the most south- westerly outcrops of the Moine Supergroup.
- Constrain age(s) of metamorphism in the Glenfinnan Group.
- Date peak metamorphism in Sutherland, is there a Knoydartian event?
- Constrain ages of Moine and Sgurr Beag thrusts.
- Date peak metamorphism of the Yell Sound Division.

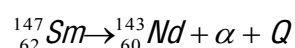
- Provide metamorphic evidence for the Scandian orogeny within the Moine Supergroup.

This study will focus on Lu-Hf and Sm-Nd dating of garnets with some Rb-Sr dating of muscovites and biotites, most of which was carried out as part of a Nuffield Foundation funded project (McDermott).

2.1 Chemical properties of Sm-Nd and Lu-Hf

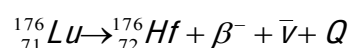
Sm, Nd and Lu are all rare earth elements (REE) with atomic numbers of 62, 60 and 71, respectively. Hf is a high field strength element (HFSE) with an atomic number of 72 and a valence of 4. Sm is a medium REE and has four stable isotopes ^{144}Sm , ^{150}Sm , ^{152}Sm and ^{154}Sm , and three radioisotopes, ^{147}Sm , ^{148}Sm and ^{149}Sm , and has a valence of 3. The radioisotopes decay by alpha decay to isotopes of Nd. Nd is a light REE and is composed of five stable isotopes ^{142}Nd , ^{143}Nd , ^{145}Nd , ^{146}Nd and ^{148}Nd , and two radioisotopes ^{144}Nd and ^{150}Nd and has a valence of 3. The decay of ^{147}Sm is shown below.

Equation 2-1; Decay of ^{147}Sm



Lu is the heaviest of the REE and has a valence of 3. Lu has two naturally occurring isotopes ^{175}Lu (97.4%) and ^{176}Lu (2.6%). ^{176}Lu is radioactive and decays by beta emission to ^{176}Hf (atomic number 72) or by electron capture to ^{176}Yb (atomic number 70). Hf has 32 isotopes whose half-lives are known, with mass numbers 154 to 185. Of these, five are stable ^{176}Hf , ^{177}Hf , ^{178}Hf , ^{179}Hf and ^{180}Hf . The decay of ^{176}Lu is shown below.

Equation 2-2; Decay of ^{176}Lu



2.2 Sm-Nd and Lu-Hf geochronology in garnets

Garnet is commonly used in many pressure-temperature determinations; therefore its stability relationships are generally well understood allowing for good interpretation of ages achieved (e.g. Spear and Peacock 1989). Geochronology of garnets is particularly useful for Sm-Nd and Lu-Hf because garnet has high $^{147}\text{Sm}/^{144}\text{Nd}$ and $^{176}\text{Lu}/^{177}\text{Hf}$ ratios, thus it is possible to achieve high resolution dating (e.g. Mezger et al. 1992; Duchene et al. 1997). As both Sm and Nd are REE they show limited fractionation in garnet and lower Sm/Nd ratios when compared with Lu/Hf, thus giving a lower age precision. As Lu is a heavy REE (HREE) and Hf is a HFSE, this allows them to have a larger

fractionation in garnets and higher Lu/Hf ratios, potentially giving better age precision than Sm/Nd. This is due to HREE being compatible within the garnet matrix and the incompatible nature of HFSE, giving a high HREE/HFSE ratio. The fact that the parent elements of the Sm-Nd and Lu-Hf isotope systems are both REEs results in an overall coherent behaviour between the two isotopic systems, whereas the distinctly different characters of the daughter elements, especially the strong affinity of Hf for zircon with consequent Hf/REE fractionation, may lead to isotopic decoupling during crustal anatexis and, more importantly, during sediment transport (Patchett et al. 1984).

2.3 ^{176}Lu decay constant and CHUR parameters

Unlike the decay constant for ^{147}Sm ($6.54 \times 10^{-12} \text{ yr}^{-1}$), the ^{176}Lu decay constant has been a contentious issue since the 1960s. Early determinations came from counting experiments, and provided estimates ranging from $1.39 \times 10^{-11} \text{ yr}^{-1}$ (Sakamoto, 1967) to $3.18 \times 10^{-11} \text{ yr}^{-1}$ (Donhöffer, 1964). More recently this scatter has been reduced. Table 2-1 shows the ^{176}Lu decay constant estimations since 1939.

Table 2-1 summary of previously published ^{176}Lu decay constants, radiogenic refers to Lu-Hf dating of geological samples.

λ ^{176}Lu (10^{-11} yr^{-1})	Method	References
0.949 ± 1.000	β counting	Libby (1939)
3.223 ± 1.075	γ counting	Arnold (1954)
1.520 ± 0.150	$2\pi\beta$	Dixon et al. (1954)
3.300 ± 0.100	γ counting	Glover & Watt (1957)
3.194 ± 0.175	Radiogenic	Herr et al. (1958)
1.925 ± 0.050	γ counting	McNair (1961)
3.179 ± 0.030		Donhoff (1964)
1.883 ± 0.070	γ sum counting	Brinkman et al. (1965)
1.386 ± 0.015	γ sum counting	Sakamoto (1967)
2.119 ± 0.120	Liq. Scint. Coincidence	Prodi et al. (1969)
2.100 ± 0.250	Radiogenic	Boudin & Deutsch (1970)
1.828 ± 0.015	γ sum counting	Konmura et al. (1972)
1.963 ± 0.080	Radiogenic	Patchett & Tatsumoto (1980)
1.699 ± 0.005	γ counting	Norman (1980)
1.941 ± 0.070	Radiogenic	Tatsumoto et al. (1981)
1.930 ± 0.030	γ - γ coincidence	Sguigna et al. (1982)
1.833 ± 0.005		Sato et al. (1983)
1.711 ± 0.045	γ counting	Gehrke et al. (1990)
1.858 ± 0.025	γ counting	Dalmaso et al. (1992)
1.858 ± 0.005	γ counting	Nir-el & Lavi (1998)
1.865 ± 0.015	Radiogenic	Scherer et al. (2001)
1.699 ± 0.015	γ - γ coincidence	Grinyer et al. (2003)
1.983 ± 0.029	Radiogenic	Bizzarro et al. (2003)
1.885 ± 0.038	γ counting	Nir-El & Haquin (2003)
1.867 ± 0.008	Radiogenic	Söderlund et al. (2003)
1.957 ± 0.035	β counting	Luo & Kong (2006)

The first Lu-Hf isochron was constructed by Patchett & Tatsumoto (1980) on a suite of planetary igneous rocks, eucrite meteorites (achondrites) of a known age of 4550 Ma. Using this known age, they constructed a ten point isochron which yielded a decay constant of $1.96 \pm 0.08 \times 10^{-11} \text{ yr}^{-1}$. This decay constant was improved to $1.94 \pm 0.07 \times 10^{-11} \text{ yr}^{-1}$ by the addition of three extra points later (Tatsumoto et al. 1981). However, the eucrites at the higher end of the isochron may have a formation age that is 100 Ma younger than the main population (Mittlefehldt et al. 1998). The decay constant from the isochron was very similar to one calculated from the weighted means of five physical half-life determinations made between 1960 and 1980 (Patchett & Tatsumoto, 1980), thus the decay constant of $1.94 \times 10^{-11} \text{ yr}^{-1}$ was used from 1981 to 1997 (Patchett & Tatsumoto, 1980; Tatsumoto et al. 1981).

In 1997, a decay constant of $1.93 \pm 0.03 \times 10^{-11} \text{ yr}^{-1}$ was adopted by Blichert-Toft & Albarède (1997), which had been determined by absolute counting (Sguigna et al. 1982). This value was similar to the one used previously by Patchett & Tatsumoto (1980), thus only had a small effect of the Hf isotopic studies. However, Nir-El & Lavi published a physically determined (e.g. using a semiconductor to measure gamma radiation) decay constant of $1.878 \pm 0.01 \times 10^{-11} \text{ yr}^{-1}$ which was consistent with another physically determined value from Dalmaso et al. (1992) of $1.858 \pm 0.025 \times 10^{-11} \text{ yr}^{-1}$. It was proposed to use the weighted average of the two values, resulting in a decay constant of $1.876 \pm 0.009 \times 10^{-11} \text{ yr}^{-1}$ (Albarède et al. 2000). However Scherer et al. (2001) calibrated Lu-Hf against the U-Pb decay scheme to determine the ^{176}Lu decay constant, using a sample with minerals rich in Lu and U, which had cooled quickly so the effects of closure temperature were minimised, and the sample must have remained closed systems with respect to Lu-Hf and U-Pb since formation. The value determined was $1.865 \pm 0.015 \times 10^{-11} \text{ yr}^{-1}$, which is the decay constant used throughout this study. This is very similar to the values Nir-El & Lavi (1998), Dalmaso et al. (1992) and Nir-El & Haquin (2003) achieved physically. Other more recent physically determined decay constants include $1.7 \times 10^{-11} \text{ yr}^{-1}$ (Grinyer et al. 2003), and $1.95 \times 10^{-11} \text{ yr}^{-1}$ (Luo & Kong, 2006). The latter value is similar to the value from Patchett & Tatsumoto (1980) and is in agreement with a study undertaken by Blichert-Toft et al. (2002) where they re-examined 21 eucrites of Patchett & Tatsumoto. Sm-Nd analysis of 18 samples gave an age of $4464 \pm 75 \text{ Ma}$ (MSWD = 1.26). Using the old ^{176}Lu decay constant of $1.94 \times 10^{-11} \text{ yr}^{-1}$ a similar age of $4470 \pm 22 \text{ Ma}$ was obtained, however this age was only

for the three samples that were rejected for Sm-Nd, therefore there is no direct comparison. A Lu-Hf age for all 21 of the samples is not meaningful, however the basaltic eucrites give of 4604 ± 39 Ma (MSWD = 4.52) using the old decay constant which is within error of 4565 Ma which is the latest estimate of the time of differentiation of the eucrite parent body. Blichert-Toft et al. (2002) use this as evidence against the new ^{176}Lu decay constant ($1.865 \pm 0.015 \times 10^{-11} \text{ yr}^{-1}$). However, the spread of data used to construct this isochron provides a relatively weak constraint on the decay constant. Using the new decay constant, the age achieved would be 4743 ± 180 Ma, which is within error of the earliest solar system ages of 4567 Ma (Amelin et al. 2002). Therefore the eucrite data alone cannot prove that the new decay constant is not correct. More evidence against the new decay constant was obtained from the study of Bizzarro et al. (2003), where Lu-Hf isotopic measurements were undertaken on chondrites and basaltic eucrites and gave an initial $^{176}\text{Hf}/^{177}\text{Hf}$ ratio of 0.279628 ± 0.000047 . This implies a ^{176}Lu decay constant of $1.983 \pm 0.033 \times 10^{-11} \text{ yr}^{-1}$ using an age of 4560 Ma for the chondrite-forming event. A more recent study by Söderlund et al. (2003), has cross-calibrated U-Pb and Lu-Hf isotopic systems on mineral fractions from Proterozoic samples from Sweden and Finland. The calibration yielded a ^{176}Lu decay constant of $1.867 \pm 0.008 \times 10^{-11} \text{ yr}^{-1}$ which is in good agreement with the terrestrial value obtained by Scherer et al. (2001).

The estimates for the ^{176}Lu decay constant show a discrepancy between the terrestrial value (e.g. Söderlund et al. 2003; Scherer et al. 2001) and the meteorite value (e.g. Bizzarro et al. 2003; Blichert-Toft et al. 2002). This introduces a lot of uncertainty into the interpretation of Hf isotopic data, in terms of geochronology and crust-mantle evolution models. As this research concentrates on dating metamorphism within terrestrial rocks, the terrestrial value will be used in this study.

Coupled with the problem of establishing the ^{176}Lu decay constant is the problem of determining the CHUR parameters, especially the chondritic initial $^{176}\text{Hf}/^{177}\text{Hf}$ ratio. Hf ratios were especially hard to measure until the development of the MC ICP MS because of the very low abundances of Hf within chondrites and due to the poor precision on Hf analysis by TIMS or hot-SIMS. Initially, the composition of CHUR was determined from the intersection of the eucrite meteorite isochron and the $^{176}\text{Lu}/^{177}\text{Hf}$ ratio of 0.0334 derived from carbonaceous chondrites. This gave a

$^{176}\text{Hf}/^{177}\text{Hf}$ present day average CHUR value of 0.28286 (Patchett & Tatsumoto, 1981). Development of the MC ICPMS allowed analysis of Hf isotopes, and gave a present day average CHUR value of 0.28277 ± 3 (Blichert-Toft & Albarede, 1997). Both of these values are similar to the Bulk Earth Hf isotope ratio determined from the intersection of chondritic $^{143}\text{Nd}/^{144}\text{Nd}$ with Nd, Hf isotope array defined by ocean island basalts. The changes in the ^{176}Lu decay constant have had a large effect on the ϵ_{Hf} values as they change the slope of the chondritic growth line. This has important implications for the use of ϵ_{Hf} values as tracers of crust or mantle evolution.

2.4 The effect of inclusions on garnet geochronology

There is evidence in the literature that many bulk total dissolution garnet Sm-Nd analyses have been affected by inclusions (e.g. Prince et al. 2000; Scherer et al. 2000). This is also true for the Lu-Hf system although this is not as well documented. LREE-enriched inclusions (e.g. monazite) may have a large effect on Sm-Nd ages, whereas zircon inclusions contribute most towards influencing Lu-Hf ages. Figure 2-1 shows the effect of old detrital zircon inclusions on the measured Lu-Hf age from a garnet. The mixing of the zircon inclusions within the garnet potentially flattens the isochron, thus makes the age appear younger than it should be. Scherer et al. (2000) suggest that if an entirely inclusion-free garnet is selected and the whole rock Hf content is dominated by inherited zircons then the isochron will be steepened making the age appear older. This could be resolved by using another phase to construct the isochron (Scherer et al. 2000). However, the garnet must grow from a common reservoir which may include some inherited zircon, and may be the same as the whole rock depending on how much older zircon has been dissolved in the whole rock digestion, thus it may be that picking only a pure garnet will have a lesser effect than expected.

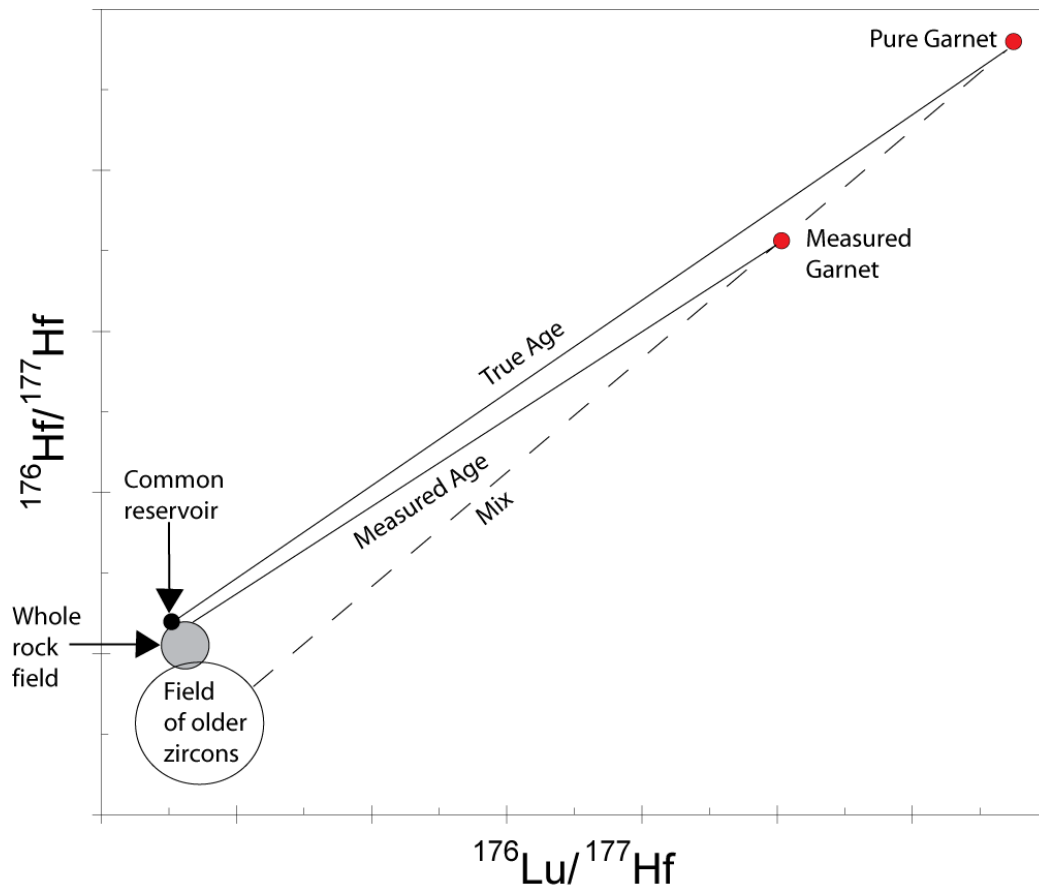


Figure 2-1, Simplified isochron, showing the effect of a zircon inclusion within a garnet on a Lu-Hf age. The True Age and Measured Age isochrons are labelled on the diagram. The whole rock field is shown, where in this field the measured whole rock fraction lies depends on the amount of older zircon inclusions that were dissolved during digestion. The field of older zircons is shown in the diagram. The common reservoir is what the garnet grew from. The measured garnet, pure garnet and the mix are also indicated within the figure.

2.4.1 The effect of zircon within this study

It is assumed that the majority of the zircons within garnets and the whole rock are inherited and are substantially older than the time of garnet growth, thus as explained above this could flatten the isochrons and make the measured age appear younger than it actually is. The extent of this effect depends on the quantity of zircon which has been incorporated within the garnet. Establishing Hf ratios of the zircon inclusions within the garnets is unfortunately not a part of this study, thus the effect of zircon inclusions on the ages achieved cannot be accurately modelled. However there are some crude estimates that can be made to approximate the effect. The first is very simple; in the circumstance where a garnet core and rim have been dated by both Lu-Hf and Sm-Nd methods, the difference between the core and rim ages for the two systems can be

compared. If the difference is similar then it can be assumed that the zircons (or monazites in the case of Nd) are not dominating the Hf ratios, and the difference is down to cooling or another phase of garnet growth. Another assumption is that the small zircons incorporated within the garnet should be representative of the whole rock population so the zircon effect within the whole rock should, at least partially, cancel out the effect from the inclusions within the garnet. This latter assumption should be fairly accurate even if inclusion-free garnets were preferentially picked the zircon inclusions would be too small to see through the binocular microscope so would be incorporated within the garnet fraction.

This study models the effect of zircon inclusions on the garnet ages by assuming a ‘worst case’ zircon. This zircon has a Lu concentration of 84 ppm, Hf concentration of 9603 ppm and a Zr concentration of 384112ppm, these values were estimated from studies by Corfu & Noble (1992), Goodge & Vervoort (2006), Kemp et al. (2006) and Goodge et al. (2008). The amount of zircon within the sample fraction was found by using Equation 2-3, which uses the measured Hf concentration in the sample fraction, the estimated pure garnet Hf concentration from LA ICPMS data and the estimated Hf concentration from the literature.

Equation 2-3, measures the amount of zircon in the sample fraction using the measured Hf concentration from the sample, the estimated pure Hf concentration from LA ICPMS data and the estimated Hf concentration from zircon. (zrn = zircon; grt = garnet; m = measured; est = estimated)

$$\text{zrn in frac} = \frac{\text{grt Hf ppm (m)} - \text{Pgrt Hf ppm (est)}}{\text{zrn Hf ppm (est)} - \text{Pgrt Hf ppm (est)}}$$

The $^{176}\text{Hf}/^{177}\text{Hf}$ was estimated using examples from the literature where the U-Pb age of zircons and the $^{176}\text{Hf}/^{177}\text{Hf}$ had been obtained (Corfu & Noble 1992; Goodge & Vervoort 2006; Kemp et al. 2006; Goodge et al. 2008) and is shown in Figure 2-2. Using the gradient of the line and the expected age of the inherited zircon inclusions within the garnets (Cawood et al. 2004, 2007; Kirkland et al. 2008; Cutts et al. 2010), it is possible to determine a $^{176}\text{Hf}/^{177}\text{Hf}$ value, which can then be used in the model.

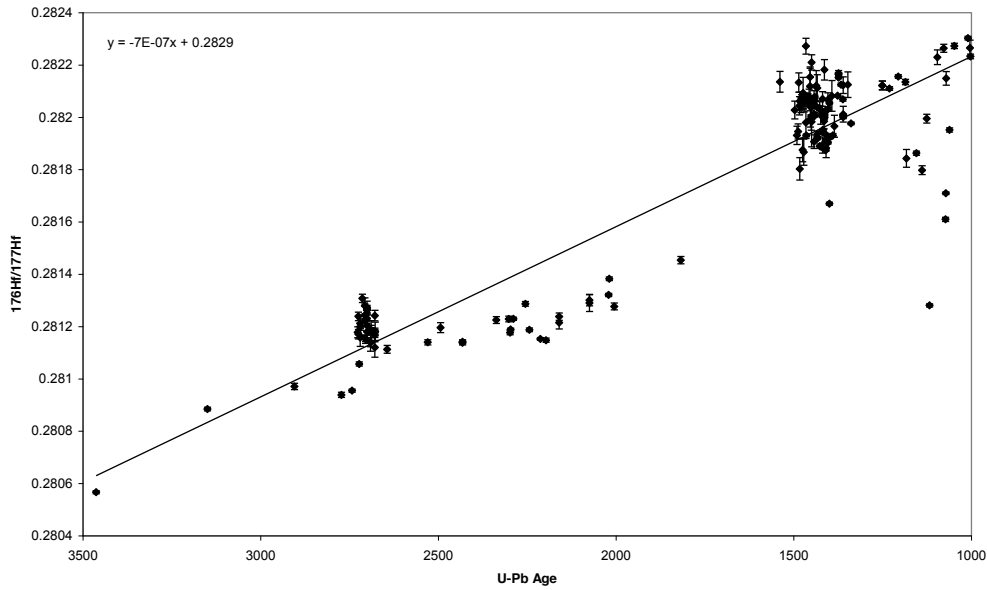


Figure 2-2, zircon U-Pb age against $^{176}\text{Hf}/^{177}\text{Hf}$ ratio using data from Kemp et al. (2006); Corfu & Noble (1992); Goodge et al. (2008) and Goodge & Vervoort (2006).

Equation 2-4 uses the measured $^{176}\text{Hf}/^{177}\text{Hf}$ (the mix) of the sample and the $^{176}\text{Hf}/^{177}\text{Hf}$ of the zircon inclusion to calculate the pure garnet Hf ratio, however this formula also uses the ^{177}Hf concentration of the zircon, which is unknown which means there are two unknowns.

$$\frac{^{176}\text{Hf}}{^{177}\text{Hf}}^{\text{m}} = \frac{\frac{^{176}\text{Hf}}{^{177}\text{Hf}}^{\text{Pgrt}} + \left(\frac{^{176}\text{Hf}}{^{177}\text{Hf}}^{\text{zrn}} \frac{^{177}\text{Hfzrn}}{^{177}\text{Hfgrt}} \right)}{\frac{^{177}\text{Hfzrn}}{^{177}\text{Hfgrt}} + 1}$$

Equation 2-4, shows how $^{176}\text{Hf}/^{177}\text{Hf}$ of pure garnet was calculated. (m = measured; Pgrt = pure garnet; grt = garnet; zrn = zircon).

It is possible to use iteration to obtain the $^{176}\text{Hf}/^{177}\text{Hf}$ pure garnet value by inputting an initial calculated ^{177}Hf zircon/ ^{177}Hf garnet ratio by using Equation 2-5.

Equation 2-5, to estimate an initial ^{177}Hf zircon/ ^{177}Hf garnet ratio to start the iteration process using the amount of zircon and garnet in the sample fraction, the % abundance of ^{177}Hf 0.18606 and the concentrations of Hf in zircon and garnet. (i = initial; zrn = zircon; grt = garnet; P = pure).

$$\frac{^{177}\text{Hfzrn}}{^{177}\text{Hfgrt}}^{\text{i}} = \frac{\text{zrn in fract} (^{177}\text{Hf abundance} \times \text{zrn Hf ppm})}{\text{grt in fract} (^{177}\text{Hfabundance} \times \text{Pgrt Hf ppm})}$$

Later ^{177}Hf zircon/ ^{177}Hf garnet ratios are calculated using the initial value obtained from Equation 2-5 and Equation 2-6.

Equation 2-6, uses the initial estimated ^{177}Hf zircon/ ^{177}Hf garnet ratio, Hf abundances, $^{176}\text{Hf}/^{177}\text{Hf}$ of the pure garnet and zircon to calculate the correct ^{177}Hf zircon/ ^{177}Hf garnet ratio. The standard values used for the calculation are $174/177 = 0.00866$, $176/177 = 0.02644$, $178/177 = 1.46733$, $179/177 = 0.7325$ and $180/177 = 1.88689$.

$$\frac{^{177}\text{Hf}_{\text{zrn}}}{^{177}\text{Hf}_{\text{grt}}} = \frac{\frac{^{177}\text{Hf}_{\text{zrn}}}{^{177}\text{Hf}_{\text{grt}}} (173.9401 \times 174/177 + 175.9414 \times \frac{^{176}\text{Hf}}{^{177}\text{Hf}} \text{Pgrt} + 176.9432 + 177.9437 \times 178/177 + 178.9458 \times 179/177 + 179.9466 \times 180/177)}{173.9401 \times 174/177 + 175.9414 \times \frac{^{176}\text{Hf}}{^{177}\text{Hf}} \text{zrn} + 176.9432 + 177.9437 \times 178/177 + 178.9458 \times 179/177 + 179.9466 \times 180/177}$$

The pure garnet $^{176}\text{Hf}/^{177}\text{Hf}$ ratios are guessed using Equation 2-7. Equation 2-6 and Equation 2-7 are repeated until Equation 2-7 continues to give the same answer.

Equation 2-7, used to guess $^{176}\text{Hf}/^{177}\text{Hf}$ ratio of the pure garnet using the measured $^{176}\text{Hf}/^{177}\text{Hf}$ ratio, the $^{176}\text{Hf}/^{177}\text{Hf}$ ratio of zircon and the ^{177}Hf zircon/ ^{177}Hf garnet ratio. (m = measured; Pgrt = pure garnet; zrn = zircon; grt = garnet).

$$\frac{^{176}\text{Hf}}{^{177}\text{Hf}} \text{Pgrt} = \frac{^{176}\text{Hf}}{^{177}\text{Hf}} \text{m} \left(\frac{^{177}\text{Hf}_{\text{zrn}}}{^{177}\text{Hf}_{\text{grt}}} + 1 \right) - \left(\frac{^{177}\text{Hf}_{\text{zrn}}}{^{177}\text{Hf}_{\text{grt}}} \times \frac{^{176}\text{Hf}}{^{177}\text{Hf}} \text{zrn} \right)$$

The Hf and Lu concentrations of the pure garnet are calculated using Equation 2-8. The $^{176}\text{Lu}/^{177}\text{Hf}$ ratio is then calculated in the usual way but substituting the new pure garnet values into the equation.

$$C_{\text{grt}} = \frac{C_{\text{m}} - X_{\text{i}} \times C_{\text{i}}}{X_{\text{grt}}}$$

Equation 2-8, where C_{grt} is the concentration of the element in the pure garnet, C_{m} is the measured concentration in the mix, C_{i} is the concentration of the element in the inclusions, X_{i} is the proportion of the inclusion that makes up the fraction (wt% in fraction), X_{grt} is the proportion of the garnet that makes up the fraction.

2.5 Closure temperature (T_{C}) in garnet

The closure temperature (T_{C}) is the temperature at which the loss of the element of interest becomes negligible compared with its rate of accumulation. In minerals that have been heated past their T_{CS} , the age obtained from the isotopic system used will reflect the time when the system cooled enough to reach the T_{C} . In minerals that have not been heated above T_{C} the age obtained will reflect mineral growth. The T_{C} of a diffusing species in a mineral undergoing cooling during exhumation has been a topic of significant interest. It can provide information on cooling rate, reflecting exhumation by plotting T_{C} of different geochronological systems against mineral ages. Knowing the T_{C} is critical to interpreting metamorphic mineral ages, establishing whether the age obtained reflects mineral growth, peak metamorphism or cooling. In addition, it is also

crucial for pressure-temperature interpretations. The factors that control the T_C of a mineral include the diffusivity of the element, the effective diffusion radius and the cooling rate; these factors are related to the grain size, shape, chemistry and cooling history, no unique number can universally be assigned to any one system in all rocks.

Dodson (1973) defined the T_C of a geochronological system as its temperature at the time corresponding to its apparent age. He proposed the following model; a given mineral (garnet) is considered to be physically connected with a large reservoir through which the daughter nuclide (e.g. ^{143}Nd) can be lost, probably by volume diffusion. The rate of loss depends either on the size of the entire mineral grain or some smaller volume, which could be controlled by cleavages, lamellae, fractures or some other imperfection in the crystal structure. Dodson's equation is shown below as Equation 2-9.

$$T_C = \frac{E/R}{\ln \left[\frac{AR(T_C)^2 D_0 / a^2}{E(dT/dt)} \right]}$$

Equation 2-9, T_C is closure temperature, E is the activation energy for diffusion, D_0 is the pre-exponential diffusion coefficient, R is the gas constant, A is the geometric factor and a is length scale for diffusion (for a sphere, $A = 55$ and a is the radius; for a cylinder, $A = 27$ and a is the radius; and for a plane sheet $A = 8.7$ and a is the half width). dT/dt is the cooling rate.

Estimates using the Dodson equation tend to run into problems as many parts of the equation have to be assumed, for example it is unlikely that one will know the cooling rate without knowing the conditions of peak metamorphism and the age of the sample when it reached peak conditions. The other main unknown when applying Dodson's equation to a system is D_0 which is the pre-exponential diffusion coefficient. Previously this has been estimated by first finding the chemical diffusivity (D), shown in Equation 2-10. This partial differential equation can be solved using a numerical scheme like the Crank and Nicolson scheme (Crank 1979) which can require use of programming such as Fortran.

$$\frac{\partial C}{\partial t} = D \frac{\partial^2 C}{\partial x^2}$$

Equation 2-10, D is the chemical diffusivity, C is the concentration of the diffusing species, x is the position on the garnet grain and t is time in seconds.

The pre-exponential diffusion coefficient can be calculated by the method shown in Equation 2-11, where D is the chemical diffusivity, D_0 is the pre-exponential diffusion coefficient, E is the activation energy for diffusion, T is the temperature in Kelvins and

R is the gas constant. However, Equation 2-11 uses the activation energy of diffusion which is not well known for Lu, Hf, Sm or Nd, resulting in an imprecise D_0 . Another issue is that T_C relies heavily on the activation energy, and the activation energy is a function of the crystalline material, therefore it follows that each mineral will have a different activation energy for diffusion.

$$D = D_0 \exp \left(\frac{-E}{RT} \right)$$

Equation 2-11, D is the chemical diffusivity, D_0 is the pre-exponential diffusion coefficient, E is the activation energy for diffusion, T is the temperature in Kelvins and R is the gas constant.

The metamorphic samples best suited for thermochronology are those displaying textural and chemical evidence for one single progressive metamorphic event. Establishing the T_C for garnets from the Moine Supergroup is problematical because the garnets have been subjected to more than thermal deformation phase. In some cases the garnet core has grown and then further heating has lead to growth of the rim (Vance et al. 1998; Cutts et al. 2009). This means that the T_C concept is not directly applicable to Moine Supergroup garnets.

2.5.1 Previous T_C estimates

There have been few T_C estimates for Lu-Hf; instead most studies compare Lu-Hf results to Sm-Nd ages and use the difference to estimate cooling rate and T_C . However, even this comparison is speculative as Sm-Nd T_C estimates are controversial with lower estimates being around 500°C for a pyrope-rich garnet (e.g. Mezger et al. 1992; Burton et al. 1995) ranging up to around 800°C for a grossular garnet (Jagoutz 1988). Previous Sm-Nd T_C estimates have been carried out by comparing ages from different isotopic systems, for example U-Pb, Rb-Sr and Sm-Nd in the work of Burton et al. (1995) or by experimental work (Ganguly et al. 1998). Mawby et al. (1999) and Buick et al. (2001) suggest that zircon U-Pb SHRIMP ages can show that Sm-Nd can record peak metamorphism in some instances, where the garnet grains have a radii >4.5 mm and have cooled at a rate of around 4°CMa⁻¹ they could have a T_C greater than or equal to 760°C. It has been suggested that garnets with a radius of 1 mm may have a T_C of around 750°C for a cooling rate of 10-100°CMa⁻¹ (Becker 1997). As mentioned briefly above, garnet chemistry may influence T_C with an estimate from an almandine-rich garnet of 730°C, this garnet had a radius of 2 mm and had cooled at a rate of 10°CMa⁻¹. These results show that establishing the T_C for the Sm-Nd system is difficult

and that certainly one T_C or restricted temperature range cannot be applied to all garnets.

Several studies have estimated Lu-Hf T_C in garnet. Scherer et al. (2000) undertook a study to constrain the Lu-Hf T_C by comparing Lu-Hf to Sm-Nd. They concluded that the closure temperature of the Lu-Hf system is equal to, if not higher than the Sm-Nd system, but were unable to assign a temperature range. Anczkiewicz et al. (2007) dated garnets from granulites and suggested that, in the granulite which had not been affected by fluids, which disturbs the HREE profile in the garnets, the T_C may have been as high as $>900^\circ\text{C}$, however in the granulite which had been affected by fluids, the HREE trace had been disturbed and gave a younger age.

The trace element profiles in many garnets can show whether the garnets have been subjected to temperatures above T_C (e.g. Skora et al. 2008; Lapen et al. 2003). Skora et al. (2008) suggest that ages obtained from garnets that have not been heated above T_C reflect prograde garnet growth ages. One might expect Lu-Hf and Sm-Nd ages in this instance to record the same date; however Lapen et al. (2003) reported an 8 Ma difference between the two systems which they attributed to the distribution differences between LREE and HREE within garnet. As HREE are concentrated within the garnet cores, Lu-Hf ages will be skewed towards garnet core growth and potentially give an older date than Sm-Nd which are concentrated at the garnet rims (Lapen et al. 2003; Skora et al. 2009; Dutch & Hand 2009). LA ICPMS analysis of garnets within this study has been undertaken to establish REE profiles which will determine whether the garnets record prograde growth or cooling.

2.6 Method of Sm-Nd and Lu-Hf dating

2.6.1 Age Calculation

Isochron ages and uncertainties were calculated using Isoplot version 3.72 (Ludwig 2010) and decay constants of 1.865×10^{-11} for ^{176}Lu (Scherer et al. 2001) and 6.54×10^{-12} for ^{147}Sm (Gupta & Macfarlane 1970).

The $^{176}\text{Lu}/^{177}\text{Hf}$ ratio was calculated by using the mass ratios from the mixed solution standards ran during Hf and Lu analyses using Equation 2-12. The standard values used for the calculation are $174/177 = 0.00866$, $176/177 = 0.02644$, $178/177 = 1.46733$,

$179/177 = 0.7325$ and $180/177 = 1.88689$ and together with the concentrations obtained from the MC ICPMS analysis they can be used to calculate the $^{176}\text{Lu}/^{177}\text{Hf}$ ratio.

Equation 2-12, demonstrating how the $^{176}\text{Lu}/^{177}\text{Hf}$ ratio was calculated for all samples analysed within the study, m = value measured from the sample, s = standard ratio value. The Lu and Hf concentrations were obtained from MC ICPMS analysis.

$$\frac{^{176}\text{Lu}}{^{177}\text{Hf}} = \frac{\left(\frac{\text{Lu ppm}}{\text{Hf ppm}}\right) \times \left(174 \frac{174}{177} s + 176 \frac{^{176}\text{Hf}}{^{177}\text{Hf}} m + 177 + 178 \frac{178}{177} s + 179 \frac{179}{177} s + 180 \frac{180}{177} s\right)}{\left(176 + 175/\frac{176}{175} s\right)}$$

2.6.2 Two point isochrons

In the literature there has been some discussion on the meaningfulness of two point isochrons (e.g. Ludwig 2003). Some of this uncertainty is well grounded, to quote Ludwig, the creator of Isoplot “the reliability of isochron ages for regression lines with only three or four data points and no resolvable ‘geological’ scatter can be significantly less than suggested by the uncertainties calculated by most regression algorithms...” Two point isochrons allow zero degrees of freedom and therefore a MSWD cannot be derived. However, this study uses two point garnet-whole rock isochrons as they can date a garnet growth event, which correlates to a specific metamorphic event. A multi-mineral isochron would provide an average metamorphic age as it would include minerals that grew and closed at different times during metamorphism (Baxter et al. 2002). Another important benefit of using two point isochrons is that it allows more samples to be dated, providing a wide regional picture of metamorphism within the Moine Supergroup.

2.6.3 Garnet core and rim dating

In several of the samples within this study, garnet cores were separated from the rims and an age determined for each separate. The separation was carried out by hand picking different coloured garnet under a binocular microscope. These ages provide valuable information about the tectonic processes from within the Northern Highland Terrane but dating just two zones can often miss the detailed information on garnet growth rate, for example did the garnet grow continuously or in pulses which could relate to tectonic events. An example is shown in Figure 2-3 from Pollington & Baxter (2011) where models of garnet growth have been calculated with varying growth rates based on core and rim ages that differ by as little as 1.4 Ma (Vance & O’Nions 1992) to

as much as 14.7 Ma (Christensen et al. 1989). Figure 2-3 shows that is impossible to accurately model garnet growth rates based only on one core and one rim age.

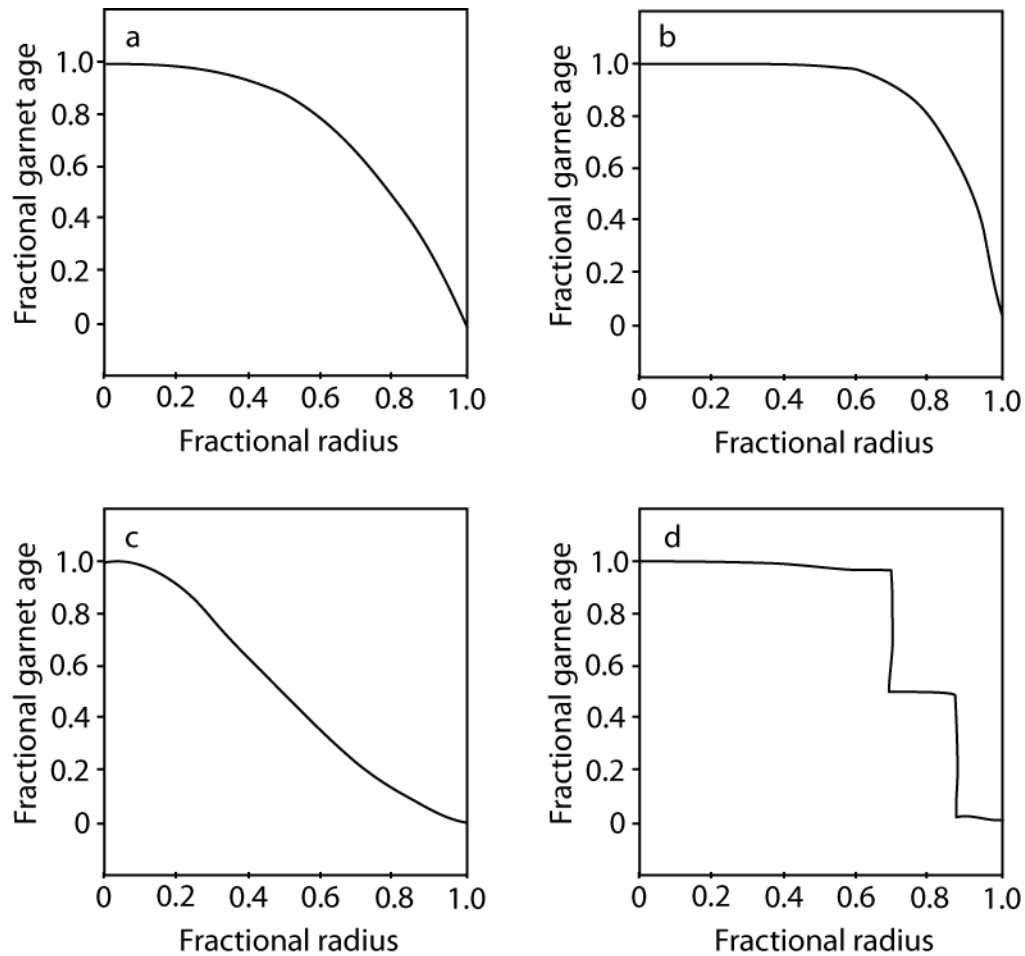


Figure 2-3, from Pollington & Baxter (2011) showing models of garnet age, total growth is equal to 1 fractional radius and total time is equal to fractional age. a) constant volumetric growth rate resulting in total growth in total time, b) decelerating growth rate; decelerating by 5% of the previous value every 0.1 mm, c) accelerating growth rate, accelerating by 5% of the previous value every 0.1 mm, d) pulsed growth rate.

High precision microsampling of garnet zones could make it possible to accurately date the individual zones and determine garnet growth rates. This would be an extremely valuable technique to apply to garnets from the Moine Supergroup as they record a very long and complex history but is not part of this project, as it is an extremely detailed and time consuming method.

2.7 Analytical techniques

2.7.1 Sampling methodology

Samples ranging in size from 2-8 kg were collected from each of the nappes within the Northern Highland Terrane, Shetland, the Dava and Glen Banchor Succession and the northern part of the Dalradian Supergroup. Sampling was undertaken in order to cover as much of the Northern Highlands as possible, to re-sample areas where previous work had already been undertaken, and to sample possible equivalents in Shetland and the Dalradian Supergroup. The localities were decided prior to fieldwork by studying thin sections, BGS reports and published work to establish where garnets were of a suitable size for Lu-Hf and Sm-Nd analyses. Areas with weathered garnets were avoided, as this usually indicated retrogression of the sample.

2.7.2 Rock crushing

Weathered surfaces were removed from all rock types using a sledge hammer; use of the hydraulic splitter was unsuccessful as samples were too large and flattened instead of braking. Once all altered surfaces had been removed, the sample was crushed into chips ($\sim 1\text{cm}^3$) using a jaw crusher. Some samples were run through the jaw crusher twice, the first time with the crusher set to produce $\sim 3\text{cm}^3$ before setting the crusher to produce $\sim 1\text{cm}^3$ chips. The sample tray in the jaw crusher was lined with clean paper for each sample to aid sample recovery and minimise contamination. Between samples excess dust and rock fragments were removed from the jaws and the area around the jaw crusher using a steel brush and a Hoover. The jaws were then removed to enable removal of material lodged behind them and cleaned with acetone. Approximately 50-100g of chipped material was reduced to a fine powder for whole rock Sm-Nd, Lu-Hf, Rb-Sr and XRF analyses using a tungsten carbide TEMA mill. Powders were stored in new glass jars previously cleaned with acetone. The TEMA was cleaned with water and acetone between each sample. In the cases where samples contained a high proportion of mica it was necessary to put the sample through the TEMA twice, agitating the sample between millings to free up any large mica plates which were stuck underneath the rings. Occasionally with very pelitic samples, a clay-like material adhered to the inside of the TEMA which was removed by grinding glass powder before washing.

2.7.3 Mineral separation (Lu-Hf, Sm-Nd and Rb-Sr analyses)

The chips retained from the jaw crusher were sieved, and the 500 μm -1mm and 250-500 μm size fractions were retained. The fractions were then rinsed with MQ and put in an ultrasonic bath for 15 minutes at a time, rinsing with MQ in between until the water was clean. The fractions were then dried in the oven before being magnetically separated using the Franz Magnetic Separator, which produced garnet-, biotite-, and muscovite-rich fractions. Garnets were then handpicked from the 0.5-1mm magnetic fraction rich in garnet, using a binocular microscope, from the 0.5-1mm magnetic fraction for Lu-Hf and Sm-Nd analysis. This allowed those garnets showing signs of alteration or with lots of inclusions to be discarded. Muscovites and biotites were handpicked from the 250-500 μm fractions for Rb-Sr analyses. Muscovites and biotites with inclusions were avoided.

2.7.4 X-ray fluorescence spectrometry – major and trace element analysis

Fused glass disc preparation

Prior to fusion the whole rock powders were dried in the oven over night to remove any adsorbed moisture. Loss on ignition was determined by igniting ~0.7g of sample at 1100°C in covered platinum crucibles. After ignition, spectro-flux was added to the sample in a ratio of 6:1 of 6 parts flux to one part sample and returned to the 1100°C furnace for a further 30 minutes. During heating the sample loses some weight from the flux, so once the sample was cool it was weighed and the deficit between the required and actual weight made up with the spectro-flux. The flux loss on ignition was then calculated; allowing the amount of flux added to be adjusted to compensate for the loss on reheating resulting in the correct weight after casting. Samples were heated over 3 meker burners for 5 minutes to re-melt the sample and the added flux was incorporated into the melt by gently swirling the melt. The discs were cast onto Al plattens using an aluminium plunger on a hotplate at 180°C. The discs were left on the hotplate to cool before clipping and storing in individual plastic sample bags. Between batches the platinum crucibles were cleaned by boiling in 50% HCl until all remaining melt was dissolved and then stored in distilled water. Prior to use they were rinsed in fresh distilled water and dried over a meker burner and the inside checked for any remaining deposits.

Pressed pellet preparation

Pressed pellets for trace element analysis were prepared using ~7g of sample. The sample was mixed with 8 drops of mowiol binder before being pressed into a disc on a tungsten carbide die. The disc is backed with boric acid and pressed under 10 tons/in² for 1 minute. Pellets are pumped in a desiccator for 30 minutes prior to running to remove surface moisture.

XRF Analysis

The XRF used for analyses was a Philips PW1480. Pressed pellets were analysed for trace elements and were run twice using both the tungsten and the rhodium tubes. Fused glass discs were analysed for major elements using the tungsten tube and were analysed once. The XRF run parameters are shown in Table 2-2. To assess the reproducibility of XRF, a sample was repeated 6 times. This sample was not from this study but was run over the same period of analysis; the results are shown in Table 2-3 and Table 2-4 where it can be seen the reproducibility is extremely good.

Table 2-2 XRF parameters for each element analysed. Abbreviations; C – coarse collimator; F – fine collimator; FL – flow counter; FS – flow and scintillation counters. Crystal numbers; 1 – Lithium fluoride 220 (LiF 220); 2 – Lithium fluoride 200 (LiF 200); 3 – Germanium; 4 – Pentaerythritol; 5 – Thallium acid phthalate; 6 – Indium antimonide.

	Kv	Ma	Collimat or	X- crystal	+offs	-offs	detector	LL	UL
SiO ₂	60	45	C	6			FL	25	76
Al ₂ O ₃	60	45	C	4		5	FL	27	78
Fe ₂ O ₃	60	45	F	2		1.6	FL	14	69
MgO	60	45	C	5	3		FL	24	70
CaO	60	45	F	2		4.5	FL	26	72
Na ₂ O	60	45	C	5	3.3		FL	26	72
K ₂ O	60	45	F	2	3.5		FL	25	75
TiO ₂	60	45	F	2	0		FL	28	75
TiO ₂ Rh	95	30	F	2	3.74		FL	27	75
MnO	60	45	F	2		0.9	FL	14	70
P ₂ O ₅	60	45	C	3	3.2		FL	35	70
Ni	60	45	F	2		0	FL	14	71
Cr	60	45	F	1		1.5	FL	13	76
V	60	45	F	1		2.5	FL	32	70
Sc	60	45	F	2		0	FL	28	63
Cu	60	45	F	2	0.6	0.4	FL	15	70
Zn	60	45	F	2	0	0.8	FL	15	68
Cl	60	45	F	4	2		FL	36	74
Ga	90	30	F	2	0.6		FS	20	70
Pb	90	30	F	2	0.78		FS	25	73
Sr	90	30	F	2	0.7		FS	25	73
Rb	90	30	F	2			FS	25	73
Ba	90	45	F	7	1.8	3	FL	28	63

Zr	90	30	F	2		FS	25	73
Nb	90	30	F	2	0.4	FS	25	73
Th	90	30	F	2		FS	25	73
Y	90	30	F	2	0.56	FS	25	73
La	60	45	F	1	2	FL	27	58
Ce	60	45	F	1	1.68	FL	13	76
Nd	60	45	F	1	4.3	FL	13	76

Table 2-3 major element XRF results for the sample that was replicated 6 times.

	I112	I112	I112	I112	I112	I112	Mean	2sd
SiO ₂	45.51	45.43	45.59	45.60	45.62	45.62	45.56	0.15
Al ₂ O ₃	13.87	13.82	13.86	13.90	13.86	13.98	13.88	0.11
Fe ₂ O ₃	12.74	12.69	12.73	12.71	12.68	12.57	12.68	0.12
MgO	10.08	9.96	9.98	10.05	10.01	10.09	10.03	0.11
CaO	11.17	11.17	11.17	11.20	11.19	11.14	11.17	0.04
Na ₂ O	2.25	2.30	2.28	2.29	2.32	2.29	2.29	0.04
K ₂ O	0.784	0.787	0.783	0.785	0.779	0.782	0.78	0.01
TiO ₂	2.642	2.634	2.648	2.654	2.649	2.635	2.64	0.02
MnO	0.203	0.197	0.199	0.194	0.194	0.193	0.20	0.01
P ₂ O ₅	0.443	0.455	0.454	0.457	0.455	0.449	0.45	0.01
Total	99.69	99.44	99.70	99.83	99.75	99.75	99.69	0.27

Table 2-4 trace element XRF results from the sample repeated 6 times.

	I112	I112	I112	I112	I112	I112	Mean	2sd
Ni	172.2	172.8	173.1	172.3	172.2	171.9	172.4	0.89
Cr	482.4	480.9	477.6	478.9	475.5	480.3	479.3	4.95
V	359.7	359.8	360.6	364.4	364.3	363.1	362.0	4.41
Sc	34.3	34.4	34.4	34.2	34.0	33.9	34.2	0.42
Cu	68.8	68.6	67.7	69.0	68.3	69.2	68.6	1.08
Zn	86.7	87.5	85.3	85.8	85.4	85.3	86.0	1.82
Cl	186	163	78	138	71	143	129.6	91.97
Ga	16.8	16.7	16.3	15.7	16.7	15.7	16.3	1.02
Pb	2.6	1.4	2.1	1.8	1.4	1.1	1.7	1.10
Sr	437.0	438.6	437.9	439.0	439.0	438.9	438.4	1.60
Rb	15.3	15.5	15.9	15.8	15.8	15.4	15.6	0.50
Ba	335	334	333	332	334	340	334.7	5.13
Zr	159.4	158.5	159.1	158.6	159.3	159.3	159.0	0.78
Nb	39.0	39.1	39.3	39.2	39.3	39.5	39.2	0.35
Th	1.8	1.6	1.7	1.3	1.3	1.3	1.5	0.46
Y	23.7	24.2	23.8	23.8	24.0	24.4	24.0	0.54
La	26.8	26.5	26.4	26.8	26.8	26.9	26.7	0.40
Ce	59.6	60.4	59.0	59.5	60.1	62.7	60.2	2.62
Nd	30.0	29.0	29.9	29.9	31.3	30.5	30.1	1.52

2.7.5 Mineral chemistry – major and trace element analysis

Sample preparation

Hand-picked garnets and micas were mounted in epoxy resin before being ground to expose a flat surface of all phenocrysts, this surface was covered in a thin layer of graphite for electron probe analysis to dissipated the electrical charges that may be generated by the electron beam. The layer of graphite was ground off before LA

ICPMS analysis, otherwise it would have to get ground off in a pre-ablation run which adds extra time to the analysis. This block was used to analyse minerals for both major and trace elements. For later analyses on the LA ICPMS, the garnets and micas were analysed in situ in a thick thin section.

Major element mineral analyses by electron probe

Garnets from some of the samples were subjected to major element analyses on the Cameca SX50 wavelength-dispersive electron microprobe at the Natural History Museum. Points for analysis were programmed in for overnight analyses. Quantitative analyses for elements with an atomic number greater than five (boron) gave typical detection limits in the order of 0.01 wt.%. Standards ran during analysis are shown in Table 2-5.

Table 2-5 standards ran during EPMA analysis.

Standard	Composition
JAD3 STD048	O : 47.6%, Na : 11.28%, Mg : 0.05%, Al : 13.33%, Si : 27.79%, Ca : 0.08%, Fe : 0.0%
FOR STD277	O : 45.48%, Mg : 34.55%, Si : 19.98%
BER STD015	Al : 22.1242%, P : 25.3977%, O : 52.4782%
CEL3 STD026	O : 34.84%, S : 17.45%, Sr : 47.7%
HAL2 STD042	Na : 39.3373%, Cl : 60.6627%
KBR3 STD075	K : 32.8551%, Br : 67.1449%
WOL STD097	O : 41.04%, Si : 23.8%, Ca : 34.16%, Fe : 0.6%, Mn : 0.05%
MNT STDIC	Mn : 36.4219%, Ti : 31.756%, O : 31.8221%
CRO2 STDIC	Cr : 68.4195%, O : 31.5805%
FAY STD278	O : 31.4%, Si : 13.78%, Fe : 54.81%
PCO STD121	Co : 100.0%
NIO2 STDIC	Ni : 78.5839%, O : 21.4161%
COR4 STD028	Al : 52.9242%, O : 47.0758%

Mineral analyses by LA-ICP-MS

Garnets from all samples were subjected to analyses by the RESolution L50 LPXPRO220 Excimer 193nm laser ablation system with a two volume laser ablation cell which is coupled to a quadrupole ICPMS at Royal Holloway. The SiO₂ contents obtained by electron microprobe from the Natural History Museum (above) were used as an internal standard; however the SiO₂ values were very constant varying from 37% to 39.2%. External standardisation was done by undertaking two runs of NIST SRM-612 glass standard at the beginning and end of each run, Table 2-6 shows a comparison between MgO and CaO concentrations obtained from the LA ICPMS and the EMPA for several of the garnets from within this study. On days when drift was noted in NIST 612, a drift correction was also applied to the data. The spot size was 44 µm for data acquisition, the repetition was 15 Hz and the raster speed was 0.5 mm/min. For the pre-

ablation the spot size was 74 μm , the raster speed was 12 mm/min which gave a 90% overlap and the repetition was 25 Hz. The attenuator was taken out giving a full strength beam giving 9.5 J/mm²; the energy density of the beam was constant and homogeneous across the beam.

Table 2-6 comparison between CaO and MgO concentrations obtained from EPMA and LA ICPMS for several of the garnets analysed within this study.

	LA ICPMS		EPMA	
	CaO %	MgO %	CaO %	MgO %
AB07-02	5.06	1.45	4.56	1.66
AB07-08	6.71	1.62	9.49	0.61
AB07-09	8.19	8.57	10.83	7.33
AB07-11	7.32	0.96	8.56	1.11
AB07-12	1.6	7.18	4.17	6.28
AB07-13	1.15	4.24	5.10	3.69
AB07-14	5.65	5.71	6.37	4.71
AB07-17	6.55	2.44	7.55	2.13
AB07-18	7.04	6.55	8.09	5.09
AB07-22	11.01	1.47	12.77	1.13
AB07-23	10.78	4.66	9.87	3.84
AB07-27	4.75	0.88	6.54	1.02

Table 2-6 compares CaO and MgO concentrations obtained from the EPMA and the LA ICPMS for several of the garnets analysed in this study. The concentrations are averaged across the garnet which may explain several of the discrepancies between the two methods, as the EPMA only analysed one to three points on each garnet whereas the LA ICPMS analysed a transect across the garnet which may be made up of ~1200 points.

2.7.6 Preparation for Lu-Hf and Sm-Nd analyses

Sample leaching and dissolution

The procedures for sample leaching and dissolution generally followed the guidelines described by Anczkiewicz and Thirlwall (2003). Lu-Hf and Sm-Nd analyses were performed on a single total dissolution. Garnet preparation was undertaken using Savillex beakers that had been cleaned in concentrated HCl for >24 hours at 175°C and concentrated HNO₃ for >24 hours at 175°C before being stored in MQ water. Prior to use the beakers were boiled for 20 minutes in MQ water then placed sealed on the hotplate at 120°C with ~1ml TD HNO₃ and ~4ml TD HF. Garnets were crushed under acetone in an agate mortar until the chips were less than 75 μm , the chips were placed in the savillex beaker using a pipette and put on the hotplate until the acetone had

evaporated. 1ml of sulphuric acid was added to the crushed garnets and left sealed in the beaker on the hot plate at 180°C for 24 hours to leach out phosphate inclusions (Anczkiewicz and Thirlwall 2003) then rinsed multiple times with MQ H₂O. The garnets were weighed before and after the sulphuric stage. From this point onwards the whole rocks and the garnets were treated in the same way. 0.05g of powdered whole rock was weighed into the beakers along with the ¹⁴⁹Sm-¹⁵⁰Nd and ¹⁷⁶Lu-¹⁸⁰Hf spikes. The required spike amount was estimated from elemental concentration data for each sample measured by LA-ICPMS for the garnets and XRF for the whole rock powders in order to achieve a target isotopic ratio shown in Table 2-7.

Table 2-7 target isotopic ratios for spiking.

Spike	Targeted Ratios
¹⁸⁰ Hf/ ¹⁷⁷ Hf	2 – 4
¹⁷⁶ Lu/ ¹⁷⁵ Lu	0.006 – 0.5
¹⁵⁰ Nd/ ¹⁴⁴ Nd	0.28 – 0.65
¹⁴⁹ Sm/ ¹⁴⁷ Sm	1.18 – 2.5

After the spike was added the samples were digested using 3:1 HF: HNO₃ on the hotplate for 48 hours at 160°C then evaporated to dryness. 0.5ml of TD concentrated HNO₃ was added and evaporated to get rid of fluorides. Once this was evaporated, 4ml of SB~8M HCl was added and left on the hotplate for 24 hours at 120°C. The solution was centrifuged to check sample has dissolved completely, any solid that was left was returned to the savillex beaker for further attack by SB~8M HCl. This was repeated until the entire sample was dissolved, the remaining solution was evaporated followed by the addition of a mixture of 2ml of 1M HCl - 0.1M HF ready for cation column chemistry. No zircon was ever seen, thus it was assumed that the majority of the zircon was dissolved along with the sample fraction.

Separation chemistry

A series of columns were used to separate the element fractions summarised in Table 2-8 below.

Table 2-8 columns used for mineral separation.

Fraction added to column	Columns Used	Fractions collected	Fraction analysed	Isoprobe programme used
Sample dissolution	AG50W-X8 (mesh size 200-400) cation resin	Hf, LREE and HREE. HFSE requires a second pass through the same columns to minimize the HREE in this fraction		
LREE fraction	Eichrom LN resin (mesh size 50-100, part no. LN-B25-S)	Nd and Sr	Nd and Sr	Sm147ax Nd143ax
HFSE (after second pass through cation)	Eichrom LN resin (mesh size 50-100, part no. LN-	Hf	Hf	Hf174ax

columns)	B25-S)			
HREE fraction	Eichrom LN resin (mesh size 50-100, part no. LN-B25-S)	Lu and Yb	Lu Part of Yb fraction was added to Lu fraction	YBLUREE

Column Calibration

To achieve the split needed in the Eichrom LN resin columns which were used for separating Lu from Yb, Hf from Zr and Sm from Nd from LREE and MREE it became apparent that careful calibration was needed. This was undertaken by running a standard through the columns then comparing to the standard which had not been put through the columns on the IsoProbe. An example of a calibration is shown below.

Table 2-9, Lu column calibration testing columns 1, 3, 4 and 8. The fractions are arranged in the order they came off the columns, the first fraction should have LREE and MREE, in the second fraction some Yb may be seen, the third fraction is where the majority of the Yb comes off and the last fraction is where Lu is found. The voltage was corrected for the amplifier offset.

Fraction	Masses Tested	Columns Tested (Voltage) Standard 174 – 3 V and 175 – 1.1 V			
		1	3	4	8
4ml load and 3 M HCl Elute	142	0.4			
	144	0.3			
	149	0.6			
	163	0.2	Not tested	Not tested	Not tested
	159	0.003			
	155	0.3			
2 nd ml of 3ml Elute of 4 M HCl	149	-	-	-	-
	163	-	-	-	-
	159	-	-	-	-
	155	-	-	-	-
	172	0.001	-	-	-
	174	0.005	0.0002	0.0001	0.001
	175	-	-	- 0.001	-
	167	-	-	-	-
3 rd ml of 3ml Elute of 4 M HCl	174	0.46	0.31	0.34	0.20
	175	-	-	-	-
4 th ml of 3ml Elute of 4 M HCl	174	0.39	0.50	0.43	0.50
	175	-	-	-	-
5 th ml of 3ml Elute of 4 M HCl	174	0.015	0.023	0.017	0.04
	175	0.018	0.06	0.008	0.0001
2ml 8 M HCl	174	-	- 0.001	-	
	175	0.76	0.10	0.74	Not Tested

Table 2-9 shows when Lu starts coming off the column and the split between Lu and Yb. Next a sample with known Lu and Yb concentrations was run through the columns to test if matrix differences would affect the separation and it gave a similar result.

2.7.7 Lu, Hf, Sm and Nd Mass spectrometry

The analyses were undertaken using the micromass GV IsoProbe MC ICP MS at RHUL. The IsoProbe uses a hexapole collision cell, which reduces the energy spread of ions produced in the plasma and eliminates interferences. Its multicollector has 9 moveable Faraday cups and 3 ion counting detectors. All analyses for this project were run in soft extraction which suppresses secondary ionisation within the interface by applying a slight positive potential instead of a large potential charge between the extraction and skimmer cones. This reduces the machine memory which is very useful when analysing Lu and Hf.

The Sm, Nd and Lu separates were dissolved in 0.1-0.5 ml of 2% HNO₃ and the Hf separate was dissolved in 0.4ml of 2% HNO₃: 0.5% HF. The samples were introduced by a Cetac Aridus nebulizer at a constant uptake rate of about 50 ml/min. The inlet system was cleaned between analyses with 5% HNO₃. In the case of Hf analyses, this was followed by 5% HNO₃: 5% Hf. One issue with analyses using a MC ICPMS is the problem of mass bias, which is preferential extraction of heavier ions. This can be corrected by internal normalisation to a known constant isotope ratio of the same element. Processing of the data yielded by the IsoProbe followed the procedures described by Thirlwall and Anczkiewicz (2004). The IsoProbe measurements were first corrected for the baselines using on peak zeros (OPZ) measured during integrations of the blank solution (2% HNO₃: 0.1% HF for Hf), immediately prior to the analysis of the sample. These OPZ include instrumental memory and amplifier offsets. Corrections for the contribution to peak intensity from adjacent peaks (“tail”), (Thirlwall, 2001) and electronic crosstalk between the Faraday amplifiers (Thirlwall and Anczkiewicz, 2004) are then applied. The collector configuration used for Hf, Lu, Nd and Sm analyses is shown in Table 2-10.

Table 2-10, MC ICPMS collector configurations for Hf, Lu, Nd and Sm analysis.

L3	L2	L1	Ax	H1	H2	H3	H4	H5	H6
Hf									
172	174	-	175	176	177	178	179	180	182
	Hf		Lu	Hf Lu Yb	Hf	Hf	Hf	Hf Ta W	W
Lu									
155	159	163	164	171	172	174	175	176	177
								Lu Yb	Hf
Gd	Tb	-	¹⁴⁸ NdO Dy	Yb GdO GdOH	Yb GdO GdOH DyO	Yb Hf GdO GdOH DyO	Lu TbO GdOH	Hf TbOH GdO DyO	GdOH DyO DyOH
Nd									
140	142	-	143	144	145	146	147	149	150
Ce	Nd Ce		Nd	Nd Sm	Nd	Nd	Sm	Sm	Nd Sm
Sm									
-	143	-	145	146	147	148	149	-	152
-	Nd		Nd	Nd	Sm	Sm Nd	Sm		Sm (Gd)

Instrumental drift, if present, was monitored by running standards every 3 – 6 samples. Hf isotopic ratios were determined using a static procedure and the standard used was JMC 475 97ppb, Figure 2-4 shows its value over the period of time analyses for this project were being carried out.

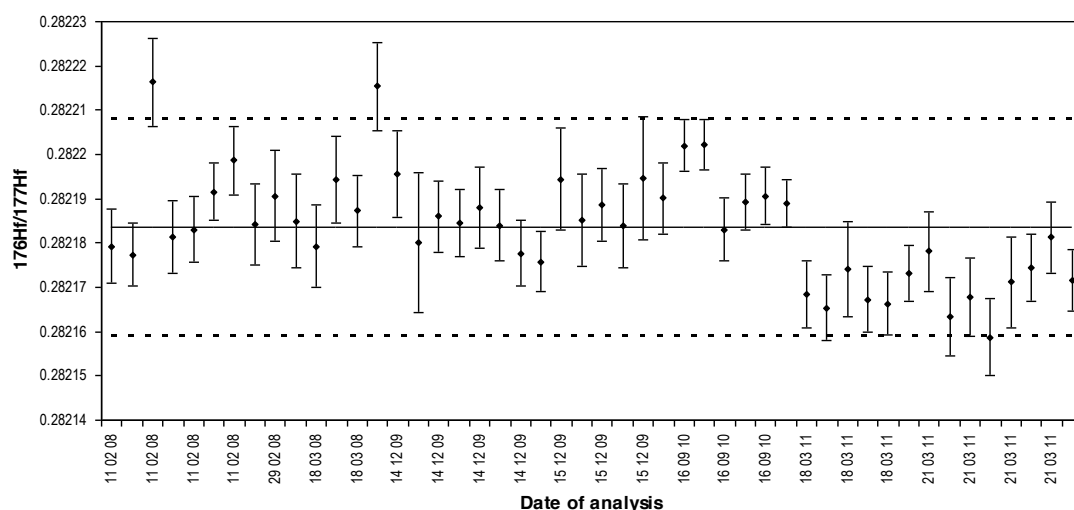


Figure 2-4, standard JMC 475 97ppb over the period of use. It should give a value of 0.282165. The solid line shows the long term mean and the dashed lines mark the 2sd on the long term mean.

120 ppb Sm-40 ppb Nd and 300 ppb Aldrich Nd standards were used for Sm analysis. For Lu analyses 40 ppb Yb-20 ppb Lu and 100 ppb Yb-20 ppb Lu were ran interspersed between the samples to monitor natural $^{176}\text{Yb}/^{175}\text{Yb}$ and $^{175}\text{Lu}/^{176}\text{Lu}$. Gd ~20 ppb, Dy ~40 ppb and ^{159}Tb ~70 ppb were also analysed at the start and end of each day's run to

determine oxide production rates of GdO, GdOH, DyO, TbO and TbOH. Two standards were used for Nd analysis, 200 ppb Aldrich Nd and 200 ppb Aldrich Nd Ce. 200 ppb Aldrich Nd which was corrected to $^{143}\text{Nd}/^{144}\text{Nd}$ values of 0.511407 and 200 ppb Aldrich Nd + 125 ppb Ce was used to determine the value of $^{142}\text{Ce}/^{140}\text{Ce}$ used to correct $^{144}\text{Ce}/^{142}\text{Ce}$ to monitor for Ce interference. The two standards were run every 4 to 6 samples, over the period of study and they gave a mean value of 0.511288 ± 0.000080 (2 sd). This information is shown in Figure 2-5 below with the area between the dashed lines representing the long term mean. The diagram shows a large spread in data which is due to non-exponential mass bias correlation (Thirlwall and Anczkiewicz, 2004), however a correlation between $^{143}\text{Nd}/^{144}\text{Nd}$ and $^{142}\text{Nd}/^{144}\text{Nd}$ can be used to correct the data.

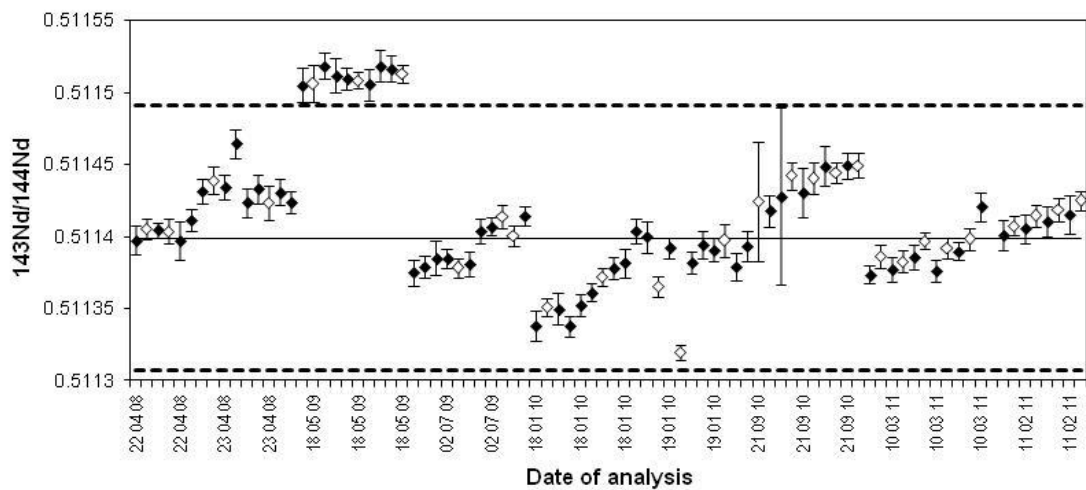


Figure 2-5, $^{143}\text{Nd}/^{144}\text{Nd}$ for 200 ppb Aldrich Nd (black symbols) and 200 ppb Aldrich Nd+Ce (Open symbols) standards should be 0.511407, the area between the dashed lines shows the long term mean.

The measured $^{143}\text{Nd}/^{144}\text{Nd}$ and $^{142}\text{Nd}/^{144}\text{Nd}$ ratios from the standards were used to determine the $^{143}\text{Nd}/^{144}\text{Nd}$ ratios from the samples, which was used to calculate the age. This is done by plotting $^{142}\text{Nd}/^{144}\text{Nd}$ against $^{143}\text{Nd}/^{144}\text{Nd}$ from the standards ran on the day, as shown in Figure 2-6, which make a positive correlation.

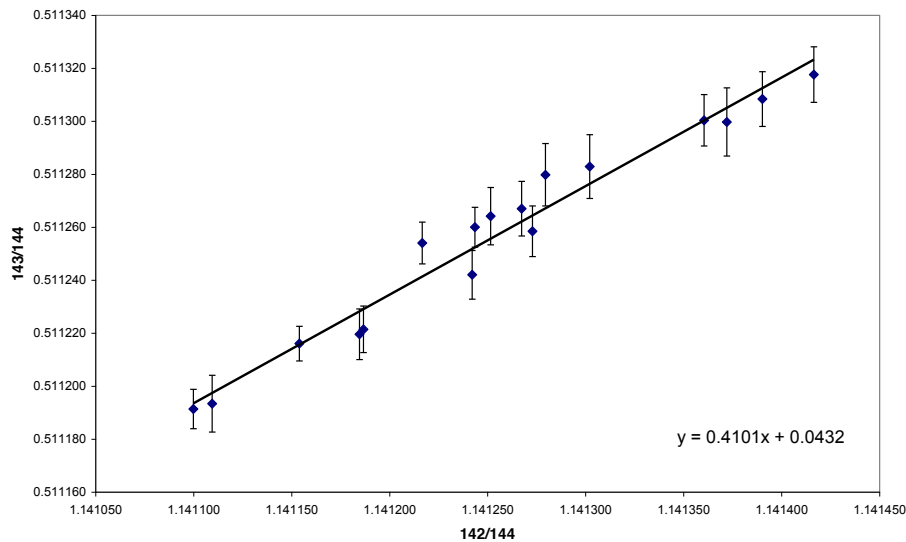


Figure 2-6, $^{143}\text{Nd}/^{144}\text{Nd}$ values from 200 ppb Aldrich Nd and 200 ppb Aldrich Nd Ce plotted against $^{142}\text{Nd}/^{144}\text{Nd}$. The gradient is used to calculate the $^{143}\text{Nd}/^{144}\text{Nd}$ values in the samples.

The gradient from the measured $^{142}\text{Nd}/^{144}\text{Nd}$ versus $^{143}\text{Nd}/^{144}\text{Nd}$ standards (Figure 2-6) and the correct $^{142}\text{Nd}/^{144}\text{Nd}$ standard value are used to calculate the sample $^{143}\text{Nd}/^{144}\text{Nd}$, using the formula shown in Equation 2-13. This corrects for drift during the day and differences between the measured value and the actual standard value.

$$\frac{^{143}\text{Nd}}{^{144}\text{Nd}} = \frac{^{143}\text{Nd}}{^{144}\text{Nd}}m + \text{gradient} \times \left(\frac{^{142}\text{Nd}}{^{144}\text{Nd}}sv - \frac{^{142}\text{Nd}}{^{144}\text{Nd}}m \right)$$

Equation 2-13, shows how $^{143}\text{Nd}/^{144}\text{Nd}$ for the samples was calculated. Abbreviations are m – measured; sv – standard value.

2.7.8 Rb-Sr analysis

Sample dissolution and column chemistry

The muscovites and biotites were picked from the 250-500 μm sieved fraction and then were ultrasonicated in ultra-pure water. Then they were purified by lightly grinding in acetone in an agate mortar then sieving, the mica flakes did not pass through the sieve. The samples were added to clean savillex beakers, which were cleaned using the method detailed above. From this point the whole rocks and the micas were treated in the same way. 0.05g of powdered whole rock was weighed into the beakers along with the mixed ^{87}Rb - ^{84}Sr spike. The mixed Rb-Sr spike was also added to the muscovite fraction. A mixed ^{87}Rb - ^{84}Sr spike with a high Rb/Sr was added to the biotite fraction.

After the spike was added the samples were dissolved using 2ml of TD concentrated HNO_3 and 4ml of HF was added to the samples and they were left sealed on the hotplate at $\sim 150^\circ\text{C}$ overnight then evaporated at $\sim 120^\circ\text{C}$. Then 2ml TD HNO_3 was evaporated, then 6ml 6M HCl was added, and the remaining solution was evaporated followed by the addition of 1 ml of 8M HNO_3 ready for column chemistry. Before loading onto the columns the samples were centrifuged again to separate any solid that may be remaining.

The columns to separate Sr were made by inserting 70 μ frits into pipette tips and then soaked in 10% HNO_3 for ~ 24 hours. The columns were cleaned with 4 M HNO_3 and MQ before adding ~ 5 drops of Eichrom Sr-spec resin. This was then cleaned with 4 M HNO_3 and MQ before being conditioned with 8 M HNO_3 . The sample was then loaded using pasture pipette which had been cleaned in 8 M HNO_3 . The Sr fraction was eluted with ultra pure water and collected in cleaned beakers. The collected was then evaporated, a few drops of TD concentrated HNO_3 was added and evaporated again. The remaining fraction from the columns was retained to separate Rb.

The Rb and K-rich fraction remaining from the columns was evaporated, and then a few drops of concentrated HNO_3 were added and evaporated. 1 ml of 5% HNO_3 was added to each sample and ran through large cation columns.

Bead making and loading procedures

Sr isotopic analyses were run on Re filaments. These were prepared by grinding any old filament material off the bead before spot welding new Re filament into place. These were then cleaned in MQ in a ultrasonic bath to remove any loose material and rinsed before boiling for 10-20 minutes in fresh MQ. After drying the beads were degassed at 5A at a pressure of $< 1.10^{-5}$ mbar and then stored in a bead box for at least 24 hours prior to loading to allow the filaments to oxidise. The samples were loaded onto single Re filaments using H_3PO_4 and once dried the current was raised to $\sim 2\text{A}$ to burn off any excess H_3PO_4 .

2.7.9 Rb and Sr Mass spectrometry

The Sr analyses were undertaken on a VG 354 TIMS at RHUL. The samples were loaded into a 16 sample turret under a pressure of 10^{-7} mbar and were run automatically. The Sr isotopic compositions were determined using a multidynamic programme which

used all five collectors. The multidynamic programme allowed correction for ^{87}Rb interference on ^{87}Sr and recovers both Sr concentration and $^{87}\text{Sr}/^{86}\text{Sr}$ corrected for spike. Two standards of SRM 987 were run alongside the samples usually in turret positions 5 and 12. The standard values over the period of analysis are shown in Figure 2-7 with the area between the dashes lines showing the long term mean.

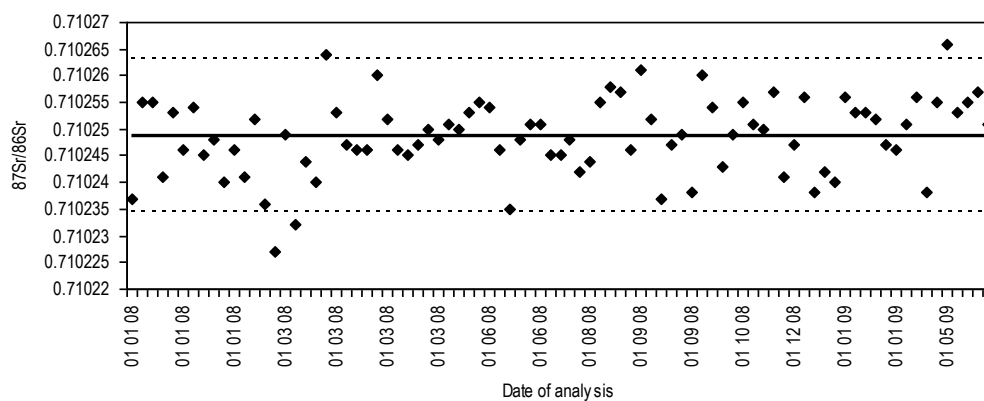


Figure 2-7 Exponential and tail corrected $^{87}\text{Sr}/^{86}\text{Sr}$ for SRM run throughout the period of study. The area between the dashed lines is the long term mean.

Rb was run on the micromass GV IsoProbe MC ICP MS at RHUL, which is described above. As Rb only has two isotopes the data was normalised to Zr to correct mass bias.

3.1 Synopsis

This chapter provides evidence for: 1) early Mesoproterozoic metamorphism at ~1670 Ma and ~1640 Ma within the Borgie inlier in Sutherland and the Eastern Unit of the Glenelg-Attadale inlier respectively, and 2) late Mesoproterozoic eclogite-facies metamorphism at ~1200 Ma within the Eastern Unit of the Glenelg-Attadale inlier. Evidence for 1670-1640 Ma metamorphism has also been reported from the Western Unit of the Glenelg-Attadale inlier by Storey et al. (2010). This event could conceivably correlate with the later Laxfordian events recorded on the Caledonian foreland in Scotland (Kinny et al. 2005; Wheeler et al. 2010) which from a broader perspective are most likely linked with Labradorian (NE Laurentia) and Gothian (Baltica) events (Park 1995; Buchan et al. 2000). The timing of the younger eclogite-facies event is significantly older than that proposed by Sanders et al. (1984). It is suggested here that this event corresponds to the Elzevirian phase of the Grenville orogeny in NE Laurentia (Karlstrom et al. 1999; 2001). A corresponding high-grade metamorphism event is not recorded in Baltica, suggesting a Laurentian affinity for the Scottish basement inliers.

Ages that range between 1020 Ma and 912 Ma recorded by Sanders et al. (1984), Storey et al. (2010), Brewer et al. (2003) and in this chapter have been thought to reflect thermal reworking of the Glenelg-Attadale inliers during the Ottawan phase of the Grenville orogeny. However, data from other parts of this study show that a range of early Neoproterozoic ~980-900 Ma metamorphic events also affected the overlying Moine Supergroup and so are not restricted to the basement inliers. These younger ages recorded from within the Glenelg-Attadale inliers may therefore result, at least in part, from variable to complete degrees of isotopic resetting.

3.2 Introduction

Metamorphic events within the Glenelg-Attadale inlier have previously been dated using Sm-Nd and Lu-Hf geochronology applied to garnets and pyroxenes (Sanders et al. 1984; Storey et al. 2010). Ages between 1082-1010 Ma have been obtained from

the Eastern Unit of the Glenelg-Attadale inlier and 1322-1750 Ma from the Western Unit. The late-Mesoproterozoic ages from the Eastern Unit were interpreted to relate to the latest phase of the Grenvillian Orogeny. The mid-Mesoproterozoic ages from within the Western Unit have been interpreted to relate to the high pressure equivalent of the lower pressure Laxfordian events recorded in the Lewisian Gneiss Complex. The aim of this chapter was to re-analyse rocks from the Eastern Unit to evaluate the Mesoproterozoic age and compare to the more recent ages obtained by Storey et al. (2010) from the Western Unit. This chapter also dates garnets from one of the more northerly inliers to compare with the ages from Glenelg and to published U-Pb zircon ages (Friend et al. 2008).

3.3 Regional Geology

Within the Moine Supergroup there are numerous inliers of highly deformed high grade rocks which are very different from the surrounding Moine in their metamorphic histories and their lithologies (e.g. Ramsay & Spring 1962; Holdsworth 1989). The locations of the inliers are shown in Figure 3-1. They are concentrated in three main areas; northern Sutherland below the Naver Thrust; the Scardroy-Fannich area; and immediately above the Moine Thrust in the Glenelg-Attadale Inlier, and either occupy the cores of major early isoclinal folds (Powell 1974) or lie along thrust planes (Tanner et al. 1970; Rathbone & Harris 1979; Grant & Harris, 2000; Kelley & Powell, 1985).

The basement inliers are always found at the bottom of the Moine lithological succession once the successions have been structurally restored. The inliers usually consist of tonalitic to dioritic hornblende-rich gneisses that are strongly deformed and are often banded with pegmatitic material (e.g. Ramsay 1958; Holdsworth 1989; Friend et al. 2008; Storey et al. 2008). Several of the inliers, including the Glenelg-Attadale inlier, have thin strips of metasediments which usually consist of pelites and marbles and represent an important part of the basement assemblage.

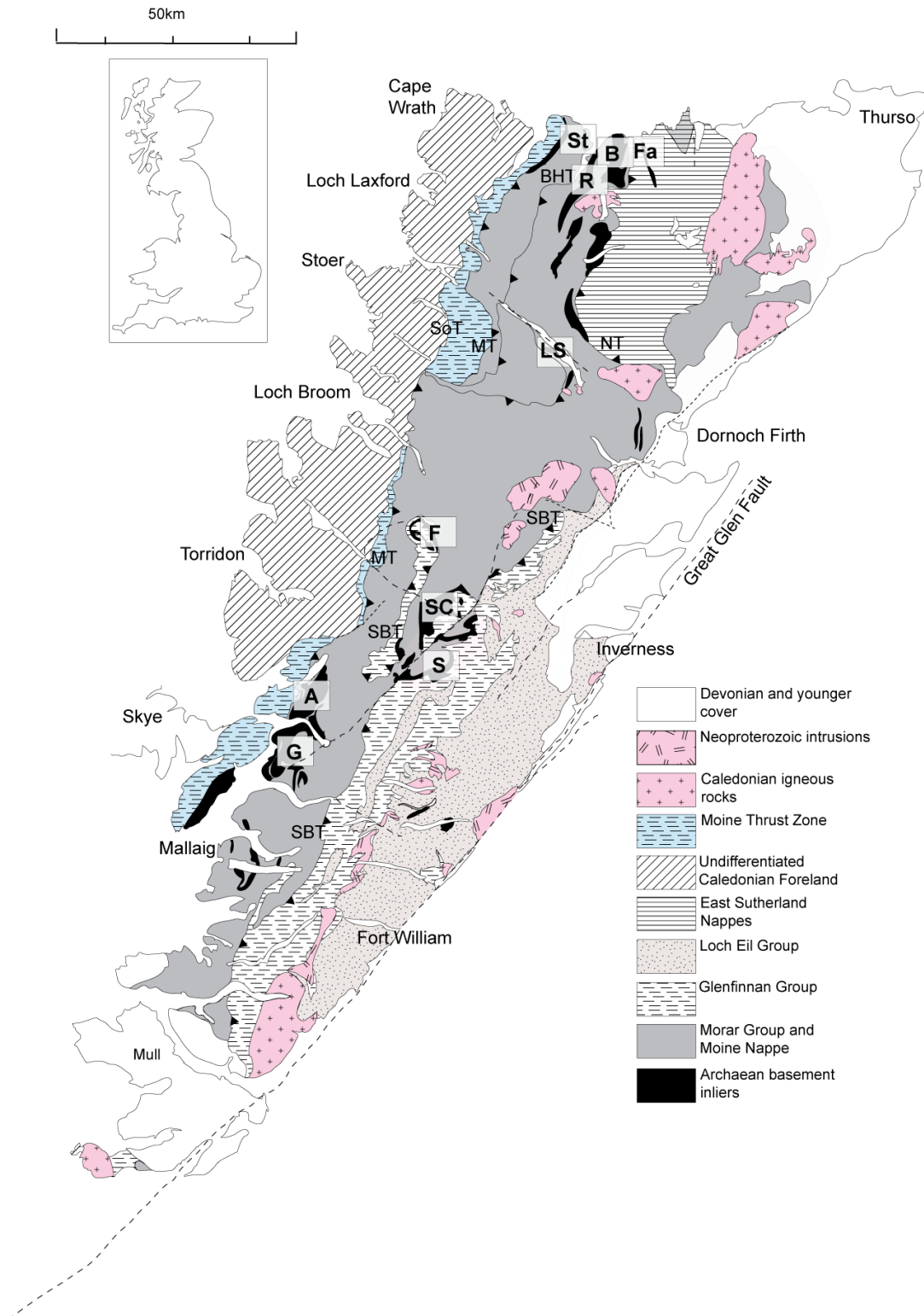


Figure 3-1 sketch map of the Northern Highland Terrane showing the relationship with the basement inliers and the Moine Supergroup. BHT – Ben Hope Thrust; MT – Moine Thrust; NT – Naver Thrust; SBT – Sgurr Beag Thrust; SoT – Sole Thrust. Inliers are: A – Attadale; B – Borgie; F – Fannich; Fa – Farr; G – Glenelg; LS – Loch Shin; R – Ribigill; S – Glen Strathfarrar; SC – Scardroy; St – Strathan.

The prevailing metamorphic grade seen in all the inliers is now amphibolite facies or lower, as the gneisses have been extensively reworked and retrogressed during Knoydartian (840-700 Ma) and Caledonian (480-420 Ma) orogenic events. However some inliers locally preserve evidence of high-grade metamorphic assemblages, these include the Glenelg-Attadale inlier where relict granulite and eclogite assemblages are preserved (e.g. Barber & May 1975; Sanders 1979; Storey 2004; Storey et al. 2010). Early high grade assemblages have also been reported from the Borgie inlier, where retrogressed garnet-clinopyroxene-bearing mafic gneisses have been reported (Moorhouse 1976; Holdsworth et al. 2001).

3.4 Regional basement (pre-1 Ga) geology of NW Scotland and related areas

Figure 3-2 shows the pre-Mesoproterozoic setting of Laurentia and Baltica, and the possible areas which could be correlated with the basement inliers within the Moine Supergroup. The following section discusses these possible correlations and compares them to the previously published data from the basement inliers within the Moine Supergroup.

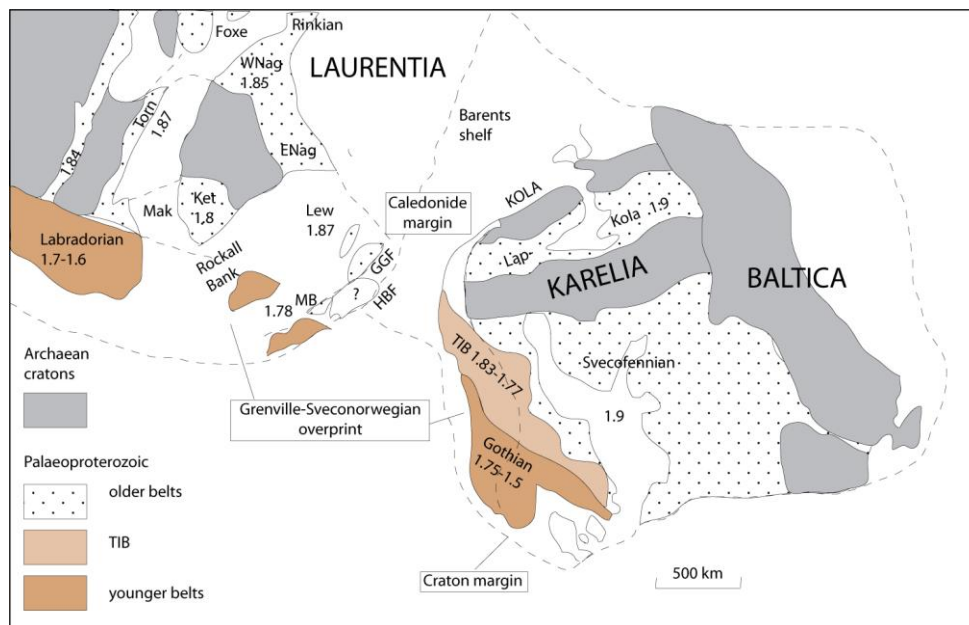


Figure 3-2, from Park (1985), reconstruction of eastern Laurentia and Baltic between 1900-1500 Ma. Abbreviations Lew – Lewisian; HBF – Highland Boundary Fault; NAC – North Atlantic Craton (Nain); SUP – Superior craton; Mak – Makkovik belt; Ket – Ketilidian belt; Lap-Kola – Lapland-Kola belt; TIB – Trans-Scandinavian igneous belt; W Nag – W NagssuGrtoqidian belt; E Nag – E NagssuGrtoqidian (or Ammassalik) belt; B – BABEL deep seismic reflection line.

3.4.1 The Lewisian Gneiss Complex

The tectonic relationship of the basement inliers with the overlying Moine has been a source of controversy since the early work of the Geological Survey. Early work correlated the inliers with the Lewisian basement of the Caledonian foreland to the west (e.g. Johnstone 1975; Rathbone & Harris 1979), because of their high grade nature and lithological similarities to the gneisses of the Lewisian Gneiss Complex (e.g. Flett 1905; Peach et al. 1907, 1910, 1913).

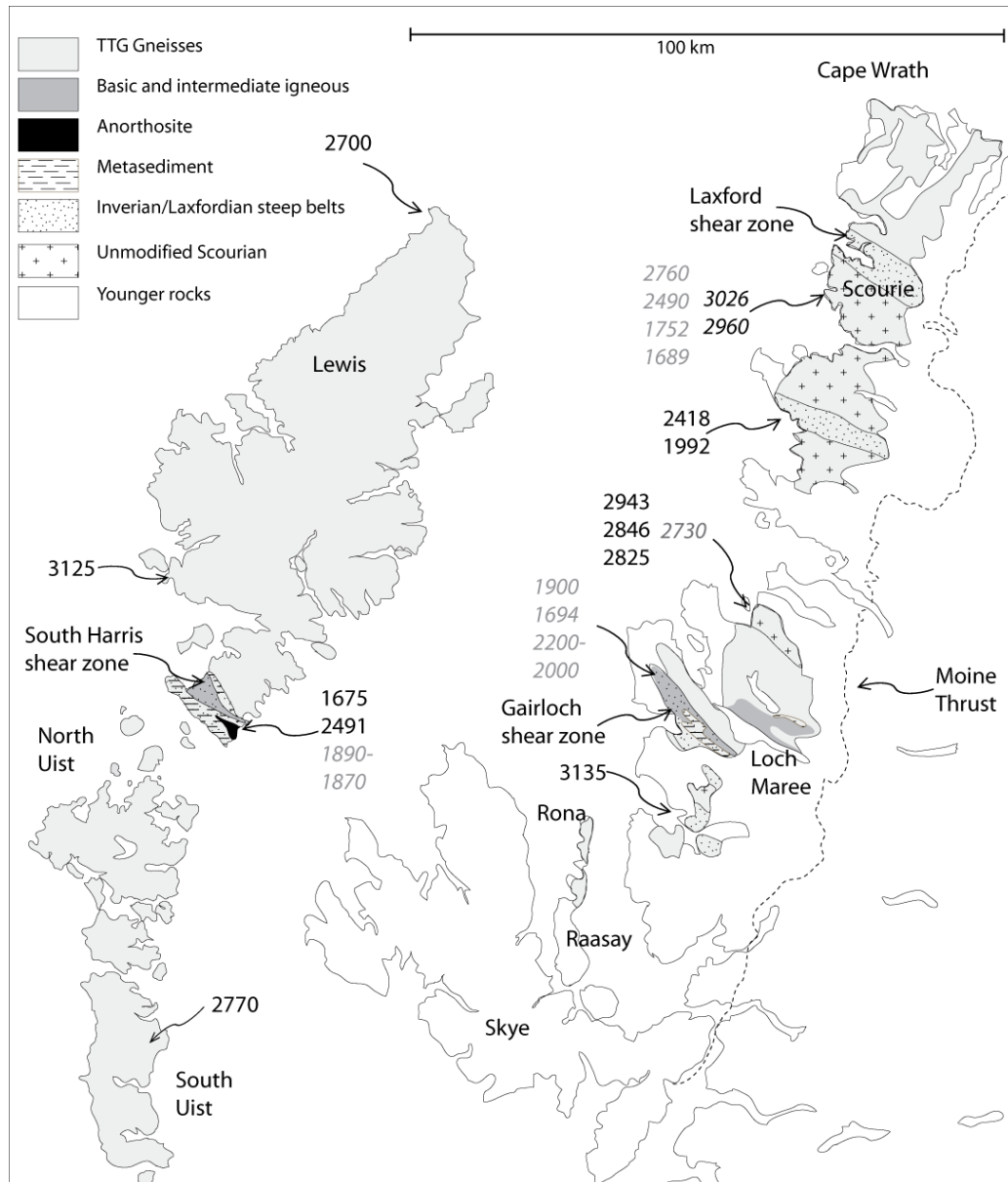


Figure 3-3. Adapted from Wheeler et al. 2010. Rock types, protolith and metamorphic ages from the Caledonian Foreland. Protolith ages are shown in normal text and metamorphic ages are shown in grey italics. Ages are mainly U-Pb zircon ages and are detailed in Table 3-1.

Another view was that the inliers were integral parts of the Moine Succession (Sutton & Watson, 1953, 1954), prompting the famous ‘Lewisian inlier’ controversy of the 1950’s. However, the detailed work of Ramsay (1958) reestablished the basement affinities of the inliers and this has been confirmed by isotopic dating (Moorbath & Taylor 1974; Friend et al. 2008).

The Lewisian Gneiss Complex is dominantly composed of Archaean TTG-gneisses with protoliths as old as 2960-3030 Ma (Friend & Kinny 2001) and a few occurrences of metasediments and meta-volcanics. The Lewisian is composed of distinct crustal units or terranes which were assembled at various times during the Proterozoic (Kinny & Friend 1997; Whitehouse et al. 1997; Friend & Kinny 2001; Whitehouse & Bridgewater 2001; Love et al. 2004). Metamorphic events have been recorded at 2700-2800 Ma within the Outer Hebrides and the Mainland terranes. Later events have been recorded at 2490 Ma from within the Assynt terrane and 1800-1600 Ma within Tarbet, Rhiconich, Assynt, Gairloch, Rona and Ialltaig terranes. These are shown in Figure 3-3. There is some geochronological evidence that supports correlation of the inliers with the Lewisian Gneiss Complex, summarised in Table 3-1.

Table 3-1 summary of geochronology from basement rocks of NHT and the Lewisian Gneiss Complex, adapted from Wheeler et al. (2010). Abbreviations; EU – Eastern Unit; WU – Western Unit.

Date	Area	Lithology	System	Technique	Mineral(s)	Event	Reference
995	Inlier EU	eclogite	U-Pb		zircon	Amphibolite retrogression	Brewer et al 2003
1010	Inlier EU	eclogite	Sm-Nd			Amphibolite retrogression	Sanders et al 1984
1082	Inlier EU	eclogite	Sm-Nd	ID-TIMS	grt-omp-WR		Sanders et al 1984
1322	Inlier WU	eclogite	Sm-Nd	MC-ICPMS			Storey et al 2010
1586	Inlier WU	granulite	Sm-Nd	MC-ICPMS			Storey et al 2010
1667	Inlier WU	eclogite	Lu-Hf	ID-TIMS	grt-omp	Eclogite facies	Storey 2008
1675	South Harris	granite	U-Pb	SHRIMP	zircon	Intrusion	Friend & Kinny 2001
1689	Scourie	Scourie dyke (norite)	U-Pb	ID-TIMS	rutile	Metamorphism	Heaman & Tarney 1989
1694	Tollie	pegmatite	U-Pb	ID-TIMS	zircon	syntectonic to D3	Park et al 2001
1718	Inlier WU	Granulite	Lu-Hf	MC-ICPMS		Granulite facies	Storey et al 2010
1750	Inlier WU	mafic dyke	U-Pb			Minimum age for eclogite meta morphism	Storey et al 2010
1752	Scourie	metasediment	U-Pb	Ion microprobe	monazite	Amphibolite	Zhu et al 1997
1855	Laxford	granite	U-Pb	SHRIMP	zircon	Intrusion	Friend & Kinny 2001
1870	South Harris	meta-anorthosite	Sm-Nd	ID-TIMS	4 mineral isochron	Cooling after granulite	Cliff et al 1983
1888	South Harris	diorite, norite	U-Pb	ID-TIMS	zircon	Intrusion	Mason et al. 2004
1903	Ard gneiss	metagranitoid	U-Pb	ID-TIMS	zircon	Syntectonic to	Park et al 2001

						D1/D2	
1992	Assynt	Scourie dyke (gabbro)	U–Pb	ID-TIMS	baddeleyite	Intrusion	Heaman & Tarney 1989
2000	Loch Maree	metasediment	U–Pb	Ion microprobe	zircon	Source area	Whitehouse et al 1997
2418	Assynt	Scourie dyke (picrite)	U–Pb	ID-TIMS	baddeleyite	Intrusion	Heaman & Tarney 1989
2490	Scourie	TTG	U–Pb	SHRIMP	zircon	Granulite facies	Friend & Kinny 2001
2490	Scourie	basic gneiss	Sm–Nd	ID-TIMS	4 or 5 mineral isochrons	Closure, 600 °C	Humphries & Cliff 1982
2490	Scourie	felsic granulite	U–Pb	ID-TIMS	zircon	Granulite facies	Corfu et al 1994
2491	South Harris	anorthosite	U–Pb	ID-TIMS	zircon	Intrusion	Mason et al. 2004
2526	Scourie	metasediment	U–Pb	Ion microprobe	monazite in grt	Granulite facies	Zhu et al 1997
2677	Inlier WU	retrogressed gneiss					Friend et al 2008
2680	Northern District	hbl-bt mafic tonalite	U–Pb	SHRIMP	zircon	Youngest TTG in Northern District	Kinny & Friend 1997
2730	Gruinard Bay	tonalitic granulite	U–Pb	SHRIMP	zircon	Granulite facies	Love et al 2004
2700	N tip Lewis	diorite	U–Pb	Ion microprobe	zircon	Intrusion	Whitehouse & Bridgewater 2001
2760	Scourie	metasediment	U–Pb	Ion microprobe	monazite in grt	Granulite facies	Zhu et al 1997
2770	Corodale	mafic gneiss	Sm–Nd	ID-TIMS	WR	Intrusion	Whitehouse 1993
2825	Gruinard Bay	tonalitic granulite	U–Pb	SHRIMP	zircon	Intrusion	Love et al 2004
2840	Northern District	biotite gneiss	U–Pb	SHRIMP	zircon	Oldest TTG in Northern District	Kinny & Friend 1997
2846	Gruinard Bay	hornblende-metagabbro	Sm–Nd	ID-TIMS	WR	Intrusion	Whitehouse et al 1996
2880	Inlier Borgie	felsic gneiss				Protolith	Friend et al 2008
2905	Farr inlier	felsic gneiss				Protolith	Friend et al 2008
2943	Gruinard Bay	main amphibolite	Sm–Nd	ID-TIMS	WR	Intrusion	Whitehouse et al 1997
2960	Central District	tonalitic granulite	U–Pb	SHRIMP	zircon	Youngest TTG in Central District	Friend & Kinny 2001
3026	Scourie	tonalitic gneiss	U–Pb	SHRIMP	zircon	Oldest TTG in Central District	Kinny & Friend 1997
3125	South Harris	migmatitic gneiss	U–Pb	SHRIMP	zircon	Intrusion	Friend & Kinny 2001
3135	Torridon	TTG	U–Pb	SHRIMP	zircon	Oldest TTG in Southern District	Kinny et al 2005

Friend et al. (2008) dated zircons from orthogneisses samples from four basement inliers in order to test potential correlations with the Lewisian Gneiss Complex. A U–Pb zircon age of 2.9 Ga was obtained from within the Borgie inlier in Sutherland, although this age is very discordant with a lower intercept of 1600 Ma. The 2.9 Ga protolith age is shared by the Farr and Ribigill inliers. The 2.9 Ga age is seen in the Assynt terrane of the foreland and the 2.8 Ga age is seen the Rhiconich terrane, thus demonstrating some potential correlation between the inliers and the foreland. More evidence of a similarity was provided by Moorbath & Taylor (1974) who obtained an Rb–Sr whole rock age of

2810 ± 120 Ma from the Scardroy Inlier, an age of 2741 ± 120 Ma (MSWD 7.3) is obtained by employing the more recently determined ^{87}Rb decay constant of $1.42 \times 10^{-11} \text{ yr}^{-1}$ instead of $1.39 \times 10^{-11} \text{ yr}^{-1}$. Friend et al. (2008) suggested that the differences between the inliers and the Lewisian are no greater than those recorded between the different terranes within the Lewisian, which could suggest that the inlier gneisses could be a part of the Lewisian Gneiss Complex. However, this evidence only suggests a similarity between the protolith ages of the inliers and the foreland and not their metamorphic histories, thus is not definitive proof of correlation.

Evidence that the inliers and the Lewisian Gneisses may share metamorphic events includes recent ages from the Western Unit (WU) of the Glenelg-Attadale inlier. A granulite within the WU gave an age of $1718 \pm 6 \text{ Ma}$ using a Lu-Hf isochron defined by clinopyroxene and two garnet fractions and the WU eclogite gave a Lu-Hf age (also using two garnet fractions and a clinopyroxene fraction) of $1667 \pm 6 \text{ Ma}$ (Storey et al. 2010). A mafic sheet was also dated and gave a U-Pb zircon age of $1750 \pm 17 \text{ Ma}$ which has been interpreted as the minimum age of eclogite facies metamorphism, as the zircon fraction of the dated eclogite lies on the same regression line (Storey et al. 2010). These ages are similar to U-Pb rutile and monazite ages of 1689 Ma and 1752 Ma from Scourie which are interpreted to date amphibolite-facies metamorphism (Heaman & Tarney, 1989; Zhu et al. 1997).

If the basement inlier of the Northern Highland terrane were to correlate with the Lewisian Gneiss Complex, there would be no need for the Moine Supergroup and its associated basement to be grossly allochthonous relative to the Caledonian foreland (Bluck et al. 1997).

3.5 The Rhinns Complex and Annagh Gneiss Complex

Two other areas of basement rocks within the British Isles with which the basement inliers of the Northern Highland terrane could be correlated with are the Rhinns Complex and the Annagh Gneiss Complex of north-west Ireland (Figure 3-4).

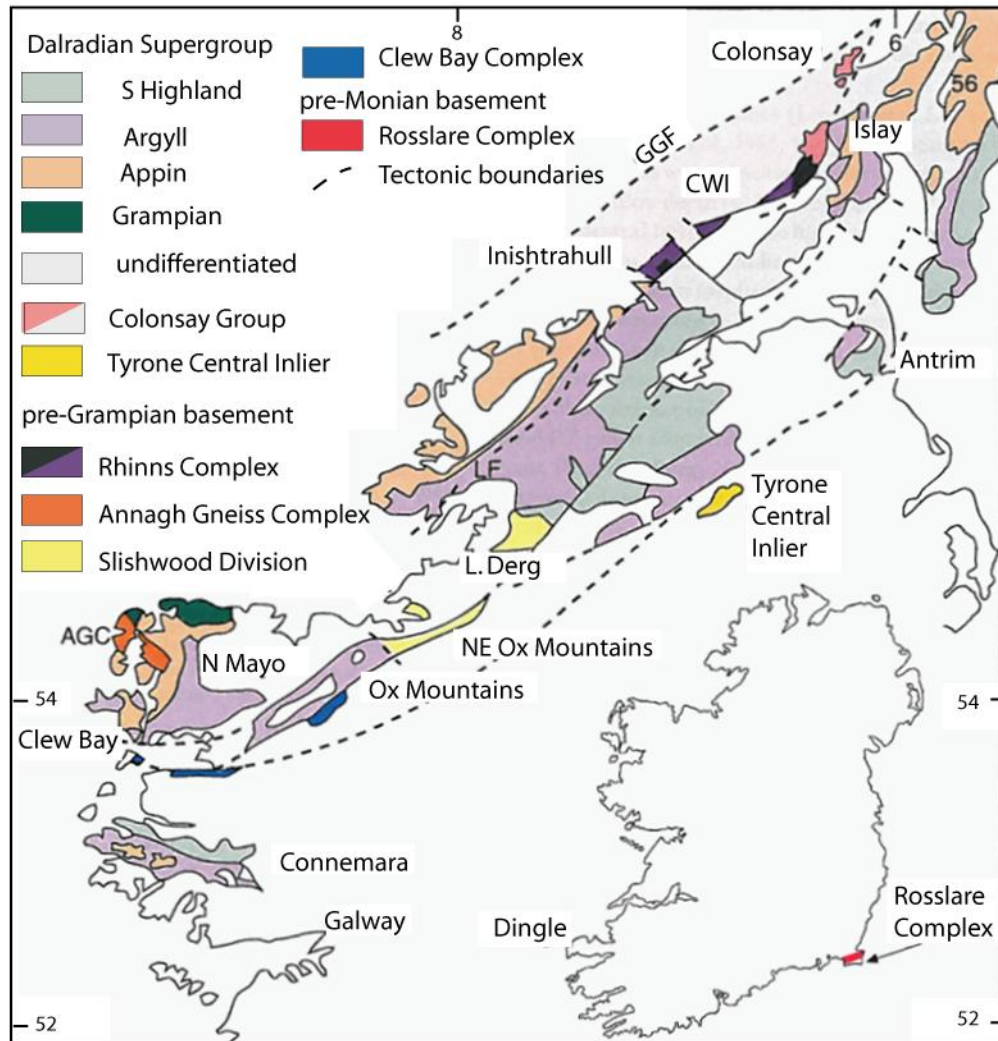


Figure 3-4 map showing the location of Precambrian rocks in Ireland and SW Scotland. Abbreviations: AGC – Annagh Gneiss Complex; CWI – Colonsay West Islay block; GGF – Great Glen Fault; LF – Leannan Fault (Daly 2009).

The Rhinns Complex occurs within the Colonsay West Islay block (Figure 3-4) and consists of metamorphosed alkaline igneous rocks with intruded syenites and gabbros. The rocks are gneissose and generally have been metamorphosed to amphibolite-facies except where they have been retrogressed. The gneisses are overlain by Neoproterozoic meta-sediments which have been assigned to the Dalradian Supergroup (Daly 2009).

One of the syenitic gneisses of the Rhinns Complex in Ireland has given a crystallisation U-Pb zircon age of 1779 ± 3 Ma (Daly et al. 1991); a U-Pb zircon age of 1782 ± 5 Ma was also recorded from the Rhinns Complex in Islay which is also interpreted as a crystallisation age (Marcantonio et al. 1998). Sm-Nd model ages give

dates between 1978-1912 Ma (Daly 2009). Metamorphic zircons from the Rhinns Complex on Islay yielded ages of 1725-1729 Ma (Loewy et al. 2003), which is similar to a $^{40}\text{Ar}/^{39}\text{Ar}$ age of 1710 Ma from a metagabbro which is also interpreted to date metamorphism. These ages are similar to the age of high pressure metamorphism recorded within the WU of the Glenelg-Attadale inlier, and the Laxfordian event of the Lewisian Gneiss Complex (Corfu et al. 1994; Storey et al. 2010).

The Annagh Gneiss Complex is located in the North Mayo Inlier, and structurally underlies Dalradian metasediments (Figure 3-4, Figure 3-5). It is composed of intermediate to acid orthogneisses which have been partially migmatized in places. Amphibolized basic bodies are also present which are generally concordant with the main fabric. Later pegmatites have intruded cross-cutting the main fabric making it possible to deduce a geological history (Daly 2009).

The Annagh Gneiss Complex has been split into three units, the Mullet gneisses, Cross Point gneisses and Doolough gneisses, based on U-Pb zircon ages (Figure 3-5). The Mullet gneisses give U-Pb zircon ages of ~1750 Ma, the Cross Point gneisses give ~1280 Ma and the Doolough gneisses give ~1180 Ma (Daly 1996; Fitzgerald et al. 1996). Sm-Nd model ages for the Annagh Gneiss Complex are in the range of 2.0-1.7 Ga. Magmatism within the Cross Point gneisses was dated using U-Pb zircon at 1287-1271 Ma which was interpreted to be anorogenic and related to melting of pre-existing Mullet gneisses (Daly 2009). The Annagh Gneiss Complex has undergone at least three phases of deformation which are thought to relate to the Grenville orogeny. The earliest two phases occurred between 1177-1015 Ma which could relate to the Ottawa orogeny. The later phase occurred between 980-940 Ma and could relate to the main Grenville deformation phase in Labrador which occurred at 1010-990 Ma and was followed by the intrusion of granites at 966-956 Ma (Gower 1996). These events are seen to young to the east, thus the youngest deformation phase recorded within the Annagh Gneiss Complex could relate to this younging of deformation towards the east (Daly 2009).

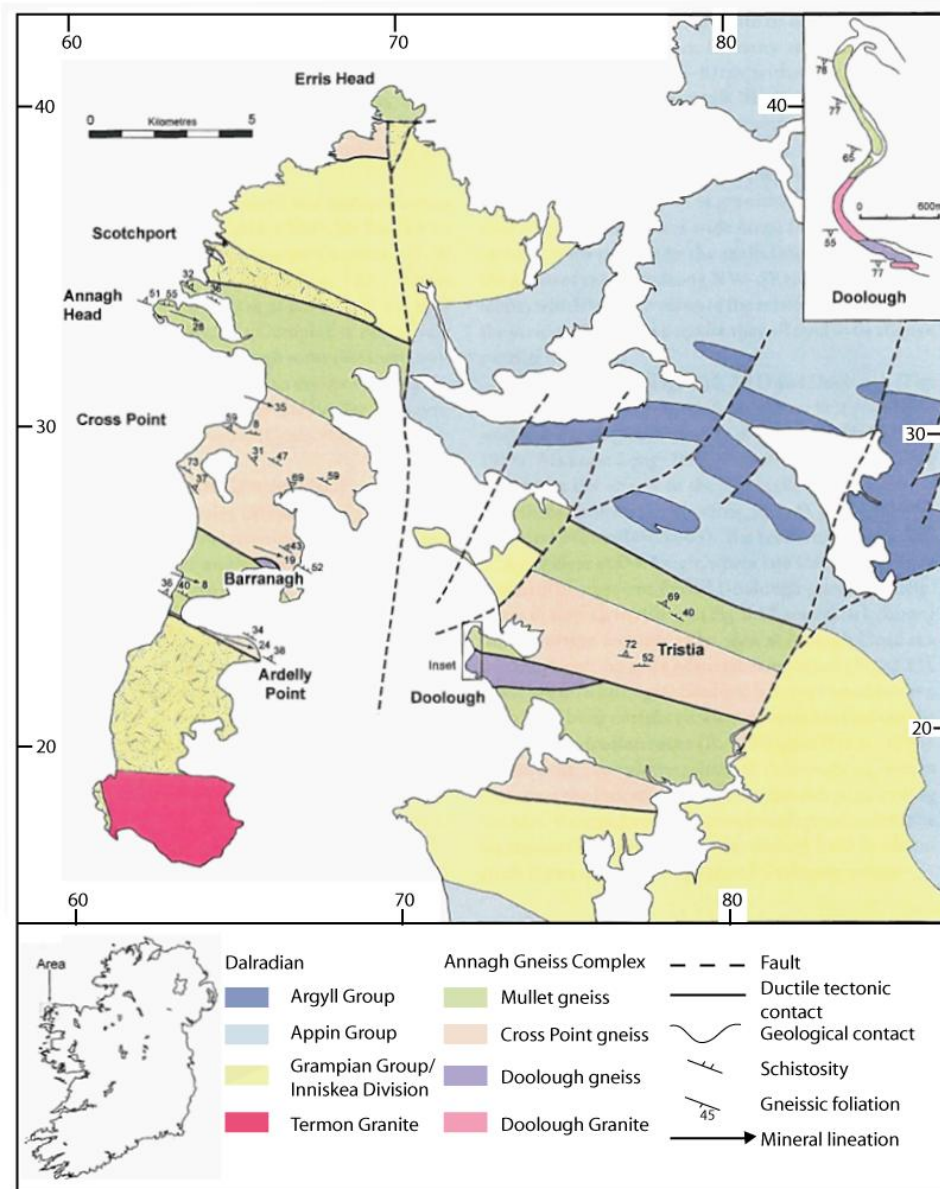


Figure 3-5 sketch map of the Annagh Gneiss Complex within the North Mayo Inlier showing the subdivisions of the Annagh Gneiss Complex (Daly 2009).

Both the Rhinns Complex and the Annagh Gneiss Complex yield ~1750 Ma intrusion ages and Sm-Nd model ages that range between 2.0-1.7 Ga, suggesting that they cannot correlate directly with the Lewisian Gneiss Complex as the latter gives dominantly Archaean protolith ages. The Rhinns Complex records amphibolite-facies metamorphism at ~1730-1710 Ma which could suggest there was a common metamorphic event shared by the Rhinns Complex, the WU and the Lewisian Gneiss Complex. The Annagh Gneiss Complex shows extensive deformation related to the Grenville orogeny which is similar to the Eastern Unit of the Glenelg-Attadale inlier.

3.5.1 East Greenland

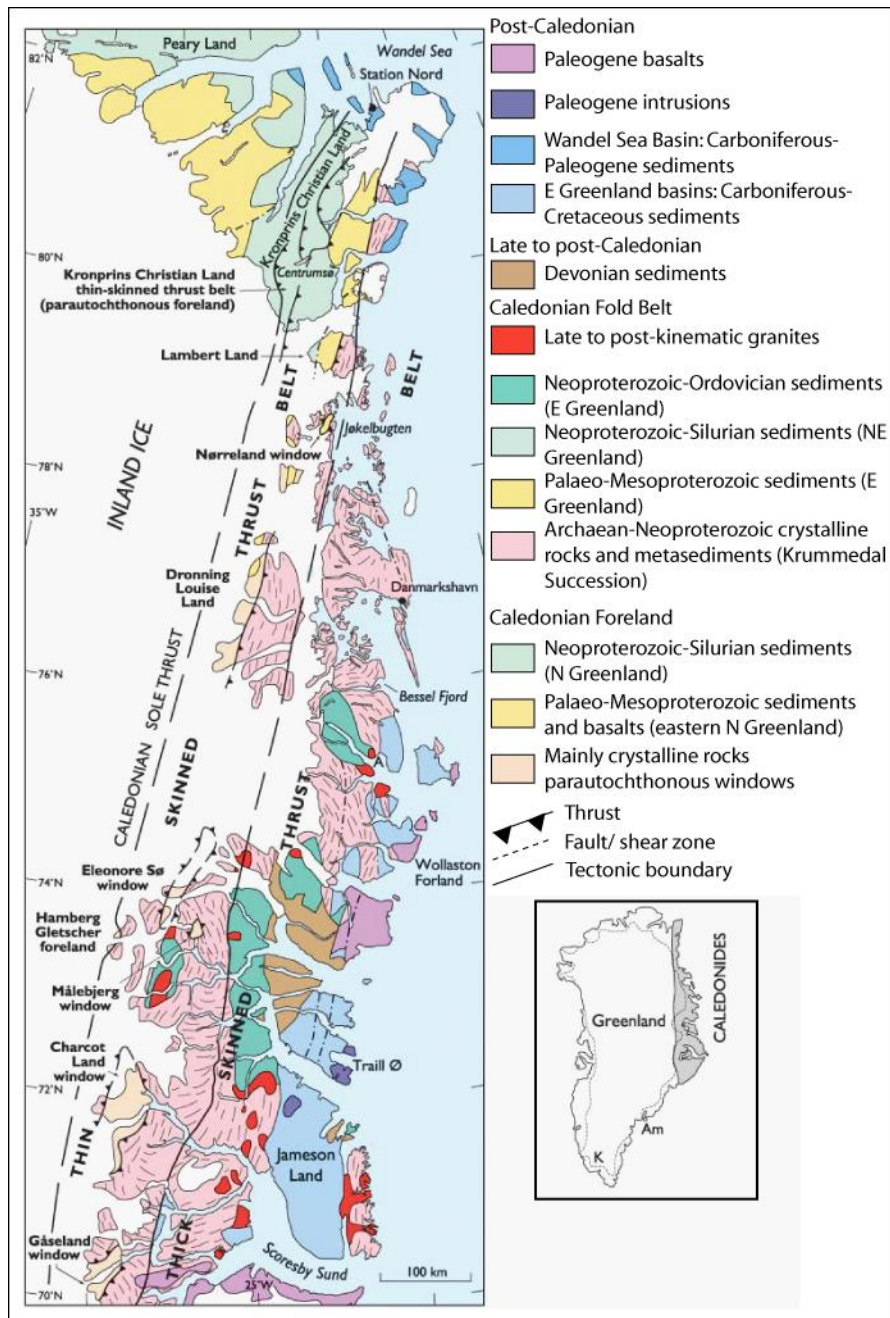


Figure 3-6 simplified geological map of the East Greenland Caledonides from Higgins et al. (2004). The western limit of deformation is largely concealed by Inland Ice. Abbreviations A – Ardencaple Fjord; Am – Ammassalik; K – Ketilidian orogen.

The Caledonides of East Greenland (Figure 3-6) share a Neoproterozoic to lower Palaeozoic geological with the Scottish Highlands, as both regions have Laurentian foreland successions and parautochthonous successions that can be correlated (Leslie et al. 2008), thus it seems likely that their basements may be correlatable. The comparable

sequence of Moine meta-sediments in East Greenland is represented by the Krummedal succession (Higgins, 1988), widely distributed in both the Niggli Spids and the Hagar Bjerg thrust sheets. The Krummedal succession appears to have shared a similar provenance to the Moine Supergroup (Friend et al. 2003), indicating that late Mesoproterozoic sedimentary basins extended over a very large area ($>1000 \text{ km}^2$), and the Krummedal succession may represent a northward continuation of marine dispersal of parts of the Moine Supergroup (Leslie et al. 2008). The Dalradian Supergroup is of a similar age to the Eleonore Bay Supergroup, the overlying Tillite Group and the Kong Oscar Fjord Group within the Franz Joseph Allochthon, Figure 3-6 (Higgins & Phillips 1979; Higgins et al. 2004).

The basement of the East Greenland Caledonian fold belt is Archaean/ Proterozoic orthogneisses with local supracrustals rocks comprising of paragneisses, marbles and amphibolites (Chadwick & Friend 1991). The north-eastern part of the basement consists of Palaeoproterozoic orthogneisses. The orthogneisses give Rb-Sr whole rock ages which lie on a $\sim 2.0 \text{ Ga}$ isochron (Kalsbeek et al. 1993) and zircon SHRIMP U-Pb ages of $1774 \pm 17 \text{ Ma}$, $1764 \pm 20 \text{ Ma}$ and $1739 \pm 11 \text{ Ma}$ (Kalsbeek et al. 1993; Nutman & Kalsbeek 1994), the two younger ages are within error of ages from the Lewisian Gneiss Complex, the Western Unit of the Glenelg-Attadale Inlier, the Rhinns Complex and the Annagh Gneiss Complex. Two ages of $1909 \pm 6 \text{ Ma}$ (Tucker et al. 1993) and $1960 \pm 15 \text{ Ma}$ (Kalsbeek et al. 1993) have been obtained using U-Pb zircon dating which are similar to the first age quoted above suggesting a significant crustal formation event (Kalsbeek et al. 1993). Sm-Nd model ages range from 2.11-3.39 Ga suggesting that many of the samples contain an older crustal component (Kalsbeek et al. 1993).

The basement rocks to the south give Archaean ages as well as Palaeoproterozoic protolith ages. Metamorphic ages of $\sim 1900 \text{ Ma}$ and 1000 Ma have been found for two sequences of supracrustal rocks, the latter age is coeval with ages of $\sim 1050\text{-}800 \text{ Ma}$ from granitic intrusions. This suggests that the southern part of the basement has been affected by the Grenville orogeny and the northern part has not, which could indicate a similarity to the Annagh Gneiss Complex and the Glenelg-Attadale inlier. The Eastern Greenland basement also records Caledonian metamorphism.

3.5.2 The Grenville Belt

The Grenville-Sveconorwegian orogeny culminated in the formation of the super-continent Rodinia. The Grenville orogeny resulted from the collision between Amazonia and Laurentia (e.g. Tolver et al. 2005; Karlstrom et al. 1999; Bartholomew & Hatcher 2009), the Sveconorwegian arm of this collision formed from the collision between Baltica and Laurentia (e.g. Bingen et al. 2008). Figure 3-7 shows the spatial relationship between the Northern Highland terrane basement inliers and the rest of the Grenville margin and Laurentian geology.

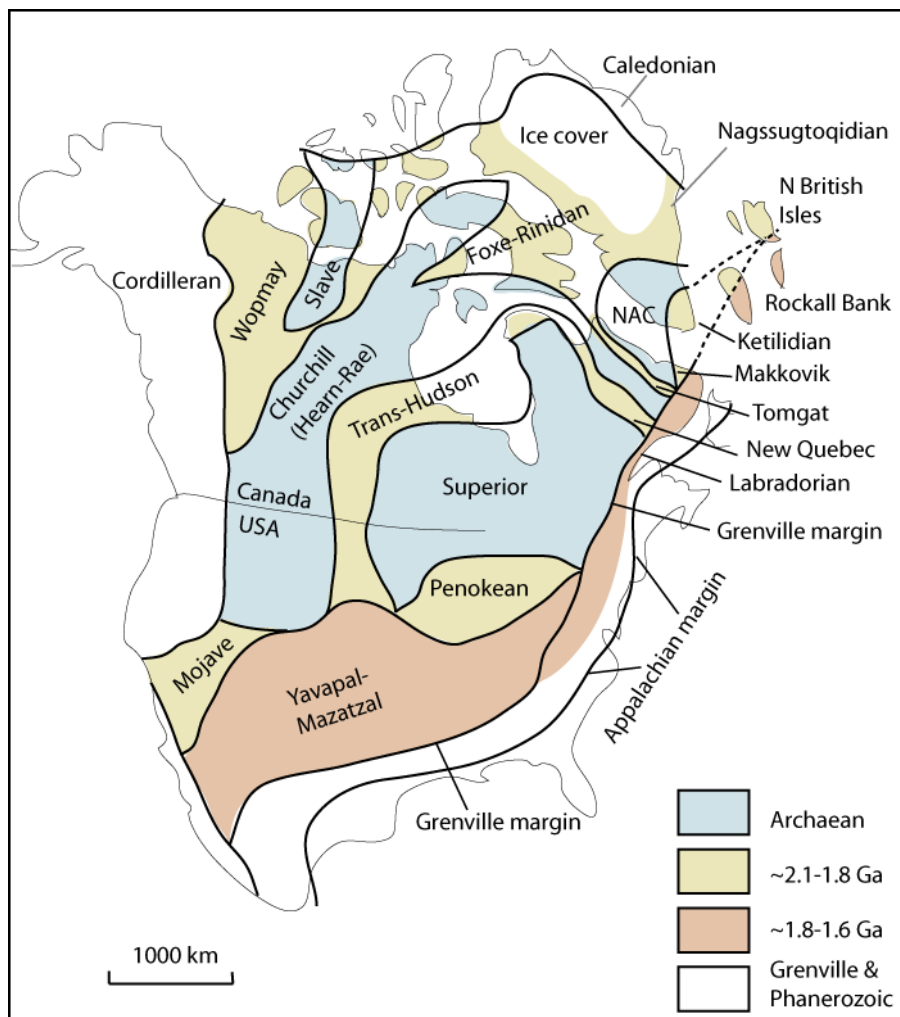


Figure 3-7 Geology of Laurentia (Buchan et al. 2000). Greenland, Rockall Bank and northern British Isles are shown in a pre-Mesozoic reconstruction with respect to the rest of Laurentia. NAC – North Atlantic craton, comprising the Nain Province of eastern North America and its equivalent in southern Greenland.

In NE Canada, the Grenvillian rocks are divided into allochthonous terranes which form a south-easterly dipping thrust stack emplaced over the southern margin of the Archaean

age Superior Province and reflect the accretionary growth of south-eastern Laurentia (Karlstrom et al. 2001). Rocks within the thrust stack range from Archaean to late Mesoproterozoic in age, with older units occupying the lower levels of the thrust stack, and the younger units within the higher levels to the south east. Other than the youngest intrusive granites, all the rocks within the Grenville Province were highly deformed at 1220-980 Ma, and comprise a variety of rock types including marbles, pelites, meta-volcanics, granulites, eclogites, granites and migmatites. The Grenville orogenic cycle comprised mostly amphibolite to granulite facies metamorphism (Karlstrom et al. 2001). High-K calc-alkali granitoids from within south-west Norway suggests that subduction beneath Baltica continued to as late as 1040 Ma (Bingen & van Breemen, 1998), which could explain the young metamorphic ages from eclogites within SW Sweden which have yielded a ion probe zircon age of 972 ± 14 Ma and a U-Pb titanite age of 945 ± 4 Ma (Johansson et al. 2000).

Assembly of the Grenville orogenic belt may have taken place in several stages. The earliest stage was the Elzevirian event (1250-1200 Ma) which was caused by collision of an island arc with the continental margin, this is viewed by some authors as the earliest part of the Grenville orogenic cycle (e.g. Karlstrom et al. 2001; McLelland et al., 1996) and by others as a separate earlier orogeny (e.g. Bartholomew & Hatcher 2009; Gower & Krugh, 2002). For the purposes of this chapter it will be discussed as an integral part of the Grenville orogeny. The Elzevirian is most strongly recorded within the allochthonous units in the southern western part of the orogen in NE Canada (Figure 3-8) and is largely absent south of the Green Mountains (McLelland et al., 1996). It was followed between 1200-1150 Ma by the Shawinigan phase and between 1080-1020 Ma the Ottawan phase which is recorded in the allochthonous belt (Figure 3-8) and was characterised by orogen-wide terrane accretion and magmatism (Rivers, 2009). The latest Rigolet phase (1020-1000 Ma) which is recorded within the parautochthonous belt (Figure 3-8) and was associated with collision with the micro-continent Oaxaquia (Rivers, 2009).

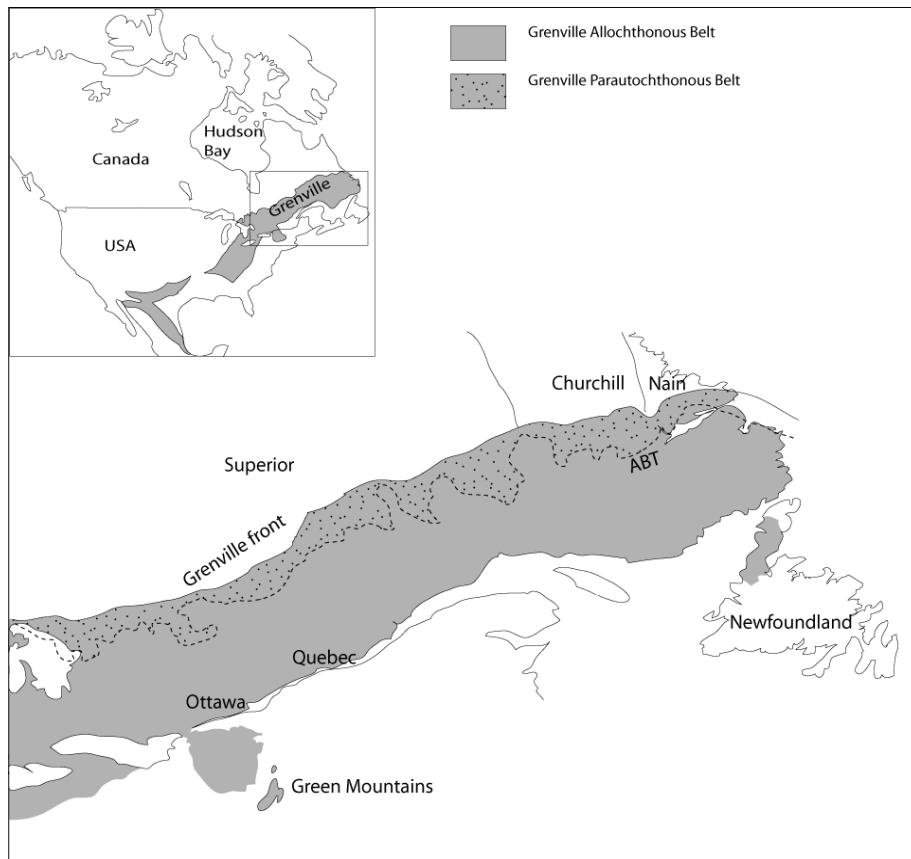


Figure 3-8. Sketch map of the Grenville orogenic belt of America and Canada (adapted from Corriveau et al. 2007 and Rivers 2009). The Archaean crustal blocks, Superior, Churchill and Nairn are indicated as is the Grenville front; ABT is the Allochthon Boundary Thrust between the allochthonous and parautochthonous belts.

Evidence that some of the basement inliers in Scotland record Grenville-Sveconorwegian metamorphism comes from the Eastern Unit (EU) of the Glenelg-Attadale inlier. The EU eclogites have been dated by garnet-clinopyroxene-whole rock Sm-Nd isochron and have given an age of 1028 ± 24 Ma (Sanders et al. 1984). This was interpreted as close to the age of eclogite formation and proposed to have resulted from the Grenville orogeny (Sanders et al. 1984). However, according to Brewer et al. (2003), this age is unlikely to represent peak metamorphism due the enrichment of MREE within the garnets which would skew the ages to yield younger dates. A U-Pb age of 995 ± 8 Ma obtained from zircon overgrowths has been interpreted to date retrogressive metamorphism within the EU (Brewer et al. 2003). An age from a garnet-clinopyroxene-whole rock Sm-Nd isochron of 1010 ± 13 Ma might also date retrogression (Sanders et al. 1984), however is within error of the Sm-Nd age cited by the same study for peak metamorphism and it also has MREE enrichment in the garnets

which might have resulted in a spuriously young age (Brewer et al. 2003). A lower intercept U-Pb zircon age of 943 ± 77 Ma has been obtained from the WU and interpreted to result from late Grenville reworking (Storey et al. 2010). This amphibolite facies retrogression was interpreted to indicate major crustal reworking in NW Scotland during the Grenville-Sveconorwegian (Brewer et al. 2003). This would indicate that during this time NW Britain was located within the Grenville-Sveconorwegian orogen, in contrast to existing palaeomagnetic data, which places NW Britain on the margin of the orogen (Buchan et al. 2000). This evidence shows a correlation with the Grenville-Sveconorwegian, however, it does not indicate whether the inliers are related to the Laurentian craton or the Fennoscandian craton.

3.5.3 The Fennoscandian Nordic basement

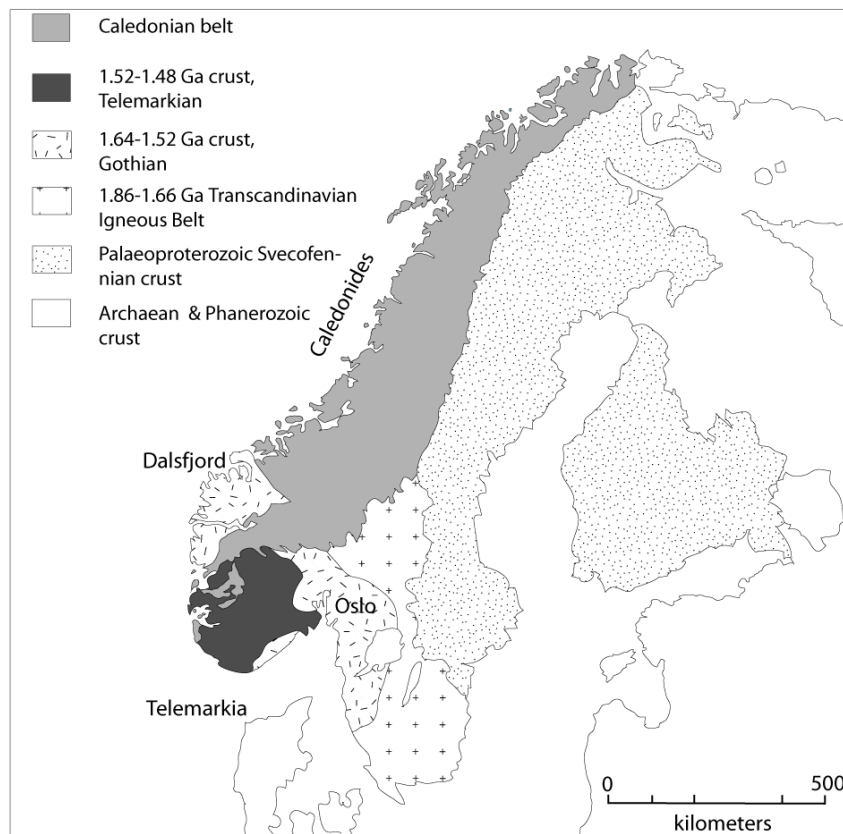


Figure 3-9. Adapted from Bingen et al. (2008). Sketch map of Fennoscandian crust showing main age areas.

The Nordic Mesoproterozoic basement rocks outcrop in Fennoscandia, the relationship between Baltica and Laurentia during the Mesoproterozoic is shown in Figure 3-2

which also shows many of the distinct terranes and relative ages. The Nordic basement rocks are thought to have been affected by an extensional regime during the Mesoproterozoic, which lead to the emplacement of dykes, granites, flood basalts and the formation of sedimentary basins, shown in Figure 3-9. During this time there were at least two accretionary events, Gothian (1640-1520 Ma) and Telemarkian (1520-1480 Ma) along the south-western active margin. Following this was the Hallandian-Danopolonian event (1470-1420 Ma) which included high grade metamorphism and granitic intrusions within the southern part of Fennoscandia. The Sveconorwegian orogeny (1140-970 Ma) occurred after a period of magmatism and sedimentation and is related to the Grenville and resulted from the collision of Baltica and Laurentia.

3.6 The Glenelg-Attadale Inlier

The majority of the basement gneisses within the Glenelg-Attadale Inlier were formed from trondhjemitic and granitic protoliths in the Neoarchaeon, and thus have similarities with gneisses of the Lewisian Gneiss Complex (Friend et al. 2008). The major difference is in the presence of eclogite and metasediments, which do not have a direct comparison with the Lewisian, although there are some possible metasediments in the Gairloch and Stoer areas and in the Outer Hebrides.

The Glenelg-Attadale inlier can be divided into the Western and Eastern Units which are separated by a major ductile shear zone, the Barnhill Shear Zone (BSZ), Figure 3-10. The BSZ dips east-southeast and has a top-to-the-west sense of shear (Storey et al 2004). Morar Group metasedimentary rocks can be identified within the BSZ also recording top-to-the-west shear, EU and WU rocks next to the BSZ are ultramylonitic. Storey et al (2004) dated titanites within the BSZ using U-Pb and determined an age of 661 ± 31 Ma; this age is not an exact date of movement on the shear as retrograde fabric (995 Ma) within the EU can be correlated with fabrics developed within the BSZ. This gives a period of movement on the BSZ of 995-670 Ma (Storey et al. 2010). The WU and the EU were initially assumed to have shared a similar metamorphic history; however the recent ages mentioned in the previous section demonstrate that peak metamorphism happened ~600 Ma earlier in the WU (Storey et al. 2010).

The EU is structurally overlain by Morar Group rocks and separated from it by the Inverinate Shear Zone (ISZ), which has a dextral sense of shear (Temperley & Windley

1997; Storey et al. 2004). The EU contains mafic and felsic rocks which are often inter-layered, the mafic rock is commonly made up of relict garnet, omphacite. Eclogite is often preserved within the mafic rock as patches where there are fewer veins and less deformation. The felsic rock is often coarse grained and consists of omphacite, garnet, kyanite and plagioclase. Ultrabasic rocks are also present within the EU as garnet-bearing olivine websterites and garnet-absent olivine websterites. Meta-sediments include pelites ranging from manganiferous to calcareous in character, marbles and iron formations. A PT estimate was made for the streaky eclogite of the EU by Sanders (1989) who used calcite-dolomite and garnet-clinopyroxene thermometry, and garnet-omphacite-quartz and garnet-plagioclase-kyanite-quartz barometry to establish peak PT conditions at 16.5 ± 1 kbar and $730 \pm 25^\circ\text{C}$. Storey et al. (2005) later achieved PT estimates of 20 kbar and $750\text{-}780^\circ\text{C}$ from the streaky eclogite and a coarse grained felsic gneiss using GADS barometer (Powell & Holland 1988) and the garnet-clinopyroxene Fe-Mg exchange thermometer (Powell 1985). Rawson et al. (2001) estimated PT of the garnet-bearing olivine websterites of ~ 20 kbar and 730°C . These PT estimates indicate that the whole of the EU shared this ~ 20 kbar and $730\text{-}750^\circ\text{C}$ event and indicates that the EU was buried to depths of 70 km most likely as a result of deep subduction of continental crust in a collision zone. The metasediments and the eclogite protoliths may have formed as part of a volcano-sedimentary sequence that accumulated on pre-existing trondhjemitic gneisses probably around 2.0 Ga (Storey et al. 2010).

The WU is made up of TTG acid gneisses with subordinate basic and ultrabasic rocks which generally preserve granulite facies; there is only one small area of eclogite. Friend et al. (2008) dated zircons from the WU using SHRIMP and found that the oldest age obtained was 2800 Ma, with the least disturbed population giving an age of 2677 ± 16 Ma, and a youngest age of ~ 1277 Ma. Friend et al. (2008) suggested that the younger analyses appeared to plot on a second discordant line which implied a complex history.

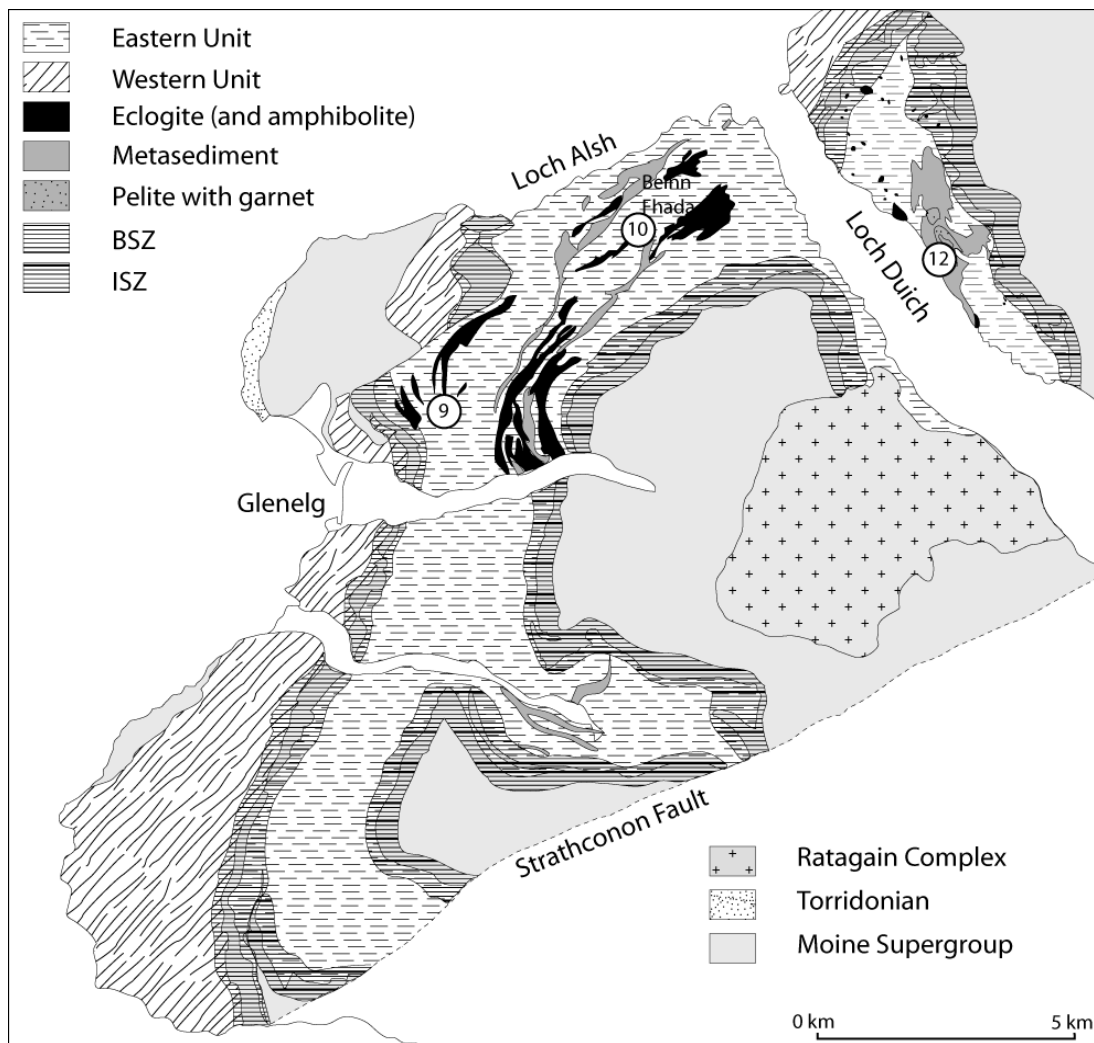


Figure 3-10. Simplified geological map of the Glenelg-Attadale Inlier from Storey et al. 2010. The numbers indicate the sample localities; 9 – AB07-09, 10 – AB07-10, and 12 – AB07-12. BSZ – Barnhill Shear Zone; ISZ – Invernate Shear Zone.

3.6.1 AB07-09 – Streaky Eclogite

This sample was collected from a prominent ridge north of Cnoc Mór (NG 8411 2142), which is referred to as the “ridge of streaky eclogite” by Storey (2007), the location for this is shown in Figure 3-10. The sample was collected from a mafic lithology, which is cut by a network of quartzo-feldspathic veins (“streaks”) that range in size from millimetre to tens of centimetre scale. According to Sanders (1988), the veins/ streaks formed during eclogite facies metamorphism. There are also hydrated layers of amphibolitised material cutting through the eclogite pods. The rock is strongly tectonised with a dominant D_1 fabric and has prominent lineations which plunge $\sim 20^\circ$ which Sanders (1988) interpreted to possible transcurrent shearing during eclogite

metamorphism. XRF analysis undertaken at RHUL indicates that the protolith for this sample was tholeiitic basalt.

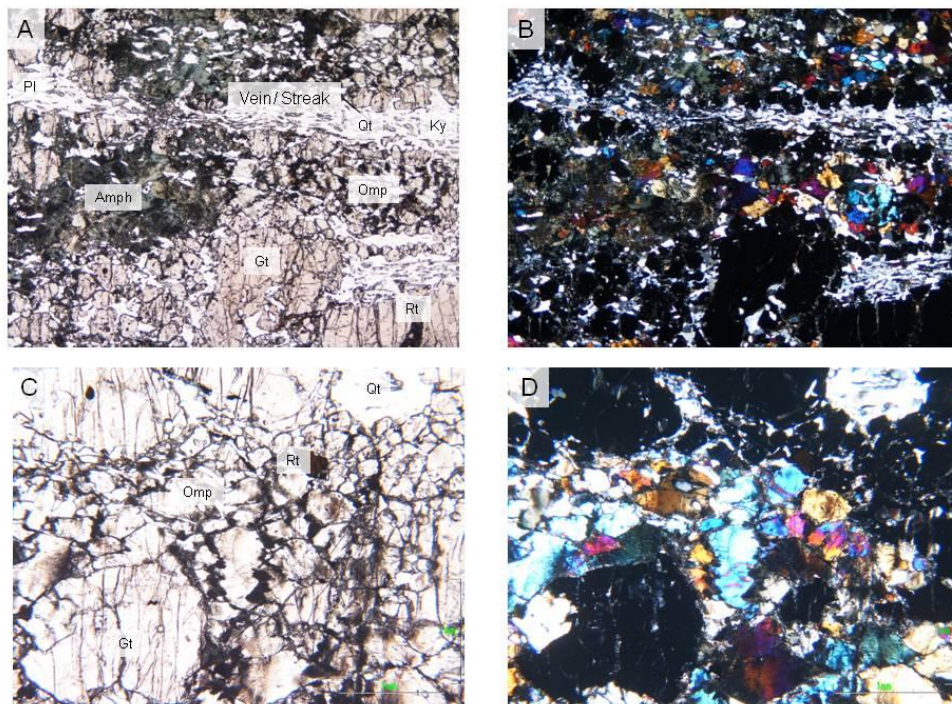


Figure 3-11, AB07-09 in thin section, A shows one of the veins/ streaks consisting of quartz, plagioclase and kyanite fish and an amphibolitised area of the sample. B shows the same view in XP. C shows a fresher part of the sample and D shows the same view in XP.

In thin section the sample has a coarse granoblastic polygonal texture (up to 4 mm). It is made up of garnet, omphacite, rutile and quartz, Figure 3-11. The veins/ streaks contain quartz, plagioclase and kyanite. The kyanite sometimes forms asymmetric fish, indicating non-coaxial shearing within the streaks. Garnets are quite inclusion-free with some alteration to amphibole around the rims. Omphacite grains are colourless in thin section with symplectites of diopside and plagioclase and replaced around their rims by hornblende. Omphacite has patchy and undulose extinction and is distinguished from diopside by its larger optic angle. Rutile has been replaced round the rims by ilmenite. The veins of amphibolitisation are much greener as more hornblende occurs and more symplectites are also present. The garnets are up to 4 mm in size and are extremely plentiful. They have inclusions of rutile, omphacite, quartz, zircon and opaques which sometimes appear to be present as linear trails.

Figure 3-12 shows LA ICPMS transect across a garnet from AB07-09. The major elements represented by MgO and CaO are flat reflecting the high grade nature of this sample.

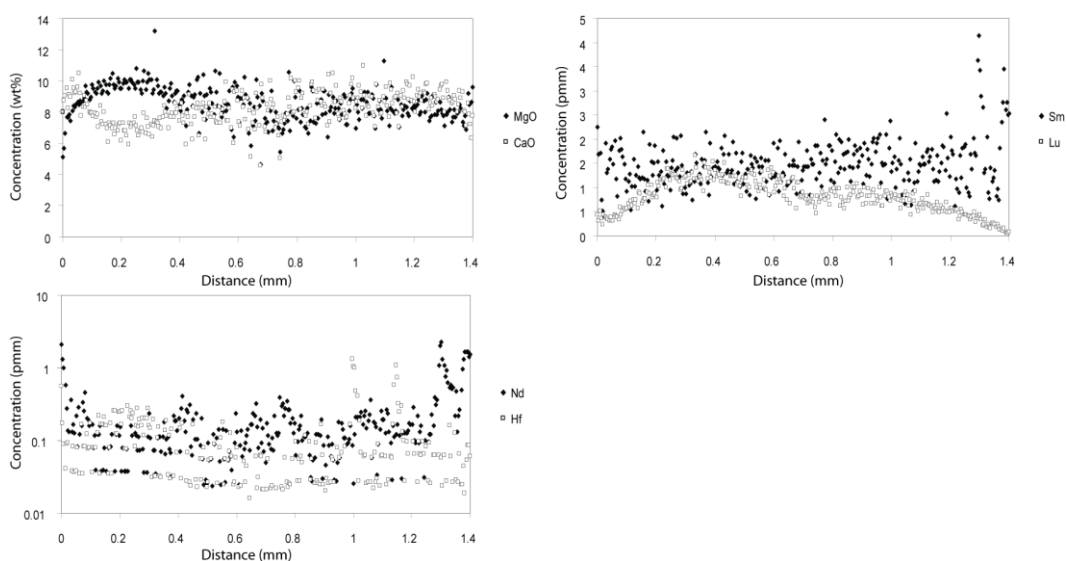


Figure 3-12, MgO, CaO, Lu, Hf, Sm and Nd profile across a garnet from AB07-09 undertaken on the LA ICPMS at Royal Holloway, University of London. The sample was normalised internally to 39.30% SiO₂ obtained from the electron microprobe at the Natural History museum and externally to SRM 612.

Lu increases towards the garnet core suggesting that the Lu-Hf age from this sample may represent garnet growth and that the age obtained should be meaningful. Sm and Nd are flat apart from where they have been affected by inclusions. Hf is very close to the LA ICPMS detection limit, shown by the flat parallel traces. It is expected that Lu-Hf and Sm-Nd should yield reliable garnet growth ages from this sample.

3.6.2 AB07-10 – Beinn Fhada Eclogite

This sample was collected from further north east along the “ridge of streaky eclogite” from very close to the sample site of Sanders et al. (1984) (NG 8603 2343), shown in Figure 3-10. The streaks described above are also present within this sample; it also has the same strong deformation fabric.

In thin section it is evident that this rock is much more retrogressed than the previous sample, shown in Figure 3-13. Rutile intergrowths and inclusions have in some cases almost entirely been replaced by framboidal rims of titanite. The matrix is dominated by symplectitic intergrowths which are probably of diopside, plagioclase and quartz,

and a blue-green amphibole is replacing the omphacite. There are patches of white streaks with plagioclase, quartz, and very small kyanite (<0.4 mm). The garnets are up to 6 mm in size and have inclusions of omphacite, quartz, rutile, opaques and zircon. XRF data from this sample indicates that the protolith for this rock was a basalt that was more enriched than sample AB07-09.

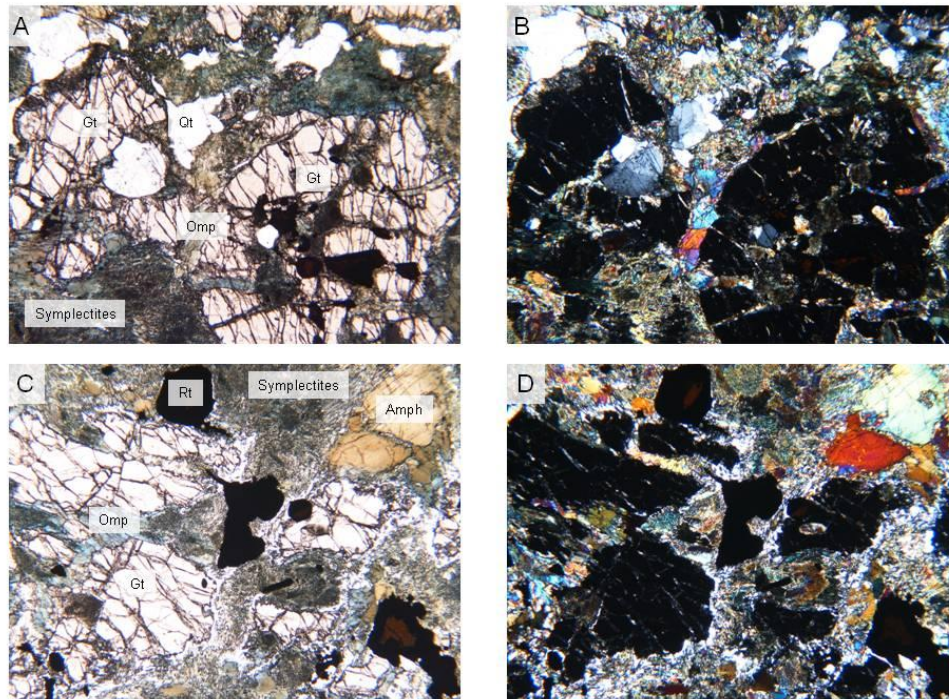


Figure 3-13, shows AB07-10 in thin section, A shows one of the euhedral garnets with omphacite and opaque inclusions, B shows the same view in XP. C and D show the symplectitic texture which dominates this sample and a large amphibole.

Figure 3-14 shows LA ICPMS data across a garnet from AB07-10. The most notable feature is the large inclusion (omphacite?) seen in most of the traces. There is no obvious zoning seen in any of the traces, and apart from the large inclusion the traces are reasonably flat. This is most likely related to the high grade nature of this sample. This sample is likely to give reliable Lu-Hf and Sm-Nd ages, as the traces have not been affected by many inclusions and are flat lying so will likely give cooling ages for each system. .

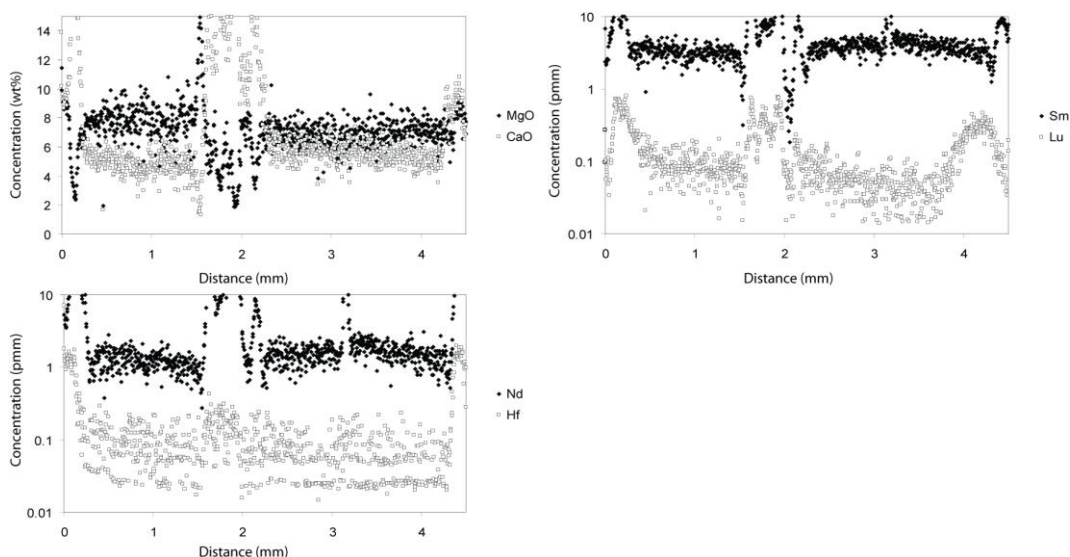


Figure 3-14, MgO, CaO, Lu, Sm and Nd profile across a garnet from AB07-10, undertaken on the LA ICPMS at Royal Holloway, University of London. The sample was normalised internally to 39.30% SiO₂ obtained from the electron microprobe at the Natural History museum and externally to SRM 612. Hf profile is not included for this sample as its concentration was less than the detection limit on the LA ICP MS.

3.6.3 AB07-12 – Garnet-kyanite-pelite

The garnet-kyanite-pelite is part of the meta-sedimentary rock series of the EU and was sampled at NG 9049 2330, shown in Figure 3-10. The meta-pelite shows a strong S₂ schistosity (Rawson 2002) and is associated with marble. It contains mauve coloured garnet porphyroblasts up to 5 mm in size, the kyanite is not seen in hand specimen. The white mica in this sample has been studied by Rawson (2002) who found it to be phengitic in composition indicating that they may be relicts of the eclogite facies.

In thin section, (Figure 3-15), it contains garnet, biotite, plagioclase, quartz, white mica, chlorite, rutile, sillimanite and kyanite. The biotite, white mica and quartz define the schistose fabric which is wrapping the garnets. Kyanite is not common and is always associated with biotite. The garnets have inclusions of quartz, mica, opaques and quite large zircons (70µm). Zircons are also present within biotites where they have pleochroic halos. Sillimanite is present in very small needles which cluster at the rims of plagioclase grains.

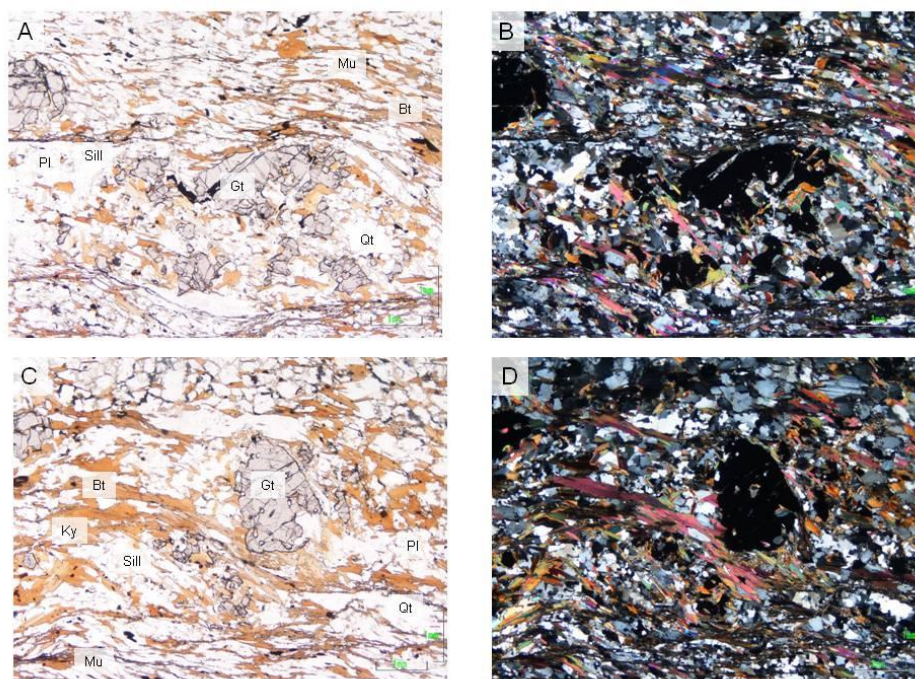


Figure 3-15, AB07-12 in thin section, A and B highlight the fabric which wraps the garnets. C and D shows a similar view with kyanite present associated with biotite.

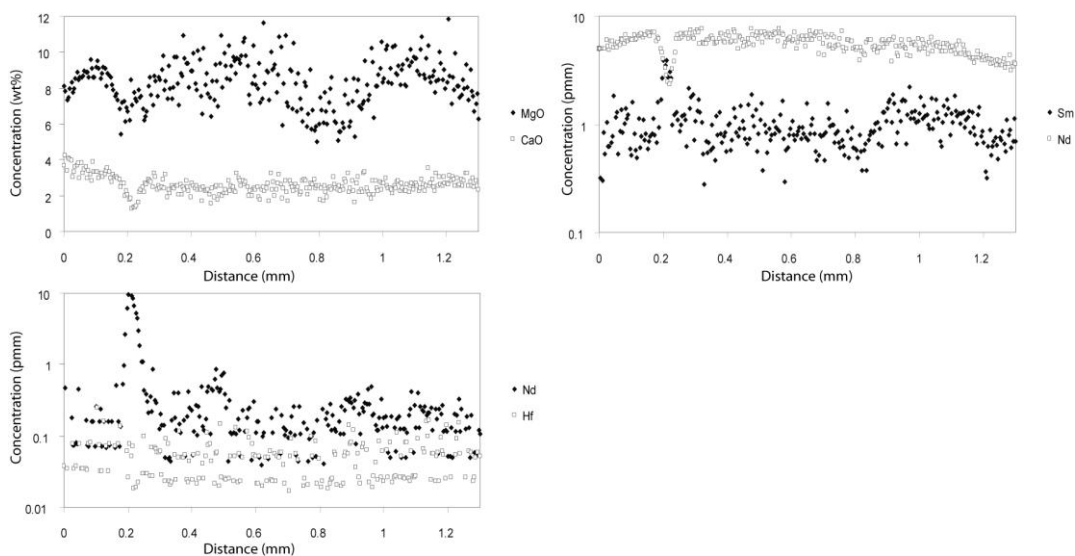


Figure 3-16, MgO, CaO, Lu and Sm profile across a garnet from AB07-12, undertaken on the LA ICPMS at Royal Holloway, University of London. The sample was normalised internally to 38.41% SiO_2 obtained from the electron microprobe at the Natural History museum and externally to SRM 612. Hf and Nd profiles are not included for this sample as their concentrations were less than the detection limit on the LA ICP MS.

The LA ICPMS from this sample is shown in Figure 3-16; CaO shows zoning across the garnet. MgO does not show zoning and is quite irregular. Lu increases towards the garnet core indicating that the Lu-Hf age should relate to garnet growth. Sm and Nd do

not show zoning, suggesting that the Sm-Nd age will not relate to garnet growth. Hf and Nd are close to the detection limit of the LA ICPMS which is shown by the flat parallel traces. One inclusion affects the Nd and Sm profiles which is likely to be feldspar.

3.7 The Borgie Inlier

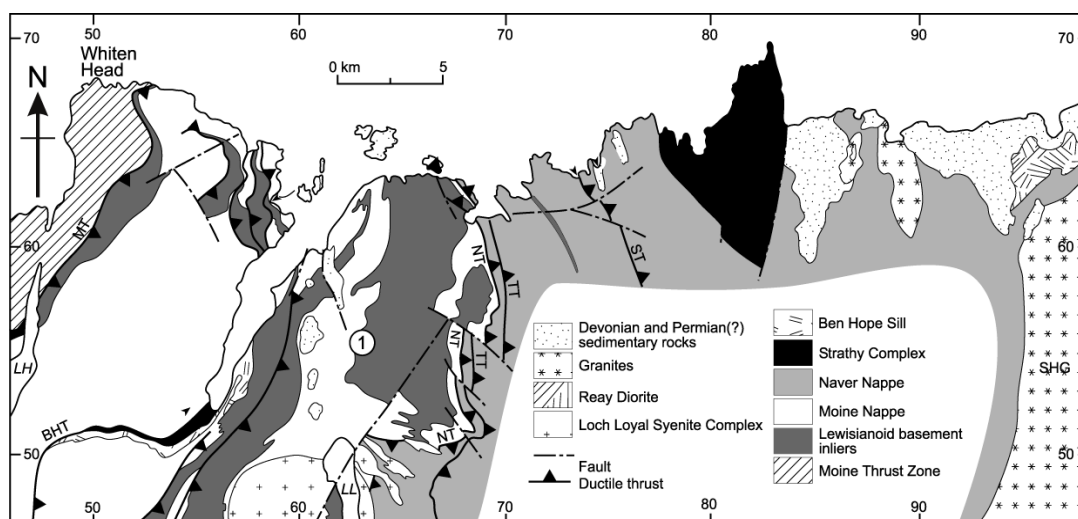


Figure 3-17. Adapted from Strachan et al. (2010). Simplified geology map of north Scotland, circled number 1 is the location of sample AB07-18. BHT – Ben Hope Thrust; MT – Moine Thrust; NT – Naver Thrust; TT – Torrisdale Thrust; ST – Swordly Thrust; SHG – Strath Halladale Granite; LL – Loch Loyal.

The Borgie inlier is the largest basement inlier on the north coast of Sutherland, Figure 3-17, and occupies an antiformal fold between the Ben Hope Thrust and the Naver Thrust (Moorhouse 1976; British Geological Survey 1997; Holdsworth et al. 2001). It consists of banded felsic to intermediate gneisses, which enclose mafic and ultramafics rafts up to hundreds of metres long (Friend et al. 2008). The banded felsic to intermediate gneisses contain hornblende and biotite and are K-feldspar poor. A strong east to south-east dipping foliation and a south-east plunging lineation are parallel, respectively, to the S_2 and L_2 in the surrounding Moine lithologies, suggesting that this fabric is at least in part related to the Caledonian orogeny. This is supported by a $^{40}\text{Ar}/^{39}\text{Ar}$ age of 421 Ma from a hornblende within the gneisses (Dallmeyer et al. 2001). Some of the mafic rafts are characterised by garnet-clinopyroxene metamorphic assemblages which are indicative of high grade metamorphism and are cut by narrow retrogressive shear zones made of hornblende schist. In some places the mafic rafts

have completely been converted to hornblende schist (Moorhouse 1976; Holdsworth et al. 2001).

Friend et al. (2008) dated zircons from within the Borgie inlier and obtained U-Pb ages of ~2880 Ma which were interpreted as protolith ages, although the whole array is discordant. The lower intercept for the array is ~1600 Ma which was interpreted to represent a significant isotopic disturbance.

3.7.1 AB07-18 – Borgie Granulite

The sample was collected from a mafic pod within the inlier. The sample had no obvious fabric or lineations and was composed mainly of garnet and clinopyroxene. XRF data indicates that the protolith for this sample was a tholeiitic basalt.

In thin section the sample comprises garnet, clinopyroxene, amphibole, quartz and plagioclase, Figure 3-18. The garnets are euhedral to subhedral in shape often with some amphibole around the edges, and contain inclusions of clinopyroxene, rutile and opaques. The amphibole typically is replacing the clinopyroxene around grain rims and sometimes along cleavage planes. The plagioclase is multiple twinned and has inclusions of clinopyroxene.

Figure 3-19 shows LA ICMS across a garnet from AB07-18. MgO shows some zoning decreasing towards the garnet rims and CaO decreases towards the garnet core. Lu shows a slight increase towards the garnet core, and Hf is fairly flat with one small peak. This suggests that the Lu-Hf age from this sample should yield a reliable age. Sm and Nd show no zoning and are quite homogeneous throughout the garnet suggesting that the Sm-Nd age should also be reasonable and will most likely reflect cooling from peak metamorphism.

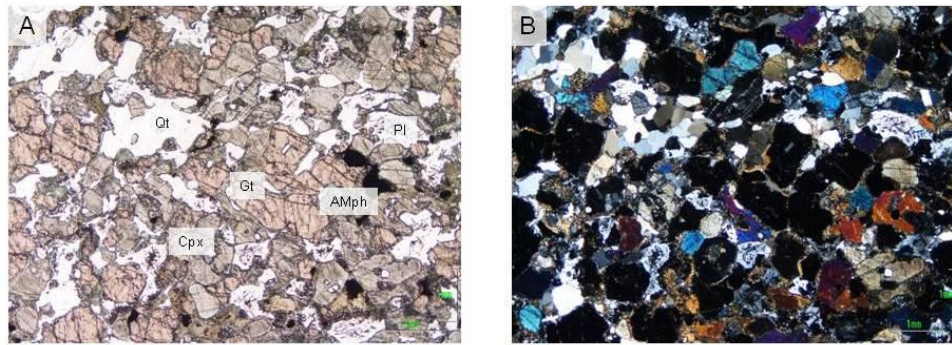


Figure 3-18 shows AB07-18 in thin section, A and B highlight the granulitic texture. Clinopyroxene and garnet are often seen with a rim of amphibole.

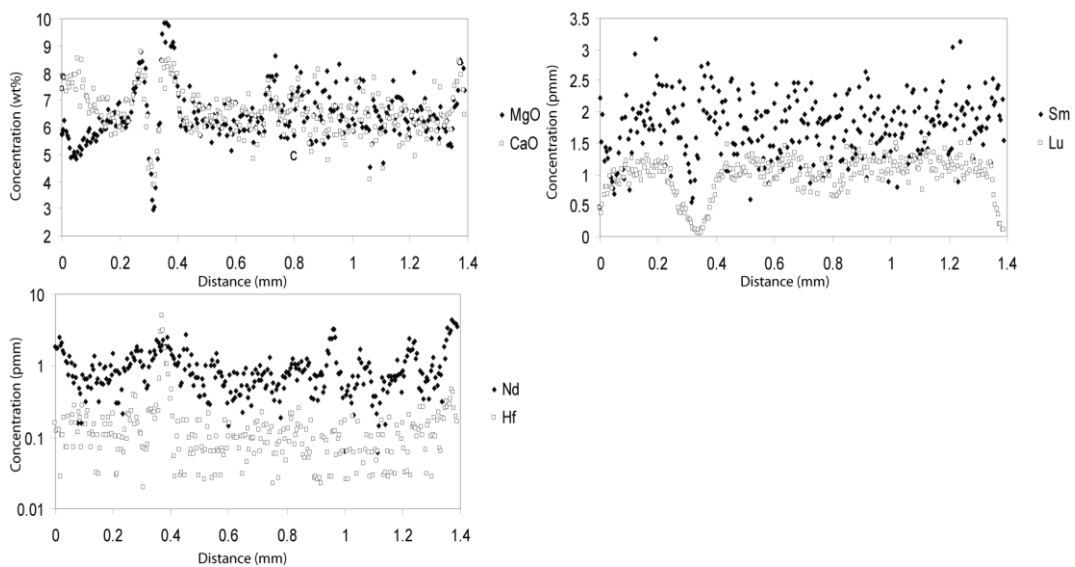


Figure 3-19 MgO, CaO, Lu, Sm and Nd profile across a garnet from AB07-18, undertaken on the LA ICPMS at Royal Holloway, University of London. The sample was normalised internally to 38.27% SiO_2 obtained from the electron microprobe at the Natural History museum and externally to SRM 612. Hf profile is not included for this sample as its concentration was less than the detection limit on the LA ICP MS.

In summary, all of the LA ICPMS data for the samples in this study suggest that all of the Lu-Hf and Sm-Nd ages should be meaningful. In all cases the Sm and Nd traces are flatter than the Lu traces, suggesting that the Sm-Nd age is more likely than the Lu-Hf age to reflect cooling.

3.8 Results and interpretation

The results are summarised in Table 3-3 and Table 3-4. Two garnet fractions were dated from AB07-09 using garnet + whole rock isochrons and yielded two Lu-Hf ages of 1220.5 ± 6.2 Ma (AB07-09 Grt 1) and 1173.2 ± 9.3 Ma (AB07-09 Grt 2), which are 31.8 Ma outside of error. They give a three point isochron age of 1201 ± 510 Ma with a MSWD of 178, as the points do not lie within error of the isochron, shown in Figure 3-21. The LA ICPMS trace suggests that there should be little effect from inclusions. The Hf concentration can be estimated from part of the pure garnet using the LA ICPMS trace by looking at parts of the trace which were above the detection limit and were not affected by zircon inclusions. This shows little influence from inclusions as the ID Hf concentrations are very similar to that of the pure garnet (0.187 ppm and 0.260 from ID and 0.213 ppm from LA ICPMS). AB07-09 gave a three point Sm-Nd isochron of 983.0 ± 110 Ma with an MSWD of 22, shown in Figure 3-22. AB07-09 Grt 1 gives a two point isochron age of 984.9 ± 4.2 Ma and AB07-09 Grt 2 gives 972.8 ± 5.0 Ma, which are 2.9 Ma outside of error. The LA ICPMS gave a Nd concentration of 0.231 ppm for pure garnet, while ID gave 1.884 ppm for AB07-09 Grt 1 and 2.562 ppm for Grt 2 suggesting that some Nd-rich inclusions were incorporated in the digestion. AB07-09 gave an NdT_{DM} model age of 2969 Ma, which is similar to the protolith ages from the Borgie and Farr inliers (Friend et al. 2008). It gave a ϵ_{Nd} value of 1.2 suggesting a mantle source. All the ϵ_{Nd} values in this chapter are quoted for an age of 2000 Ma.

AB07-10 Grt 1 gave a Lu-Hf two point isochron age of 1204.8 ± 4.6 Ma and AB07-10 Grt 2 gave a Lu-Hf age of 1175.9 ± 4.2 Ma. These fractions give a three point isochron age of 1207.0 ± 150 Ma with a MSWD of 85, shown in Figure 3-21. The LA ICPMS from this sample gives an Hf concentration of 0.212 ppm, the garnet fractions gave concentrations of 0.187 ppm and 0.387 ppm, which suggests that inclusions have not affected these ages. AB07-10 gave a three point Sm-Nd isochron age of 939.0 ± 86 Ma with an MSWD of 6, shown in Figure 3-22. The LA ICPMS gave a pure garnet Nd concentration of 1.783 ppm, and ID gave 5.333 ppm for AB07-10 Grt 1 and 13.423 ppm for AB07-10 Grt 2. This suggests that the ages may have been influenced by Nd-rich inclusions, for example, epidote, this is particularly evident in AB07-10 Grt 2 where only ~13% of the Nd has come from the garnet. If we assume that AB07-09 and AB07-

10 are co-genetic then we can plot both samples can be plotted on the same isochron, this gives a Lu-Hf six point isochron age of 1203 ± 27 Ma with an MSWD of 22 and a Sm-Nd six point isochron of 1016 ± 120 Ma with an MSWD of 986, shown in Figure 3-21 and Figure 3-22. This sample gave a Nd_{DM} model age of 2354 Ma and a ϵ_{Nd} value of 1.5, suggesting a mantle source for the rock.

AB07-12 Grt 1 gave a two point Lu-Hf isochron age of 1669.6 ± 28 Ma and AB07-12 Grt 2 gave a Lu-Hf age of 3156 ± 170 Ma (Figure 3-21). The age from AB07-12 Grt is not meaningful; the $^{176}\text{Lu}/^{177}\text{Hf}$ and $^{176}\text{Hf}/^{177}\text{Hf}$ ratios from the garnet fraction are very close to the whole rock ratios suggesting that it is not very radiogenic. AB07-12 Grt 2 also yielded a lower Lu concentration and higher Hf concentration than AB07-12 Grt 1 which would lower the $^{176}\text{Lu}/^{177}\text{Hf}$ ratio. The Hf concentration obtained from LA ICPMS from pure garnet was close to the detection limit making it difficult to estimate a concentration, whereas the Hf concentration from ID was 1.020 ppm from AB07-12 Grt 1 and 1.387 ppm from AB07-12 Grt 2 suggesting that inclusions have affected the ages obtained. AB07-12 gave a precise Sm-Nd three point isochron age of 912.5 ± 2.1 Ma, shown in Figure 3-22. The LA ICPMS Nd concentration for the pure garnet was ~ 0.382 ppm and the ID concentration for AB07-12 Grt 1 was 1.271 ppm and AB07-12 Grt 2 was 1.197 ppm suggesting some effect from Nd-rich inclusions. AB07-12 gave Nd_{DM} age of 2400 Ma and a ϵ_{Nd} value of -1.4, suggesting a crustal source. AB07-12 also gave a two point Rb-Sr (Table 3-4) white mica+ whole rock age of 1025.4 ± 9.6 Ma, and although the white mica was not widely radiogenic there is no reason to suspect that this age is not meaningful. A two point biotite + whole rock age of 412 ± 0.42 Ma was also obtained and this age will be discussed in more detail in Chapter 7.

AB07-18 gave a precise Lu-Hf three point isochron age of 1634.9 ± 9.4 Ma with an MSWD of 0.4 (Figure 3-21). The LA ICPMS gave a pure garnet Hf concentration of 0.283 ppm, which is higher than the values obtained from ID (0.239 ppm for AB07-18 Grt 1, 0.179 ppm for AB07-18 Grt 2), suggesting that there has been no interaction with Hf-rich inclusions. AB07-18 Grt 1 gave a Sm-Nd two point isochron age of 1457.8 ± 3 Ma and AB07-18 Grt 2 gave an age of 1476.9 ± 15 Ma, these ages are only 1.1 Ma outside of error. Figure 3-20 shows the initial $^{143}\text{Nd}/^{144}\text{Nd}$ from the three fractions used to construct the isochron with their corresponding errors; this type of diagram enhances the error which makes it easier to see which points lie within error. All three points

from this sample are within error, which should suggest that a three point isochron age would be meaningful with a small error and small MSWD. However, the three point isochron age using Isoplot is 1461.9 ± 180 Ma with a MSWD of 6.2, (Figure 3-22), which suggests that Isoplot may overestimate error for ages calculated using only two or three points.

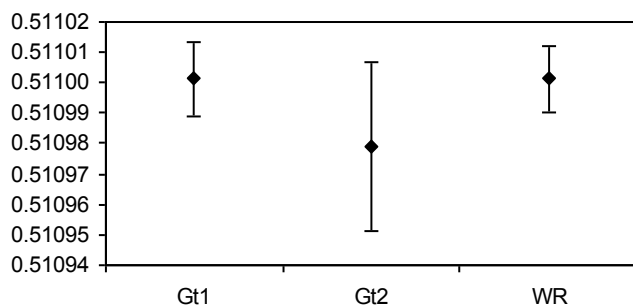


Figure 3-20, initial $^{143}\text{Nd}/^{144}\text{Nd}$ ratios for AB07-18.

The LA ICPMS gave an Nd concentration of 1.098 ppm for pure garnet which is higher than the concentrations obtained by ID (0.891 ppm AB07-18 Grt 1, 0.900 ppm AB07-18 Grt 1), suggesting little influence from inclusions. AB07-18 gave a ϵ_{Nd} value of -1.7 which suggests a crustal component. A crustal component is supported by an NdT_{DM} age of 1363 Ma.

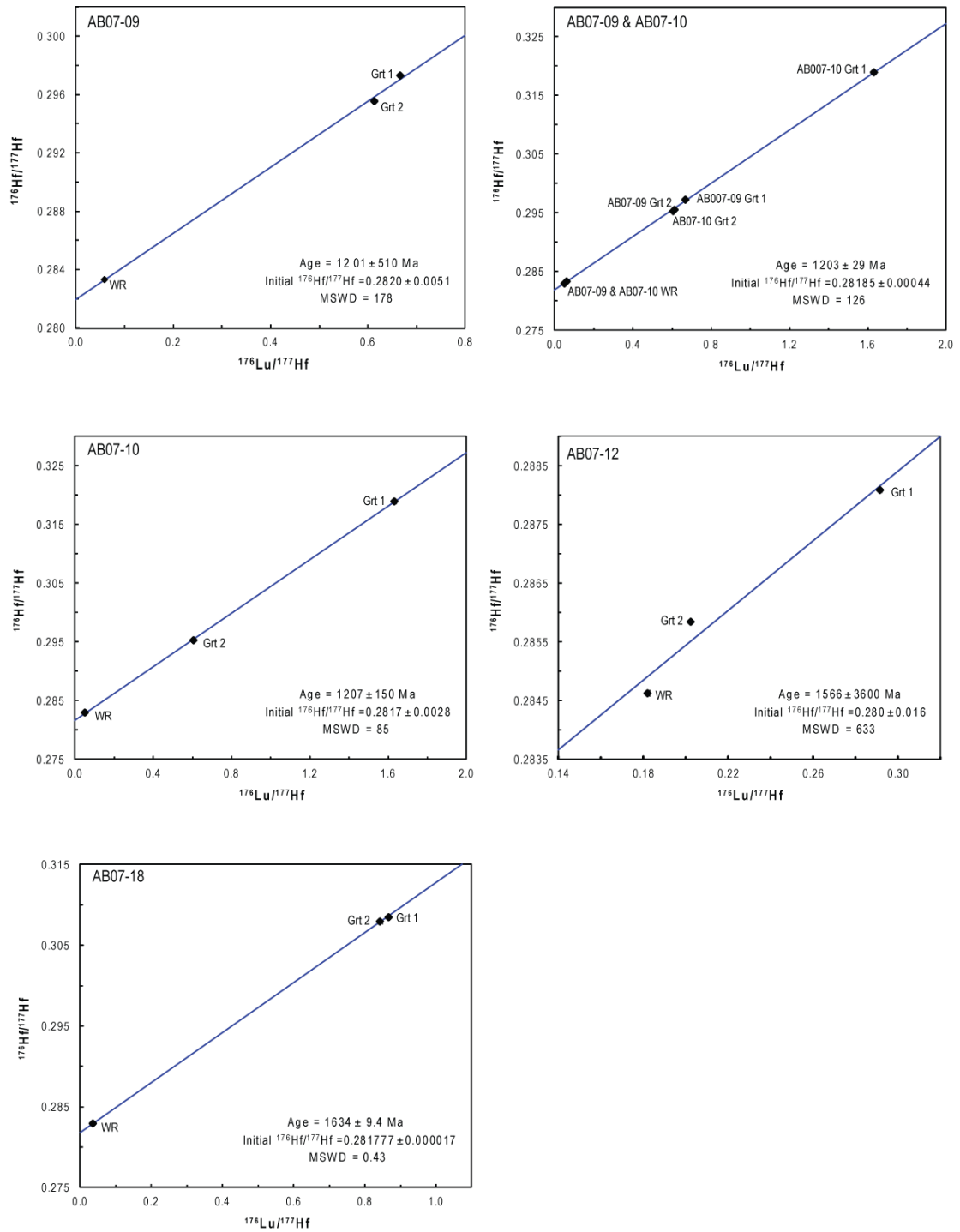


Figure 3-21 showing isochron diagrams for all samples which gave three point or more Lu-Hf ages. The different garnet fractions are labelled and the whole rock is indicated by WR. Error bars are included on the diagram but in most cases they are smaller than the symbol.

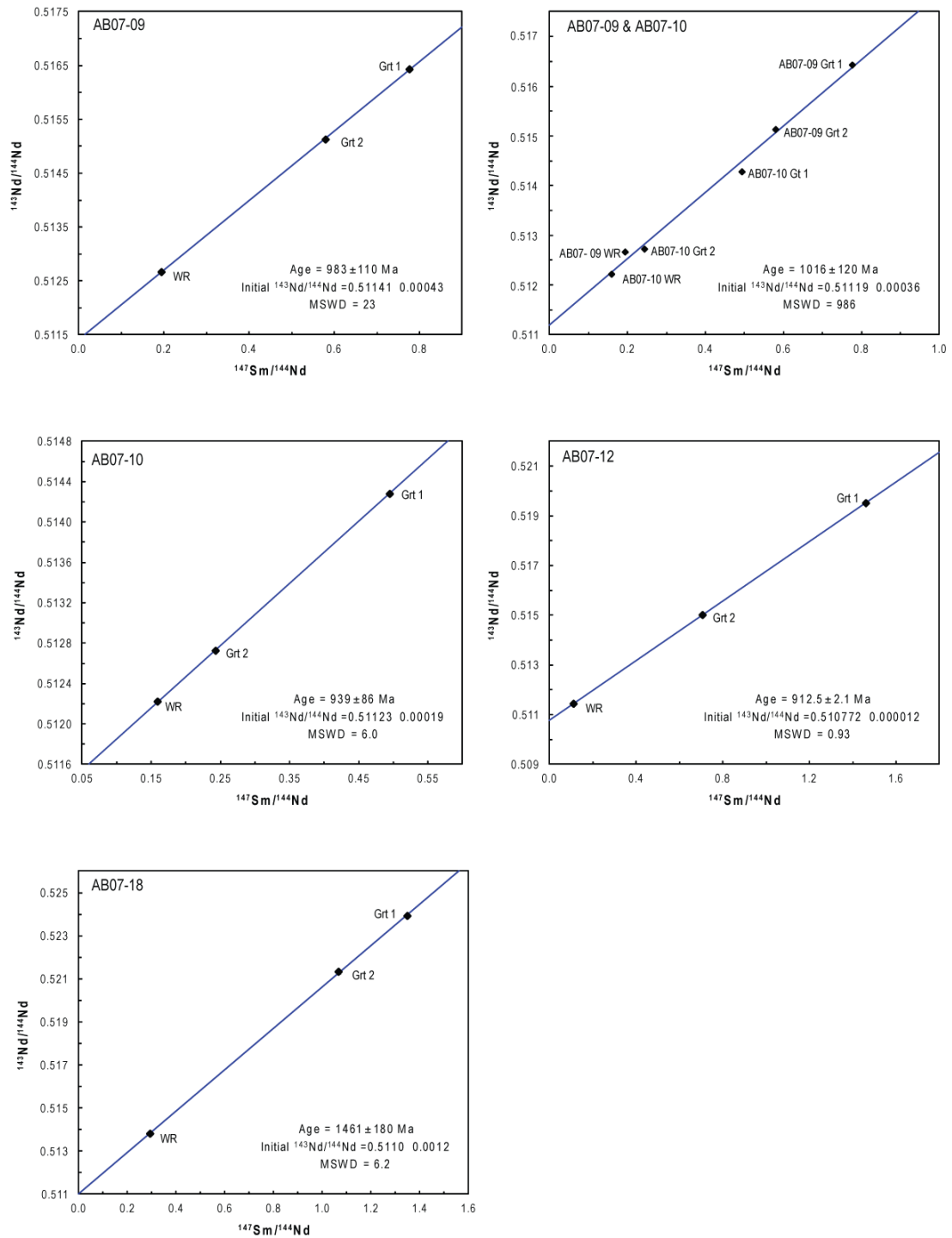


Figure 3-22 showing isochron diagrams for all samples which gave a three point or more Sm-Nd age. The garnet fractions are labelled and the whole rock is indicated by WR. Error bars are included on the diagram but in most cases they are smaller than the symbol.

Table 3-2 summarising the Lu-Hf results from the basement inliers. Ages marked with an * are interpreted to be not geologically meaningful.

Sample Fraction	Lu ppm	Hf ppm	$^{176}\text{Hf}/^{177}\text{Hf}$	2se	$^{176}\text{Lu}/^{177}\text{Hf}$	Initial $^{176}\text{Hf}/^{177}\text{Hf}$	Lu-Hf Age (Ma)	Nr points on isochron	MSWD
AB07-09 Grt 1	1.224	0.260	0.297296	0.000021	0.666	0.281953	1220.5 ± 6.2	2	
AB07-09 Grt 2	0.808	0.187	0.295553	0.000042	0.612	0.282006	1173.2 ± 9.3	2	
AB07-09 WR	0.330	0.791	0.283311	0.000024	0.0590	0.281850	1203.0 ± 29	6	126
AB07-10 Grt 1	2.141	0.187	0.318905	0.000023	1.632	0.281827	1204.8 ± 4.9	2	
AB07-10 Grt 2	1.642	0.387	0.295300	0.000017	0.606	0.281854	1175.9 ± 4.2	2	
AB07-10 WR	0.434	1.257	0.282935	0.000013	0.0488	0.281700	1207.0 ± 150	3	85
AB07-12 Grt 1	2.102	1.020	0.288088	0.000016	0.291	0.278874	1669.6 ± 28	2	
AB07-12 Grt 2	1.982	1.387	0.285848	0.000012	0.202	0.273594	3156 ± 180*	2	
AB07-12 WR	0.324	0.252	0.284631	0.000048	0.182				
AB07-18 Grt 1	1.416	0.239	0.307908	0.000016	0.842	0.2817797	1634.9 ± 9.4	3	0.43
AB07-18 Grt 2	1.093	0.179	0.308522	0.000034	0.866				
AB07-18 WR	0.226	0.883	0.282895	0.000013	0.0361				

Table 3-3 summarising the Sm-Nd results from the basement inliers. Ages marked with an * are interpreted to be not geologically meaningful.

Sample Fraction	Sm ppm	Nd ppm	$^{143}\text{Nd}/^{144}\text{Nd}$	2se	$^{147}\text{Sm}/^{144}\text{Nd}$	Initial $^{147}\text{Sm}/^{144}\text{Nd}$	Sm-Nd Age (Ma)	Nr points on Isochron	MSWD
AB07-09 GRT 1	2.415	1.884	0.516424	0.000012	0.776	0.511410	983.0 ± 110	3	23
AB07-09 GRT 2	2.452	2.562	0.515123	0.000008	0.579				
AB07-09 WR	2.601	8.092	0.512667	0.000009	0.194	0.511190	1016 ± 120	6	986
AB07-10 GRT 1	4.360	5.333	0.514281	0.000010	0.494	0.511230	939.0 ± 86	3	6
AB07-10 GRT 2	5.393	13.423	0.512722	0.000008	0.739				
AB07-10 WR	8.195	31.166	0.512220	0.000010	0.159				
AB07-12 GRT 1	3.066	1.271	0.519517	0.000012	1.461	0.510772	912.5 ± 2.1	3	0.93
AB07-12 GRT 2	1.395	1.197	0.515006	0.000027	0.705				
AB07-12 WR	6.408	35.132	0.511431	0.000011	0.110				
AB07-18 GRT 1	1.983	0.891	0.523934	0.000012	1.349	0.511000	1461.0 ± 180	3	6.2
AB07-18 GRT 2	1.582	0.900	0.521312	0.000028	1.065				
AB07-18 WR	2.396	4.965	0.513802	0.000011	0.292				

Table 3-4 summarising the Rb-Sr results from the basement inliers.

Sample Fraction	Rb ppm	Sr ppm	$^{87}\text{Sr}/^{86}\text{Sr}$	2se	$^{87}\text{Rb}/^{86}\text{Sr}$	Initial $^{87}\text{Rb}/^{86}\text{Sr}$	Rb-Sr Age (Ma)
AB07-12 Biotite	296.20	8.99	1.32793	0.000150	100.7439	0.73864	411.98 ± 0.42
AB07-12 Muscovite	194.69	248.95	0.75305	0.000010	2.2646	0.71983	1025.40 ± 9.6
AB07-12 WR	128.81	192.91	0.74818	0.000014	1.9327		

3.9 Discussion

The Lu-Hf and Sm-Nd dates presented for each sample within this chapter are significantly different. There are three possible explanations for reasons these differences. The first is that both the Lu-Hf and Sm-Nd ages are cooling ages and the garnet had been subjected to temperatures higher than T_C for both systems. A second interpretation is that these samples only went through Sm-Nd T_C and did not go through T_C for Lu-Hf. This would suggest that the Lu-Hf ages are garnet growth ages and the Sm-Nd ages correspond to the time of cooling. A third option is that the Lu-Hf ages record peak metamorphism, or close to it, and the Sm-Nd ages reflect partial resetting during a younger metamorphic event. The third option is most likely as the first option suggests that both ages are cooling ages but in some cases that would suggest ~200 Ma of cooling, which is unlikely. The second option suggests that both ages are growth ages thus in some cases there would be ~200 Ma of garnet growth which is also unlikely.

3.9.1 1750 - 1600 Ma events

AB07-12 (EU metasediment) and AB07-18 (Borgie granulite) record Lu-Hf ages of 1669.6 ± 28 Ma and 1631.8 ± 9.6 Ma respectively which are broadly similar to the Lu-Hf age of 1667 ± 6 Ma obtained from a WU eclogite (Storey et al. 2010). This suggests that a ~1650 Ma event is shared by the WU, the Borgie inlier and the EU metasediments. This is further supported by the U-Pb zircon lower intercept age of ~1600 Ma from the Borgie Inlier (Friend et al. 2008) which was interpreted to represent a significant isotopic disturbance.

The 1750-1600 Ma metamorphic events are the oldest yet recorded within the basement inliers and overlap with the Palaeoproterozoic events found in the Lewisian Gneiss Complex and the Rhinns Complex. These events are broadly contemporaneous with the Labradorian and Gothian events from Laurentia and Baltica, the location of these belts is shown in Figure 3-2. The 1750-1600 Ma eclogite metamorphism recorded in the WU Glenelg inlier could represent the high-pressure convergent margin to the lower-pressure (amphibolite-facies) event recorded in the Caledonian foreland and in the Rhinns Complex (Storey et al. 2010). The Gothian and Labradorian belts are dominated by subduction-related activity involving separate orogenic events related to subduction

along the western margin of Baltica including calc-alkaline magmatism and deformation due to arc accretion (Karlstrom et al. 2001); this type of metamorphism could be easily responsible for the production of the WU eclogites and granulites.

3.9.2 1250 - 1200 Ma events

The Lu-Hf ages obtained from the EU eclogites (AB07-09 and AB07-10) give a six point isochron of 1203.0 ± 26 Ma. The ~ 1200 Ma ages confirm the Grenville-Sveconorwegian affinities of the eclogites. More specifically, they can now be assigned to the Elzevirian phase of the Grenville orogeny in NE Laurentia, thus supporting a general Laurentia rather than Baltican origin for the basement inliers in the Northern Highland Terrane (Friend et al. 2008; Storey et al. 2010).

3.9.3 1020 - 900 Ma events

The significance of the 1020-900 Ma ages is uncertain. One option is that they relate to the Ottawan phase of the Grenville orogeny (Sanders et al. 1984; Brewer et al. 2003). An alternative view is that they could be the consequence of partial resetting during early Neoproterozoic metamorphic events which have been recorded in the Moine Supergroup (see Chapter 4 this thesis), the Westing Group of Shetland (Cutts et al. 2009) and the Krummedal Succession of East Greenland (Leslie & Nutman 2003).

The EU eclogites yield Sm-Nd garnet ages of 983 Ma and 939 Ma respectively which is similar to the U-Pb zircon rim age of 995 Ma from Brewer et al. (2003). These ages are almost within error of two Sm-Nd ages of 1028 ± 24 Ma and 1010 ± 13 Ma from the EU eclogite and the Rb-Sr white mica age of 1025 ± 9.6 Ma from the EU metapelite. These ages are similar to the Ottawan orogeny (1080-1020 Ma) from the Laurentian sector of the Grenville belt and the Sveconorwegian orogeny (1200-900 Ma) from the Baltica sector. The ages are also similar to late-Mesoproterozoic/ Neoproterozoic ages from the Rhinns Complex and the Annagh Gneiss Complex which are also interpreted to relate to the Ottawan orogeny. This complements the suggestion from the ~ 1650 Ma and ~ 1200 Ma ages that the Moine basement inliers of the Northern Highland terrane share an affinity with Laurentia.

A second option for the 1020-900 Ma ages is that they represent partial/ full resetting of the Sm-Nd and Rb-Sr systems during Neoproterozoic metamorphic events. This study shows (Chapter 4) there is substantial evidence for 980-903 Ma garnet growth events

within the Moine Supergroup that unconformably overlies the basement inliers. Several of the ages from within the basement inliers, especially the Sm-Nd age from AB07-12 of 912.5 ± 2.1 Ma, fall within this age bracket. This could potentially represent the time when the Moine Supergroup and the basement inliers were first deformed and metamorphosed together and may not be related to the Grenville orogenic cycle at all.

The preservation of ~ 1650 Ma Lu-Hf garnet ages within the EU metapelite (AB07-12) is perhaps surprising, given that wholesale isotopic resetting might have been expected during eclogite facies metamorphism at ~ 1200 Ma. However, if these lithologies had been tectonically interleaved at a later stage, perhaps during extension, then this would explain the preservation of these older ages. This is supported by a schematic cross-section drawn by Temperley & Windley (1997) of kinematic textures present in the rocks along the edge of Loch Duich, shown in Figure 3-23, which shows the boundary between the gneissic meta-pelites and the gneisses as a shear.

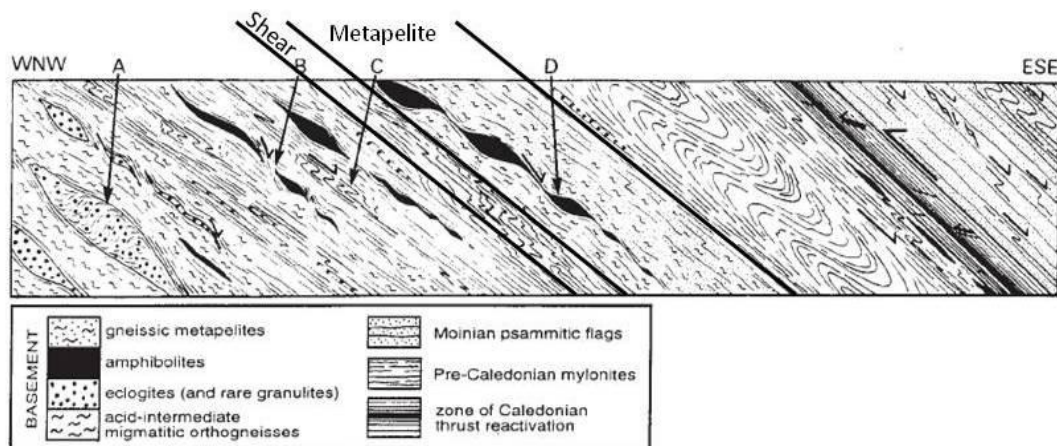


Figure 3-23. From Temperley & Windley 1997, schematic section based on exposures along the NE and SE shores of Loch Duich. A – deflection of earlier fabrics, B – secondary shear foliations, C – vergence of shear folds, and D – low angle asymmetric boudins. Structures demonstrate top-to-east shear, which is also observed within the overlying Moine.

The only shear zone in this area which has given any dates is the BSZ and the movement on it occurred between 995 Ma and 669 Ma, which could suggest that the other shear zones are of a give similar age. If this is the case then there is no reason why the EU meta-pelite and the EU eclogites should share an identical history prior to their juxtaposition, thus explaining the contrasting isotopic ages.

3.10 Conclusions

This chapter provides evidence for ~1650 Ma and ~1200 Ma metamorphic events within the basement inliers. It is likely that the inliers are part of the 1000 kms long belt that make up the Laurentian-Baltica south facing margin and record ~1650 Ma metamorphism which is also seen in Laurentia (Labradorian) and Baltica (Gothian). The Lu-Hf ages from AB07-09 and AB07-10 record eclogite metamorphism at ~1200 Ma which does not correlate with events seen in Fennoscandia but does match the Elzevirian orogeny of the Laurentian craton, which could suggest that the inliers share more of affinity with Laurentia than Baltica, although according the reconstruction of Park (1995) and Karlstrom et al. (2001) Scotland was located between the continents (Figure 3-2). The Sm-Nd and U-Pb ages of 900-1020 Ma recorded by Sanders et al. (1984), Storey et al. (2010) and Brewer et al. (2003) and in this chapter might reflect thermal reworking of the EU and WU during the Ottawa part of the Grenville orogeny. However, this study also shows that 980-903 Ma metamorphism affected the overlying Moine Supergroup. In that context, these younger (1020-900 Ma) isotopic ages recorded within the basement inliers may correspond to the first deformation and metamorphic event that they share with the Moine cover rocks.

4.1 Synopsis

Previous research indicated that the Caledonian Orogeny (470-420 Ma) has extensively overprinted Neoproterozoic deformation fabrics and metamorphic assemblages within the Moine Supergroup. The aim of the chapter is to apply Lu-Hf and Sm-Nd geochronological techniques in order to provide further constraints on the timing and nature of these hitherto rather cryptic Neoproterozoic events. The new data reported here from the Morar Group suggest that there was an early garnet growth event at ~950 Ma to 900 Ma, followed by renewed growth between 880 Ma and 830 Ma seen from Lu-Hf ages and Sm-Nd ages. The events recorded in the Morar Group are different from the garnet growth events recorded within the Glenfinnan Group. This suggests that the two units were separate until at least 740 Ma. The Glenfinnan Group apparently records three phases of garnet growth at 740 Ma, 700-680 Ma and 640 Ma. The early Lu-Hf ages recorded from the Morar Group indicate that deposition must have ceased prior to ~950 Ma. The youngest published precise detrital zircon age is 980 ± 4 Ma (Cawood et al. 2007) which gives approximately 30 Ma to deposit the Morar Group. The early (>900 Ma) ages from the Morar Group link with areas in the North Atlantic region that record 'Renlandian' orogenesis (Cawood et al. 2010). The younger ages relate to the Knoydartian Orogeny which Cawood et al. (2010) describe as consisting of three discrete events, 830-820 Ma, 800-790 Ma and 730-710 Ma. Many of the ages presented within this chapter are too old to fit into any of these established groups, suggesting that definitions of the Knoydartian event require revision.

4.2 Introduction

The Caledonian Orogeny (470-420 Ma) is the most recent orogenic event that the Scottish Highlands has experienced and this was associated with variable overprinting of the evidence for Neoproterozoic orogenies. Despite the intensity of Caledonian deformation and metamorphism, the aim of this chapter was to resolve the timing of these often cryptic Neoproterozoic tectonothermal events. Published Neoproterozoic mineral ages can broadly be separated into three age brackets; ~870, 820-790 Ma and 740-730 Ma. The earliest group dates the granitic protoliths of the West Highland

Granitic Gneiss. The later groups of ages have been interpreted to record prograde metamorphism which suggests that the Knoydartian consists of at least three events. Vance et al. (1998) dated the Knoydartian Orogeny by Sm-Nd geochronology on garnets from the Morar Group, which gave ages between 820-790 Ma. This was thought to date prograde metamorphism during crustal thickening. There is evidence for a younger metamorphic event from a titanite U-Pb prograde age of 737 ± 5 Ma from the Loch Eilt area, which suggests that there may have been more than one phase of Neoproterozoic prograde metamorphism (Tanner & Evans 2003). Establishing the cause for this tectonothermal Neoproterozoic event(s) has been the subject of much controversy since the 1970s and since the later Caledonian deformation has overprinted much of the record it is difficult to see back to the Knoydartian. Cawood et al. (2010) suggest that the Knoydartian was part of the Valhalla Orogen and suspect there were at least two tectonothermal episodes, the Renlandian (980-910 Ma) (Cutts et al. 2010a) and the Knoydartian (830-710 Ma). This chapter focuses on the geochronology of Neoproterozoic metamorphic events within the Northern Highland Terrane, and whether the Grampian Terrane has been affected by any early deformation. It is also important to determine when peak metamorphism occurred, to establish if it was recorded at the same time throughout the Moine Supergroup and the tectonic implications of the deformation recorded which could shed some light on the palaeotectonic setting of the Moine Supergroup during the Neoproterozoic.

4.3 Previous Geochronology

The first recognition that the Moine rocks had been affected by Precambrian metamorphism resulted from the work of Giletti et al. (1961) who dated muscovites from a series of foliated pegmatites from Knoydart and Morar. They obtained Rb-Sr ages from white micas of 740 ± 15 Ma, 740 ± 25 Ma, 725 ± 15 Ma from the Knoydart mica mine and $665 \pm$ Ma from Sgurr Breac, (Figure 4-1). The authors concluded that the Moine sediments in those areas were older than 740 Ma and that the pegmatites were formed at the time of early metamorphism of the Moine sediments. This event has been referred to as both the Knoydartian (Bowes 1968) and the Morarian (Lambert 1969). Since the early work of Giletti et al (1961), a lot of geochronological work has been undertaken with the aim of determining the nature of the Neoproterozoic

metamorphism. Published ages, together with errors and techniques are summarised below in Table 4-1.

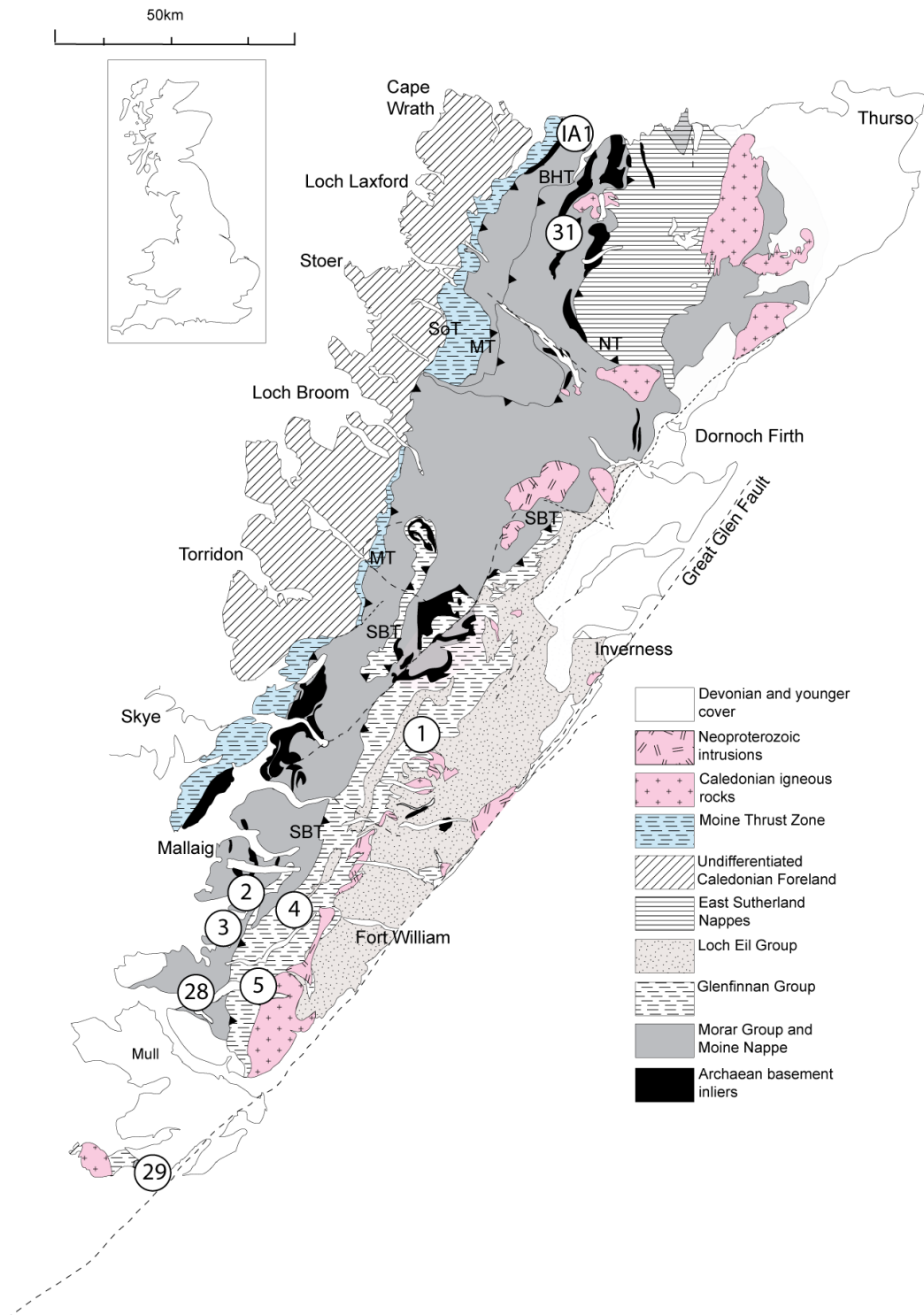


Figure 4-1, abbreviations 1 – AB08-01; 2 – AB07-02; 3 – AB07-03; 4 – AB07-04; 5 – AB09-05; 28 – AB07-28; 29 – AB07-29; 31 – AB07-31; IA1 – IA1; BHT – Ben Hope Thrust; K – Knoydart mica mine; MT – Moine Thrust; SBc – Sgurr Breac; SBT – Sgurr Beag Thrust; SoT – Sole Thrust.

Table 4-1 summary of previous Neoproterozoic geochronology. Mineral references use Kretz (1983).

Date (Ma)	Area	Lithology	System	Technique	Mineral(s)	Event	Reference
1028 ± 43	Ardgour Gneiss	Granitic gneiss	Rb-Sr	XRF & TIMS	WR	Metamorphism	Brook et al 1976
1024 ± 96	Druimindarroch Morar Pelite	Pelite	Rb-Sr	XRF & TIMS	WR	Metamorphism	Brook et al 1977
873 ± 6	Glen Doe WHGG	Metagabbro	U-Pb	TIMS	Zrn	Intrusion age	Miller 1999
873 ± 7	Ardgour Gneiss	Granitic gneiss	U-Pb	TIMS & SIMS	Zrn	Intrusion age	Friend et al 1997
870 ± 30	Fort Augustus Granite Gneiss	Loch Eil Group	U-Pb	SHRIMP	Zrn	Intrusion age	Rogers et al 2001
827 ± 2	Ardnish pegmatite	Pegmatite	U-Pb	TIMS	Mnz	Pegmatite generation age	Rogers et al 1998
825 ± 18	Drumna drochit	Garnet migmatite	U-Pb	LAICPMS	Mnz inclusion in Grt	Metamorphism	Cutts et al 2010
822 ± 5	Polnish	Morar Group Grt core	Sm-Nd		Grt core+WR	Prograde metamorphism	Vance et al 1998
815 ± 21	Glen uig	Morar Group	Sm-Nd		Grt+WR	Prograde metamorphism	Vance et al 1998
813 ± 5	Mallaig	Morar Group	Sm-Nd		Grt+WR	Prograde metamorphism	Vance et al 1998
788 ± 4	Polnish	Morar Group	Sm-Nd		Grt rim+WR	Metamorphism	Vance et al 1998
784 ± 1	Sgurr Breac	Pegmatite	U-Pb	TIMS	Zrn	Pegmatite generation age	Rogers et al 1998
761 ± 18	Loch Beag	Morar Group	Sm-Nd		Grt+WR	Metamorphism	Vance et al 1998
760 ± 15	Ardnish pegmatite	Pegmatite	Rb-Sr	TIMS	Ms	Minimum estimate for pegmatite generation	Powell et al 1983
740 ± 25	Knoydart mica mine	Pegmatite	Rb-Sr	TIMS	Ms	Pegmatite generation age	Giletti et al. 1961
740 ± 30	Loch Monar	Pegmatite	U-Pb	TIMS	Zrn	Pegmatite generation age	van Breemen et al 1978
737 ± 5	Lochailort Morar	Pelite	U-Pb	TIMS	Ttn	Titanite growth during D2	Tanner & Evans 2003
731 ± 44	Carn Gorm	Pegmatite	U-Pb	TIMS	Zrn	Pegmatite generation age	van Breemen et al 1974
730 ± 19	Glenfinnan	Pegmatite	U-Pb	TIMS	Zrn	Pegmatite generation age	van Breemen et al 1974
727 ± 6	Glenfinnan Group	Migmatite	U-Pb		Zrn	Migmatisation	Cutts et al. 2010
725 ± 15	Knoydart mica mine	Pegmatite	Rb-Sr	TIMS	Ms	Pegmatite generation age	Giletti et al 1961
724 ± 6	Drumna drochit	Garnet migmatite	U-Pb	LAICPMS	Mnz inclusion within Grt	Metamorphism	Cutts et al 2010
665 ± 15	Sgurr Breac	Pegmatite	Rb-Sr	TIMS	Ms	Pegmatite generation age	Giletti et al 1961
647 ± 20	Loch Eilt	Pegmatite	Rb-Sr				Long & Lambert 1963

Rb-Sr geochronology was also undertaken on foliated pegmatites at Loch Eilt, Carn Gorm, Kinlochourn and Ardnish and generally yielded ages between 730 Ma and 760 Ma with one younger date at 647 ± 20 Ma (Long & Lambert 1963; van Breeman et al. 1974, 1978; Powell et al. 1983; Piasecki & van Breemen 1983; Piasecki 1984). Monazite and zircon U-Pb analyses also yielded ages of 784 ± 1 Ma, 780 ± 10 Ma, 740 ± 30 , 815 ± 30 Ma and 827 ± 2 Ma (van Breemen et al. 1974, 1978; Rogers et al. 1998). Thus, the ages suggest Neoproterozoic activity between 740 Ma and 780 Ma. Rb-Sr whole rock analyses were undertaken on the Ardour Granite Gneiss of the West Highland Granite Gneiss (WHGG) and yielded a controversial age of 1028 ± 46 Ma (Brook et al. 1976). A similar age was obtained from the Morar Pelite of 1024 ± 96 Ma (Brook et al. 1977) and this was thought to represent the early prograde metamorphism of the Moine rocks which occurred during the end of the Grenville Orogeny (Harris et al. 1985; Powell et al. 1988). The Grenville ages suggested that the 740-780 Ma event recorded in the pegmatites did not represent a real Precambrian event, instead they were the result of partial resetting of Grenville ages during the Caledonian Orogeny (Powell et al. 1983). The field relations of the pegmatites are difficult to interpret as they show a lot of Caledonian strain and recrystallisation which obscures much of the original textures, which made it difficult to determine whether the pegmatites were emplaced syn-metamorphically or alternatively might simply represent a series of intrusions, perhaps related to Iapetus rifting (e.g. Powell et al. 1983; Soper & Anderton 1984; Powell & Phillips 1985). The Grenville ages, mentioned above, from Brook et al. (1977) were substantially older than the ages obtained from the pegmatites. Later U-Pb dating of bulk zircon fractions from the Ardour granite gneiss gave upper intercepts at 1517 Ma and 1556 Ma and lower intercepts at 556 Ma and 574 Ma, and thus did not support the Grenville ages (Pidgeon & Aftalion 1978; Aftalion & van Breemen 1980). More recent ages from the Ardour granite gneiss also show no evidence for Grenville emplacement. An age of 873 ± 7 Ma was obtained using TIMS and SIMS U-Pb on individual zircons, ages in the range of 1900-1100 Ma were also obtained from rounded zircon grains which were interpreted as detrital grains (Friend et al. 1997). The 873 Ma age is similar to the age of the Ardnish pegmatite described above (Rogers et al. 1998) and an age of 870 ± 30 Ma from the Fort Augustus Granite Gneiss within the Loch Eil Group (Rogers et al. 2001). These ages demonstrate that the granite gneisses formed at ~ 870 Ma. The ages could also suggest that the pegmatites were formed from the in-situ

melting of the Moine sediments and were contemporaneous with the WHGG and local garnet growth. This indicated that the pegmatites were Knoydartian in age and the 30 Myr difference in ages could suggest that the Knoydartian was either diachronous or comprised different thermal events. Rogers et al (2001) and Friend et al. (1997) also showed that the Moine sediments were deposited after the Grenville Orogeny, due to the presence of inherited grains of 950-1000 Ma from within the Fort Augustus body. This is supported by more recent studies which confirm the presence of 1100-1000 Ma inherited zircons within Moine sediments (Friend et al. 2003; Cawood et al. 2004; Kirkland et al. 2008). The ~870 Ma ages supplied evidence for a Neoproterozoic granite-forming event, but in which tectonic regime the granites were formed was still not known. It was argued that the granites were a syn-tectonic melting event related to the D₁ isoclinal folding of the Moine, thus a compressional event (Barr et al. 1985; Friend et al. 1997). Evidence for this was the lack of a thermal aureole surrounding the granites which suggested that the country rock was hot at the time of intrusion; and migmatitic leucosomes within the granites locally cross-cut the S₁ gneissic fabric which has been dated at 870 Ma. Another interpretation was that the granitic protolith of the gneiss was entirely pre-tectonic and formed during crustal extension and the formation of the Moine sedimentary basins (Millar 1999). This is supported by the presence of amphibolites which have tholeiitic protoliths and were interpreted to represent dykes and sills related to extension as they lack compressional structures (Soper 1994; Soper & Harris 1997; Millar 1999 and Dalziel & Soper 2001). U-Pb zircon ages of 873 ± 6 Ma from the Glen Doe meta-gabbro of the West Highland granitic gneiss support an extensional event (Millar 1999).

Although the nature of the ~870 Ma event is controversial, the younger events appear to have stronger evidence for their mode of deformation. Vance et al. (1998) using Sm-Nd on post-D₁ garnets from the Morar Group obtained core ages of between 814-823 Ma and a rim age of 788.3 ± 4.4 Ma, which suggests that the garnets grew over a time span of 34 Ma. These ages are similar to the age obtained from the Ardnish and Sgurr Breac pegmatites described above (Rogers et al. 1998). Vance et al. (1998) used THERMOCALC to model expected assemblages and mineral compositions on a pressure temperature pseudosection. By matching the garnet core composition from the sample with a garnet composition on the pseudosection it was seen that the garnet cores grew at approximately 5 kbar and 525°C. The same could be done for the garnet rims

giving 12-14 kbar and 675°C, for rim growth, thus showing garnet growth could only accompany burial as the pseudosection pressures need significant heating which requires significant crustal thickening during the Neoproterozoic; this was the first substantial evidence of the Knoydartian as a collisional orogenic event instead of an extensional event (Dalziel & Soper 2001). These PT estimates have recently been recalculated using the same mineral assemblage and mineral chemical data with an updated version of THERMOCALC to show that the metasediments record more modest pressures of 7.5 kbar. This would imply burial to around 21 km, suggesting that the Knoydartian thickening was less significant than originally thought and could be associated with extension (Cutts et al. 2009). Monazite inclusions within a garnet bearing migmatite of the Glenfinnan Group near Drumnadrochit give ages in the range of 825-780 Ma, and PT estimates of 650°C and 7 kbar (Cutts et al. 2010). These ages suggest peak metamorphism at ~820 Ma which could suggest that the Rb-Sr ages of ~750 Ma from the pegmatites around Ardnish, Sgurr Breac and various other localities (Piasecki & van Breemen 1983; Piasecki 1984; Hyslop 1992; Rogers et al. 1998) represent cooling from peak metamorphism (Strachan et al. 2008). Added to the complexity of the early metamorphic history of the Moine is a U-Pb titanite age of 737 ± 5 Ma from a calc-silicate pod within Morar Group rocks near Lochailort close to the Sgurr Beag thrust. The titanites grew during progressive sillimanite zone regional metamorphism (Tanner & Evans 2003). As the Morar and Glenfinnan Groups appear to record the same Neoproterozoic deformation events, Tanner & Evans (2003) suggest that the Sgurr Beag thrust is Neoproterozoic in age, not Caledonian as previously thought. A U-Pb zircon age of 727 ± 6 Ma was recorded from Glenfinnan Group migmatites near Drumnadrochit; this is complemented by 724 ± 6 Ma U-Pb monazite and 725 ± 4 Ma SIMS zircon inclusion ages from the middle zone of garnet which grew at 650°C and 6 kbar (Cutts et al. 2010). These ages are thought to date a younger metamorphic event (Strachan et al. 2008; Cutts et al. 2010). Another younger age was recorded within the Barnhill Shear Zone of the Glenelg inlier from syn-kinematic titanites which gave 669 ± 31 Ma. The shear zone contains Morar Group psammites which have been deformed at the same time as the titanite age is thought to date top to the west compression (Storey et al. 2004).

There is also evidence of Neoproterozoic deformation south east of the Great Glen Fault within the Dava Succession. Highton et al (1999) dated zircon rims using U-Pb from a

migmatised gneissose psammite and reported an age of 840 ± 11 Ma, which has been interpreted to date peak metamorphism. There are also ages from pegmatites and mylonitic rocks within the Grampian Shear Zone of 806 ± 3 Ma, (U-Pb monazite, Noble et al. 1996), and 750 Ma ages from pegmatites within the Appin Group (Piasecki and van Breemen, 1983), which confirm Neoproterozoic deformation within the Dava Succession.

4.4 Sample descriptions

The locations of the samples analysed within this chapter are shown on Figure 4-1, several of the samples had LA ICPMS and electron probe undertaken on them. LA ICPMS and electron probe were used to establish the spatial distribution of major and trace elements within the garnets. The garnets are almandine in composition with appreciable amounts of grossular. This is the classic composition of a garnet from a garnet-mica schist of regional metamorphism. The data also provided information about the inclusions within the garnets and their compositions. The LA-ICPMS measurements were normalised to silica values obtained from the electron probe data. This data is detailed below with thin section photograph; the mineral abbreviations use Kretz (1983).

AB07-02 – Polish Pelite

The Polish Pelite is part of the Morar Group and is a garnet mica schist sampled within 10 metres of the sample site of Vance et al. (1998) at NM 7445 8392. Vance et al. (1998) obtained an age of 822.7 ± 4.6 Ma from the garnet core and an age of 788.3 ± 4.4 Ma from the garnet rim using a Sm-Nd two point garnet + whole rock isochron. The rationale for re-dating garnets from this locality was to undertake Lu-Hf and Sm-Nd analyses to compare with the ages that Vance et al. (1998) reported, and compare the ages from the different isotopic systems.

In the field, the sample was dark with obvious pink-purple garnets protruding from the surrounding rock wrapped by a mica fabric. In thin section it comprises plagioclase, muscovite, biotite, garnet, quartz, chlorite and clinocllore. The schistosity is layered, with quartz and plagioclase-rich layers and micaceous layers, which may define the original bedding. The garnets are wrapped by an S_2 fabric. Clinocllore is present around the edges of the garnets which may indicate some retrograde deformation. The

garnets range from 0.1 mm to 6.5 mm in diameter and several are elongate in shape which leads to the suggestion that they may be pseudomorphs after chloritoid or chlorite (Leslie 2011 pers. comm.). The garnets form idio to xenoblastic crystals in all the samples and in some of the samples the garnets show three different textural zones, zone 1, 2 and 3 shown in Figure 4-2.

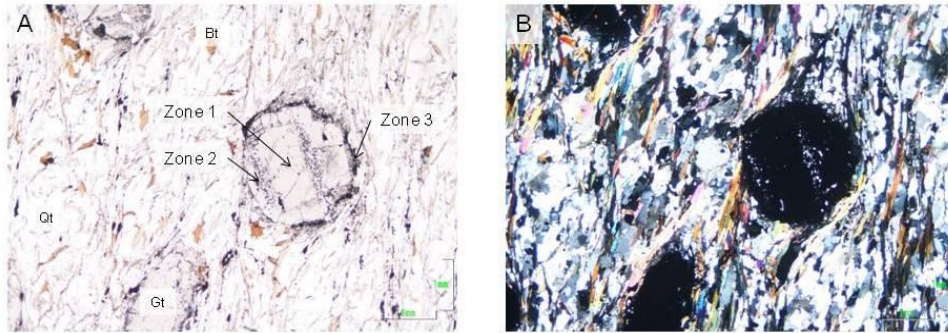


Figure 4-2, A and B shows AB07-02 in thin section. A shows three different textural zones within the garnet. The S_2 fabric, made up of quartz, white mica and biotite can be seen to be wrapping the garnets.

The zones do not occur in every crystal, and there seems to be no correlation between crystal size and zones present. The garnet core, zone 1, has few inclusions which are parallel to the S_1 schistosity; the boundary between zone 1 and zone 2 is marked by an accumulation of graphite and by a colour change from orange to purple. Zone 2 has more inclusions than zone 1; the inclusions follow on from the inclusion trails in zone 1 and are still aligned with the planar S_1 fabric. Zone 3 is not always present and does not preserve the planar S_1 fabric. It is more inclusion-rich than any of the other zones and is very dusty. The planar inclusion fabric recorded in zones 1 and 2 represent a pre-garnet fabric. The inclusions in the garnets are smaller than the crystals of the same material in the matrix, which indicates that substantial matrix recrystallisation has probably taken place. While picking these samples, the inner zone could be distinguished from the outer zones by the strong colour difference so were picked separately to obtain two ages from each rock.

MacQueen and Powell (1977) demonstrate that the zoning in the garnet from AB07-02 was developed during prograde metamorphism. They report that the FeO, MnO and CaO in the inner zone and part of the middle zone is similar to that reported by other

authors for whole crystals; showing that the growth of these crystals was continuous from nucleation to at least the first part of the middle zone.

Figure 4-3 shows LA ICPMS data for AB07-02. It shows marked manganese zoning, which on the electron probe changed from 0.1 wt% at the rim to 5.8 wt% in the core. Magnesium and iron show the opposite trend, increasing in concentration from core to rim, the electron probe data shows FeO decreasing from 34.7% in the rim to 30.8 wt% in the core. Calcium stays fairly constant in the core then shows a sharp decrease in the rim. The kinks in the data here are likely to represent the inclusions at zone boundaries. The zones have been marked on this graph. The progressive decrease in manganese and increase in iron and magnesium is consistent with growth resulting from prograde metamorphism; it is consistent with the consumption of chlorite which is characteristic of pelites subjected to increasing temperature.

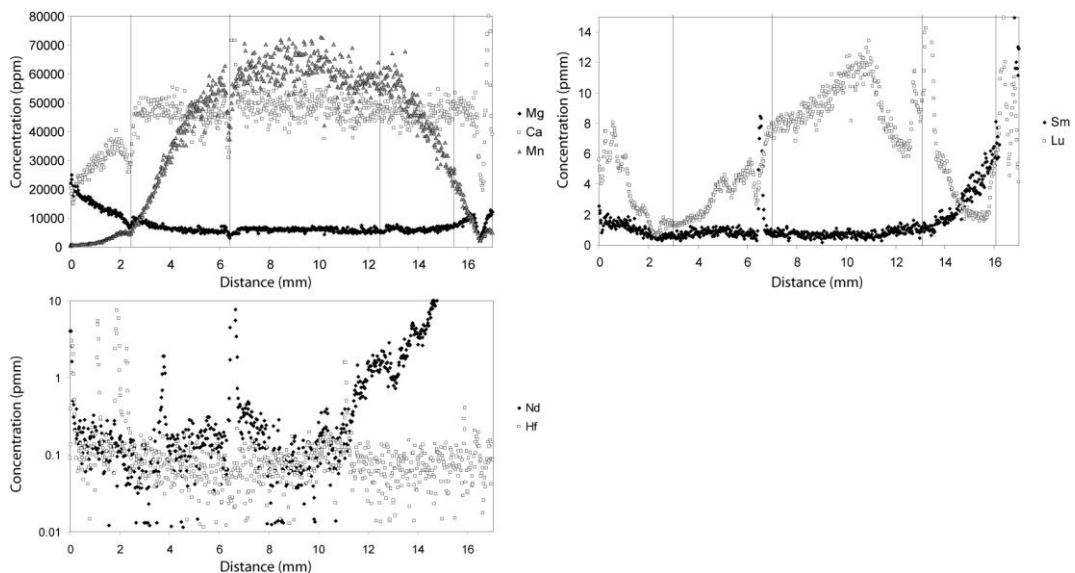


Figure 4-3, LA ICPMS element zonation across AB07-02 going from garnet rim to core to rim.

Figure 4-3 shows the concentrations of Lu and Sm across a garnet from AB07-02. The traces show typical HREE enrichment in Zones 1 and 2, shown by the increased Lu concentrations. HREE are strongly compatible in garnet and show Rayleigh-like profiles with steep fall of concentrations from core to rim. Such distribution is commonly accepted as reflecting prograde garnet growth conditions. In the case for this garnet the Lu trace implies partial redistribution of the original growth zonation during post-growth evolution in zone 3, shown by the increase in Lu concentration from the zone 2/3 boundary to the garnet rim. Hf is quite homogeneous throughout the garnet

and appears to only been affected by few zircon inclusions. The Nd profile has been affected by several large inclusions which have also affected Ca and Sm suggesting that they are phosphate inclusions. This may indicate that the age derived from the zone 1 (core) is likely to be representative of peak metamorphism but the rim age probably does not represent peak metamorphism as it has partially been reset. Figure 4-3 also shows the concentration of Sm across a garnet from the sample. Peaks in Sm indicate phosphate inclusions. The Sm trace increases towards the garnet rims, which is due to LREE being incompatible in garnets (Dutch & Hand 2009).

AB07-03 – Glenuig Pelite

The Glenuig Pelite is a garnet mica schist sampled within ~10 metres of the sample site of Vance et al. (1998) at NM 6707 7756. Vance et al. (1998) reported a garnet + whole rock age of 815 ± 21 Ma. The rationale for this sample is similar to that of AB07-02 where the aim is to replicate the Sm-Nd results and compare the Lu-Hf and Sm-Nd isotopic systems.

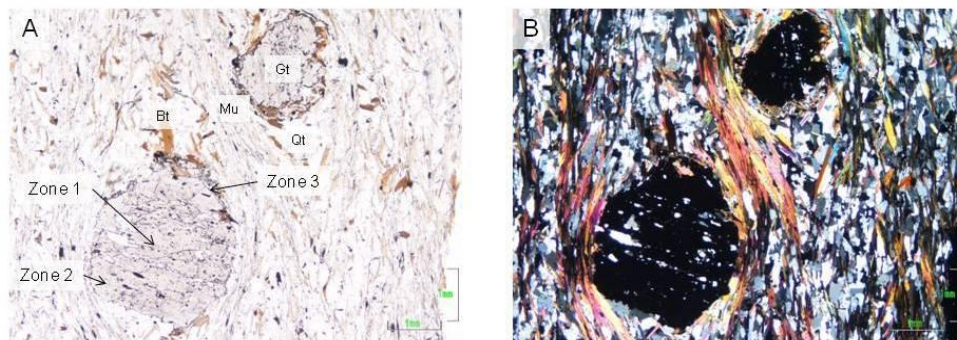


Figure 4-4, thin section photographs for AB07-03, A shows garnets with zoning and S_1 planar inclusions. The S_2 fabric made up of biotite, muscovite, feldspar and quartz is wrapping the garnets.

In the field the sample had a similar appearance to AB07-02 and was dark with dark garnets protruding from the surrounding rock. In thin section (Figure 4-4) it comprises plagioclase, muscovite, biotite, garnet, quartz, chlorite and clinochlore. The schistosity is layered, with quartz and plagioclase rich layers and micaceous layers. The garnets are wrapped by an S_2 fabric and are not as plentiful as AB07-02, however the garnets are larger, ranging from 0.2 mm to 7 mm. The garnets are euhedral and show zoning but not as obviously as AB07-02. The cores have fewer inclusions than the rims and the

inclusion trails are planar and are oblique to the fabric. The garnet rims are more inclusion-rich and are dusty in appearance. The boundary between the core and the rim is not as well defined as AB07-02, however, during picking the inner zone could be distinguished by colour differences from the outer zones so were picked separately to obtain two ages from each rock. The inclusions consist of quartz, mica, opaques are zircons and are smaller than the crystals of the same material in the matrix, which indicates that substantial matrix recrystallisation has probably taken place. The planar inclusion fabric observed is likely to represent a pre-garnet fabric.

AB07-04 - Loch Eilt Semi-pelitic Gneiss

This sample is a semi-pelitic gneiss from east of Loch Eilt within the Glenfinnan Group. The rationale for this sample was to help to constrain the age(s) of early metamorphism within the Glenfinnan Group, which at present is poorly constrained.

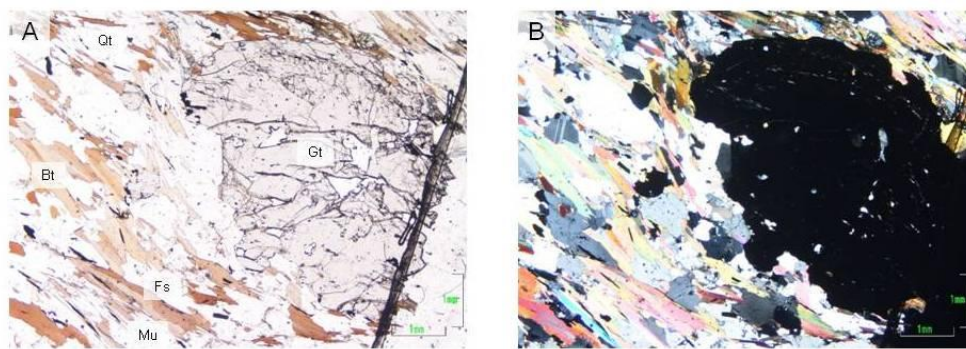


Figure 4-5, thin section photographs showing the relation of garnet and the surrounding fabric. A shows the sample in PP and B shows the sample in XP.

In thin section the sample contains kyanite, staurolite, muscovite, biotite and garnet with accessory rutile, apatite and zircon, (Figure 4-5). The sample is coarse with garnets up to 1 mm in size with inclusions of plagioclase, quartz and muscovites up to 4 mm in size. The planar fabric is defined by biotite, muscovite, quartz and plagioclase and wraps the garnets which have pressure tails. The kyanites are small > 0.5 mm and appear to be reacting in, usually associated with biotite, which could suggest that this sample has crossed into the kyanite zone. The biotites have zircon inclusions with pleochroic halos; the staurolites are small and well-formed.

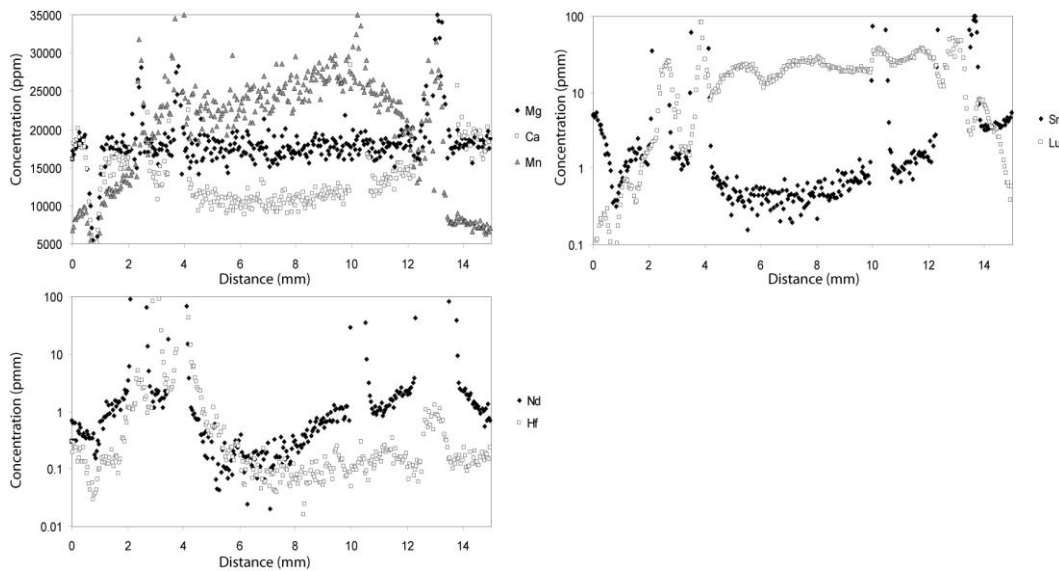


Figure 4-6, LA ICPMS trace for AB07-04.

Figure 4-6 shows Mg and Mn traces across a garnet from AB07-04. Mn shows Rayleigh-like zoning towards the garnet core and Mg shows a slight increase towards the garnet rims. Ca increases towards the garnet rims and has been affected by several inclusions.

Sm and Lu show the inverse of each other with Sm increasing towards the garnet rim and Lu increasing towards the garnet core, this suggests that the garnet records prograde growth thus the ages obtained should reflect peak metamorphism. The peaks in the Sm and Nd profile are also seen in the other LREE, some MREE and Ca which suggest that they are phosphate inclusions. Hf has been affected by few zircon inclusions.

AB07-28 – Glenborrowdale Pelite

AB07-28 was sampled from the part of the Morar Pelite close to the contact with the Upper Morar Psammite in Glenborrodale [NM 6101 6084]. In the field the sample was very garnetiferous with numerous small (<1.5 mm) dark garnets. In thin section the sample is made up of muscovite, biotite, garnet, plagioclase and quartz. The garnets are clearly zoned in thin section (Figure 4-7) with very small >1 mm inclusion-free cores with several inclusion-rich intermediate zones, the inclusions in these zones are curved. The outer zone is also inclusion-rich; however the inclusions are smaller in size and follow on from the curved inclusions in the intermediate zones. Often around this rim has a dusty dark appearance. All the garnets have chlorite surrounding them, and

pressure tails which also consist of chlorite. In some places the garnets are completely replaced by chlorite. The fabric is made up of mica-rich layers and quartz/ feldspar-rich layers which wrap the garnets and is clearly crenulated.

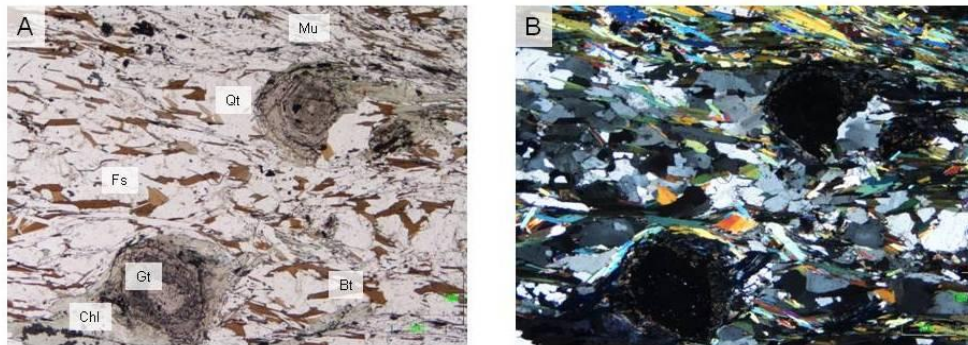


Figure 4-7, A shows AB07-28 in PP and B shows the sample in XP. The garnets can be seen to be complexly zoned and surrounded by chlorite. The matrix is crenulated and is made up of quartz, biotite, white mica and feldspar.

AB07-29- Shiaba Pelite

AB07-29 was sampled from part of the Shiaba Pelite which forms part of the Morar Group on the Ross of Mull [NM 4438 1890]. The rationale for this sample was to establish the age of high-grade metamorphism in the most southerly outcrops of the Moine. The Shiaba Pelite is a garnet-mica schist, and locally contains thin granitic pegmatites (Harris 2010).

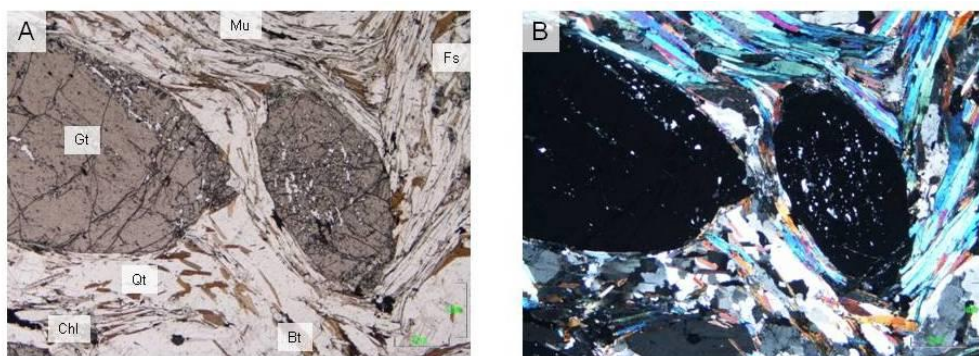


Figure 4-8, A shows AB07-29 in PP and B shows the sample in XP. The fabric can be seen to have been crenulated and consists of muscovite, feldspar, biotite and quartz.

The sample consists of garnet, muscovite, biotite, chlorite and quartz with accessory opaques, zircon, titanite and apatite, Figure 4-8. The garnets are up to 5 mm in size and show zoning with a fairly inclusion-poor core and an extremely inclusion-rich rim. The inclusions mainly consist of opaque minerals and quartz, zircon, titanite and chlorite.

Chlorite is present round the edges of many of the garnets and is reacting with the garnet. The majority of the small garnets (<0.4 mm) have been completely replaced by chlorite. Within the biotite layers there is evidence of another mineral that has been completely replaced by biotite, it was likely to have been kyanite or staurolite as it was elongate with high relief. The matrix is crenulated and consists of quartz and plagioclase rich layers and muscovite and biotite rich layers. Elongate opaque minerals are also present within the matrix.

AB07-31- Meadie Pelite

AB07-31 is the Meadie Pelite from the Morar Group of Sutherland. The rationale for this sample was to use Lu-Hf and Sm-Nd to establish the timing of peak metamorphism.

The sample is a garnet-staurolite-kyanite schist, Figure 4-9. In thin section the garnets are up to 8 mm and the few inclusions are of quartz and opaques. The garnets show zoning with more inclusions in the core than in the rims. The staurolites are up to 5 mm and do not have a good crystal shape, the edges are rough and have inclusions of quartz. The garnets and the large staurolite porphyroblasts are wrapped by the matrix.

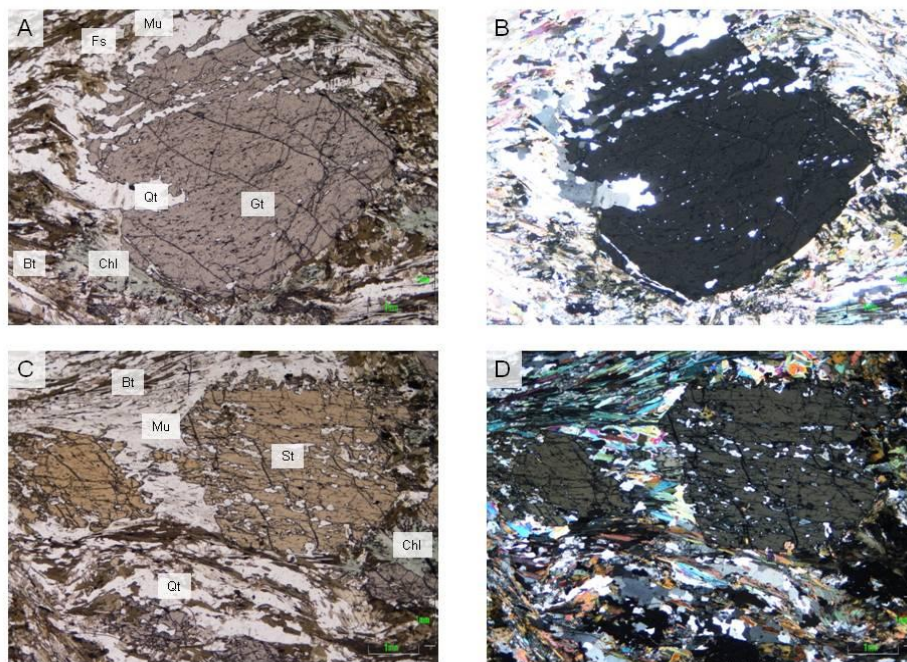


Figure 4-9, A shows one of the garnets from AB07-31 in PP, showing the curved inclusion trails which join up with the fabric. Chlorite is present round the edges of the garnets. B shows the same view in XP. C shows two of the large staurolites within the sample in PP, D shows the same view in XP.

Smaller staurolite porphyroblasts are present within the matrix and are found next to poorly-formed kyanite crystals, this is likely to represent the staurolite-out reaction $\text{staurolite} + \text{muscovite} + \text{quartz} = \text{Al}_2\text{SiO}_5 + \text{biotite} + \text{H}_2\text{O}$. The matrix consists of quartz, K feldspar, muscovite, bitotie and chlorite. Chlorite is mostly present round the edges of the garnet porphyroblasts. The biotites have zircon inclusions which have pleochroic haloes.

Figure 4-10 shows an elemental profile across a garnet from AB07-31. MgO increases towards the garnet core and CaO increases towards the garnet rim, which is a typical garnet growth profile. The depressions correlate to quartz inclusions. AB07-31 shows notable Lu zoning, with Lu increasing towards the core. Sm and Nd do not show any obvious zoning perhaps reflecting several phases of garnet growth. Hf is fairly homogeneous throughout the garnet and has been affected by a few zircon inclusions. The Lu-Hf age should reflect garnet growth; the Sm-Nd age should also reflect garnet growth but as the profile may reflect several phases of growth different garnet fractions may give very different ages.

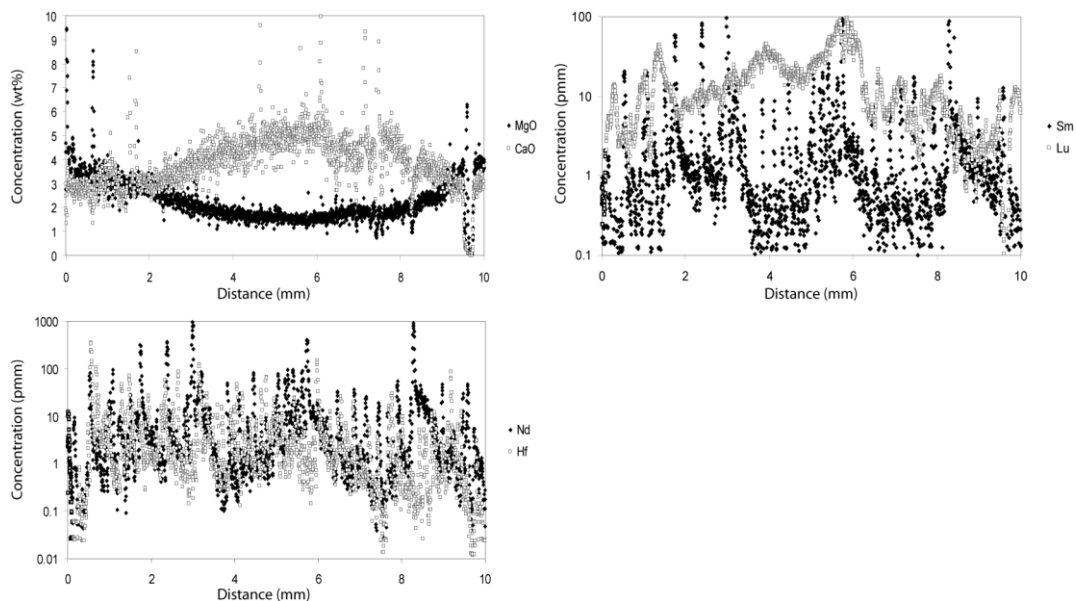


Figure 4-10, LA ICPMS profiles for AB07-31 across one garnet.

AB08-01 – Glenfinnan Group Garnet Gneiss

AB08-01 is a Glenfinnan Group garnet gneiss collected from the summit of Sgurr Clach nan Geala [NH 1850 1735], north of Loch Fannich. This sample was collected close to

Sgurr Beag Thrust. The rationale was to establish the timing of early high-grade metamorphism within the Glenfinnan Group in central Ross-shire.

In thin section it contains garnet, biotite, plagioclase, quartz, rutile and sphene, Figure 4-11. The garnets are euhedral and are up to 8 mm in size; they are wrapped by the fabric and sometimes have chlorite around the garnet rims. The garnet cores are more inclusion-rich than the rims, the inclusions consist of quartz, sphene and apatite. The fabric is made up of biotite, plagioclase and quartz with accessory rutile and sphene. The rutiles often have black framboidal rims and are most commonly associated with the biotite. There are also zircon inclusions within the biotite with pleochroic halos.

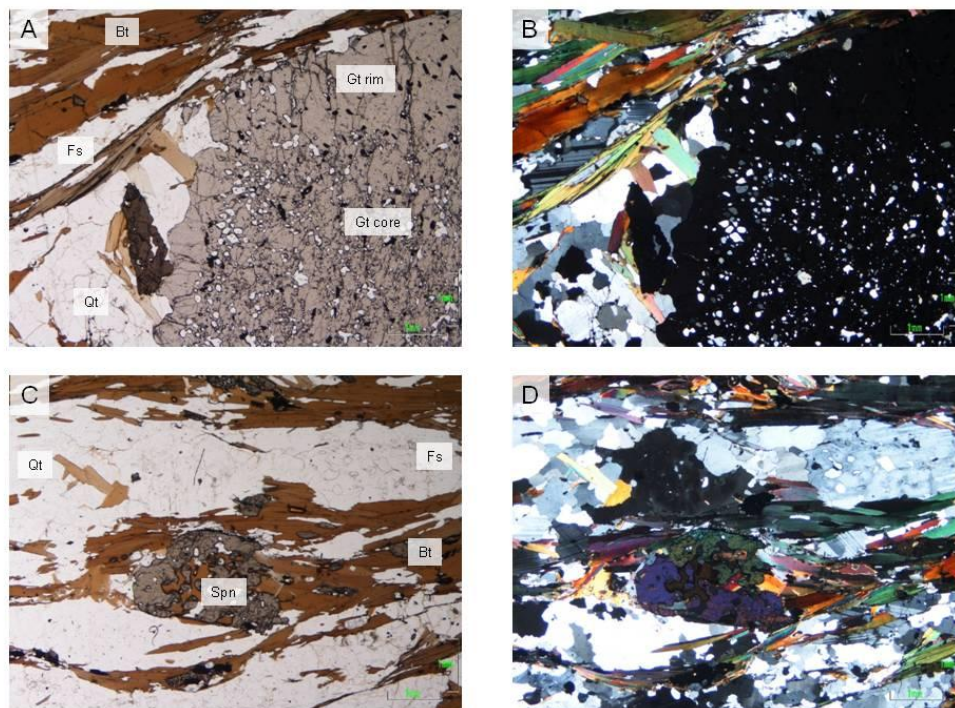


Figure 4-11, A shows one of the garnets from AB08-01 in PP, showing the clear distinction between the garnet core and rim. B shows the same view in XP and clearly shows the biotite wrapping the garnet. C shows the fabric consisting of biotite, feldspar and quartz, and one of the large sphenes present within this sample. D shows the same view but in XP.

Figure 4-12 shows the elemental profiles, rim to core from a garnet from AB08-01. The major element profile remains flat which is likely due to REE diffusing slower than major elements so they retain their prograde growth zoning profile (Dutch & Hand, 2009). There are several depressions which represent quartz inclusions. The Lu profile increase towards the garnet core and Sm profile shows a slight increase towards the

garnet rim. The Nd and Hf traces have been affected by many inclusions. The Lu-Hf and Sm-Nd ages from this sample should reflect garnet growth.

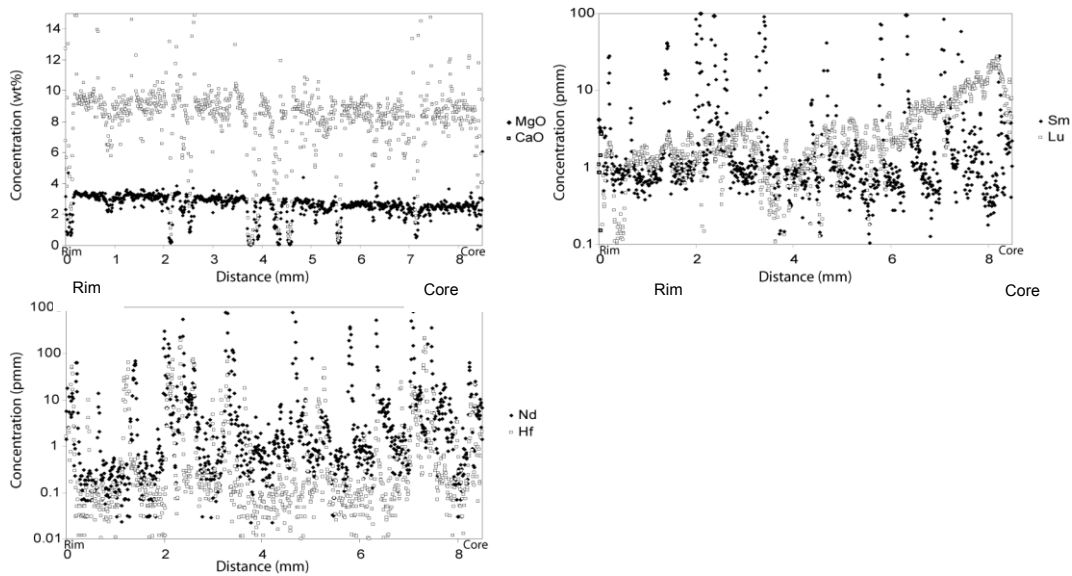


Figure 4-12, LA ICPMS profiles for AB08-01 from garnet rim to garnet core.

AB09-05 – Glenborrodale Pelitic Gneiss

AB09-05 is a garnetiferous pelitic gneiss from within the Glenfinnan Group and was collected east of Resipole Camping and Caravan site within Glenborrodale [NM 7246 6382]. The sample was collected within a pelitic layer with very fresh pink garnets up to 3 mm in size.

In thin section the sample contains muscovite, biotite, garnet, quartz and plagioclase, with kyanite which is reacting in and is usually associated with biotite, Figure 4-13. The garnets are subhedral and are mostly inclusion free, and the fabric does not wrap them perhaps indicating that they were post kinematic. The fabric consists of micaceous layers and quartz/ plagioclase layers which show a mild crenulation.

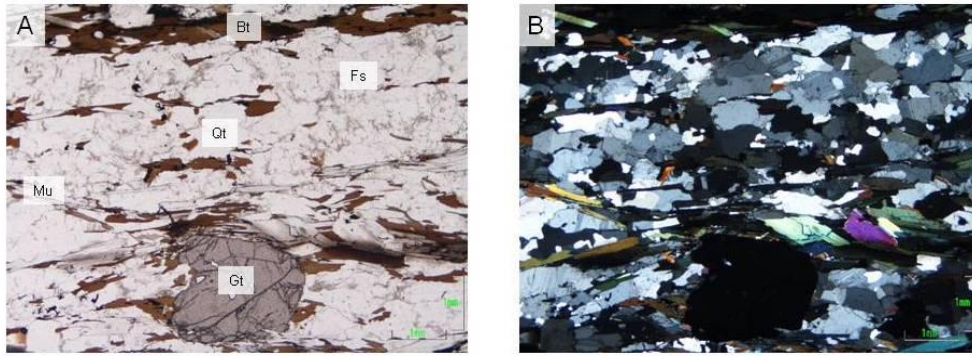


Figure 4-13, A shows AB09-05 in PP showing the fabric wrapping the garnets. B shows the same view in XP.

IA1- Creag Mhor Pelite

The sample was collected by Ian Allsop at [NC 5892 6487]; from the Morar Group of north Sutherland. In the field it had very defined zoning and large garnets up to 20 mm in size which appear to be wrapped by the fabric.

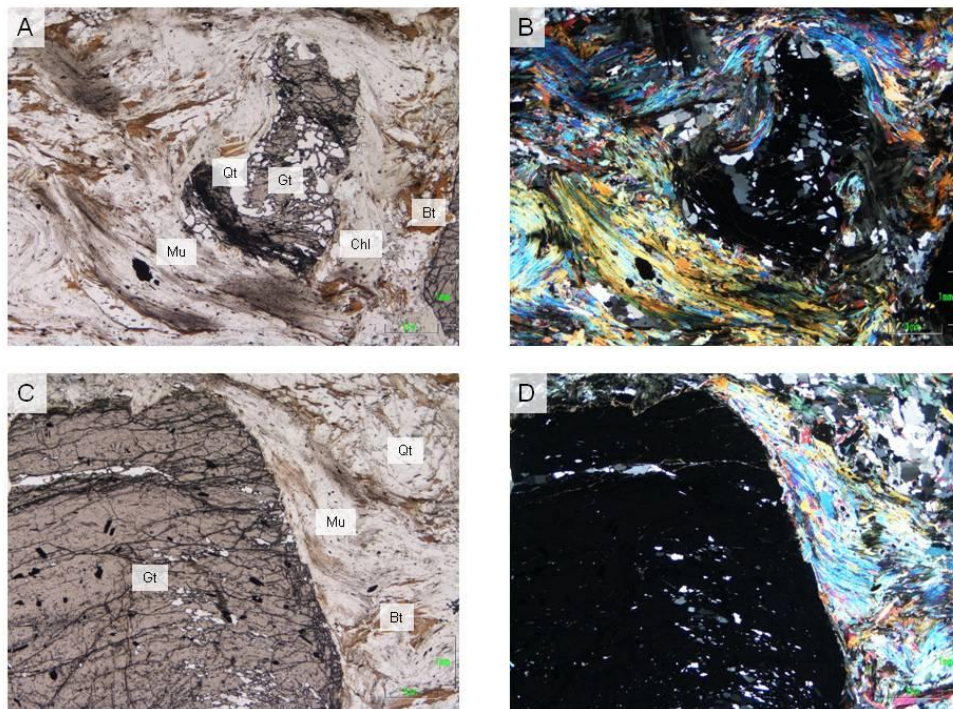


Figure 4-14, shows IA1 in thin section. A shows the fabric dominated by white mica wrapping the garnet. Chlorite is also surrounding the garnets; B shows the same view in XP. C shows a large garnet with an inclusion poor core and an inclusion-rich rim; D shows the same view in XP, the mica-rich and quartz-rich layers in the fabric can be seen clearly.

In thin section it is made up of garnet, muscovite, biotite, quartz and plagioclase with accessory rutile and apatite, Figure 4-14. The fabric is split into micaceous rich layers and quartz/ feldspar layers which are crenulated with distinct Q and P zones. The fabric wraps the garnets with chlorite appearing round the rims. The inclusions are slightly curved and are made up of quartz, opaques, zircon and muscovite. The garnets have very small inclusion free cores (>1 mm) and intermediate zone which is inclusion-rich and a dusty rim which is not always present.

4.5 Results and interpretation

4.5.1 Morar Group

The results are summarised in Table 4-2 and 4-4. From the Morar Group the oldest Lu-Hf age obtained was from the core of AB07-28 which gave a two point garnet-whole rock age of 982 ± 6 Ma. AB07-28 rim gave a two point garnet-whole rock Lu-Hf age of 490 ± 5 Ma. The thin section from this sample (Figure 4-7) shows that the garnets from this sample consist of multiple zones. The two fractions analysed here were separated during picking based on colour difference (purple core and an orange rim), this obviously bulks many of the growth zones together suggesting that these ages are likely to be mixing ages between many growth events. LA ICPMS was not undertaken for this sample, thus it is impossible to evaluate the effect of inclusions, however AB07-28 rim gave a Hf concentration of 4.100 ppm and a AB07-28 core gave a Hf concentration of 3.097 ppm. This suggests that there has been some influence from zircon inclusions and because of the high Hf concentrations both fractions gave low $^{176}\text{Lu}/^{177}\text{Hf}$ ratios, which indicates that the age should be used with some caution. AB07-28 gave two Palaeozoic Sm-Nd ages with large errors, the core gave a Sm-Nd two point garnet-whole rock age of 424 ± 81 Ma, and the rim gave a Sm-Nd two point garnet-whole isochron age of 512 ± 84 Ma. Sm-Nd was dated using the same fractions as Lu-Hf thus the many of the growth fractions have been bulked together, suggesting that the ages are not relating to a specific phase of garnet growth. The $^{147}\text{Sm}/^{144}\text{Nd}$ ratios are low from the garnet fractions and the $^{143}\text{Nd}/^{144}\text{Nd}$ ratios are similar to the whole rock ratios thus these ages are not reliable. The Nd concentrations from ID are 3.418 ppm and 3.022 ppm suggesting some influence from Nd-rich inclusions.

AB07-31 gave a core age of 947 ± 4 Ma and a rim age of 942 ± 4 Ma which are within error of each other. The core and rim were separated during picking based on a purple core and an orange rim. It has been suggested by Cutts et al. (unpublished) that the garnets from AB07-31 have three growth zones, a Neoproterozoic core, a middle zone and a thin Caledonian rim. It was impossible during picking to distinguish between the middle zone and the outer rim, thus it is likely they were picked as one fraction. The Hf concentration was estimated from part of the pure garnet using the LA ICPMS trace by looking at parts of the trace which were above the detection limit and were not affected by zircon inclusions. The LA ICPMS gave a Hf concentration of ~ 1.72 ppm for pure garnet which is just less than half of the Hf concentration from ID from both of the garnet fractions. This suggests that there has been some influence from zircon inclusions. The effect of the zircon inclusions can be modelled if the $^{176}\text{Hf}/^{177}\text{Hf}$ ratio of the zircon inclusions is known along with the concentration of Lu and Hf in the inclusions. This information is not known, however if it is assumed that the zircon inclusions are ~ 1600 Ma based on detrital zircon data from Kirkland et al. (2008) and Cawood et al. (2004, 2007), then a $^{176}\text{Hf}/^{177}\text{Hf}$ ratio can be estimated. Using Lu and Hf concentration estimates of ~ 84 ppm and ~ 9603 ppm for the zircon inclusions the effect of the zircons can be estimated. Using this information the pure garnet core is estimated to have an age of ~ 995 Ma and the garnet rim is estimated to have an age of ~ 983 Ma. However, as the oldest Sm-Nd age from AB07-31 was a two point garnet-whole rock isochron age of 951 ± 34 Ma from Gt core 2, which is within error of the Lu-Hf ages, this suggests limited influence from zircons or Nd-rich inclusions on these ages. AB07-31 core 1 gave a younger Sm-Nd age of 841 ± 9 Ma. The Sm-Nd rim ages from this sample were 773 ± 26 Ma and 701.7 ± 9.7 Ma. The Nd concentration for pure garnet from LA ICPMS was ~ 0.78 ppm, the Nd concentrations from ID ranged from 2.372 ppm to 3.401 ppm suggesting some input from Nd-rich inclusions. The spread in ages could represent physical mixing between the picked garnet core and rims, as this sample gives Sm-Nd core ages that are different by almost 100 Ma and rim ages that differ by 70 Ma. To establish whether mixing has affected any of the samples analysed here, mixing end members were calculated based on 950 Ma cores, 430 Ma rims and LA ICPMS concentrations of Sm, Nd, Lu and Hf. This information was plotted into four diagrams, a $^{176}\text{Hf}/^{177}\text{Hf}$ versus $^{176}\text{Lu}/^{177}\text{Hf}$ diagram, a $^{143}\text{Nd}/^{144}\text{Nd}$ versus $^{147}\text{Sm}/^{144}\text{Nd}$, a $1/\text{Nd}$ versus $^{147}\text{Sm}/^{144}\text{Nd}$ and $1/\text{Hf}$ versus $^{176}\text{Lu}/^{177}\text{Hf}$.

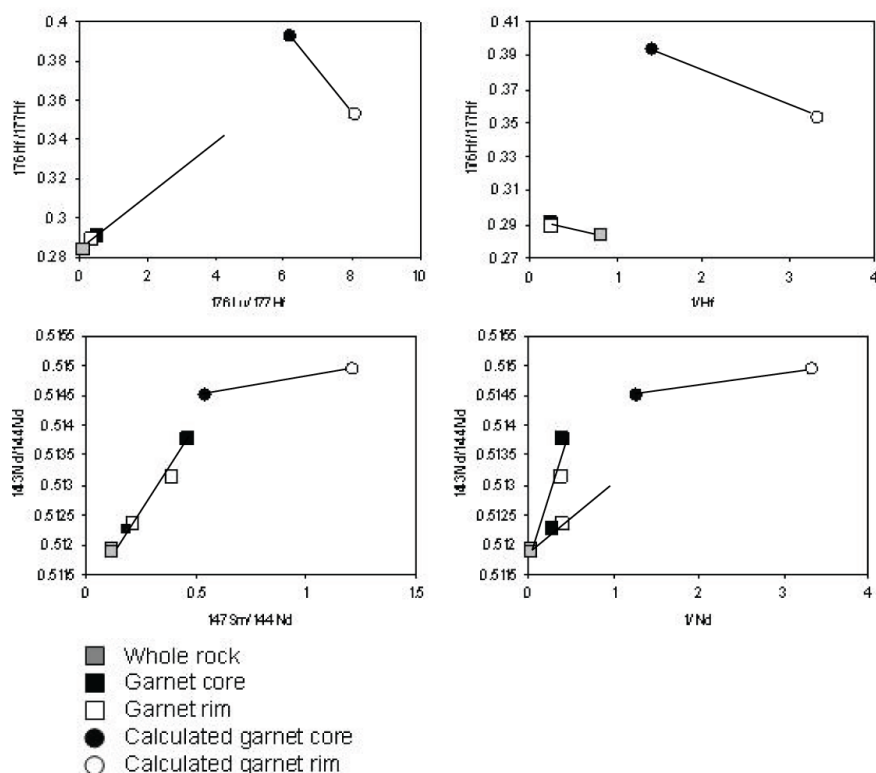


Figure 4-15 $^{176}\text{Lu}/^{177}\text{Hf}$ vs $^{176}\text{Hf}/^{177}\text{Hf}$; $^{176}\text{Lu}/^{177}\text{Hf}$ vs $1/\text{Hf}$; $^{147}\text{Sm}/^{144}\text{Nd}$ vs $^{143}\text{Nd}/^{144}\text{Nd}$ and $^{147}\text{Sm}/^{144}\text{Nd}$ vs $1/\text{Nd}$ for AB07-31. The filled black squares are the measured garnet core fractions, the empty black squares are the garnet rim fractions, the grey squares are the measured whole rock fractions, the filled black circles are the old calculated end members and the empty circles are the Caledonian end members. The end members were 950 Ma and 430 Ma.

Garnet fractions that are the result of mixing should lie on mixing lines on all diagrams, offset to some degree toward the whole rock composition as a result of inclusions. AB07-31 gave a Lu-Hf core age of 947.0 ± 4.2 Ma and a rim age of 942.1 ± 3.7 Ma, thus it is unlikely that this sample has been affected by any mixing. This is seen on the graphs in Figure 4-15. For Sm-Nd the end members were 950 Ma and 430 Ma, mixing could be interpreted to have happened on both of these diagrams, but as no mixing is seen on the Lu-Hf diagrams no physical mixing has occurred.

AB07-03 gave a core Lu-Hf age of 903.2 ± 2.9 Ma and a rim Lu-Hf age of 843.4 ± 3.3 Ma. This sample had no LA ICPMS undertaken on it making it difficult to assess the influence of inclusions on the Lu-Hf age. The ID Hf concentrations were 1.629 ppm for the core and 2.524 ppm for the rim; this could suggest some influence from zircon inclusions, especially for the garnet rim which has a higher Hf concentration. Sm-Nd

for this sample yielded a core age of 757 ± 14 Ma and a rim age of 683 ± 38 Ma. The garnet rim fraction has a significantly higher Nd concentration than the garnet core fraction (2.020 ppm compared to 0.619 ppm), suggesting that the rim has been influenced by Nd-rich inclusions.

AB07-29 gave a Lu-Hf two point garnet-whole rock isochron age of 878 ± 3 Ma and a Lu-Hf rim two point garnet-whole rock isochron age of 832 ± 3 Ma. This sample also had no LA ICPMS; however the ID Hf content was 3.679 ppm for the core fraction and 3.518 ppm for the rim fraction suggesting influence from zircon inclusions. AB07-29 gave a Sm-Nd age of 665 ± 9 Ma from the garnet rim and the garnet core yielded an age of 253.4 ± 3.0 Ma. Both of the $^{147}\text{Sm}/^{144}\text{Nd}$ and the $^{143}\text{Nd}/^{144}\text{Nd}$ ratios for these ages seem to be high enough to yield meaningful ages, thus it is unclear why the core has given such a young age. The analysed garnet fraction gave Nd concentrations of 1.776 ppm (core) and 1.507 ppm (rim) suggesting little influence from Nd-rich inclusions.

AB07-02 gave a Lu-Hf core two point garnet-whole rock isochron age of 860.7 ± 2.7 Ma and a Lu-Hf rim two point garnet-whole rock isochron age of 828.8 ± 3.5 Ma. The LA ICPMS gave pure garnet core and rim concentrations of 0.138 ppm and 0.225 ppm respectively. This suggests that the rim age may have been affected by zircon inclusions. Using the modelling described above the pure garnet core gave an age of ~ 866 Ma confirming little or no effect from zircon inclusions and the rim gave an age of ~ 918 Ma suggesting that the rim could have been affected by zircon inclusions. Sm-Nd from this sample gave a two point garnet-whole rock core age of 795.9 ± 2.4 Ma and a two point garnet-whole rock rim age of 772.6 ± 2.4 Ma. ID gave Nd concentrations of 0.237 ppm for the core and 0.360 ppm for the rim, which is similar to a pure garnet value of 0.268 ppm suggesting little input from Nd-rich inclusions on these ages. Figure 4-16 shows the Lu-Hf mixing graphs for this sample, the Lu-Hf end members calculated for AB07-02 were 945 Ma and 460 Ma and Sm-Nd the end members were 940 Ma and 460 Ma. On both the Lu-Hf and Sm-Nd isochron diagrams mixing could be interpreted to have occurred but as there is no sign of mixing on the $1/\text{Hf}$ or $1/\text{Nd}$ diagrams it indicates that there is no mixing.

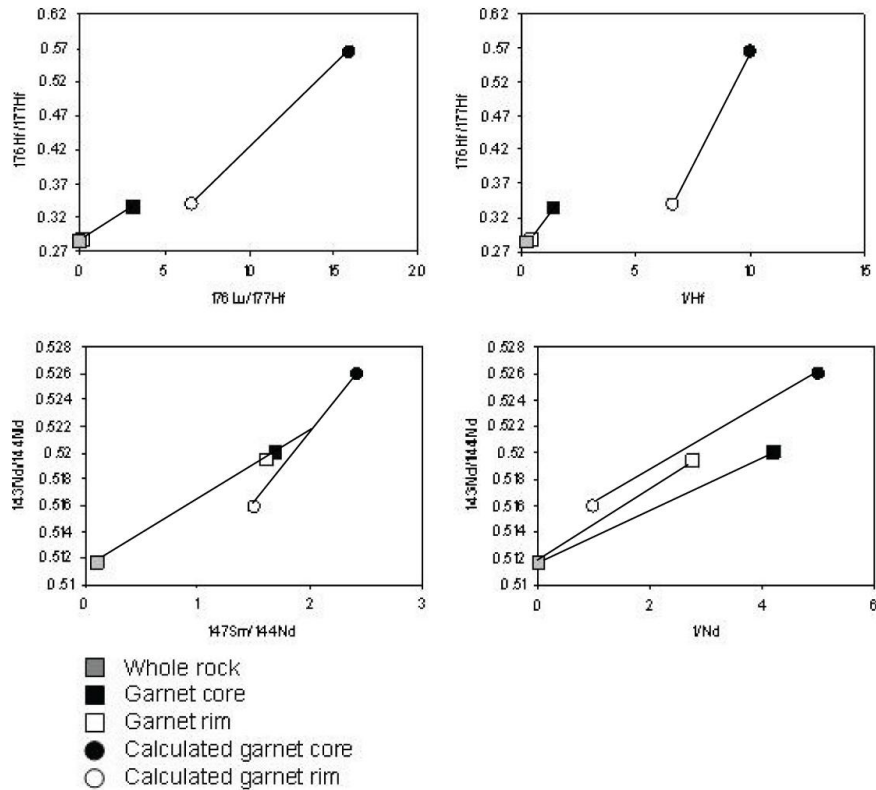


Figure 4-16 $^{176}\text{Lu}/^{177}\text{Hf}$ vs $^{176}\text{Hf}/^{177}\text{Hf}$; $^{176}\text{Lu}/^{177}\text{Hf}$ vs $1/\text{Hf}$; $^{147}\text{Sm}/^{144}\text{Nd}$ vs $^{143}\text{Nd}/^{144}\text{Nd}$ and $^{147}\text{Sm}/^{144}\text{Nd}$ vs $1/\text{Nd}$ for AB07-02. The filled black squares are the measured garnet core fractions, the empty black squares are the garnet rim fractions, the grey squares are the measured whole rock fractions, the filled black circles are the old calculated end members and the empty circles are the Caledonian end members. The end members were 950 Ma and 460 Ma.

Sample IA1 gave significantly younger Lu-Hf two point garnet-whole rock isochron ages of 530 ± 5 Ma for the core and 476 ± 3 for the rim. The $^{176}\text{Lu}/^{177}\text{Hf}$ ratios for each of the garnet fractions are sufficiently high to provide meaningful ages. LA ICPMS has not been undertaken on this sample; however the higher than expected Hf concentrations of 2.213 ppm for the garnet core and 1.356 ppm for the rim suggest that these ages were influenced by zircon inclusions. A Sm-Nd age of 886 ± 76 Ma was obtained from IA1 garnet rim, this age is not reliable as the fraction has $^{147}\text{Sm}/^{144}\text{Nd}$ and $^{143}\text{Nd}/^{144}\text{Nd}$ ratios very similar to the whole rock. It also gives a high Nd concentration of 3.958 ppm, suggesting that inclusions may have affected the age. The core from this sample gave a Sm-Nd age of 4959 ± 2300 Ma, which is geologically impossible. The $^{147}\text{Sm}/^{144}\text{Nd}$ and $^{143}\text{Nd}/^{144}\text{Nd}$ ratios from this fraction were very close to the whole rock

and it gave a Nd concentration of 8.207 ppm suggesting influence from Nd-rich inclusions.

4.5.2 Glenfinnan Group

The sample that gave the oldest age from the Glenfinnan Group was AB08-01 which gave a core two point garnet-whole rock Lu-Hf age of 749 ± 6 Ma and a Lu-Hf rim two point garnet-whole rock age of 796 ± 58 Ma. This latter age is very imprecise due to the similarity of the rim $^{176}\text{Hf}/^{177}\text{Hf}$ ratio to the whole rock ratio, however as both of the $^{176}\text{Lu}/^{177}\text{Hf}$ are reasonably high the ages should be meaningful. LA ICPMS gave a pure garnet Hf concentration of ~ 0.22 ppm, while ID gave a garnet core Hf concentration of 1.389 ppm and a rim concentration of 0.503 ppm suggesting some influence from zircon inclusions. Using the zircon modelling described above for a zircon ~ 1400 Ma (Cawood et al. 2004; 2007) which is one of the most prominent zircon peaks for the Glenfinnan Group, the garnet core gives an age of ~ 720 Ma and the garnet rim gives an age of ~ 1474 Ma. AB08-01 gave a Sm-Nd two point garnet-whole rock isochron age of 686 ± 16 Ma from the garnet core, the $^{147}\text{Sm}/^{144}\text{Nd}$ is sufficiently high to provide a reliable age, however the $^{143}\text{Nd}/^{144}\text{Nd}$ ratio is quite close to whole rock which accounts for the large error. The garnet rim gave a Sm-Nd two point garnet-whole rock age of 1247 ± 52 Ma, the $^{176}\text{Lu}/^{177}\text{Hf}$ ratio for this fraction was very close to that of the whole rock suggesting that this fraction was not radiogenic. ID gave Nd concentrations of 1.340 ppm for the core and 4.510 ppm for the rim, while the pure garnet had a Nd concentration of 0.31 ppm suggesting that Nd-rich inclusions affected these ages. Figure 4-17 shows the mixing diagrams for AB08-01. As AB08-01 is from the Glenfinnan Group, the end members for Lu-Hf were 780 Ma and 460 Ma. AB08-01 does show mixing on the isochron diagrams but does not show any mixing in the 1/Hf and 1/Nd diagram.

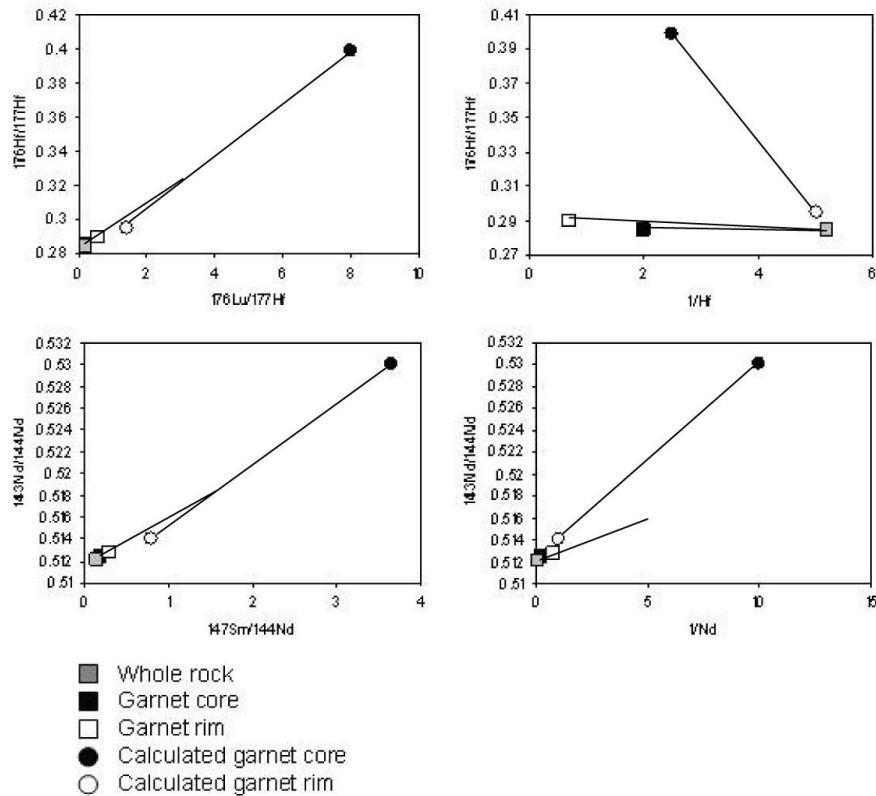


Figure 4-17 $^{176}\text{Lu}/^{177}\text{Hf}$ vs $^{176}\text{Hf}/^{177}\text{Hf}$; $^{176}\text{Lu}/^{177}\text{Hf}$ vs $1/\text{Hf}$; $^{147}\text{Sm}/^{144}\text{Nd}$ vs $^{143}\text{Nd}/^{144}\text{Nd}$ and $^{147}\text{Sm}/^{144}\text{Nd}$ vs $1/\text{Nd}$ for AB08-01. The filled black squares are the measured garnet core fractions, the empty black squares are the garnet rim fractions, the grey squares are the measured whole rock fractions, the filled black circles are the old calculated end members and the empty circles are the Caledonian end members. The end members were 780 Ma and 460 Ma.

AB07-04 gave a Lu-Hf two point garnet-whole rock isochron age of 739.5 ± 2.5 Ma for the garnet core and an age of 697.7 ± 3.1 Ma for the rim. The $^{176}\text{Lu}/^{177}\text{Hf}$ ratios for these fractions are high (0.792 for the core and 0.492 for the rim), complemented by high Lu concentrations (23.45 ppm for the core and 21.26 ppm for the rim) suggesting that these ages should be reliable. The LA ICPMS gave pure garnet values between 0.12 ppm and 0.20 ppm, ID gave Hf concentrations of 4.193 ppm for the core and 6.113 ppm for the rim suggesting that some zircon has been digested with the garnet. Using the modelling described above the garnet core gave an age of ~ 757 Ma and the rim gave ~ 731 Ma, suggesting that zircons have not had a large effect on the ages obtained from this sample. AB07-04 gave a Sm-Nd two point garnet-whole rock isochron core age of 540 ± 3 Ma and a rim age of 498 ± 2 Ma. The LA ICPMS Nd trace for this sample showed that it had been affected by several large inclusions; the pure garnet gave a

concentration ranging from ~0.33 ppm to 1.45 ppm. The $^{147}\text{Sm}/^{144}\text{Nd}$ ratios are high, especially in the rim fraction which gave a ratio of 2.149, suggesting that these ages are reliable. ID gave Nd concentrations of 0.519 ppm for the core and 0.319 ppm for the rim suggesting despite the inclusions seen using LA ICPMS there appears to have been little effect from inclusions on the ages obtained. Figure 4-18 shows the mixing diagrams for AB07-04, as this sample is from the Glenfinnan Group, the end members were 780 Ma and 460 Ma. In the Lu-Hf there is clearly no sign of mixing, however in the Sm-Nd diagrams the sample does show signs of mixing, the tie lines intersect on both diagrams. To be physical mixing, all four diagrams need to both show mixing, as this is not the case the sample has not been affected by mixing between an old core and young rim during picking. It is likely that the mixing indicated by the Sm-Nd analysis represents partial resetting of the Sm-Nd system during the Caledonian orogeny.

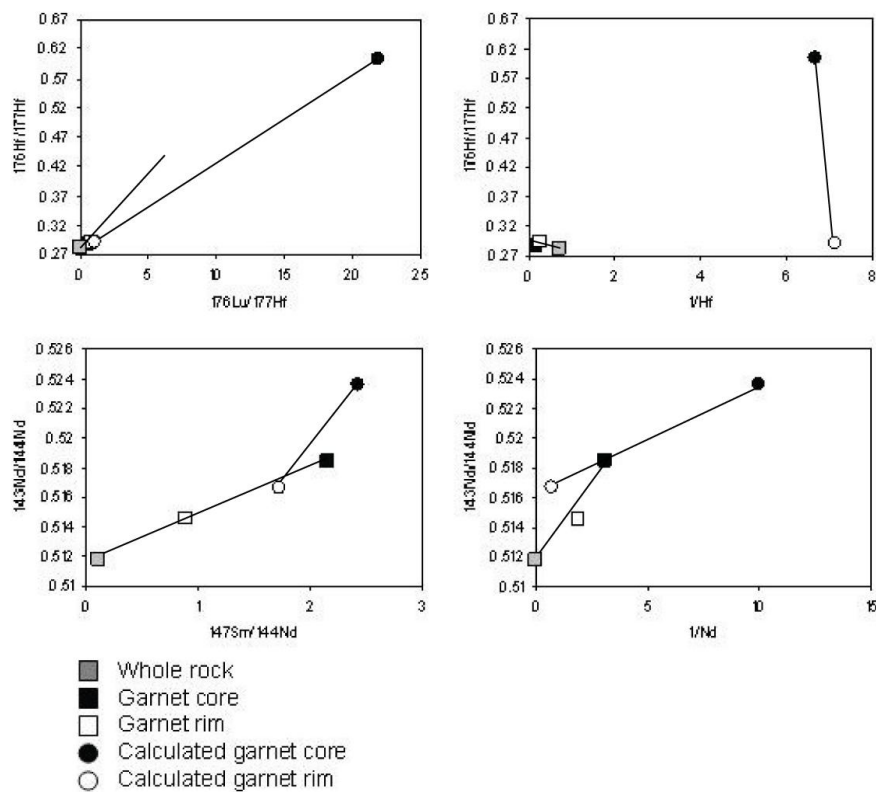


Figure 4-18 $^{176}\text{Lu}/^{177}\text{Hf}$ vs $^{176}\text{Hf}/^{177}\text{Hf}$; $^{176}\text{Lu}/^{177}\text{Hf}$ vs $1/\text{Hf}$; $^{147}\text{Sm}/^{144}\text{Nd}$ vs $^{143}\text{Nd}/^{144}\text{Nd}$ and $^{147}\text{Sm}/^{144}\text{Nd}$ vs $1/\text{Nd}$ for AB07-04. The filled black squares are the measured garnet core fractions, the empty black squares are the garnet rim fractions, the grey squares are the measured whole rock fractions, the filled black circles are the old calculated end members and the empty circles are the Caledonian end members. The end members were 780 Ma and 460 Ma.

AB09-05 gave a Lu-Hf two point garnet-whole rock core age of 685.3 ± 2.2 Ma and a rim age of 640.2 ± 2.4 Ma. The $^{176}\text{Lu}/^{177}\text{Hf}$ ratios for these fractions are 0.49 for the core and 0.36 for the rim which are reasonably high and complemented by high Lu concentrations (16.71 ppm for the core and 14.57 ppm for the rim) suggests that these ages should be reliable. LA ICPMS was not undertaken on this sample, however as the Hf concentration obtained by ID is high, 4.82 ppm for the core and 5.73 ppm for the rim; it suggests that there may have been influence from zircon inclusions. AB09-05 gave a two point garnet-whole rock isochron Sm-Nd age of 602 ± 15 Ma for the core and an age of 557 ± 8 Ma for the rim. The high errors on these ages are due to the similarity of the $^{143}\text{Nd}/^{144}\text{Nd}$ garnet ratios to the whole rock, however the $^{147}\text{Sm}/^{144}\text{Nd}$ ratios are sufficiently high to yield reliable ages. ID gave Nd concentrations of 1.491 ppm for the core and 1.168 ppm for the rim which could suggest some influence from Nd-rich inclusions.

Table 4-2; Results of Lu-Hf garnet analyses for samples which give Neoproterozoic ages. Ages marked with an * are interpreted to be not geologically meaningful.

Sample fraction	Lu ppm	Hf ppm	$^{176}\text{Hf}/^{177}\text{Hf}$	2se	$^{176}\text{Lu}/^{177}\text{Hf}$	Initial $^{176}\text{Hf}/^{177}\text{Hf}$	Lu-Hf Age (Ma)
<i>Moine Nappe</i>							
AB07-02 WR	0.562	4.162	0.282473	0.000016	0.0191		
AB07-02 Core	16.307	0.720	0.334463	0.000016	3.232	0.28216	860.7 ± 2.7
AB07-02 Rim	3.541	2.232	0.285669	0.000016	0.224	0.28218	828.8 ± 6.3
AB07-03 WR	0.631	1.695	0.282827	0.000016	0.0526		
AB07-03 Core	10.326	1.629	0.297193	0.000016	0.898	0.28193	903.2 ± 3.1
AB07-03 Rim	7.224	2.524	0.288412	0.000016	0.405	0.28199	843.3 ± 4.4
AB07-28 WR	0.851	2.333	0.282804	0.000012	0.0515		
AB07-28 Core	4.031	3.097	0.285251	0.000012	0.184	0.28185	981.5 ± 7.8
AB07-28 Rim	5.155	4.100	0.283962	0.000012	0.178	0.28233	490.0 ± 7.3
AB07-29 WR	0.612	3.206	0.282512	0.000015	0.0270		
AB07-29 Core	6.050	3.679	0.285904	0.000015	0.233	0.28207	877.8 ± 6.1
AB07-29 Rim	6.614	3.518	0.286246	0.000015	0.266	0.28209	831.8 ± 5.3
AB07-31 WR 2	0.729	1.200	0.283738	0.000009	0.086		
AB07-31 Core 2	10.956	3.963	0.289179	0.000009	0.391	0.28221	947.0 ± 4.2
AB07-31 Rim 2	14.031	3.942	0.291146	0.000010	0.504	0.28222	942.1 ± 3.7
IA1 WR	0.695	1.094	0.283129	0.000012	0.0898		
IA1 Core	3.974	2.213	0.284751	0.000012	0.254	0.28224	527.4 ± 5.9
IA1 Rim	3.618	1.356	0.285685	0.000012	0.377	0.28233	474.6 ± 3.6
<i>Glenfinnan Group</i>							
AB07-04 WR	0.660	1.444	0.282922	0.000016	0.0646		
AB07-04 Core	23.445	4.193	0.293020	0.000016	0.792	0.28203	739.5 ± 2.9

AB07-04 Rim	21.262	6.113	0.288521	0.000016	0.492	0.28208	697.7 ± 3.9
AB08-01 WR	0.263	0.193	0.284258	0.000033	0.193		
AB08-01 Core	5.448	1.389	0.289345	0.000011	0.555	0.28154	748.7 ± 6.1
AB08-01 Rim	0.804	0.503	0.284745	0.000009	0.226	0.28137	795.7 ± 58
AB09-05 WR	0.488	5.585	0.282280	0.000012	0.0123		
AB09-05 Core	16.712	4.823	0.288444	0.000012	0.490	0.28212	687.2 ± 3.4
AB09-05 Rim	14.574	5.729	0.286458	0.000012	0.360	0.28213	641.1 ± 3.2

Table 4-3; Results of Sm-Nd analyses for samples which give Neoproterozoic ages. Ages marked with an * are interpreted to be not geologically meaningful.

Sample fraction	Sm ppm	Nd ppm	$^{143}\text{Nd}/^{144}\text{Nd}$	2se	$^{147}\text{Sm}/^{144}\text{Nd}$	Initial $^{143}\text{Nd}/^{144}\text{Nd}$	Sm-Nd Age (Ma)
<i>Moine Nappe</i>							
AB07-02 WR	9.578	51.719	0.51168	0.000009	0.112		
AB07-02 Core	0.667	0.237	0.52000	0.000022	1.707	0.511093	795.9 ± 2.4
AB07-02 Rim	0.968	0.360	0.51935	0.000021	1.627	0.511110	772.6 ± 2.4
AB07-03 WR	11.393	61.900	0.51169	0.000009	0.111		
AB07-03 Core	0.385	0.619	0.51300	0.000023	0.376	0.511134	756.7 ± 14
AB07-03 Rim	0.618	2.020	0.51202	0.000016	0.185	0.511188	682.8 ± 38
AB07-28 WR	8.544	45.832	0.51175	0.000008	0.113		
AB07-28 Core	0.711	3.022	0.51183	0.000014	0.142	0.51143	423.8 ± 81*
AB07-28 Rim	0.788	3.418	0.51184	0.000012	0.139	0.51137	512.0 ± 84*
AB07-29 WR	9.571	52.156	0.51171	0.000011	0.111		
AB07-29 Core	2.495	1.776	0.51293	0.000011	0.849	0.51152	253.4 ± 3.0*
AB07-29 Rim	1.130	1.507	0.51320	0.000017	0.453	0.51122	665.2 ± 9.4
AB07-31 WR 1	5.330	26.083	0.51190	0.000012	0.124		
AB07-31 Core 1	1.883	2.457	0.51377	0.000016	0.464	0.51121	841.3 ± 8.6
AB07-31 Rim 1	1.696	2.608	0.51314	0.000013	0.393	0.51133	701.7 ± 9.7
AB07-31 WR 2	5.462	26.755	0.51188	0.000010	0.123		
AB07-31 Core 2	1.030	3.401	0.51226	0.000009	0.183	0.51111	950.9 ± 34
AB07-31 Rim 2	0.848	2.372	0.51235	0.000012	0.216	0.51126	772.5 ± 26
IA1 WR	3.397	14.662	0.51182	0.000009	0.140		
IA1 Core	1.932	8.207	0.51189	0.000010	0.142	0.50720	4959.4*
IA1 Rim	1.085	3.958	0.51197	0.000008	0.166	0.51101	885.8 ± 76*
<i>Glenfinnan Group</i>							
AB07-04 WR	12.263	66.971	0.51179	0.000012	0.111		
AB07-04 Core	0.770	0.519	0.51456	0.000012	0.896	0.51139	539.6 ± 3.2
AB07-04 Rim	1.134	0.319	0.51843	0.000024	2.149	0.51142	497.6 ± 2.0
AB08-01 WR	4.499	19.780	0.51208	0.000011	0.138		
AB08-01 Core	0.666	1.340	0.51281	0.000014	0.300	0.51146	685.9 ± 16
AB08-01 Rim	1.368	4.510	0.51245	0.000011	0.183	0.51095	1247 ± 52*
AB09-05 WR	9.502	51.801	0.51182	0.000008	0.111		
AB09-05 Core	0.645	1.491	0.51241	0.000013	0.262	0.51138	602.4 ± 15
AB09-05 Rim	0.691	1.168	0.51272	0.000012	0.358	0.51141	557.1 ± 8.1

4.6 Discussion

4.6.1 Morar Group

Vance et al. (1998) dated four samples using Sm-Nd garnet geochronology from the south-west Morar Group and the ages obtained were 813.5 ± 5.4 Ma from Mallaig, 761 ± 18 Ma from Loch Beag, Polish gave a core age of 822.7 ± 4.6 Ma and a rim age of 788.3 ± 4.4 Ma and Glenuig gave 815 ± 21 Ma. AB07-02 was sampled close to the Polish sample site and gave Lu-Hf core and rim ages of 860.6 ± 2.7 Ma and 828.8 ± 3.5 Ma respectively, and Sm-Nd core and rim ages of 795.9 ± 2.4 Ma, 772.6 ± 2.4 Ma. The difference between the Vance et al. (1998) core and rim Sm-Nd ages for Polish is 34.4 Ma, and the difference between the Lu-Hf and Sm-Nd ages achieved here is 31.8 Ma and 23.3 Ma. As Sm-Nd is not affected by zircons and Lu-Hf is not affected by monazite, the similarity of the difference between the core and rim ages shows that the ages have not been significantly affected by any inclusions of these accessory minerals. There is a 19.8 Ma difference between the Sm-Nd age obtained by Vance et al. (1998) and the Sm-Nd core age from this study and an 8.9 Ma difference between the rim ages. AB07-03 was from close to the Glenuig sample site of Vance et al. (1998) and gave Lu-Hf core and rim ages of 903.2 ± 2.9 Ma and 843.4 ± 3.3 Ma and Sm-Nd core and rim ages of 756.7 ± 14 Ma and 682.8 ± 38 Ma. The Sm-Nd age from Vance et al. (1998) is 4 Myr outside of error of the Sm-Nd core of this study, however the Lu-Hf age is significantly older. The core age from AB07-03 is also significantly older than the age of the core from AB07-02. An explanation for this could be due to the larger garnet size in AB07-03 which would make it harder to diffuse through than AB07-02, and would effectively give AB07-03 a higher closure temperature. This is further complemented by the larger difference in Lu-Hf core and rim ages in sample AB07-03 when compared with AB07-02, this is discussed in more detail in Chapter 8. Vance et al. (1998) believed that the final equilibration temperatures of these samples were ~ 650 - 700 °C, in the middle of the range of estimated closure temperatures for the Sm-Nd system in small garnets (> 0.1 mm). Larger grains, such as those studied here (0.1-6mm), should not be affected by diffusion at these temperatures (Dutch & Hand, 2009). Thus Vance et al. (1998) suggested that the ages obtained were growth ages for the garnets. The data from the LA ICPMS transects supports this interpretation suggesting that the ages obtained within this study are also garnet growth ages.

There are two samples which give surprising Lu-Hf results, the rim of AB07-28 which gives an age of 490 Ma and IA1 which gave a Lu-Hf core age of 531 Ma and a rim age of 476 Ma. The rim ages from both of these samples are likely to be related to the Caledonian orogeny, and show that there must have been significant garnet growth during the Ordovician/ Cambrian in these samples. The age from the core of IA1 is within ~30 Ma of an unpublished age from the Loch A'Mhoid meta-gabbro (Strachan et al. 2010) which is not far from where IA1 was sampled. This could suggest that in north Sutherland there was also garnet growth during the early Cambrian.

U-Pb zircon ages of ~870 Ma date intrusion of the West Highland Granitic Gneiss, (Friend et al. 1997; Millar 1999 & Rogers et al. 2001). This study has obtained several ages which are significantly older including 980 Ma from the Glenborrodale Pelite, 947 Ma from the Meadie Pelite and 903 Ma from the Glenuig Pelite. The 980 Ma age from the Glenborrodale Pelite (AB07-28) is not very radiogenic thus this age should be used with some caution, however the ages from the Meadie Pelite are considered to be reliable and show prograde garnet growth at ~947 Ma. Similar ages of 925 ± 10 Ma and 938 ± 8 Ma were obtained from the Westing Group in north east Shetland and interpreted to date amphibolite-facies metamorphism (Cutts et al. 2009). P-T estimates for the Westing Group give temperatures of $640 \pm 19^\circ\text{C}$ and pressures of 8.5 ± 0.8 kbar, P-T estimates were also made for the Meadie Pelite using near rim garnet compositions with the adjacent matrix mineral and gave an average of $651 \pm 31^\circ\text{C}$ and 9.3 ± 1.3 kbar, which is not dissimilar to the P-T estimates from the Polnish Pelite of 650°C and 7.5 kbar (Cutts et al. 2009; pers. comm.). The Krummedal Succession equivalents at Smallefjord give a metamorphic age of 955 ± 13 Ma (Strachan et al. 1995), which is within error of the Lu-Hf ages and the Sm-Nd core fraction 2 age from the Meadie Pelite. S-type granites that intrude the Krummedal Succession yield emplacement ages between 940-910 Ma (Kalsbeek et al. 200; Watt & Thrane 2001; Leslie & Nutman 2003), which is similar to the metamorphism ages from the Krummedal Succession, and the Westing Group of Shetland. These >900 Ma ages have been assigned to a 'Renlandian' orogenic event, that appears to have affected certain rock units along the eastern margin of Laurentia (Cawood et al. 2010). The Moine Supergroup had been assigned to the later phase, the Knoydartian Orogeny, however the >900 Ma ages from the Morar Group suggest that the lower part of the Moine Supergroup is related to the

same >900 Ma event that affected the Westing Group and the Krummedal Succession, and is part of the Renlandian Orogeny.

4.6.2 Glenfinnan Group

Monazite inclusions within a garnet from a Glenfinnan Group migmatite at Glen Urquhart give a 825-780 Ma core, 724 Ma middle zone and a 462 Ma from the rim (Cutts et al. 2010). The age from the middle zone is the same age as leucosomes dated within the same rock (SIMS zircon, Cutts et al. 2010) and similar to the age of 737 ± 5 Ma from just below the Sgurr Beag Thrust (Tanner & Evans 2003), which is within error of the Lu-Hf core age of 740 ± 2.5 Ma from the Loch Eilt Pelitic Gneiss (AB07-04), the core age from AB08-01 of 749 ± 6.1 Ma and the rim age from AB08-01. This demonstrates that the garnet cores within the Glenfinnan Group grew at ~740 Ma. There are several ages that range between 697.7 ± 3.1 Ma (Lu-Hf AB07-04 rim) and 685.3 ± 2.2 Ma (Lu-Hf AB09-05 core) perhaps suggesting another phase of garnet growth. AB09-05 also gives a younger Lu-Hf rims age of 640.2 ± 2.4 Ma suggesting another later phase of garnet growth. The Sm-Nd ages from AB07-04 and AB09-05 are significantly younger than the Lu-Hf ages and AB07-04 shows mixing in the Sm-Nd diagrams, suggesting that these ages reflect partial resetting of the Sm-Nd systems. Thus the Glenfinnan Group records three phases of garnet growth at 740 Ma, 700-680 Ma and 640 Ma.

4.6.3 Tectonic implications of the new data

The new older metamorphic ages from the Morar Group suggest that the younger limit of Morar Group deposition is older than previously thought (Friend et al. 1997; Millar 1999; Rogers et al. 2001). The oldest reliable age is from the Meadie Pelite (AB07-31) where Lu-Hf and Sm-Nd give ages within error of ~950 Ma. The youngest published precise detrital zircon age from the Morar group is 980 ± 4 Ma (Cawood et al. 2007) suggesting deposition occurred over at least 30 Myr.

Another important point that needs discussion is what these ages show about the driving forces behind Neoproterozoic metamorphism. As mentioned above there are conflicting views about where these rocks should be placed, depending on which palaeo-reconstruction is used. If Baltica is placed directly opposite East Greenland then the Moine Supergroup would be deposited within the interior of Rodinia (e.g. Dalziel

1997), which means deformation may have been related to the closure of an intraoceanic rift (Vance et al. 1998; Cawood et al. 2004). Another model based on more recent palaeomagnetic studies, places Baltica further south relative to East Greenland (Cawood & Pisarevsky 2006; Li et al. 2008; Cawood et al. 2010) on the periphery of Rodinia, suggesting that deformation and metamorphic processes could be related to plate boundary processes. Pressures and temperatures (~6 kbar and ~600°C) obtained from the Morar Group by Cutts et al. (2009, pers comm.) do not have to be related to compression, and could be related to an extending deep basin filling up with sediment. Thus it could be that the Neoproterozoic events recorded within the Morar Group relate to extension with heat supplied from below, for example, in an extending basin behind a subduction-related arc, which would be in agreement with the most recent interpretation of the palaeomagnetic data. The Glenfinnan Group has recorded higher pressures and temperatures of 9 kbar and ~650°C which is more suggestive of crustal thickening, perhaps suggesting that the later phases of Neoproterozoic deformation were associated with compression.

4.7 Conclusions

1. Physical mixing between the garnet core and rim fractions has not affected the samples analysed here. This indicates that the Lu-Hf ages represent discrete garnet growth episodes; this is further supported by the LA ICPMS profiles which indicate retention of the prograde Lu profile within the garnets.
2. The Lu-Hf ages from the Morar Group suggest that there was an early garnet growth event ~950 Ma to 900 Ma seen in the Lu-Hf ages from the core of AB07-03, the core of AB07-28 and the core and the rim of AB07-31. A later event between 880 Ma and 830 Ma seen from the Lu-Hf ages from the core and the rim from AB07-02, the rim from AB07-03, the core and the rim from AB07-29 and the Sm-Nd age from core fraction 1 from AB07-31.
3. The events recorded in the Morar Group are generally older than the garnet growth events recorded within the Glenfinnan Group which suggests that the Glenfinnan Group and the Morar Group were separate until at least 740 Ma (see also Tanner & Evans 2003), although they may have been separate until significantly later. This could suggest that prior to 740 Ma the Glenfinnan/ Loch

Eil Groups were separate from the Morar/ Moine Nappe and were thrust together at ~740 Ma. Glenfinnan Group records three phases of garnet growth at 740 Ma, 700-680 Ma and 640 Ma.

4. The Sm-Nd systematics in several of the samples (AB07-04, AB09-05) show evidence of mixing suggesting that these Sm-Nd ages have been partially reset.
5. The most important result from this chapter is the ages obtained from AB07-31 (Meadie Pelite), they are geologically meaningful as the Lu-Hf core and rim results are within error and one of the Sm-Nd core ages agree within uncertainty at ~950 Ma. This indicates that deposition of the Morar Group must have ceased prior to garnet growth in this sample. The youngest published precise detrital zircon age is 980 Ma which gives approximately 30 Ma to deposit the Morar Group.
6. The early (>900 Ma) ages from the Morar Group have more in common with the 'Renlandian' orogenic events identified elsewhere in the North Atlantic region (Cawood et al. 2010) than with the Knoydartian Orogeny. The younger <900 Ma ages relate to the Knoydartian Orogeny which Cawood et al. (2010) describe as consisting of three discrete events, 830-820 Ma, 800-790 Ma and 730-710 Ma. Many of the ages presented within this chapter are too old to fit into any of these established groups, suggesting that the Knoydartian is older than previously thought.

5.1 Synopsis

The new data reported within this chapter suggests that the existing two-stage model for Caledonian orogenesis in northern Scotland is over-simplistic which has implications for regional tectonic models. This is demonstrated by new Late-Ordovician Lu-Hf ages that have been obtained from prograde garnets: 449.3 ± 1.9 Ma (Talmine Pelite, within the Morar Group of Sutherland), 447.3 ± 1.7 Ma (Ben Hope Sill amphibolites, Sutherland), 448.7 ± 5.0 Ma (amphibolite within Glenfinnan Group, Ross of Mull), 446 ± 13 Ma (Strathy Complex amphibolite) and a Sm-Nd core age of 449.7 ± 2.3 Ma (Basal Pelite, Morar Group, Glenelg). These ages are within error of a Sm-Nd age of 456.2 ± 7.5 Ma also obtained from the Talmine Pelite garnets. These ages suggest a previously unrecognised event at ~ 448 Ma. This event postdates peak metamorphism in the Naver nappe by c. 17 Ma, and predates Silurian (Scandian) nappe stacking and associated deformation by at least 13 Ma. The new Late-Ordovician metamorphic ages also demonstrate that the Scandian did not reach mid to upper amphibolite facies throughout the whole Moine Supergroup.

A Lu-Hf age of 466.0 ± 2.1 Ma has been obtained from prograde garnet in Moine gneisses of the Naver nappe in Sutherland. This confirms a Mid-Ordovician age for high-grade metamorphism and migmatization, and complements the previously published U-Pb zircon (SIMS) data of 461 ± 13 Ma and 467 ± 10 Ma (Kinny et al. 1999). A Mid-Ordovician age was also obtained from syn-kinematic garnets from close to the Moine Thrust, which most likely date thrust movement. This could suggest that there may have been ~ 30 Ma of movement on the thrust with the U-Pb ages from the Loch Borrolan Complex marking the younger limit of movement (Goodenough et al. 2010).

The apparent restriction of the Late Ordovician and Silurian events to the Northern Highland terrane could reinforce the suggestion that it was far removed from the Grampian terrane until the two were juxtaposed following major end-Caledonian sinistral displacement along the Great Glen Fault. A similar record of protracted Ordovician accretion-related metamorphism is seen within the Laurentian-derived

Uppermost Allochthon of Norway. The Caledonian history of the Northern Highland terrane thus has more in common with the Laurentian-derived rocks of Baltica than with the Grampian terrane of Scotland.

5.2 Introduction

Within many collisional orogens, the final suturing of continental blocks is preceded by accretionary events that commonly occur during initial stages of oceanic closure. These events typically result from the collisions of magmatic arcs with continental margins and examples have been documented in the Himalayas (Fraser et al. 2001), the Urals (Puchkov 2009), the Appalachians (van Staal et al. 2009), and the Caledonides of Norway (Roberts 2003). Recognition of early accretionary events is relatively straightforward within orogens where the rocks affected are overlain unconformably by successor basins of known age. These successor basins will in turn be deformed during later stages of ocean closure and continental collision. However, at deeper structural levels within orogens the distinction between major tectonic events depends critically upon the isotopic dating of regional metamorphic minerals and associated fabrics. The Caledonides of the Northern Highlands and Shetland are examples where being at a deeper structural level and later strike slip faulting has made it difficult to distinguish between major deformation events.

Lower Palaeozoic Caledonian orogenesis in the North Atlantic region resulted from the collision of three continental blocks, Laurentia, Baltica and Avalonia, associated with the closure of the Iapetus Ocean (Soper & Hutton 1984; Pickering et al. 1988; Soper et al. 1992; Dewey & Strachan 2003). The final amalgamation of continental blocks in late Silurian/ early Devonian time was preceded by a series of Cambrian-Ordovician arc-continent collisions that occurred on the Iapetan margins of both Laurentia and Baltica (Dewey & Ryan 1990; van Staal et al. 1998; Dewey & Mange 1999; Roberts 2003). In Ireland and Scotland, the collision of the Lough Nafoeey arc and its likely north-eastward extension beneath the Upper Palaeozoic cover of the Midland Valley in Scotland (Figure 5-1) resulted in ophiolite obduction (Chew et al. 2010) and widespread deformation and metamorphism between 475-465 Ma of the Laurentian Neoproterozoic-Cambrian rocks of the Dalradian Supergroup within the Grampian terrane (Friedrich et al. 1999a, 1999b; Oliver et al. 2000; Flowerdew et al.

2005; Baxter et al. 2002). In western Ireland, a Silurian successor basin with early Ordovician sediments was deposited unconformably on the eroded remnants of this orogenic tract and was later deformed during the culminating collision with Avalonia (Dewey & Ryan 1990).

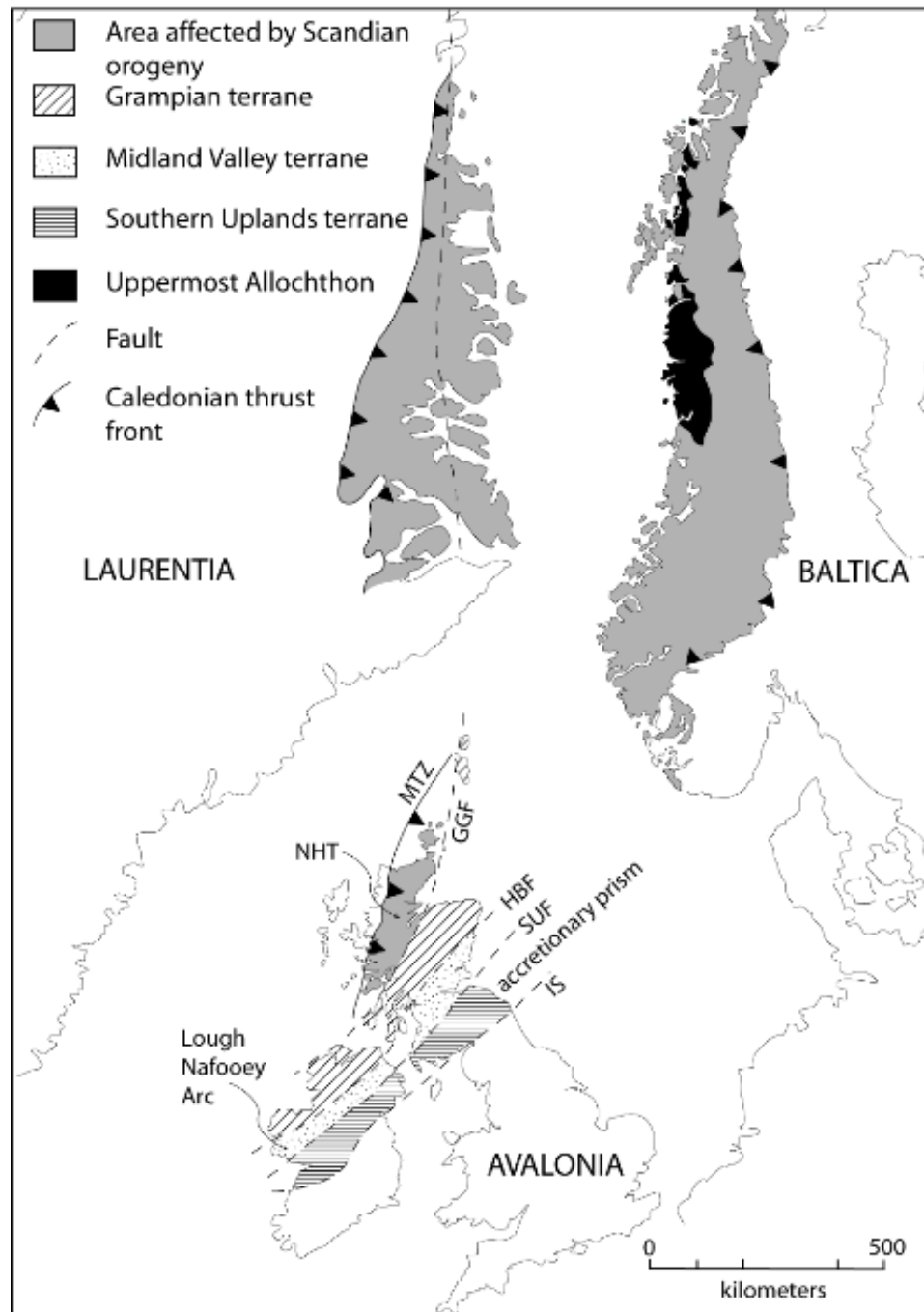


Figure 5-1, Adapted from Dewey & Strachan (2003) and Roberts (2003). Simplified tectonic map of the Caledonides in the Mid- Late Silurian, showing the main structures and areas affected by Caledonian deformation. Major faults and thrusts; GGF – Great Glen Fault; HBF – Highland Boundary Fault; SUF – Southern Upland Fault; IS – Iapetus Suture; MTZ – Moine Thrust Zone. NHT – Northern Highland Terrane.

This chapter concentrates on the youngest of the deformation events that has affected the Moine Supergroup, the Caledonian Orogeny. The Caledonian Orogeny has been split into two events, an Ordovician event and a Silurian event (Kinny et al. 1999, 2003; Rogers et al. 2001; Cutts et al. 2010) which overprint earlier Neoproterozoic metamorphism. The Ordovician event has been correlated with the Grampian accretionary event (Kinny et al. 1999), and the Silurian event attributed to the ‘Scandian’ collision between Baltica and the segment of the Laurentian margin that contained the Northern Highland terrane (Coward 1990; Dallmeyer et al. 2001; Dewey & Strachan 2003; Kinny et al. 2003). Although the Caledonian Orogeny appears to be fairly well understood, many unanswered questions remain including why the Grampian Terrane records Grampian deformation but has no evidence for any Scandian deformation. Possibly the biggest unresolved issue is that there are no peak metamorphic ages that represent the Scandian deformation within the Northern Highlands; the currently quoted ages are igneous intrusion ages or cooling ages. The new data reported here suggests that the existing two-stage model for Caledonian orogenesis in northern Scotland is overly-simplistic which has implications for regional tectonic models.

5.3 Models for the Caledonian Orogeny

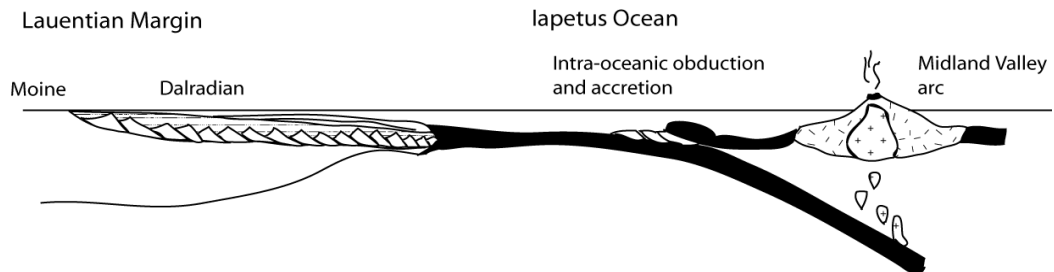
5.3.1 Grampian

During the Cambrian and into the early Ordovician the Moine Supergroup is thought to have been located on the Laurentian margin and was probably overlain by shelf sediments that passed south-east into the Dalradian. Sedimentation was terminated in the early to mid-Ordovician by the Grampian Orogenic event. Figure 5-2 shows a schematic diagram of how the Grampian event probably occurred; the top diagram is before the Grampian event and shows southward directed intra-oceanic subduction forming an island arc complex which developed during the closure of the Iapetus.

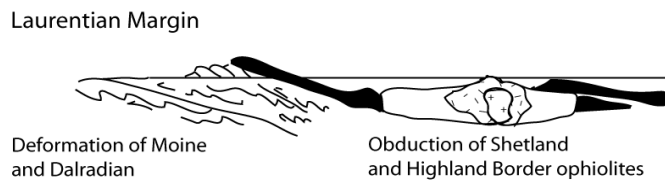
The volcanic arc then collided with the subducting margin of Laurentia as shown in the middle diagram; parts of the arc are exposed in western Ireland. The collision caused the obduction of ophiolites, nappe stacking and the deformation of the Moine and Dalradian Supergroups. Remnants of this ophiolite may be represented by the ophiolitic rocks found on Unst in Shetland and intermittently along the Highland

Boundary Fault. The last diagram shows that continued collision resulted in underthrusting and folding of the Laurentian margin and the creation of a northward-dipping subduction zone.

1) Upper Cambrian - Lower Ordovician



2) Arenig-Llanvirn Grampian Orogen - early phase



3) Grampian Orogeny - late phase

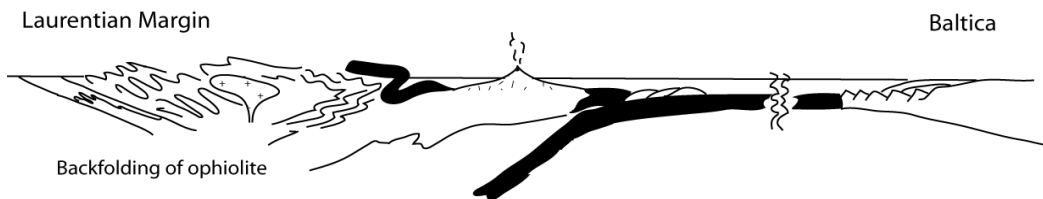


Figure 5-2. Adapted from Leslie et al. (2009). Diagram 1 shows a pre-Grampian stage showing south directed subduction forming an island arc complex. Diagram 2 shows the initial collision of the arc and the trench leading to the obduction of ophiolites and crustal thickening, deformation and metamorphism on the Laurentian margin. Diagram 3 shows continued collision resulting in folding and underthrusting of the Laurentian margin and a north-dipping subduction zone.

5.3.2 Scandian Orogeny

Whilst there is a substantial amount of evidence which describes what caused the Grampian event and the metamorphism and deformation associated with it, there is far less geochronological evidence within the Northern Highlands for the Scandian event. The Scandian represents the final collision between Avalonia, Baltica and Laurentia. The top diagram in Figure 5-3 shows how continued closure of the Iapetus was thought to be achieved by the reversal of polarity of subduction at the

end of the Grampian. This developed an active margin and created the Southern Uplands accretionary prism at the Avalonia-Laurentia interface. Baltica is thought to have collided with the part of Laurentia that contained the Northern Highlands to result in the Scandian shown in Figure 5-4 (Dallmeyer et al. 2001; Kinny et al. 2003). The bottom diagram in Figure 5-3 shows the underthrusting of Baltica beneath Laurentia and the development of east and west directed thrust systems. This culminated in the Moine Thrust (Soper & Hutton 1984; Soper et al. 1992). Scandian deformation is not recorded within the Grampian terrane, and Figure 5-4 shows one way of explaining this. Figure 5-4 is a schematic plate tectonic diagram for the Silurian at ~430 Ma.

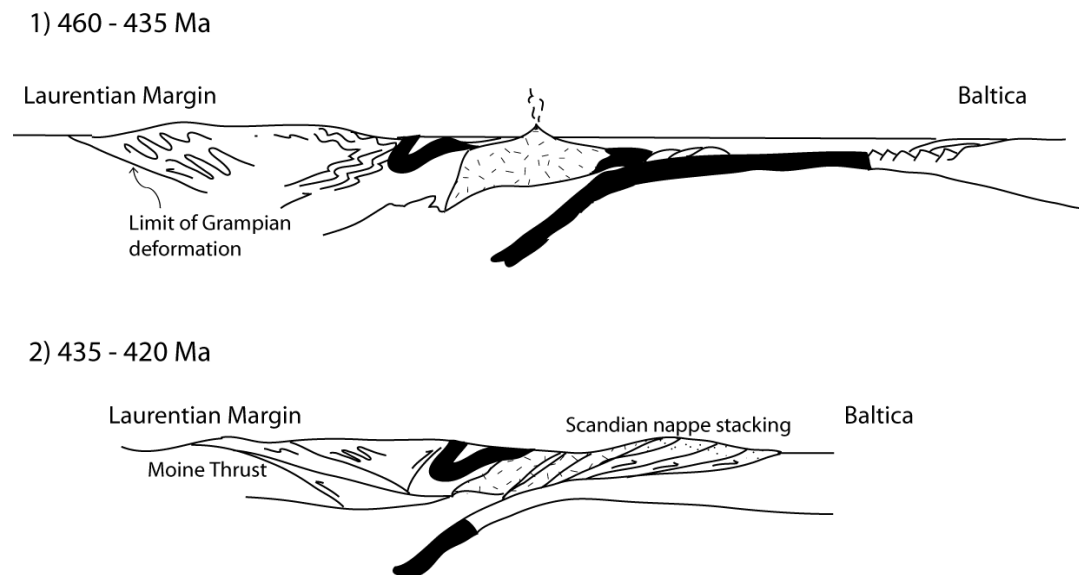


Figure 5-3, Adapted from Strachan et al. (2010). The top diagram shows how continued subduction was achieved by the reversal of polarity of subduction at the end of the Grampian developing an active margin and creating the Southern Uplands accretionary prism. The bottom diagram shows the underthrusting of Baltica beneath Laurentia and the development of E and W directed thrust systems. This was followed by strike-slip displacement along the Great Glen Fault.

The position of the Northern Highlands is shown in the box, after the main Scandian phase. It is thought by some authors (e.g. Dewey & Strachan 2003; Kinny et al. 2003) that there was >700km of sinistral movement along the Great Glen Fault. This would move the Northern Highlands to their current position next to the Grampian Terrane and explain why there is no record of Scandian deformation in the Grampian Highlands. This movement along the Great Glen Fault has to occur within 20 Ma, as movement occurs after the Scandian (430-420 Ma) and before deposition of the Old

Red Sandstone in the Moray Firth (~405 Ma) which suggests that the rate of movement was ~3.5 cm/yr.

Figure 5-5 shows Caledonian structures within the Moine Supergroup. The west-northwest to east-southeast lineations across the western Moine Supergroup are presumed to be Scandian with an indication that Grampian events are apparently confined to the eastern Moines, where the lineations are northwest to south east (Kinny et al. 2003). The formation of the Northern Highland Steep Belt (NHSB) may also be related to Scandian deformation (Strachan & Evans 2008). The eastern limit of the NHSB is defined by the Loch Quoich Line, which more or less coincides with the designated boundary between the Glenfinnan and Loch Eil groups (Roberts & Harris 1983). West of the Loch Quoich Line much of the Moine is steeply dipping; the most strongly affected area is where the Glenfinnan Group outcrops.

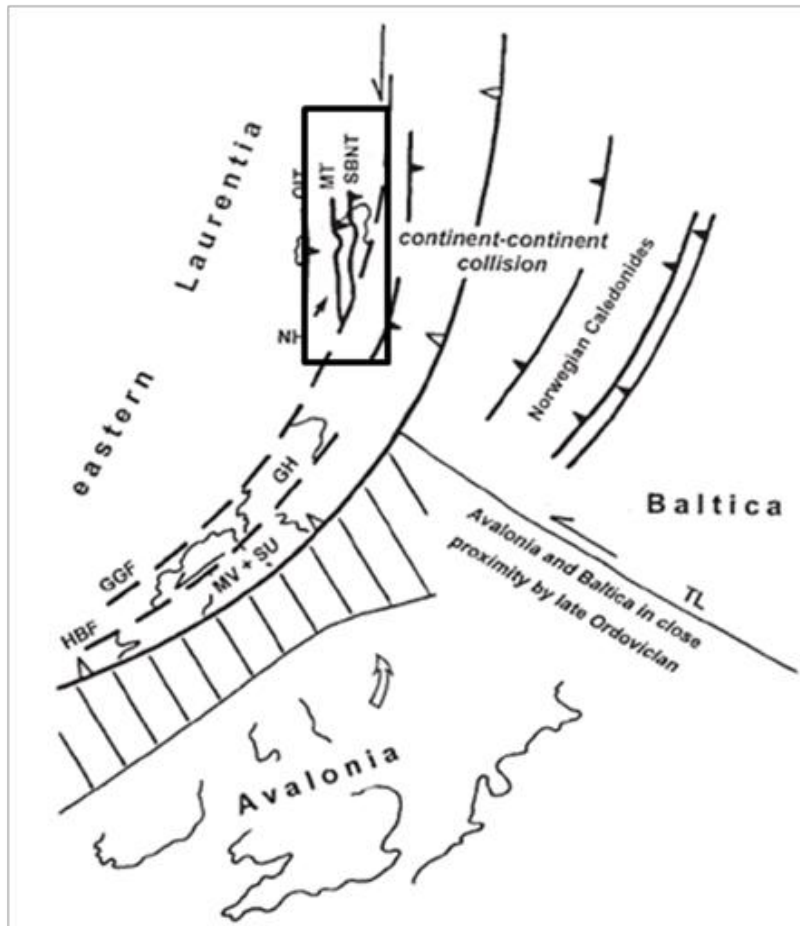


Figure 5-4 is a schematic plate tectonic diagram for the Silurian at ~430 Ma. The position of the Northern Highlands is shown in the box. It shows one way of explaining the lack of Scandian deformation in the Grampian Highlands by invoking ~700 km of sinistral displacement along the GFF (Dewey & Strachan 2003; Kinny et al. 2003).

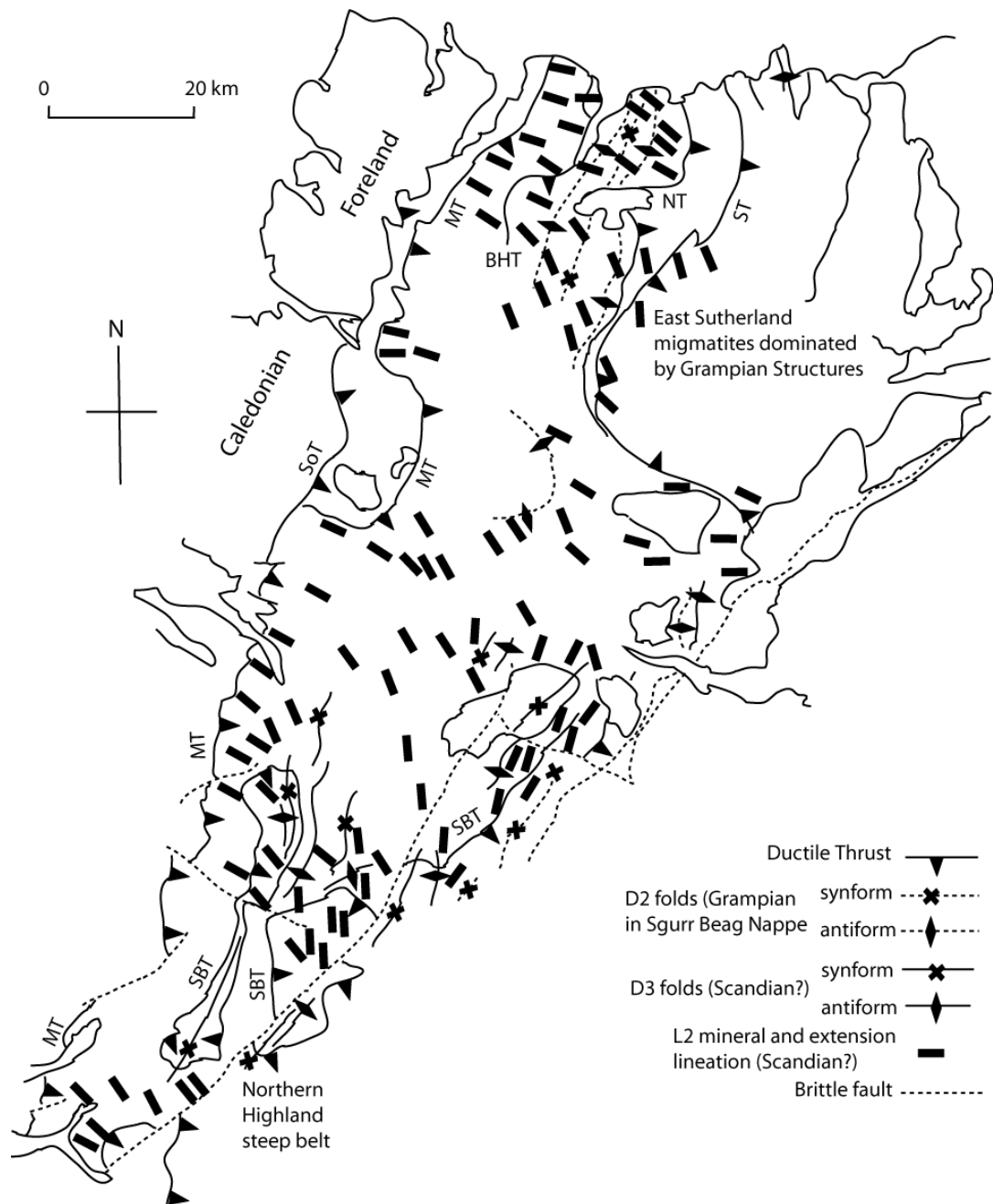


Figure 5-5 shows what are presumed to be Scandian lineations across the western Moine which are west-northwest to east-southeast with more northwesterly to southeasterly lineations in the eastern Moines which are assumed to be related to the Grampian (Kinny et al. 2003). Abbreviations BHT – Ben Hope Thrust; MT – Moine Thrust; NT – Naver Thrust; SBT – Sgurr Beag Thrust; SoT – Sole Thrust; ST – Swordly Thrust.

5.4 Previous Geochronology

The Caledonian Orogeny has been separated into two discrete events, the Grampian (470-460 Ma) and the Scandian events (435-425 Ma) (Dewey & Strachan 2003; Strachan et al. 2010). Within the lowest part of the Moine Supergroup, the Morar Group, there are no reliable isotopic evidence for Grampian deformation. Dallmeyer et al. (2001) suggest this could be due to a western “front” to Grampian deformation, which is perhaps buried underneath younger thrusts, for example the Naver or Swordly thrusts. However, Scandian deformation and metamorphism is interpreted to be widespread within the Morar Group, represented by the D₂ fabrics (Kinny et al. 2003). D₂ is represented by extensive, minor tight to isoclinal folds and a penetrative schistosity. Displacements along the Swordly, Naver, Ben Hope and perhaps the Sgurr Beag thrusts are also thought to be related to the Scandian event (Strachan & Holdsworth 1988). The Scandian deformation is thought to be responsible for the major folds within the Morar Group of Sutherland which often have basement inliers within their cores; and for the basement inliers which are present as thin allochthonous slices along the Naver, Swordly and Ben Hope thrusts (Holdsworth 1989). D₃ was associated with extensive upright folding along north-south axes; this is mostly likely associated with the formation of NHSB which, as mentioned previously, is thought to be Scandian in age (Strachan & Evans 2008).

5.4.1 Evidence for Mid-Ordovician deformation and metamorphism

Evidence for the Grampian orogenic event within the Moine Supergroup includes a U-Pb (SIMS) zircon 467 ± 10 Ma age from migmatites within the Naver Nappe and 461 ± 13 Ma from migmatites within the Kirtomy Nappe that are thought to date melting during tight-to-isoclinal folding (Kinny et al. 1999). Metamorphic studies suggest that melting occurred at 11-12 kbar and 650-700°C (Friend et al. 2000). Relict garnet-pyroxene assemblages within the metabasic rocks within the Naver Nappe are also thought to result from this event (Kinny et al. 1999). Cutts et al. (2010) obtained an age of 463 ± 4 Ma from monazite inclusions within the rims of a garnet close to Drumnadrochit with estimated pressures and temperatures of 650°C and ~7 kbar. These ages and pressures and temperatures have been correlated with

the Grampian orogenic event recognised elsewhere in Scotland and Ireland (e.g. Lambert & McKerrow 1976; Friedrich et al. 1999a, 1999b; Oliver et al. 2000).

The Fort Augustus granite gneiss gave a U-Pb titanite age of 470 ± 2 Ma which is interpreted to date amphibolite facies metamorphism (Rogers et al. 2001). Widespread tight to isoclinal recumbent folds within the Glenfinnan and Loch Eil Groups are also thought to relate to the Grampian event, as the folds pre-date the Glen Dessary syenite (445.3 ± 1.9 Ma) and the Ardgor granitic gneiss (455 ± 3 Ma) (Goodenough et al. 2010; Aftalion & van Breemen 1980). Rb-Sr 450 Ma ages have also been determined for pegmatites within the Glenfinnan Group, which have been interpreted to post-date the upright folding and have been argued to represent late Grampian intrusions (van Breemen et al. 1974).

In the Grampian terrane evidence for the Grampian event from within the Dalradian Supergroup includes the Rb-Sr muscovite, biotite and hornblende dates between 468 Ma and 484 Ma (Dempster et al. (1984), Sm-Nd garnet ages between 467-472 Ma (Oliver et al. 2000; Baxter et al. 2002), and ages for syn-tectonic granitic and gabbro intrusions between 467-489 Ma (Pankhurst et al. 1969; Fettes 1970; van Breemen & Boyde 1972; Pidgeon & Aftalion 1978; Kneller & Aftalion 1987; Friedrich et al. 1999; Oliver et al. 2000; Dempster et al. 2002). Samples from mica-schists, quartzites and granitic gneisses in Perthshire gave Rb-Sr biotite and muscovite ages of 475 ± 15 Ma (Gilletti et al. 1961). Baxter et al. (2002) estimated pressures and temperatures of garnet growth of a sample from Glen Clova within the Grampian Terrane and obtained temperatures of 550-650°C and pressures of 7.2-9.2 kbar.

5.4.2 Evidence for Silurian deformation and metamorphism

The Scandian event is thought to have happened between 435 and 425 Ma (Dewey & Strachan 2003; Kinney et al. 2003). Gilletti et al. (1961) provided one of the earliest pieces of evidence that can be used to support the Scandian event, Rb-Sr dating of biotites, microclines and muscovites and obtained ages that ranged from 435 to 405 Ma. Dallmeyer et al. (2001) undertook Rb-Sr and ^{40}Ar - ^{39}Ar analyses on mylonites from the Moine Thrust Zone and Morar Group rocks. The Rb-Sr muscovite ages of 428, 421 and 413 Ma obtained from the Moine Thrust Zone were interpreted to date regional thrusting during the Late Silurian to Early Devonian. Hornblendes and

muscovites were dated from higher metamorphic units using ^{40}Ar - ^{39}Ar and Rb-Sr. They give ages between 440-410 Ma which have been interpreted to date cooling after the regional D₂ regional thrusting. This was complemented by U-Pb zircon ages from the Loch Borrolan Complex within the Moine Thrust Zone, which gave ages of 430 ± 4 Ma, 431.1 ± 1.2 Ma and 429.2 ± 0.5 Ma (van Breemen et al. 1979; Goodenough et al. 2010). Structural relations show that the intrusion may be syn-tectonic, which would mean this age defines displacement along the Moine Thrust (van Breemen et al. 1979; Goodenough et al. 2010).

Kinny et al. (2003) dated metagranite sheets close to the Naver Thrust using SHRIMP U-Pb geochronology. They dated the Vagastie Bridge granite which is within the northern part of the Moine Nappe, close to Loch Naver, and obtained an age of 413 ± 3 Ma from titanites and 424 ± 8 Ma from zircons. The metagranites are associated with tight-to-isoclinal folding, ductile thrusting and related fabric development that has been generally assigned to D₂ (e.g. Soper & Brown 1971; Soper & Wilkinson 1975; Barr et al. 1986; Moorhouse & Moorhouse 1988; Moorhouse et al. 1988; Strachan & Holdsworth 1988; Holdsworth 1989; Holdsworth & Grant 1990; Holdsworth et al. 2001). As the zircon age represents the date of emplacement of this intrusion, they constrain the age of regional ductile thrusting and associated deformation in central and west Sutherland (Kinny et al. 2003). The 413 Ma age from the titanites within the north Sutherland metagranites (Kinny et al. 2003) is marginally younger than the corresponding magmatic zircon population and compares closely with the ages from Dallmeyer et al. (2001) from muscovites and hornblendes. These ages are interpreted to record post-metamorphic cooling during rapid exhumation of the nappe pile through a blocking temperature of 550-500 °C. The zircon ages from the metagranites in Sutherland are similar to a U-Pb zircon age from the Glen Scaddle metagabbro of 426 ± 3 Ma (Strachan & Evans, 2008). This age was interpreted to represent the age of emplacement of the gabbro, which has then been deformed indicating that it was intruded before the later phases of deformation that resulted in the Northern Highland Steep Belt. The presence of hornblende and post-D₂ kyanite within the Moine Nappe implies that deformation was accompanied by amphibolite facies metamorphism (Strachan & Holdsworth

1988; Holdsworth 1989; Holdsworth et al. 2001; Strachan, unpublished data), estimated to have occurred at 5-6 kbar and 600-650°C (Friend et al. 2000).

Widespread tight to isoclinal folding within the Morar Group as far south as Loch Duich and the lower parts of the Loch Coire migmatites and movement along the Swordly, Naver and Ben Hope Thrusts are thought to relate to the Scandian event. Tens of kilometres of movement may have occurred on the Sgurr Beag Thrust during the Scandian, although this is disputed by Tanner and Evans (2003) who argue that the thrust is cut by metamorphic gradients that predate a syn-kinematic titanite which was dated at 737 ± 5 Ma.

5.5 Sample descriptions

Figure 5-7 shows the locations for the samples discussed within this chapter. The abbreviations for the sample numbers are described below the figure.

AB07-05 – Loch Quoich Amphibolite

The Loch Quoich Amphibolite [NH 0627 0156] was intruded into the Glenfinnan Group and has been subjected to the same deformation that the group has undergone resulting in the amphibolite appearing as a series of boudins.

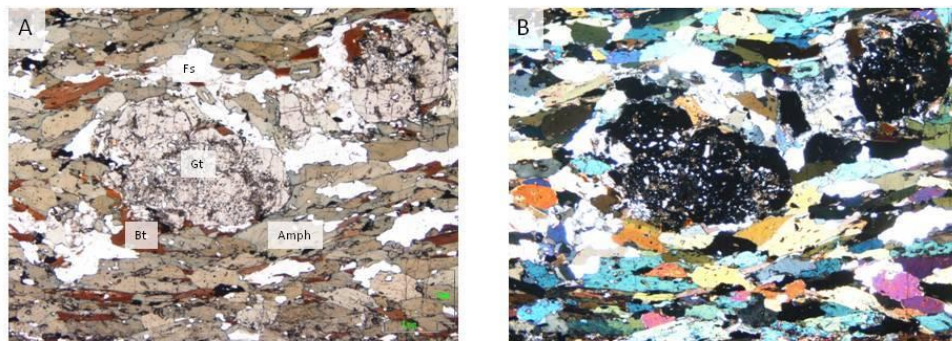


Figure 5-6 thin section photographs for AB07-05 (Loch Quoich Amphibolite). A shows AB07-05 in PP and the fabric dominated by hornblende, biotite and quartz wrapping the garnets. B shows the same view in XP. All abbreviations are from Kretz (1983).

In thin section, the amphibolite has a weak fabric that is predominantly made up of amphibole, biotite and titanite (Figure 5-6). Garnet, plagioclase, biotite, zircon, opaques and apatite are also present. The fabric wraps the garnets which are small, only 2-3 mm in size, and are irregular in shape often surrounded by a reaction rim of

fine grained plagioclase and biotite. The garnets have a dusty interior with inclusions that are made up of titanite and quartz. The fabric also wraps large (2 mm) plagioclase porphyroblasts. LA ICPMS data were not obtained for the Loch Quoich Amphibolite.

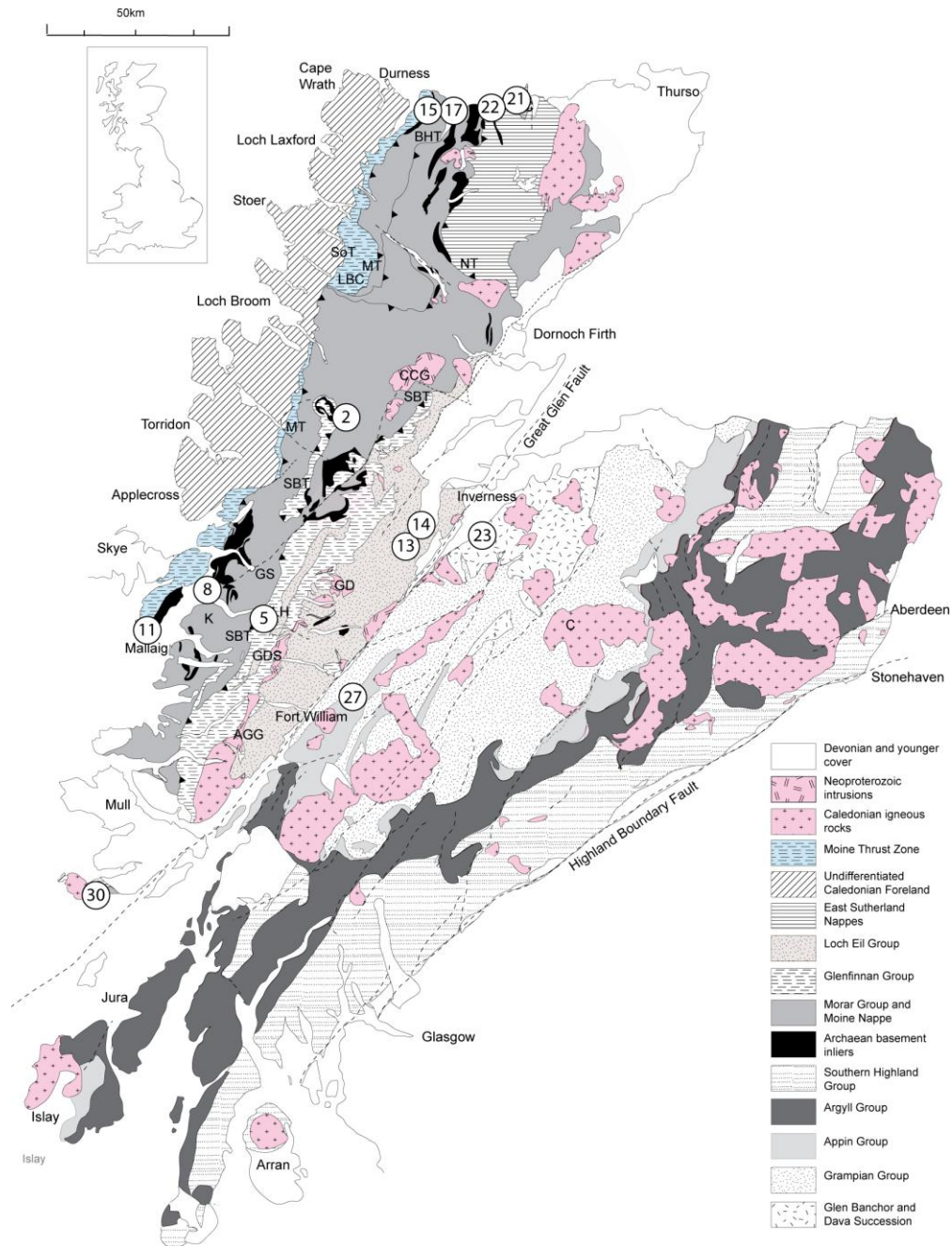


Figure 5-7, simplified geological map of the Northern Highland and the Grampian terranes, the numbers within circles represent sample numbers; 2 – AB08-02; 5 – AB07-05; 8 – AB07-08; 13 – AB07-13; 14 – AB07-14; 15 – AB07-15; 17 – AB07-17; 21 – AB07-21; 22 – AB07-22; 23 – AB07-23; 27 – AB07-27; 30 – AB07-30. Abbreviations; AGG – Ardgour Granitic Gneiss; C – Cairngorms; CCG – Carn Chuinneag Granite; GDS – Glen Dessary Syenite; GD – Glen Doe; GS – Glen Scaddle; SBT – Sgurr Beag Thrust; K – Knoydart; MT – Moine Thrust; SoT – Sole Thrust; NT – Naver Thrust; BHT – Ben Hope Thrust.

AB07-08 – Basal Pelite

This sample is from the basal pelite of the Morar Group above Lewisian basement at Sandaig, sampled at [NG 7689 1491]. The rationale for this sample was to date the post-D₁ cores and syn-D₂ rims to determine whether the garnet has separate Knoydartian cores and Caledonian rims.

In the field the Basal Pelite is a pelite comprising bands of mica schist and semi-pelitic material which is dark with very clean red garnets up to 10 mm in size. It lies between the Lewisian basement and the Moine metasediments.

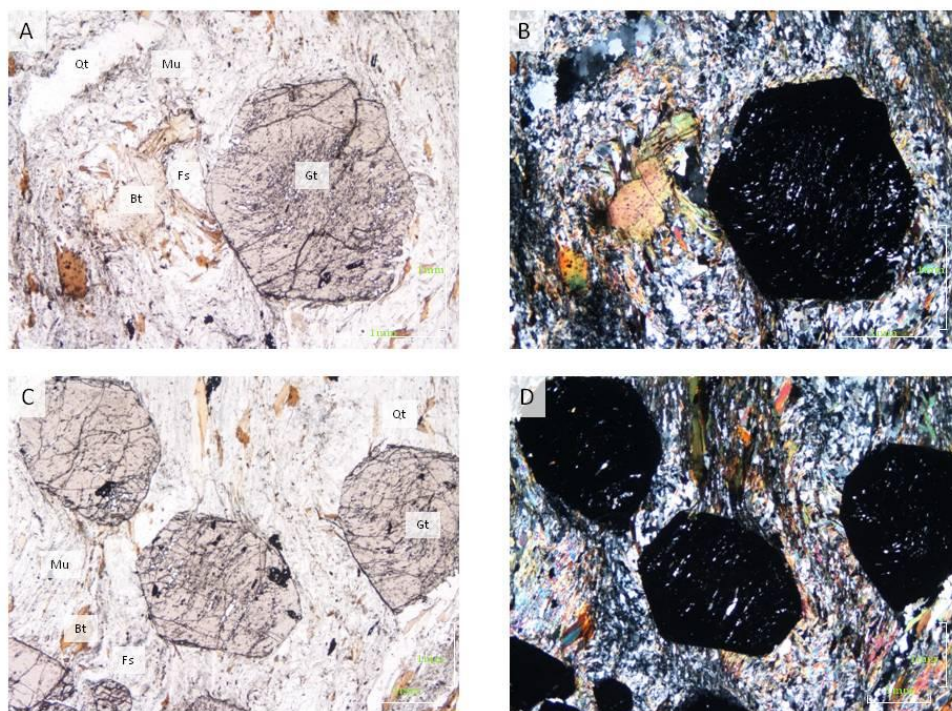


Figure 5-8, A shows a garnet from AB07-08 with curved inclusion trails which often meet up with the surrounding fabric, this garnet also shows an inclusion-rich core. B shows the same view in XP, showing a large biotite which appears to be sheared. C shows several garnets with the inclusion trails joining up with the fabric, D shows the same view in XP.

In thin section (Figure 5-8) the sample does not look fresh. There are many veins, opaques and many of the minerals have a dusty appearance; the veins tend to run along the fold hinges of the crenulation cleavage. It is comprised of garnet, muscovite, biotite, quartz and plagioclase with accessory titanite, opaques, apatite and zircon. There are biotite-rich layers interspersed with quartz and feldspar rich layers which make up the schistosity. The fabric is clearly crenulated and does not

wrap the garnets. The garnets are large, up to 10 mm in size and have curved inclusion trails which are continuous with the surrounding fabric. This suggests that the garnets are syn-kinematic and ages from the garnets should date the main deformation phase. They also have pressure tails. The garnets often have extremely inclusion-rich cores, which mainly consist of zircon with some titanite, quartz and plagioclase. Chlorite is often present around the edge of the garnets. There are large biotite porphyroblasts (up to 4 mm) which appear to have been sheared by the fabric and show signs of strain. They are also very zircon-rich in contrast to the finer biotite that forms part of the dominant fabric.

Figure 5-9 shows the LA-ICPMS profile across a garnet from the Basal Pelite (AB07-08). MgO increases towards the garnet rims and CaO shows the opposite trend increasing towards the garnet core. MgO shows a spike which correlates with a depression in the CaO profile; this is likely related to an inclusion of biotite. LREE, MREE, K₂O, Pb, Th and U are also affected by the mica inclusion.

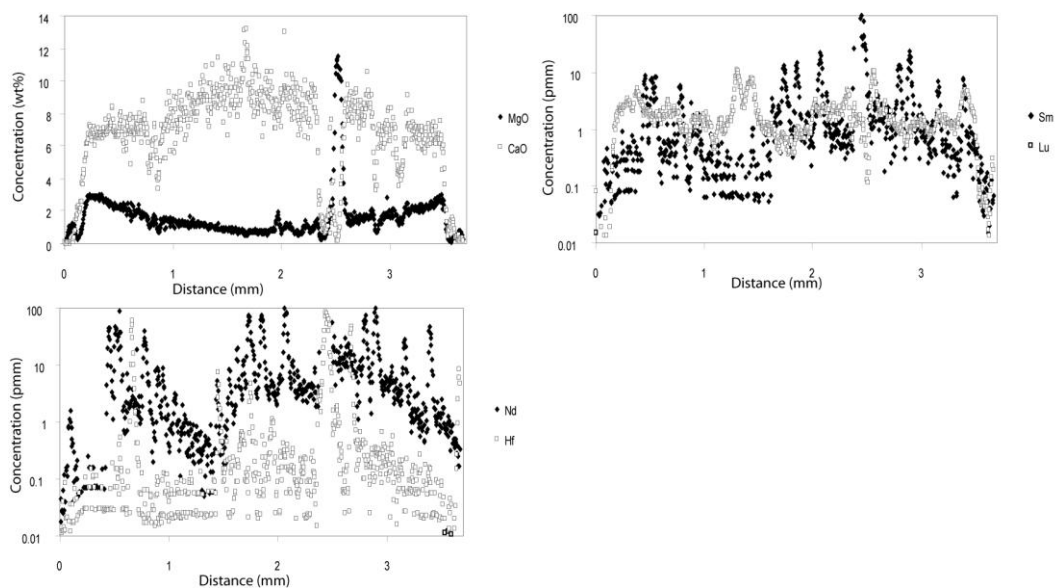


Figure 5-9, LA ICPMS data from a garnet from AB07-08 normalised to a SiO₂ content of 37.2%.

There is no obvious zoning seen in the Lu profile, which could indicate that it might be difficult to obtain a Lu-Hf age from this sample. Nd, Sm and Hf all appear to be behaving in a similar way as they are all incompatible in garnet; they also show obvious peaks relating to zircon and phosphate inclusions. The Hf trace shows flat

parallel traces with spikes; the flat traces are the result of Hf being only 1-2 CPS above background. No prograde zoning is preserved in the trace element profiles, which could suggest that the garnets grew very quickly and the ages would reflect garnet growth or the garnet has been heated to a high temperature and the ages could reflect peak metamorphism or cooling.

AB07-11- Armadale Pelite

The Armadale Pelite (AB07-11) is a mylonitic pelite from the Morar Group, structurally not far above the Moine Thrust. The garnets have been described as syn-kinematic from this locality (Strachan pers. comm.), therefore Lu-Hf and Sm-Nd ages should be the age of Moine Thrust. The sample is a mylonitic garnet mica schist and is dark and shows L_2 lineation. The garnets are dark and are marginally smaller than AB07-08.

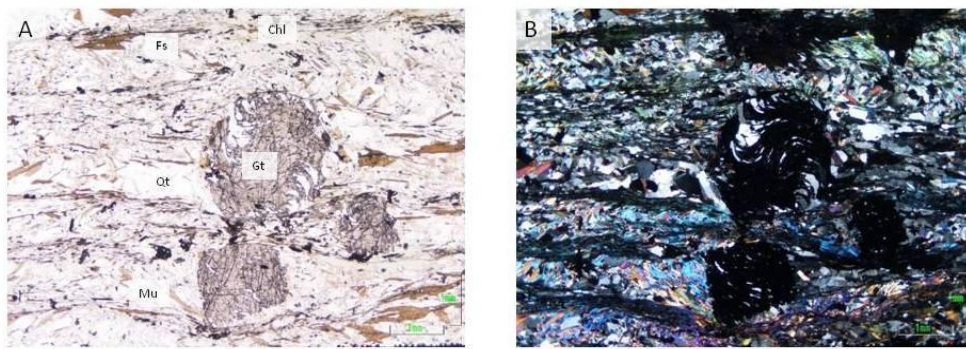


Figure 5-10, A and B show AB07-11 in thin section. The garnets show continuous inclusion trails from core to rim, pronounced pressure tails and are wrapped by the fabric.

In thin section (Figure 5-10) it is composed of plagioclase, muscovite, biotite, garnet, quartz, chlorite, and sphene. The schistosity is layered, with quartz and plagioclase-rich layers and micaceous layers. This may define the original bedding (S_0). The matrix shows a crenulation cleavage. There are large biotite porphyroblasts which have been sheared.

The garnets are between 2.5 mm and 10 mm. They are often well formed with clean edges and an inclusion-rich core, which is different from other Morar Group samples (AB07-02 and AB07-03, Chapter 4). The garnets show continuous curved inclusion fabrics from the core to the outer rim, indicating syn-kinematic growth, shown in Figure 5-10. Not all of the inclusion trails meet up with the surrounding matrix

which could suggest that there has been some recrystallisation of the schistosity. The inclusions consist of quartz, biotite, zircon and sphene. The garnets have pressure shadows suggesting pressure solution caused by high strain rates in intermediate temperatures.

All of the traces shown in Figure 5-11 have notable depressions which correlate with quartz inclusions. MgO increases towards the garnet rims and CaO increases towards the garnet core. Spikes in the CaO correlate with peaks in the Sm and Nd profiles suggesting that they are phosphate inclusions.

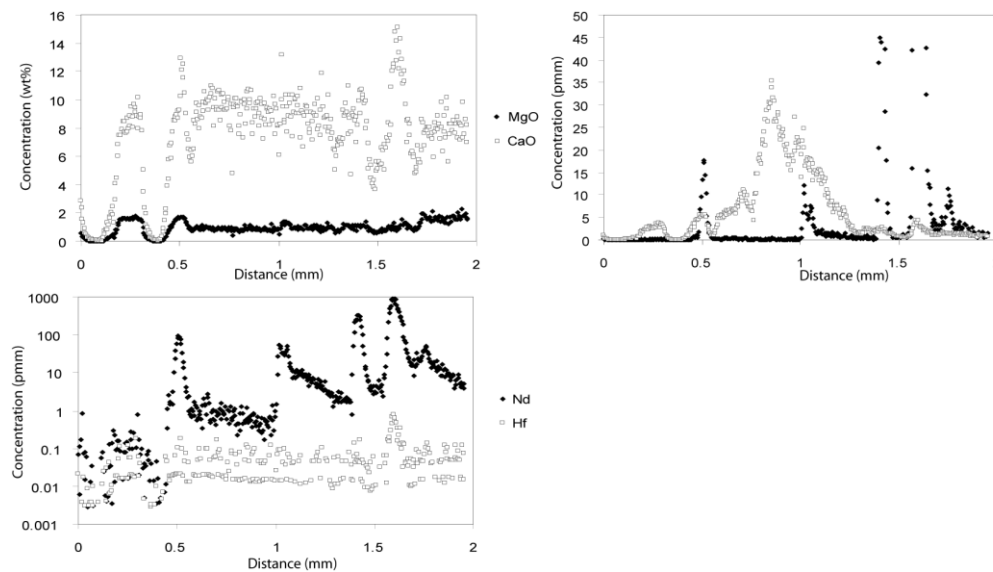


Figure 5-11, LA ICPMS data from a garnet from AB07-11 normalised to a SiO_2 value of 37.2%.

Nd and Sm have been strongly affected by inclusions and do not show prograde garnet zoning. This suggests that it may be difficult to obtain a Sm-Nd age from this sample and if an age is obtained it is unlikely to represent garnet growth. Lu shows a strong increase towards the garnet core which suggests that it retains its prograde profile. Hf levels were very close to the detection limit, indicated by the flat appear of the trace. There is only one peak in the profile which could relate to a zircon inclusion, this coupled with the prograde Lu profile indicate that a Lu-Hf age obtained from this sample will represent garnet growth.

AB07-13 – Drumnadrochit Migmatite

The rocks in this area have been strongly deformed and consist of predominantly migmatites. The Drumnadrochit Migmatite was sampled at [NH 4888 3233]; close

to the Drumnadrochit Amphibolite and close to where Cutts et al. (2010) obtained their sample for monazite and zircon geochronology which showed three zones within one of the garnets. The garnet core had inclusions which gave 825-780 Ma age range, the middle zone gave $\sim 725 \pm 6$ Ma aged inclusions and the outer zone (rim) gave $\sim 463 \pm 4$ Ma inclusions. These ages show that this area has been subjected to Neoproterozoic and Caledonian metamorphism.

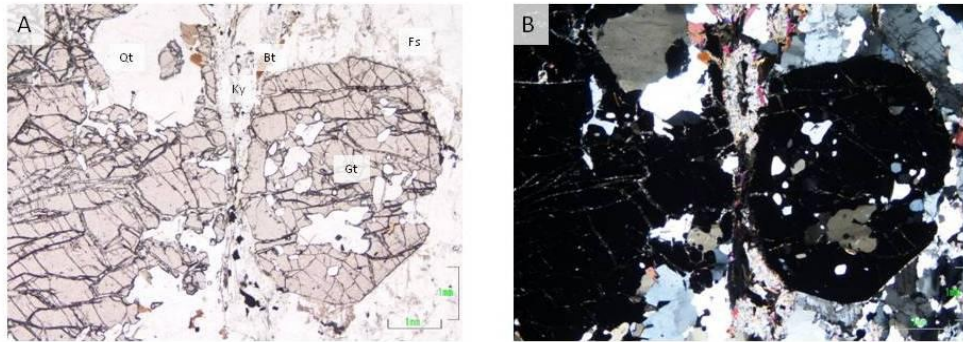


Figure 5-12, photographs of AB07-13. A shows one of the small euhedral garnets next to one of the large garnets. Kyanite is also shown with its reaction rim. B shows the same view in XP, highlighting the reaction rim.

In thin section the sample is made up of garnet, quartz, rutile, kyanite, plagioclase, biotite, muscovite and relict staurolite, shown in Figure 5-12. The garnets appear as large (up to 25 mm) poikiloblasts which are zoned or as small euhedral porphyroblasts (3 mm). The larger garnets have large inclusions (up to 1 mm) of quartz, kyanite, plagioclase, biotite, zircon, rutile and monazite; chlorite often appears in fractures and around the garnet rim. The smaller garnets have similar inclusions; however they do not have chlorite rims. Kyanite is present in the surrounding matrix where it has a reaction rim made up of micas. The fabric is made up of biotite, muscovite, plagioclase and quartz with rutile and kyanite. Chlorite is also present associated with the muscovite and biotite layers. The biotites are up to 0.5 mm in size and have zircon inclusions. The muscovites are up to 1 mm in size and have a few opaque inclusions and are often associated with the fine-grained mica that is reacting with kyanite.

The profiles in Figure 5-13 are from garnet core to its rim. The major elements, represented by MgO and CaO, do not show zoning which is most likely related to the high grade nature of these rocks.

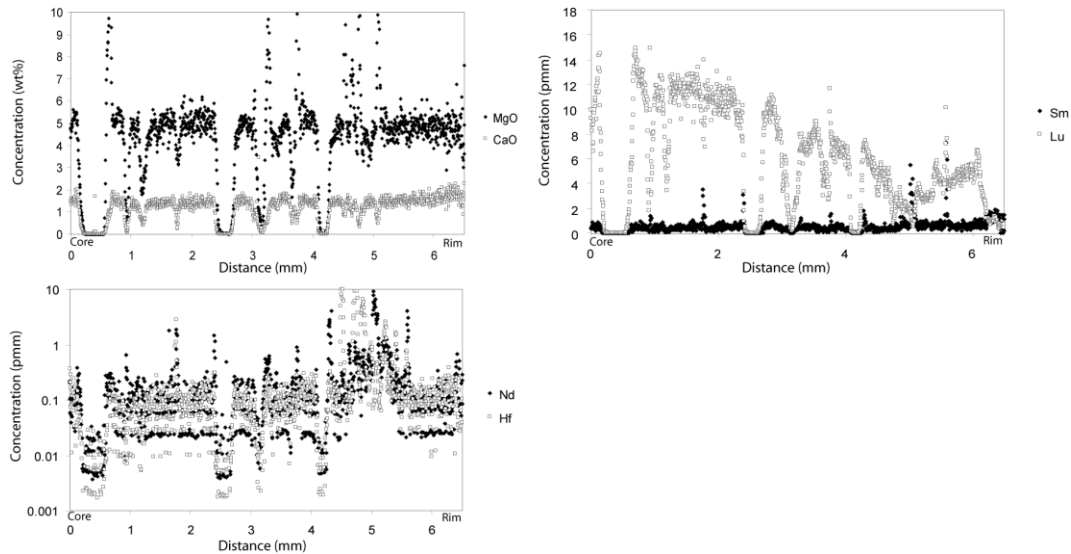


Figure 5-13, LA ICPMS data from a garnet from AB07-13 normalised to 37.6% SiO₂.

Lu shows marked zoning, decreasing from the garnet core with a slight increase closer to the rim which probably marks another zone of garnet growth. Sm shows a slight increase towards the garnet rim, this is also seen in the Nd profile. Any zoning within the Hf profile is difficult to determine as Hf concentrations were very close to the LA ICPMS detection limits, giving flat parallel points, this is also seen in Nd. All the traces show depressions which are quartz inclusions. The marked zoning of Lu suggests that a Lu-Hf age obtained from this sample would reflect garnet growth. As Sm and Nd increase towards the garnet rim it is likely that Sm-Nd could also give a prograde/ peak age.

AB07-14 – Drumnadrochit Amphibolite

The Drumnadrochit Amphibolite is part of a thin igneous sheet and was sampled at NH 4860 3255, close to AB07-13 and the sample that Cutts et al. (2010) dated. In the field the Drumnadrochit Amphibolite appears to be similar to the Loch Quoich Amphibolite as they both have intruded Glenfinnan Group rocks and been metamorphosed and boudinaged; however in thin section this sample is much coarser than Loch Quoich Amphibolite.

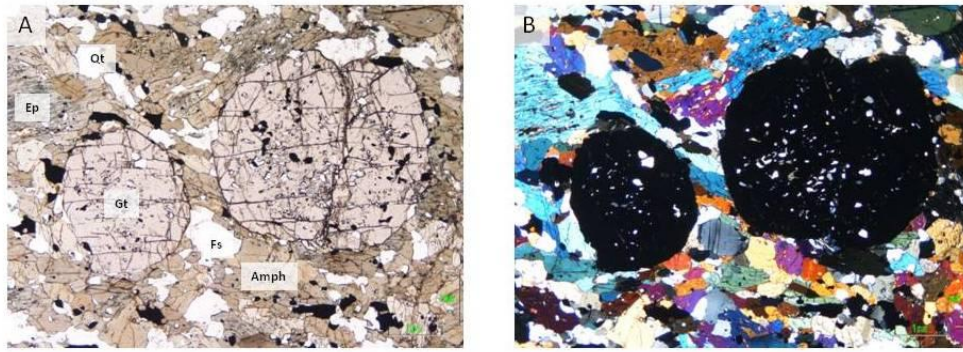


Figure 5-14, photographs of AB07-14, A shows the granoblastic texture made up of garnet, amphibolite, epidote, quartz and plagioclase. The same view is shown in B in XP.

In thin section the sample is made up of garnet, amphibole, epidote, quartz and plagioclase with accessory opaques and apatite and is granoblastic in texture, (Figure 5-14). The garnets are up to 3 mm in diameter with many inclusions of quartz, amphibole, chlorite, feldspar, apatite and opaques. The garnets are euhedral with fairly clean edges and show no zoning. The rest of the section is dominated by brown-green amphibole which regularly shows twinning and has opaque inclusions. Much of the plagioclase has a symplectitic texture where it is close to quartz veins with only a few fresh plagioclase crystals which show multiple twinning.

Figure 5-15 shows the LA-ICPMS transect across a garnet from the Drumnadrochit Migmatite (AB07-14). CaO shows an increase towards the garnet core and MgO shows an increase towards the garnet rim. MgO shows a large spike which correlates to a trough in all of the other traces shown here and in Appendix 2, this is most likely a magnetite inclusion. Lu shows a large increase towards the garnet core, and there are not many inclusions which affect the Hf trace, suggesting that the Lu-Hf ages from this sample will record prograde garnet growth. Sm and Nd show no obvious zoning, and remain fairly homogeneous. They also do not appear to be affected by many inclusions. This suggests that Sm-Nd should provide a meaningful age from this sample.

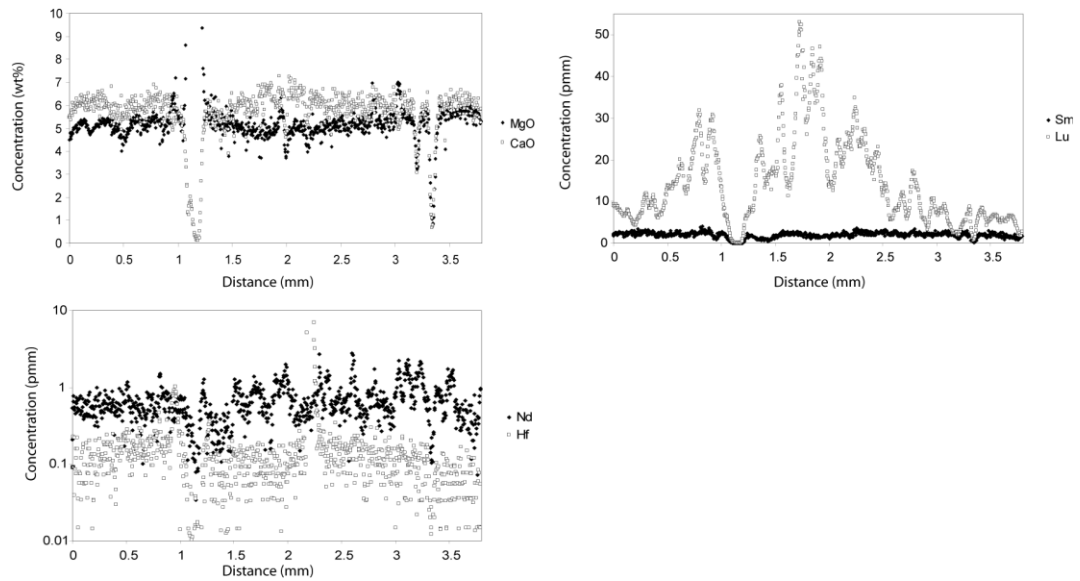


Figure 5-15, LA ICPMS data from a garnet from AB07-14 normalised to a SiO_2 value of 38.2%.

AB07-15 - Talmine Pelite

The Talmine Pelite is a discontinuous lens, c. 300m long and a few tens of metres thick, within Morar Group psammities west of the Kyle of Tongue. The pelite is a biotite-muscovite-garnet-albite-quartz schist, sampled at [NC 5735 6324]. Garnets are up to 10 mm diameter and are wrapped by a strong south-southeasterly-dipping biotite-muscovite fabric which is interpreted as S_2 . This is locally crenulated, most likely during localised F_3 folding. Quartz rods within S_2 are aligned parallel to L_2 and plunge to the south-southeast.

In thin section, Figure 5-16, garnets are generally euhedral to subhedral with sharp margins. There is no optical evidence for internal zoning. Inclusion trails consist of fine-grained quartz, opaques and biotite, and are interpreted as relics of S_1 . The quartz grains within the fabric are up to 1 mm in size, while the quartz inclusions within the garnets are up to 0.25 mm. The inclusion trails are curved and are oblique to the S_2 fabric. Some garnets contain small cracks that are filled with muscovite. The rims of many garnets are retrogressed to chlorite. The matrix also contains albite porphyroblasts that appear to be overprinted by S_2 .

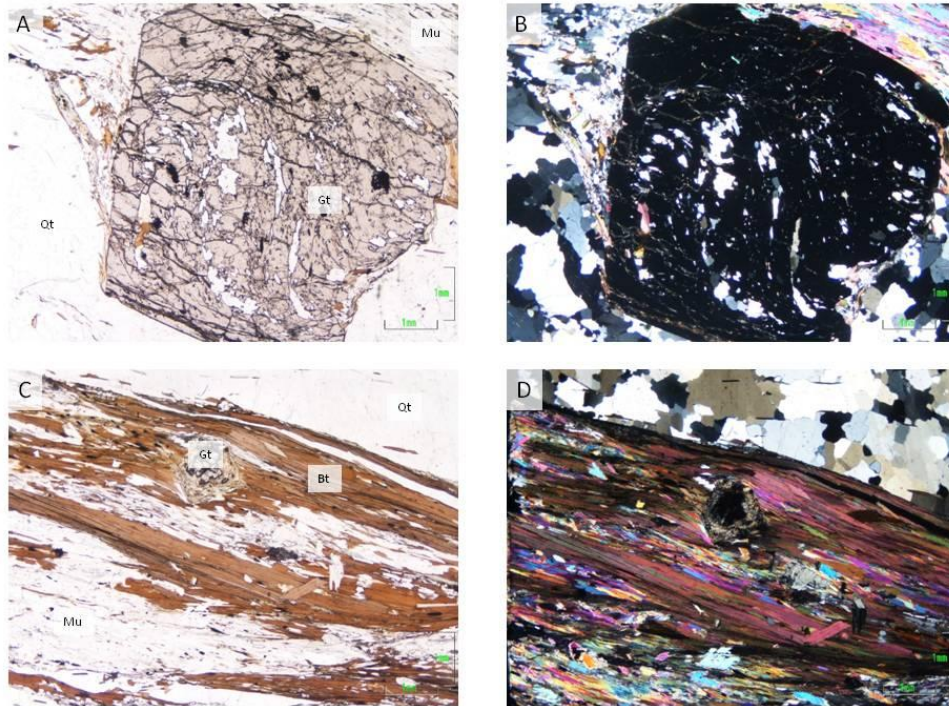


Figure 5-16, photographs of AB07-15. A and B show the curved inclusion trails within the garnets. C and D show the fabric with biotite-dominated layers and quartz-dominated layers, which wraps garnet. The garnet in C and D has a reaction rim.

The LA-ICPMS trace from the garnet from this sample was slightly offset from the centre of the grain; because of this the zoning seen in Figure 5-17 is also offset. The scaling of Figure 5-17 enhances the visibility of the zoning within the garnet and by cropping the tops off of inclusion peaks. CaO and MgO show a general increase from core to rim. The CaO trace shows large peaks which also affect Sm and the other LREE, MREE and Pb (Appendix 2), indicating these are likely to be monazite inclusions. Lu shows a significant decrease from core to rim, which suggests that Lu-Hf ages from this sample will reflect garnet growth. Sm, Nd and Hf all behave in a similar way and have all been affected by inclusions. All of the profiles are affected by a large quartz inclusion shown by a significant depression in the traces.

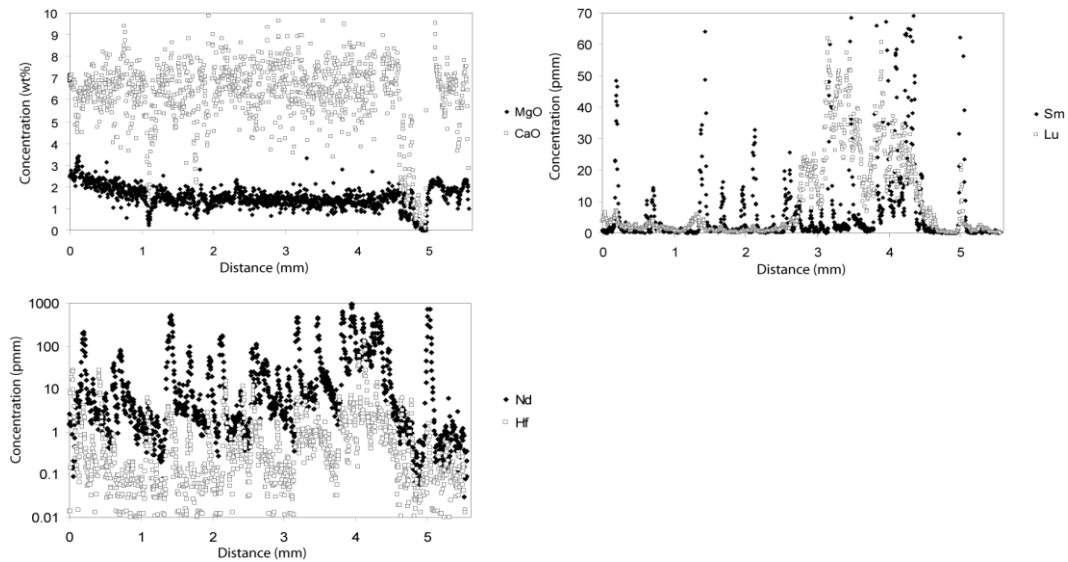


Figure 5-17, LA ICPMS data from a garnet from AB07-15 normalised to a SiO_2 value of 37.0%.

AB07/17 - Ben Hope Sill suite amphibolite

The Ben Hope Sill is a major intrusion up to 500 m thick that can be traced south from the southern Kyle of Tongue to Ben Hope (Holdsworth 1989). The intrusion carries all the structures and metamorphic fabrics present within its Moine host rocks and is therefore assumed to have been intruded pre- D_1 . It probably bifurcates northwards and is exposed on the west side of the Kyle of Tongue as a series of separate, concordant sheets (Holdsworth 1989). One of these sheets was sampled near Talmine harbour [NC 5535 5310].

The sample is dominated by hornblende-garnet-plagioclase with accessory biotite, muscovite, quartz and opaque minerals and secondary chlorite, (Figure 5-18). Abundant euhedral to subhedral garnets occur up to 20 mm in diameter. These are wrapped by S_2 , which is defined by amphibole, biotite, calcite and quartz. The garnets do not show any optical evidence for zoning. They often contain abundant inclusions of quartz, chlorite, biotite, calcite, amphibole and opaques. Prominent inclusion trails of S_1 are highly oblique to the enveloping S_2 fabric. The inclusions are linear and are made up of quartz, chlorite, opaques, biotite, chlorite and amphibole. Some garnets are extensively retrogressed to chlorite.

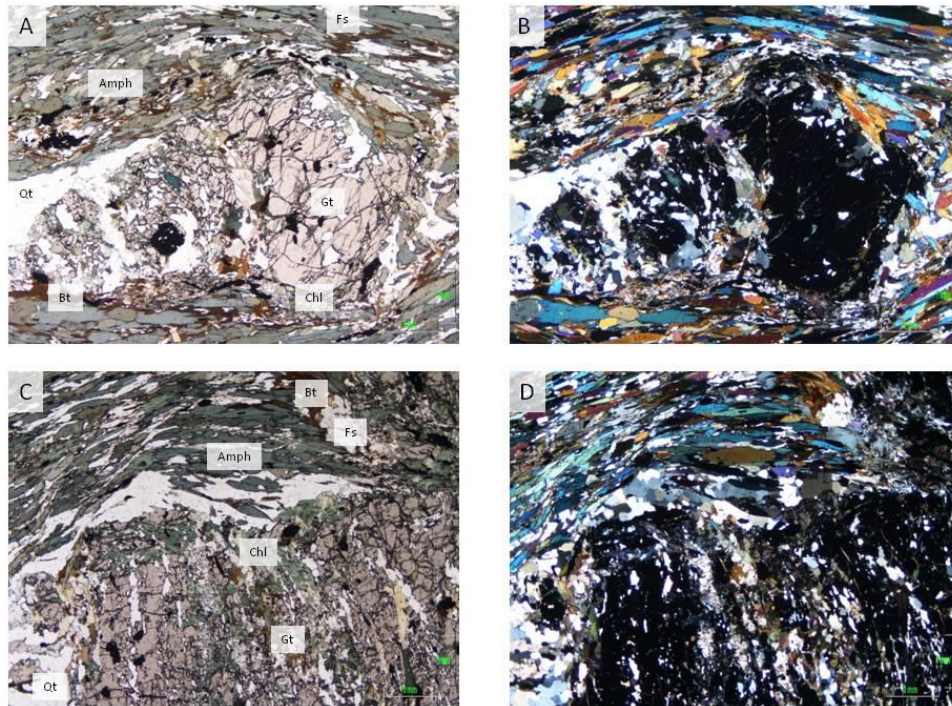


Figure 5-18, thin section images from AB07-17, A and B show the fabric, dominated by amphibole, biotite, feldspar and quartz, wrapping garnets. C and D show one of the large garnets with inclusion trails that are oblique to the main fabric.

The most notable thing about the traces from this sample are the multiple depressions evident (Figure 5-19). These depressions correspond to quartz inclusions, other inclusions seen include rutile, zircons and phosphates, seen by the Ti, Zr and Ca peaks respectively (Appendix 2).

The inclusion-rich nature of this sample makes overall zoning patterns hard to see; however, a general Lu enrichment in the garnet core is observed, with Hf concentration increasing slightly towards the rim, suggesting that the Lu-Hf age from this sample should reflect prograde growth. There Hf trace shows many peaks which probably relate to zircon inclusions which may effect the Lu-Hf age. The Sm and Nd traces are strongly affected by inclusions which suggests that it may be difficult to obtain a meaningful age from the sample.

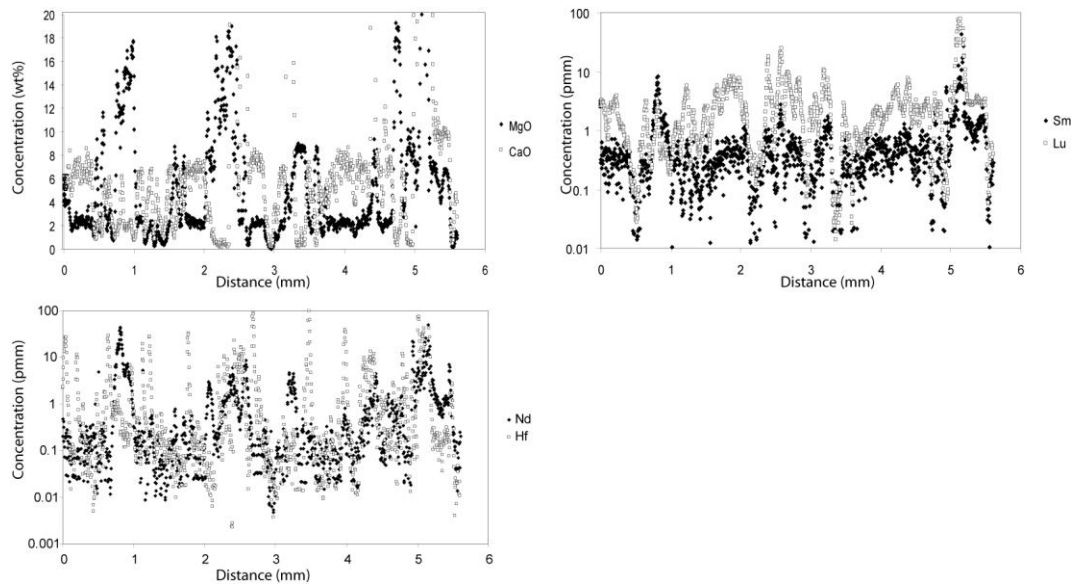


Figure 5-19, LA ICPMS data from a garnet from AB07-17 normalised to a SiO_2 value of 37.0%.

AB07/21 – Strathy Complex Amphibolite

The sample from the Strathy Complex was collected from a garnet amphibolite at Strathy Point. In the field this sample was a very coarse-grained garnetiferous amphibolite. These amphibolites occur as discrete bodies, up to 3 m thick and are usually only weakly foliated. The garnets are up to 70 mm in size with visible parallel ribbons of quartz inclusions.

In thin section (Figure 5-20) the sample comprises of garnet, gedrite (Burns et al. 2004), plagioclase, quartz, an opaque mineral, biotite and chlorite with no obvious fabric which could be due to the coarseness of this sample. The matrix mostly consists of gedrite, although this is often replaced and pseudomorphed by chlorite, and biotite is also altering to chlorite in places. The dominant inclusions within the garnets are the quartz ribbons which do not appear to be extending into the matrix. There are also inclusions of gedrite, feldspar, an opaque mineral, and biotite. LA ICPMS was not undertaken on this sample.

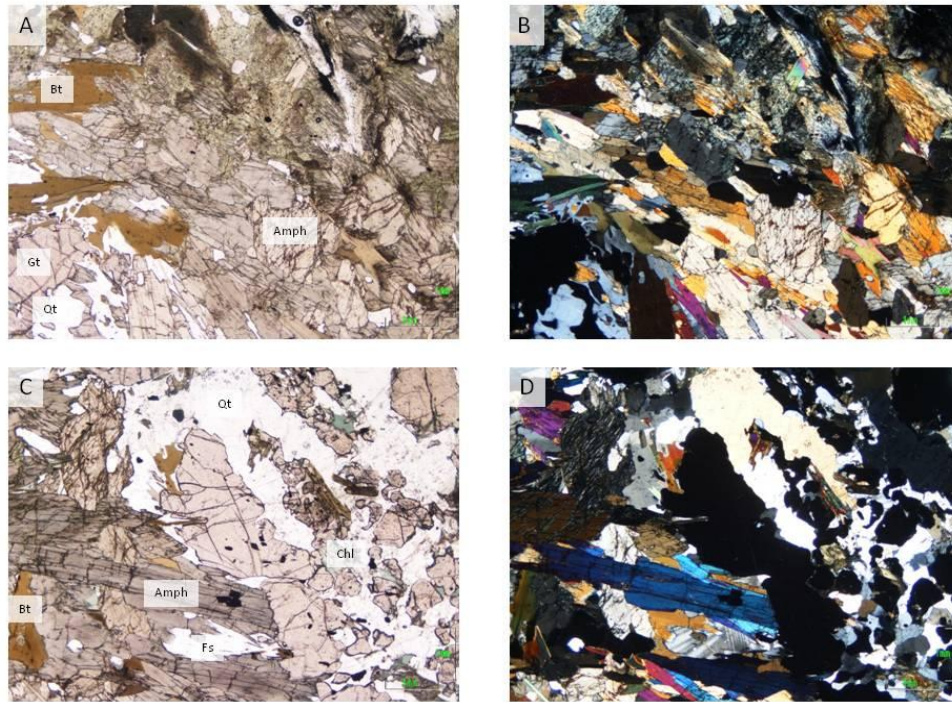


Figure 5-20 thin section photographs for AB07-21 (Strathy Complex Amphibolite). A and B show amphibole that is in equilibrium next to amphibole which is clearly not in equilibrium. C and D show the large quartz inclusions within the large garnets. All of the pictures show the weak fabric.

AB07/22 - Naver nappe garnetiferous gneiss

A sample of Moine migmatite was sampled from the Naver nappe at Kirtomy Point [NC 7511 6430]. The sample is a medium-grained garnetiferous gneiss composed of quartz-plagioclase-garnet-biotite.

In thin section, the quartz shows undulose extinction and is up to 1.5 mm in size, (Figure 5-21). The plagioclase often shows signs of recrystallisation, and is up to 2 mm in size. Minor amphibole and accessory titanite, apatite and zircon are also present, and these along with the quartz, biotite and plagioclase make up the fabric. The garnets are up to 1 mm in diameter and typically subhedral to anhedral in form. They are often characterized by a reaction rim of fine-grained plagioclase. The garnets are relatively free of inclusions and cracks, and appear to be wrapped by the fabric.

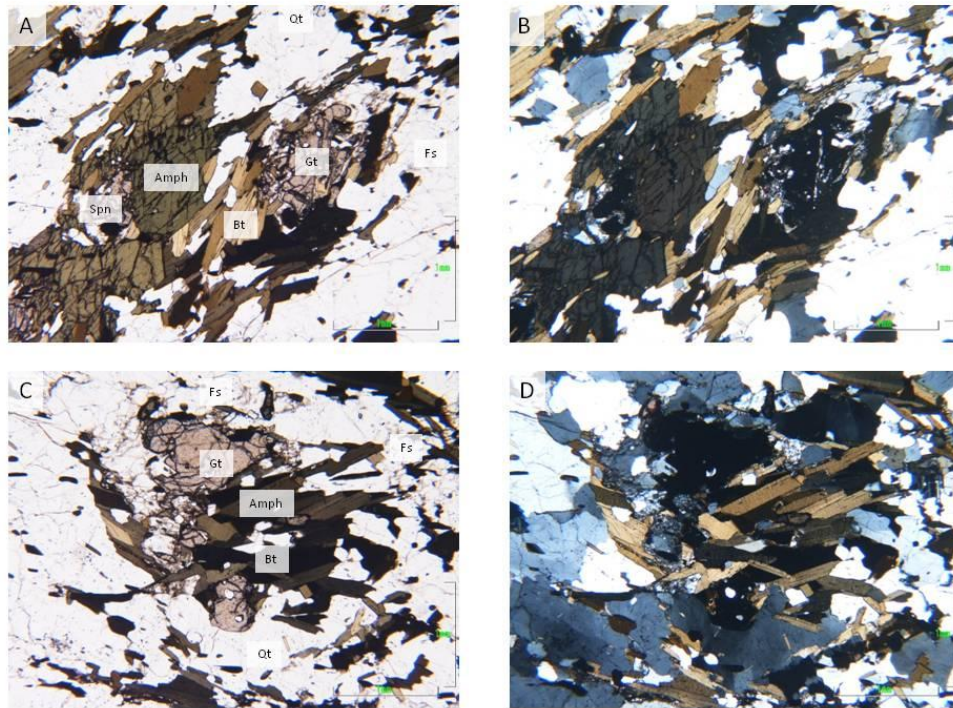


Figure 5-21 thin section photographs for AB07-22 (Naver nappe garnetiferous gneiss). A and B show the fabric defined by amphibole, biotite, quartz and feldspar. C and D show the small garnets within this sample surrounded by amphibole and biotite.

The major element profiles, shown by MgO and CaO, for this garnet are fairly homogeneous (Figure 5-22).

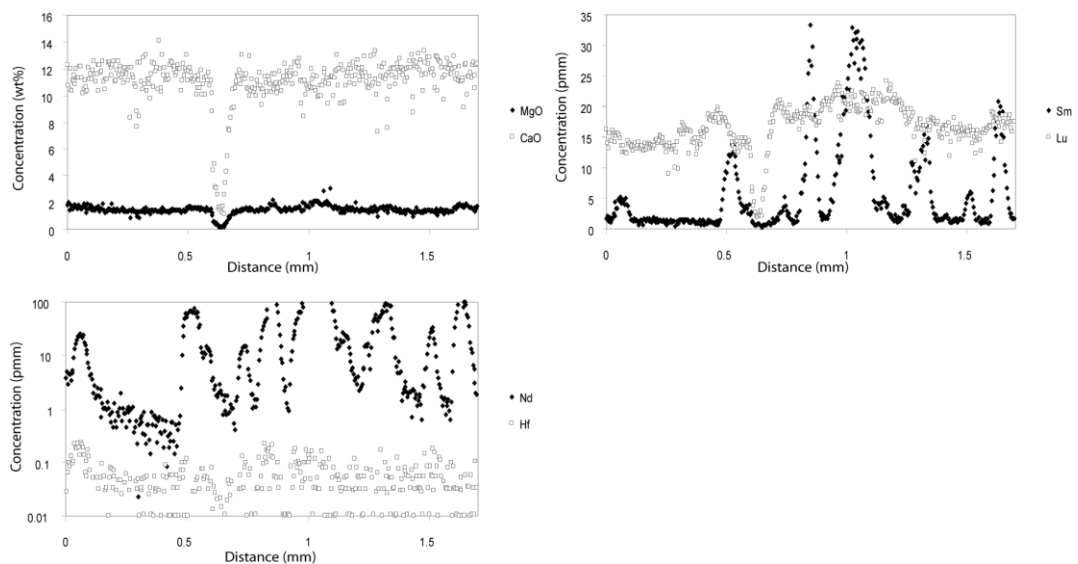


Figure 5-22, LA ICPMS data from a garnet from AB07-22 normalised to a SiO₂ value of 37.5%.

There are very few zircon inclusions, and the Lu trace increases towards the garnet core suggesting that the Lu-Hf age obtained from this sample should reflect prograde garnet growth. The Sm and Nd profiles are strongly dominated by traces from inclusions of what is likely to be amphibole as it has lower Lu, higher Sm and Nd and does not appear to be affecting MgO and CaO. Sm and Nd do appear to show zoning, suggesting that it may be difficult to get a meaningful Sm-Nd age from this sample.

AB07/23 – Dava Succession Amphibolite

A sample from within the Dava Succession was taken from a garnet amphibolite between Loch Ruthven and Loch a'Choire [NH 6283 2889]. The sample is an extremely coarse garnet amphibolite with pink garnets up to 80 mm in diameter, quartz up to 4 mm and amphibole up to 20 mm, epidote and accessory rutile, sphene and opaques are also present.

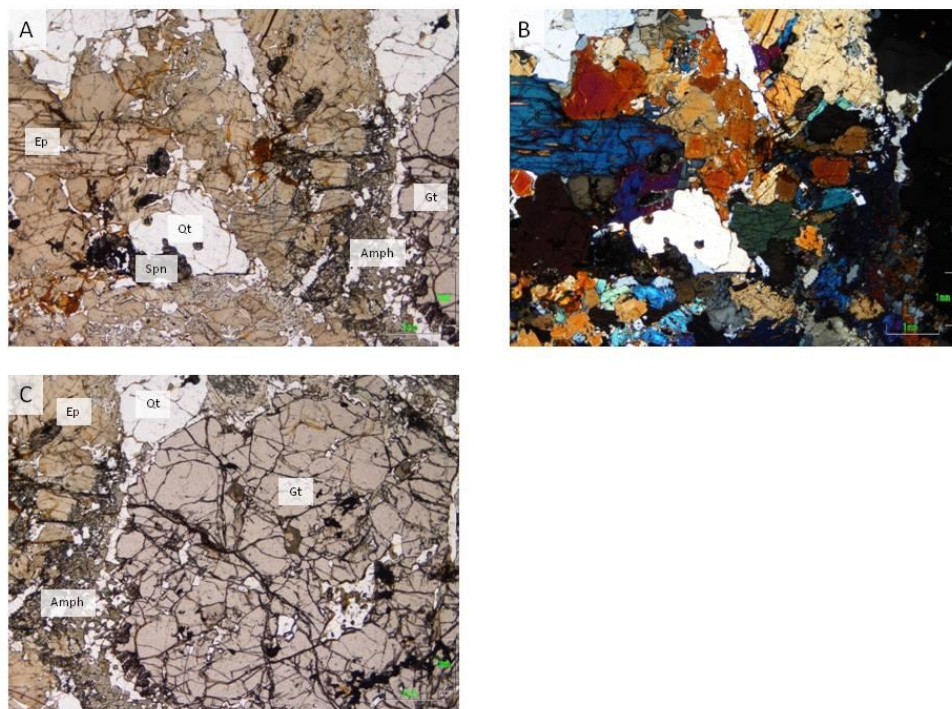


Figure 5-23, thin section images of AB07-23. A and B show the granoblastic texture made up of amphibolite, epidote, quartz, garnet and sphene. C shows a euhedral garnet surrounded by amphibole.

The garnets are euhedral to subhedral with inclusions of amphibole, quartz, sphene, rutile, epidote and opaques; they also have lots of veins and cracks and chlorite is sometimes present associated with garnet, Figure 5-23. Many of the garnets are surrounded by amphibole. The sample is granoblastic in texture. The epidote is not in equilibrium and appears to be being replaced by feldspar. In places the amphibole also looks not to be in equilibrium, perhaps fluids have affected this sample. LA ICPMS was not undertaken on this sample.

AB07/27 – Leven Schist

The sample is from part of the Leven Schist which is part of the Appin Group within the Dalradian Supergroup, sampled at NN 2611 8032. It is a biotite-garnet-mica schist with large garnet and biotite porphyroblasts.

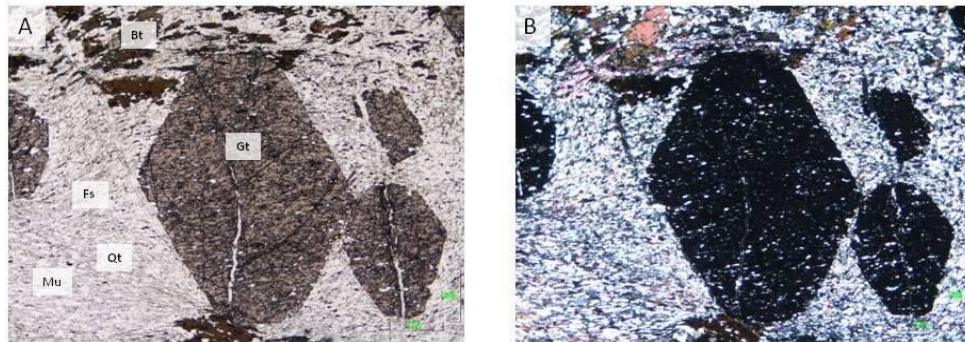


Figure 5-24 thin section photographs for AB07-27 (Leven Schist). A and B show the inclusion trails within the garnet continuing into the surrounding matrix showing that the garnets are post-kinematic. The fabric is slightly crenulated. A biotite porphyroblasts can also be seen in the top part of each picture which has been deformed.

In thin section, the garnets are up to 5 mm, euhedral and are post- D_1 as the weakly curved inclusion trails within the poikiloblasts exactly follow the crenulated matrix, (Figure 5-24). The curved inclusion trails relate to a weakly developed S_2 fabric (Phillips & Key 1992). The inclusions are the same size as their counterparts in the matrix and are made up of quartz, biotite, opaques and muscovite. The matrix is fine-grained (0.1 mm) with a weakly developed S_2 crenulation and is made up of muscovite, quartz and biotite with accessory apatite, zircon and opaques. The matrix biotite has mainly been converted to chlorite. There are larger biotite poikiloblasts with chlorite rims which are up to 2 mm in size with zircon inclusions that are

weakly curved with pleochroic halos. The biotites have been deformed during S_2 to form mica fish. Similar to the garnets the biotite poikiloblasts are post- D_1 .

The LA-ICPMS transect on this garnet went from garnet rim to the core. MgO shows an increase towards the garnet rim while CaO does not record any zoning (Figure 5-25) and is strongly influenced by inclusions.

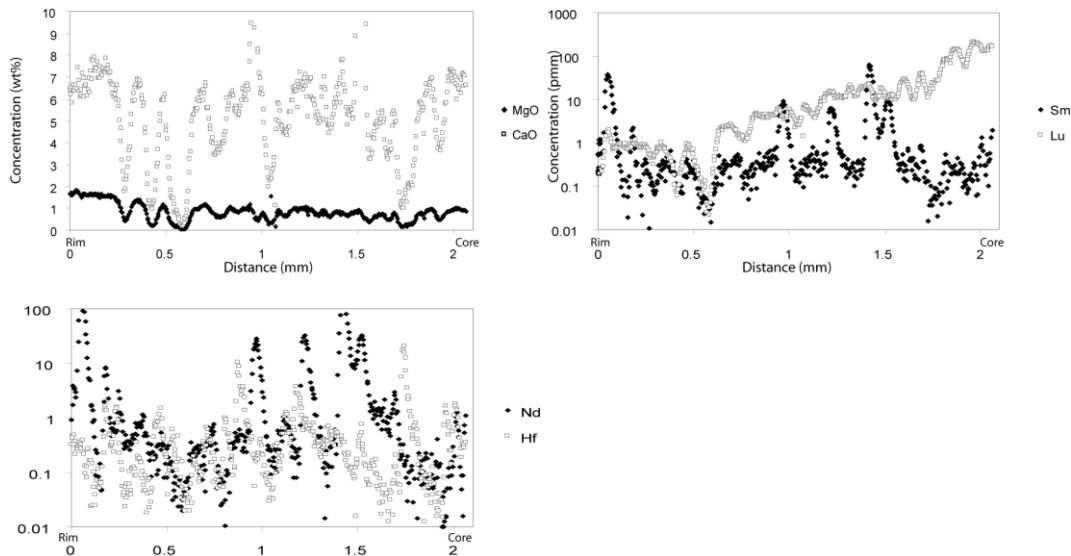


Figure 5-25, LA ICPMS data from a garnet from AB07-27 normalised to a SiO_2 value of 39.3%.

Lu shows a large increase towards the garnet core, retaining its prograde profile, indicating that a Lu-Hf age from this sample should reflect prograde garnet growth. The Hf profile shows evidence of several zircon inclusions which may affect the Lu-Hf age, although the zircons must be reasonably small as they do not show a large Hf peak. The Sm and Nd profiles are strongly influenced by inclusions which correlate with CaO peaks suggesting that these are phosphate inclusions. Sm and Nd also do not show evidence of zoning which suggests that it may be difficult to obtain a meaningful Sm-Nd age from this sample.

AB07-30 – Mull Amphibolite

This amphibolite intrudes the Glenfinnan Group on the Ross of Mull, obliquely cross-cutting the bedding within the psammities, and was sampled by Strachan in 2007 at [NM 3993 1880], close to the hinge of the Assapol Synform.

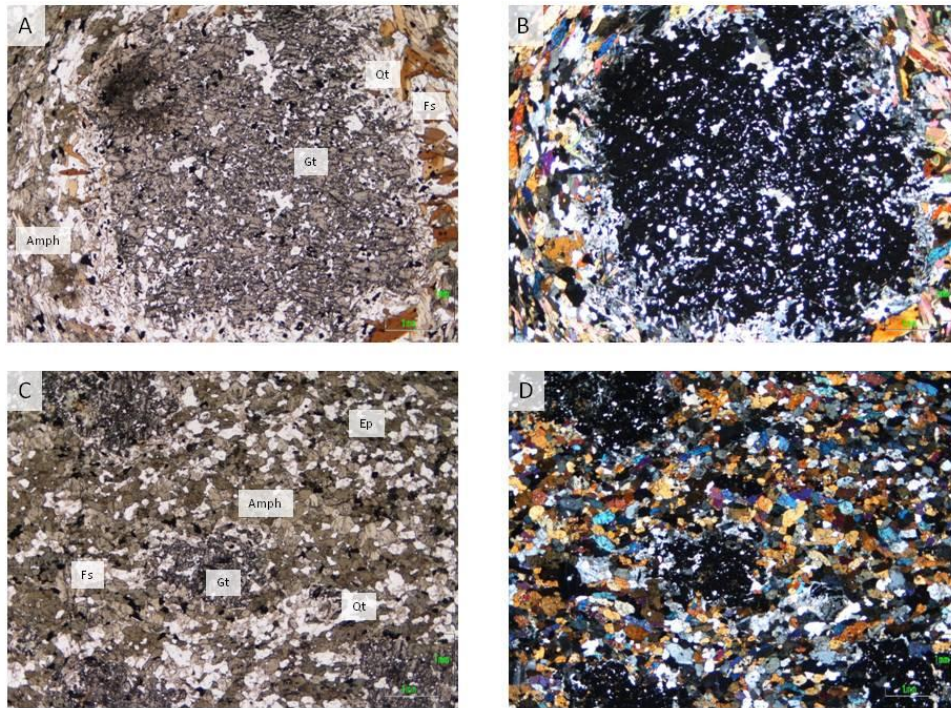


Figure 5-26 thin section photographs for AB07-30 (Mull Amphibolite). A and B show one of the large garnets which is very inclusion-rich. The inclusions are dominated by quartz. The surrounding fabric is made up of amphibole, epidote, feldspar and quartz. C and D show smaller garnets with sieve-like textures.

In thin section the sample has large garnets, between 3 mm and 10 mm in size, which have numerous inclusions of quartz, plagioclase, rutile and apatite. The garnets are wrapped by a weak fabric made up of amphibole, biotite, epidote, plagioclase and quartz with accessory rutile, zircon, opaques, titanite and apatite. The garnets are extremely inclusion-rich as shown in Figure 5-26. The plagioclase often shows signs of recrystallisation; the biotite has pleochroic halos which surround zircons. LA ICPMS was not undertaken for this sample.

AB08-02 – Vaich Amphibolite

The sample was collected at NH 20504 66427 by Strachan in early 2008. It is from part of the Morar Group close to the Sgurr Beag Thrust and was selected along with a sample from above the thrust in order to compare the timing of metamorphic events either side of this structure.

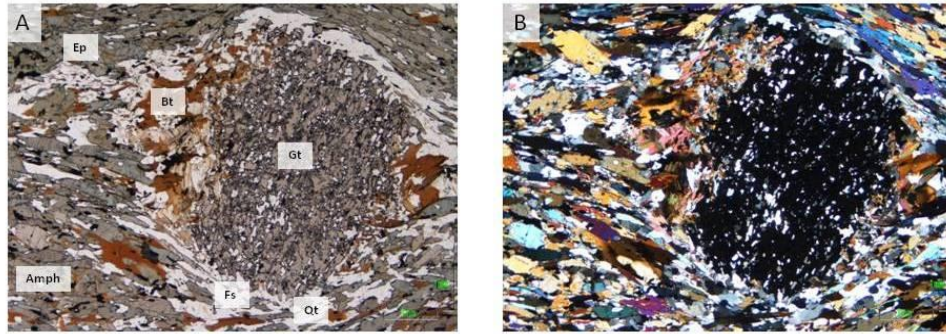


Figure 5-27 thin section photographs of AB08-02 (Vaich Amphibolite). A and B show a garnet from AB08-02 which has planar inclusion trails. The garnet is strongly wrapped by the fabric dominated by amphibole. The garnet has pressure shadows with biotite and quartz.

In thin section (Figure 5-27) it is made up of garnet, amphibole, biotite, quartz, sphene and plagioclase with accessory zircons and opaques. The garnets are up to 8 mm in diameter, are subhedral and are extremely inclusion-rich. The inclusions are made up of quartz, epidote, sphene, opaques, and zircon. The fabric is made up of amphibole, biotite, quartz and plagioclase and wraps the garnets. LA ICPMS was not undertaken on this sample.

5.5.1 Summary

The samples which show Lu enrichment towards the garnet cores and do not have many zircon inclusions will provide the best results for Lu-Hf dating. This is seen in the Armadale Pelite (AB07-11), the Drumnadrochit Migmatite (AB07-13), the Drumnadrochit Amphibolite (AB07-14), the Talmine Pelite (AB07-15), the Ben Hope Sill (AB07-17), the Naver Nappe garnetiferous gneiss (AB07-22) and the Leven Schist (AB07-27). Samples which have few inclusions that affect Sm and Nd are most likely to provide a good Sm-Nd age. Samples which should provide good Sm-Nd ages are the Drumnadrochit Migmatite (AB07-13) and the Drumnadrochit Amphibolite (AB07-14). Samples from which it may be more difficult to yield good Sm-Nd ages from are the Armadale Pelite (AB07-11), the Ben Hope Sill (AB07-17), the Naver Nappe garnetiferous gneiss (AB07-22) and the Leven Schist (AB07-27).

5.6 Results and interpretation

5.6.1 The Morar Group

The results are summarised in Table 5-1 and Table 5-2. Five samples from the Moine Nappe yielded Caledonian ages, the Basal Pelite (AB07-08), the Armadale Pelite (AB07-11), the Talmine Pelite (AB07-15), the Ben Hope Sill (AB07-17) and the Vaich Amphibolite (AB08-02).

The Basal Pelite (AB07-08) gave a Lu-Hf core age of 589 ± 17 Ma and a Lu-Hf rim age of 458.7 ± 4.5 Ma. The core and the rim were distinguished during picking based on colour, as the cores were orange and far more inclusion-rich than the purple garnet rims. The rim age is the more meaningful of the two as the core has a low $^{176}\text{Lu}/^{177}\text{Hf}$ ratio and its $^{176}\text{Hf}/^{177}\text{Hf}$ ratio is quite similar to that of the whole rock. This is due to a high Hf content of 2.493 ppm which suggests a large influence from zircon inclusions. This can be checked by comparing the Hf concentration obtained from the LA ICPMS to that obtained by isotope dilution (ID). The Hf concentration was estimated from part of the pure garnet using the LA ICPMS trace by looking at parts of the trace which were above the detection limit and were not affected by zircon inclusions. This sample gave a pure garnet core Hf concentration of ~ 0.16 ppm while a concentration of 2.493 ppm was obtained by ID. This shows that only $\sim 7\%$ of the Hf measured by the MC ICPMS came from the garnet, $\sim 93\%$ of it must have come from zircon inclusions. The Hf concentration from part of the pure garnet rim was ~ 0.38 ppm; ID gave 1.864 ppm suggesting that some zircon inclusions were mixing with the garnet rim as well. This sample also has a particularly low Lu content in the core of 1.945 ppm which leads to a low $^{176}\text{Lu}/^{177}\text{Hf}$ ratio. The effect of the zircon inclusions can be modelled if the $^{176}\text{Hf}/^{177}\text{Hf}$ ratio of the zircon inclusions is known along with the concentration of Lu and Hf in the inclusions. Although this information is not known, it may be assumed that the zircon inclusions are ~ 1600 Ma based on detrital zircon data from Kirkland et al. (2008) and Cawood et al. (2004, 2007), and for this a $^{176}\text{Hf}/^{177}\text{Hf}$ ratio can be estimated. Using the Lu and Hf concentration estimates of ~ 84 ppm and ~ 9603 ppm for the zircon inclusions and the method described in Chapter 2, the effect of the zircons can be estimated. Using this information the pure garnet core from AB07-08

gives an age of ~690 Ma, which would suggest that the garnet core from this sample grew at a similar time as the other Neoproterozoic garnet cores in the Morar Group.

The 459.7 ± 4.5 Ma age from the garnet rim could potentially be the result of physical mixing between the picked garnet old core and Scandian rims. To investigate whether mixing has affected this sample, mixing end members were calculated based on a 841 Ma core, which is similar to the Neoproterozoic ages from other parts of the Morar Group, and a 430 Ma rim. LA ICPMS concentrations of Sm, Nd, Lu and Hf. Figure 5-28 shows mixing diagrams for AB07-08. Mixing appears to have occurred according to the $^{176}\text{Lu}/^{177}\text{Hf}$ versus $^{176}\text{Hf}/^{177}\text{Hf}$ diagram as the tie lines intersect at the 430 Ma end member. However the second diagram demonstrates that the Hf content within the garnet fraction cannot be explained by mixing.

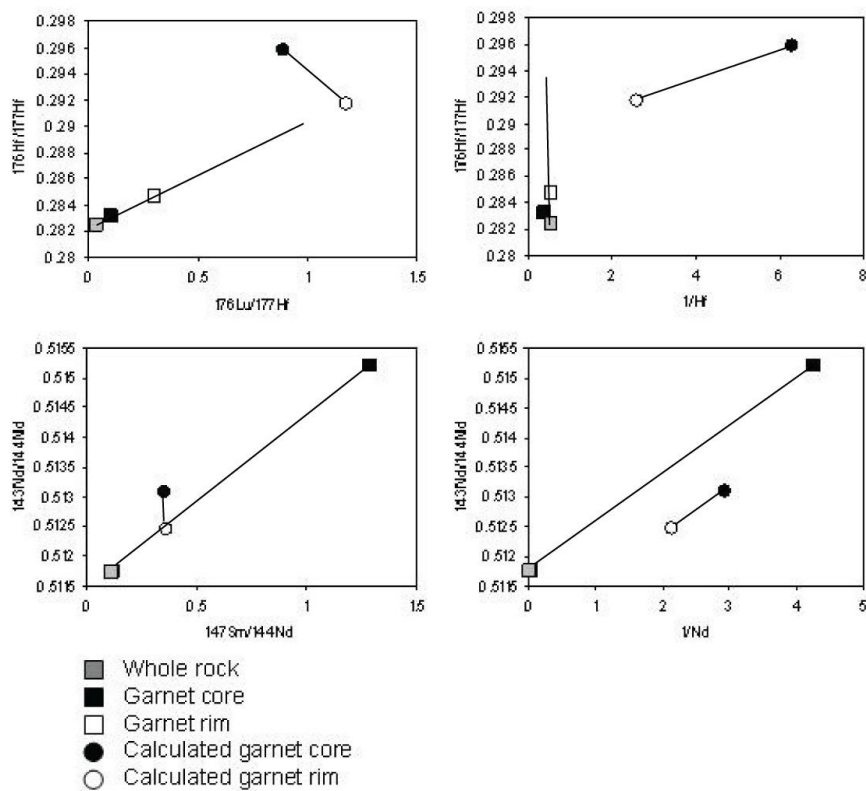


Figure 5-28, $^{176}\text{Lu}/^{177}\text{Hf}$ vs $^{176}\text{Hf}/^{177}\text{Hf}$, $^{176}\text{Lu}/^{177}\text{Hf}$ vs $1/\text{Hf}$, $^{147}\text{Sm}/^{144}\text{Nd}$ vs $^{143}\text{Nd}/^{144}\text{Nd}$ and $^{147}\text{Sm}/^{144}\text{Nd}$ vs $1/\text{Nd}$ for AB07-08. The filled black squares are the measured garnet core fraction, the empty black squares are the garnet rim fraction, the grey squares are the measured whole rock fractions, the filled black circles are a 840 Ma end member and the empty circles are a 430 Ma end member.

The Sm and Nd isochron diagram as intercepts with the 430 Ma end member but as the 1/Nd diagram does not show mixing. This sample has not been affected by mixing of an old core with a young rim.

The Basal Pelite (AB07-08) gives a Sm-Nd two point isochron age of 449.7 ± 2.3 Ma using the garnet core and the whole rock fraction. The garnet has a high $^{147}\text{Sm}/^{144}\text{Nd}$ ratio suggesting that the age is reliable. This is complemented by a low ID Nd concentration of 0.234 ppm which is similar to a pure garnet concentration (by LA ICPMS) of 0.34 ppm. The garnet rim gave an age of -20 ± 330 Ma and is clearly unradiogenic as it has a $^{147}\text{Sm}/^{144}\text{Nd}$ ratio which is the same as the whole rock. The garnet rim fraction analysed appears to have incorporated monazite inclusions as it has an ID Nd concentration of 15.54 ppm while the pure garnet rim analysed by LA ICPMS gave an Nd concentration of ~ 0.46 ppm.

The Armadale Pelite (AB07-11) gives a Lu-Hf two point isochron age of 466.2 ± 2.9 Ma. The LA ICPMS gave an Hf concentration of 0.192 ppm for the pure garnet; in contrast to the ID Hf concentration of 1.70 ppm which shows that some zircon has been incorporated in to the dissolved garnet fraction. However, as the $^{176}\text{Lu}/^{177}\text{Hf}$ and $^{176}\text{Hf}/^{177}\text{Hf}$ are high this age is reliable. This sample did not give a useful Sm-Nd age (628 ± 260 Ma) as the Nd concentration measured by ID was 19.01 ppm and the LA ICPMS value for pure garnet was ~ 0.35 ppm, which shows that there was substantial incorporation of Nd-rich inclusions.

Two garnet fractions were analysed for Lu-Hf from the Talmine Pelite (AB07-15) which do not lie on a three point isochron with the whole rock fraction, even though the individual two-point ages are within error, shown in Figure 30. The age from Grt 1 was AB07-15 449.3 ± 1.9 Ma and the age from AB07-15 Grt 2 was 443.1 ± 4.8 Ma. AB07-15 Grt 1 has a higher $^{176}\text{Lu}/^{177}\text{Hf}$ ratio than Grt 2, which is due to the significantly higher Lu concentration of 8.829 ppm compared to 5.967 ppm. The LA ICPMS gave a pure garnet Hf concentration of ~ 0.32 ppm while ID gave a Hf concentration of 2.096 ppm for AB07-15 Grt 1 and 2.108 ppm for AB07-15 Grt 2, which suggests that some zircon was dissolved along with the garnet. Using the zircon modelling described in Chapter 2 the inclusions could add ~ 78 Ma to the age obtained from AB07-15 Grt 2, while for AB07-15 Grt 1 the inclusions are estimated to add a maximum of 45 Ma to the age obtained. A Sm-Nd four point isochron has

been obtained for the Talmine Pelite sample (AB07-15), using three garnet separates and the whole rock fraction, which gives an age of 456 ± 8 Ma (MSWD = 0.68), shown in Figure 31. The LA ICPMS Nd concentration was ~ 0.95 ppm which is marginally more than that given by ID (0.701 ppm, 0.424 ppm and 0.451 ppm) indicating that there was no influence of Nd-rich inclusions on the age obtained from this sample.

A Lu-Hf four point isochron has been obtained for the Ben Hope Sill sample (AB07-17), using three garnet fractions and a whole rock, and gives an age of 447.3 ± 1.7 Ma (MSWD = 3.4) (Figure 30). The LA ICPMS gave a Hf concentration of ~ 0.11 ppm for pure garnet, while ID gave 0.133 for Grt 1, 0.094 ppm for Grt 2 and 0.246 ppm for Grt 3, which suggests no input from zircon inclusions. The whole rock fraction from this sample gave an extremely low Hf concentration of 0.188 ppm; XRF gave a Zr concentration of 90 ppm, which would usually suggest a Hf concentration of ~ 2 ppm. This could be due to not dissolving all of the zircon during the dissolution process. No useful Sm-Nd age was obtained from the Ben Hope Sill (AB07-17) as the garnets were not sufficiently radiogenic (Figure 31). The garnet fractions from the Ben Hope Sill gave ID Nd concentrations that were either close to the whole rock concentration or greater. The LA ICPMS gave a pure garnet Nd concentration of ~ 0.23 ppm showing that many Nd-rich inclusions were dissolved with the garnet fraction, which would make the $^{143}\text{Nd}/^{144}\text{Nd}$ and $^{147}\text{Sm}/^{144}\text{Nd}$ close to the whole rock value.

The Vaich Amphibolite (AB08-02) gave a Lu-Hf core age of 422 ± 5 Ma and a Lu-Hf rim age of 443 ± 6 Ma, which are just within error. This sample does not have LA ICPMS data, thus it is impossible to compare the pure garnet concentrations to the values obtained from the MC ICPMS. However, ID gave Hf concentrations of 0.977 ppm for the core and 0.729 ppm for the rim, suggesting little influence from zircon inclusions. Although the $^{176}\text{Lu}/^{177}\text{Hf}$ ratios look reasonable, the $^{176}\text{Hf}/^{177}\text{Hf}$ ratios are similar to the whole rock ratio which is giving these ages large errors. This sample gave two Sm-Nd two point garnet-whole rock isochrons, the core gave an age of 625 ± 130 Ma and the rim gave 402 ± 84 Ma. Neither of these ages are very reliable as the $^{147}\text{Sm}/^{144}\text{Nd}$ and $^{143}\text{Nd}/^{144}\text{Nd}$ ratios are close to the whole rock values.

This is most likely due to the high Nd concentrations of 15.098 ppm for the core and 11.794 ppm for the rim, suggesting influence from Nd-rich inclusions.

5.6.2 The Glenfinnan Group

Four samples have been analysed from the Glenfinnan Group that gave Caledonian ages, the Loch Quoich Amphibolite (AB07-05), the Drumnadrochit Migmatite (AB07-13), the Drumnadrochit Amphibolite (AB07-14) and the Mull Amphibolite (AB07-30). The Loch Quoich Amphibolite gave a two point Lu-Hf age of 462.9 ± 1.7 Ma, which is a reasonable age as the garnet has $^{176}\text{Lu}/^{177}\text{Hf}$ and $^{176}\text{Hf}/^{177}\text{Hf}$ ratios are significantly higher than the whole rock values. This sample did not yield a meaningful Sm-Nd age as the $^{147}\text{Sm}/^{144}\text{Nd}$ and $^{143}\text{Nd}/^{144}\text{Nd}$ ratios from the garnet are lower than that of the whole rock. The garnet fraction had an ID Nd concentration of 7.00 ppm suggesting that mixing with inclusions was the cause of the low $^{147}\text{Sm}/^{144}\text{Nd}$ and $^{143}\text{Nd}/^{144}\text{Nd}$ ratios.

No Lu-Hf ages were obtained from the Drumnadrochit Migmatite (AB07-13) as the chemistry failed for this sample, which is unfortunate because the LA ICPMS Lu profile across one of the garnets suggested that it would yield a good Lu-Hf age. The Drumnadrochit migmatite (AB07-13) gave a Sm-Nd core age of 501.7 ± 3.4 Ma and a rim age of 491.9 ± 2.7 Ma. The core and the rim were distinguished during picking based on colour, the cores were pink and the rims were orange. The ages from this sample have not been affected by Nd-rich inclusions; the pure garnet has a Nd concentration of 0.32 ppm (core) and 0.67 ppm (rim) while the ID concentrations are 0.403 ppm (rim) and 1.186 ppm (core).

Figure 5-29 shows mixing diagrams for the Drumnadrochit Migmatite (AB07-13), the end members are based on the U-Pb ages obtained from monazite inclusions within a garnet from close to where this rock was sampled, which gave core ages of 780 Ma and rim ages of 465 Ma (Cutts et al. 2010). Figure 5-29 appears to show mixing between the hypothetical rim and the measured garnet core, however the mixing diagrams do not explain the ages fully.

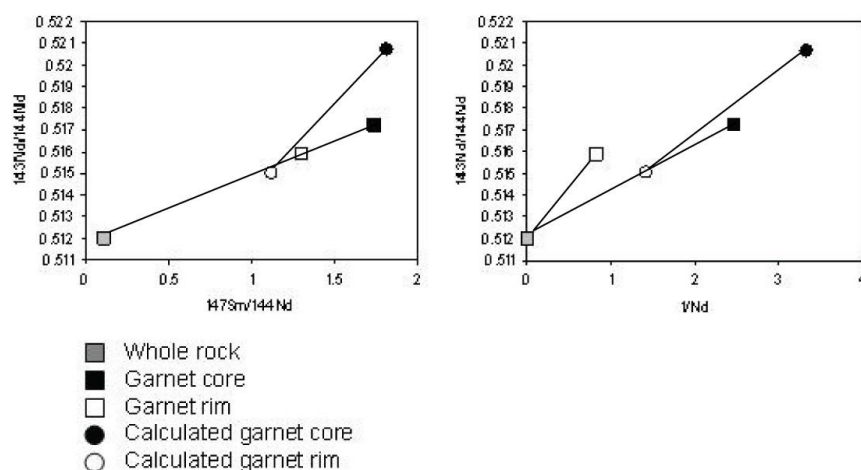


Figure 5-29, $^{147}\text{Sm}/^{144}\text{Nd}$ vs $^{143}\text{Nd}/^{144}\text{Nd}$ and $^{147}\text{Sm}/^{144}\text{Nd}$ vs $1/\text{Nd}$ for AB07-13. The filled black square is the measured garnet core fraction, the empty black square is the garnet rim fraction, the grey square is the measured whole rock fraction, the filled black circle is a hypothetical 780 Ma garnet core end member and the empty circle is a hypothetical 465 Ma end member. The end members are based on the ages of monazite inclusions within a garnet from close to this sample (Cutts et al. 2010).

The Drumnadrochit Amphibolite (AB07-14) gave a Lu-Hf three point isochron age of 474.8 ± 1.2 Ma with an MSWD of 0.9 (Figure 30). The garnet fractions have ID Hf concentrations of 0.464 ppm and 0.491 ppm which is quite similar to the value obtained from LA ICPMS of ~ 0.23 ppm. This suggests that zircon inclusions have little effect on the Lu-Hf age. The Lu profile from LA ICPMS shows that this age is a prograde garnet growth age. The Drumnadrochit Amphibolite (AB07-14) gave a Sm-Nd three point isochron age of 471.0 ± 1.5 Ma (Figure 31). The Nd concentrations from the MC ICPMS of 0.555 ppm and 0.821 ppm are similar to the concentration obtained from the LA ICPMS of ~ 0.65 ppm, suggesting that this age has not been affected by Nd-rich inclusions.

The Mull Amphibolite (AB07-30) yields a Lu-Hf three point isochron which gives an age of 448.7 ± 5.0 Ma (Figure 30). There is no LA ICPMS from this sample making it impossible to compare the concentrations from MC ICPMS and LA ICPMS, however as the sample is an amphibolite it is expected that there would be little effect from zircon inclusions. This sample did not give a meaningful Sm-Nd age as the Nd concentrations from the garnet fractions were quite high (12.480 ppm and 16.537 ppm) indicating a large influence from inclusions (Figure 31). Although

there was a significant difference between the garnet fractions and the whole rock fraction $^{147}\text{Sm}/^{144}\text{Nd}$ ratios, the $^{143}\text{Nd}/^{144}\text{Nd}$ for the garnet fractions were either almost within error or less than the whole rock ratio.

5.6.3 The Strathy Complex and the Naver Nappe

A three point Lu-Hf isochron was obtained from the Strathy Complex (AB07-21) using two garnet fractions and a whole-rock fraction, the age obtained was 446 ± 13 Ma (Figure 30). This sample had unusually Lu concentrations (0.590 ppm and 0.618 ppm) which has lead to low $^{176}\text{Lu}/^{177}\text{Hf}$ ratios, which may account for the large errors on the age calculated. It is unclear why this sample had such low garnet Lu contents and since there is no LA ICPMS data it is impossible to compare the ID and pure garnet concentrations. Sm-Nd from this sample gave a three point isochron age of 432.9 ± 1.8 Ma with an MSWD of 1.9 (Figure 31). The Nd concentrations from the garnet fractions are fairly low (1.223 ppm and 0.845 ppm) suggesting that this age has not been influenced by inclusions.

Two individual two point isochron ages were obtained for AB07-22 of 466.0 ± 2.1 Ma (AB07-22 Grt 1) and 453.9 ± 4.1 Ma (AB07-22 Grt 2), which are 7.9 Ma outside of error, the three point isochron is shown in Figure 30. AB07-22 Grt 1 gives the more reliable of the two ages as it is more radiogenic, it is also the least affected by inclusions of the two ages. Using the zircon modelling described in Chapter 2 and a 1400 Ma zircon, the zircon inclusions potentially could add ~ 31 Ma to AB07-22 Grt 2 and 26 Ma to AB07-22 Grt 1. The pure garnet has a Hf concentration of ~ 0.18 ppm (LA ICPMS), while ID Grt 1 and Grt 2 give Hf concentrations of 3.122 ppm and 3.937 ppm. The Naver nappe garnetiferous gneiss (AB07-22) gave one reasonable Sm-Nd age of 531 ± 7 Ma from Grt 2 (the three point isochron is shown in Figure 31). The pure garnet from this sample gave a Nd concentration by LA ICPMS of 0.532 ppm which is lower than the Nd concentration obtained from ID from Grt 2 (4.139 ppm), suggesting that some Nd-rich inclusions were incorporated in the dissolved garnet fraction. Grt 1 from this sample gave an Nd ID concentration of 24.892 ppm which has clearly been affected by inclusions giving a lower $^{147}\text{Sm}/^{144}\text{Nd}$ ratio than the whole rock, and an age of 1195.8 ± 180 Ma which is geologically meaningless.

5.6.4 The Dava Succession and the Dalradian Supergroup

A Lu-Hf two point garnet-whole-rock age from the Dava Amphibolite (AB07-23) gave an age of 463.2 ± 1.6 Ma. LA ICPMS is not available for this sample, thus it is difficult to determine the effect of inclusions on the age. However, the Hf concentration is low (0.130 ppm) suggesting little effect from zircon inclusions. Sm-Nd from this sample gave a two point isochron age of 431.2 ± 6.5 Ma, which may represent cooling. The $^{143}\text{Nd}/^{144}\text{Nd}$ ratios from the garnet and the whole rock are reasonably close together suggesting that this age should be considered with caution. As there is no LA ICPMS for this sample it is impossible to compare the pure garnet with that measured using MC ICPMS, however the Nd and Hf are both low, suggesting little influence from inclusions (0.846 ppm and 0.130 ppm respectively).

The Leven Schist (AB07-27) gave a Lu-Hf two point age of 470.8 ± 2.2 Ma. The pure garnet from this sample gave an Hf concentration of 0.527 ppm, the ID gave a concentration of 2.145 ppm suggesting that the age has been affected by inclusions. Using the modelling described above the maximum effect of zircon inclusions on this sample (using 1000 Ma zircons) is 13.0 Ma. This sample did not yield a reasonable Sm-Nd age as the ID Nd concentration was 20.791 ppm, which the pure garnet was ~0.34 ppm, suggesting a large effect from Nd-rich inclusions.

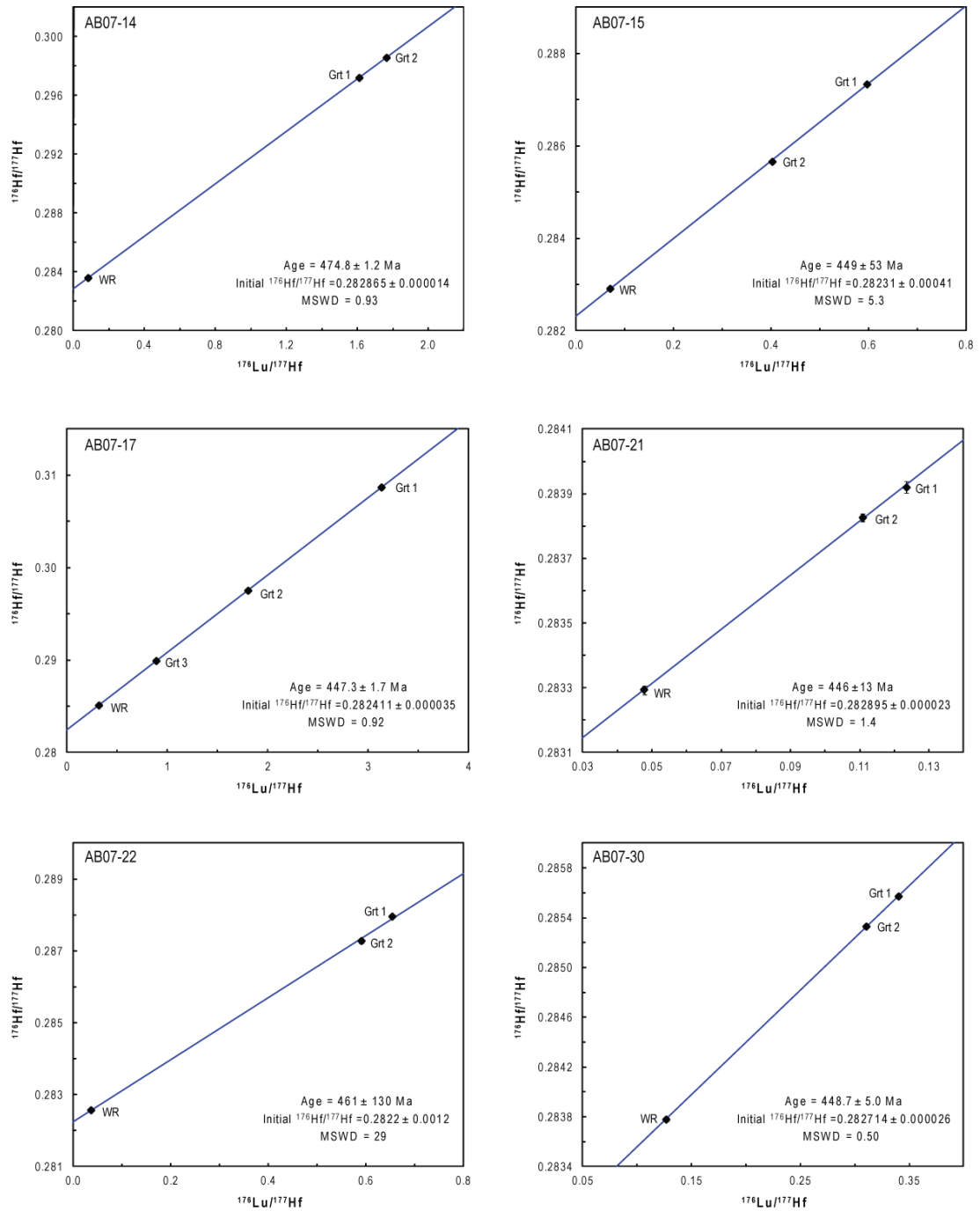


Figure 5-30 showing isochron diagrams for all samples which gave a three point or more Lu-Hf age. The garnet fractions are labelled and the whole rock is indicated by WR. Error bars are included on the diagram but in most cases they are smaller than the symbol.

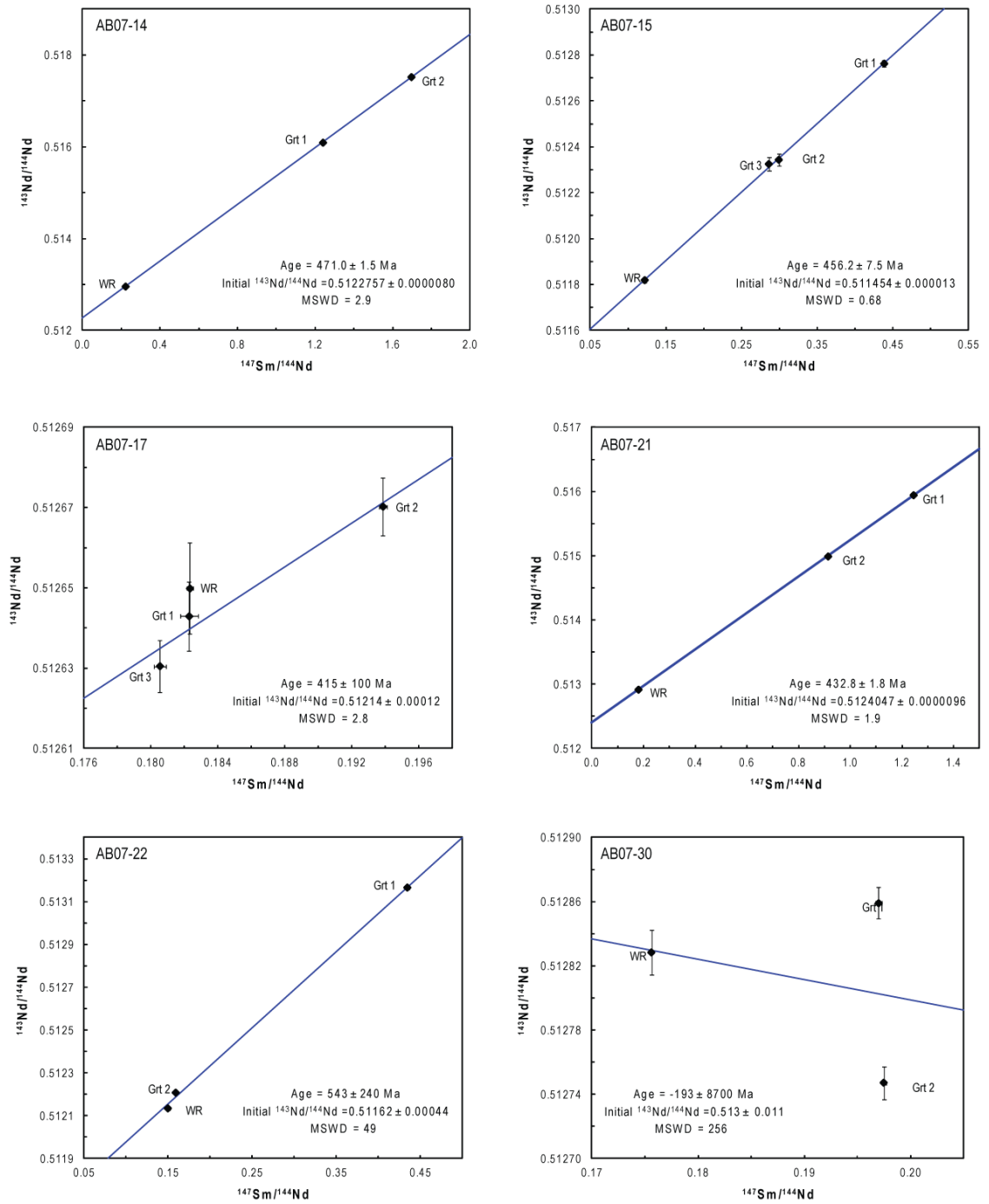


Figure 5-31 showing isochron diagrams for all samples which gave a three point or more Sm-Nd age. The garnet fractions are labelled and the whole rock is indicated by WR. Error bars are included on the diagram but in most cases they are smaller than the symbol.

Table 5-1; Lu - Hf Garnet Analyses Results for samples which gave Caledonian ages. Ages marked with an * are interpreted to be not geologically meaningful.

Sample fraction	Lu ppm	Hf ppm	$^{176}\text{Hf}/^{177}\text{Hf}$	2se	$^{176}\text{Lu}/^{177}\text{Hf}$	Initial $^{176}\text{Hf}/^{177}\text{Hf}$	Lu-Hf Age (Ma)	MSWD
<i>Moine Nappe</i>								
AB07-08 Grt Core	1.945	2.493	0.283173	0.000015	0.1103	0.281956	588.9 ± 17	
AB07-08 Grt Rim	4.053	1.864	0.284705	0.000015	0.3074	0.28207	458.7 ± 4.5	
AB07-08 WR	0.556	1.760	0.282448	0.000015	0.0446			
AB07-11 Grt	4.749	1.700	0.285343	0.000012	0.3949	0.28190	466.2 ± 2.9	
AB07-11 WR	0.488	1.928	0.282207	0.000012	0.0357			
AB07/15 Grt 1	8.829	2.096	0.287332	0.000016	0.596	0.28232	449.3 ± 1.9	
AB07-15 Grt 2	5.967	2.102	0.285660	0.000012	0.4015	0.28228	443.1 ± 4.8	
AB07-15 WR	0.565	1.137	0.282911	0.000016	0.0703			
AB07-17 Grt 1	2.074	0.0939	0.308709	0.000064	3.135			
AB07-17 Grt 2	1.700	0.133	0.297521	0.000045	1.805			
AB07-17 Grt 3	1.548	0.246	0.289866	0.000016	0.891			
AB07-17 WR	0.422	0.188	0.285081	0.000036	0.317	0.28241	447.3 ± 1.7	0.92
AB08-02 Grt Core	2.449	0.977	0.285323	0.000012	0.3545	0.28252	422.0 ± 5.2	
AB08-02 Grt Rim	1.778	0.729	0.285366	0.000018	0.3450	0.28250	443.1 ± 6.0	
AB08-02 WR	0.259	0.754	0.282906	0.000017	0.0484			
<i>Sgurr Beag Nappe</i>								
AB07-05 Grt	3.321	0.237	0.300118	0.000033	1.983	0.28292	462.9 ± 1.8	
AB07-05 WR	1.093	1.069	0.284175	0.000015	0.145			
AB07-13 Grt 1	-	-	-	-	-	-	-	
AB07-13 Grt 2	-	-	-	-	-	-	-	
AB07-13 WR	-	-	-	-	-	-	-	
AB07/14 Grt 1	5.281	0.464	0.297218	0.000019	1.612			
AB07/14 Grt 2	6.116	0.491	0.298543	0.000018	1.764			
AB07/14 WR	0.981	1.685	0.283597	0.000013	0.0823	0.28288	474.8 ± 1.2	0.93
AB07-30 Grt 1	3.573	1.485	0.285569	0.000015	0.340			
AB07-30 Grt 2	3.436	1.563	0.285330	0.000012	0.311			
AB07-30 WR	1.067	1.188	0.283780	0.000015	0.127	0.282714	448.7 ± 5.0	0.5
<i>Strathy Complex</i>								
AB07/21 Grt 1	0.618	0.708	0.283919	0.000018	0.123			
AB07-21 Grt 2	0.590	0.752	0.283827	0.000012	0.111			
AB07/21 WR	0.241	0.713	0.283293	0.000013	0.0477	0.282895	446.0 ± 13.0	1.4
<i>Naver Nappe</i>								

AB07/22 Grt 1	14.435	3.122	0.287956	0.000013	0.654	0.282247	466.0 ± 2.1
AB07-22 Grt 2	16.417	3.937	0.287270	0.000012	0.590	0.282256	453.9 ± 4.1
AB07/22 WR	2.077	8.023	0.282567	0.000013	0.0366		
<i>Dava & Grampian</i>							
AB07/23 Grt	1.838	0.130	0.300190	0.000025	2.003	0.282815	463.2 ± 1.7
AB07/23 WR	0.684	0.664	0.284078	0.000013	0.146		
AB07/27 Grt	5.752	2.145	0.285633	0.000013	0.379		
AB07/27 WR	0.965	3.640	0.282620	0.000013	0.0375	0.282290	470.8 ± 3.2

Table 5-2; Sm - Nd Garnet Analyses Results for samples which gave Caledonian ages. Ages marked with an * are interpreted to be not geologically meaningful.

Sample fraction	Sm	Nd	$^{143}\text{Nd}/^{144}\text{Nd}$	2se	$^{147}\text{Sm}/^{144}\text{Nd}$	Initial $^{143}\text{Nd}/^{144}\text{Nd}$	Sm-Nd Age (Ma)	MSWD
<i>Moine Nappe</i>								
AB07-08 Grt Core	0.499	0.234	0.515216	0.000016	1.289	0.51142	449.7 ± 2.3	
AB07-08 Grt Rim	3.051	15.540	0.511753	0.000009	0.1187	0.51177	-20.0 ± 330*	
AB07-08 WR	8.522	45.558	0.511753	0.000009	0.1131			
AB07-11 Grt	3.657	19.006	0.511728	0.000010	0.1163	0.51125	627.6 ± 260*	
AB07-11 WR	9.309	51.611	0.511698	0.000008	0.1090			
AB07-15 Grt 1	0.327	0.451	0.512762	0.000013	0.4382	0.51145	456.0 ± 7.6	
AB07-15 Grt 2	0.210	0.424	0.512343	0.000027	0.2994	0.51146	451.4 ± 24	
AB07-15 Grt 3	0.331	0.701	0.512324	0.000030	0.2859	0.51144	471.5 ± 29	
AB07-15 WR	3.027	15.006	0.511818	0.000009	0.12195	0.51148	456.2 ± 7.5	0.68
AB07-17 Grt 1	5.627	18.844	0.512630	0.000006	0.181			
AB07-17 Grt 2	2.955	9.217	0.512670	0.000007	0.194			
AB07-17 Grt 3	5.151	17.085	0.512643	0.000009	0.182			
AB07-17 WR	3.498	11.600	0.512650	0.000011	0.182	0.51218	396.0 ± 430*	2.8
AB08-02 Grt Core	3.842	15.098	0.512513	0.000011	0.154	0.51188	624.5 ± 130*	
AB08-02 Grt Rim	3.212	11.794	0.512520	0.000013	0.165	0.51209	402.2 ± 84*	
AB08-02 WR	7.376	32.064	0.512453	0.000007	0.139			
<i>Sgurr Beag Nappe</i>								
AB07-05 Grt	1.503	7.000	0.512707	0.000007	0.130	0.51206	766.4 ± 37*	
AB07-05 WR	10.244	33.498	0.512984	0.000007	0.185			
AB07-13 Grt Core	2.549	1.186	0.515853	0.000024	1.300	0.51158	501.7 ± 3.4	
AB07-13 Grt Rim	1.160	0.403	0.517202	0.000036	1.742	0.51159	491.9 ± 3.5	
AB07-13 WR	14.674	77.472	0.511958	0.000011	0.114			

AB07-14 Grt 1	1.554	0.555	0.517513	0.000015	1.695	0.51228	471.7 ± 1.7	
AB07-14 Grt 2	1.683	0.821	0.516092	0.000016	1.241	0.51228	469.1 ± 2.7	
AB07-14 WR	6.180	16.819	0.512962	0.000007	0.222	0.51228	471.0 ± 1.5	2.9
AB07-30 Grt 1	5.384	16.527	0.512859	0.000000	0.197	0.51258	219.6 ± 120*	
AB07-30 Grt 2	4.076	12.480	0.512747	0.000010	0.197	0.51348	-569.8 ± 120*	
AB07-30 WR	10.329	35.563	0.512828	0.000014	0.176			
<i>Strathy Complex</i>								
AB07-21 Grt 1	1.740	0.845	0.515939	0.000010	1.246	0.51241	432.9 ± 1.8	1.9
AB07-21 Grt 2	1.850	1.223	0.514987	0.000018	0.915			
AB07-21 WR	1.833	6.141	0.512917	0.000008	0.180			
<i>Naver Nappe</i>								
AB07-22 Grt 1	6.165	24.892	0.512133	0.000008	0.150	0.51096	1195.8 ± 180*	
AB07-22 Grt 2	2.974	4.139	0.513165	0.000010	0.434	0.51165	531.4 ± 7.0	
AB07-22 WR	12.544	47.667	0.512207	0.000008	0.159			
<i>Dava & Grampian</i>								
AB07-23 Grt	0.720	0.846	0.513924	0.000011	0.515	0.51247	431.2 ± 6.5	
AB07-23 WR	4.990	14.979	0.513037	0.000008	0.201			
AB07-27 Grt	3.757	20.791	0.511914	0.000009	0.109	0.51132	830.1 ± 250*	
AB07-27 WR	12.606	65.134	0.511957	0.000009	0.117			

5.7 Discussion

5.7.1 Timing of the Mid-Ordovician event

Sgurr Beag and Naver Nappes

The previous U-Pb (SIMS) zircon ages of 467 ± 10 Ma and 461 ± 13 Ma obtained from migmatites of the Naver nappe provided clear evidence of regional migmatization that was assigned to the Grampian orogenic event (Kinny et al. 1999). The older of the new Lu-Hf ages from the Naver nappe garnetiferous gneiss of 466.0 ± 2.1 Ma complements these ages very well and the younger age is within error of the ages from Kinny et al. (1999), providing more evidence of peak metamorphism during the Mid-Ordovician event in the Naver Nappe. This age is nearly identical to a U-Pb (SIMS) zircon age of 463 ± 4 Ma obtained from a syn-kinematic pegmatite within the eastern Moine rocks of Glen Urquhart (Cutts et al. 2010). The outer rims of garnets within nearby Moine gneisses in this area contain monazites that have yielded a U-Pb LA-ICP-MS age of 464 ± 3 Ma (Cutts et al. 2010). The age from the

Naver Nappe is within error of the Lu-Hf age from the Loch Quoich Amphibolite (AB07-05), which would suggest that the Sgurr Beag Nappe and the Naver Nappe share the same Mid-Ordovician event. A few kilometres further south, titanites from the Fort Augustus granite gneiss yielded a U-Pb age of 470 ± 2 Ma (Rogers et al. 2001), which is similar to the Drumnadrochit Amphibolite ages (Lu-Hf = 474.8 ± 1.2 Ma, Sm-Nd = 471.0 ± 1.2 Ma) obtained in this study. The Drumnadrochit Migmatite (AB07-13) gave two Sm-Nd ages of 501.7 ± 3.4 Ma and 491.9 ± 3.5 Ma which are probably mixed ages between a ~ 780 Ma core and a ~ 465 Ma rim as dated by Cutts et al. (2010).

Morar Group

Two samples from the Moine Nappe gave Mid-Ordovician garnet growth ages, the Lu-Hf garnet rim age from the Basal Pelite (AB07-08) which was 458.7 ± 4.5 Ma and the Armadale Pelite (AB07-11) which gave an age of 466.2 ± 2.9 Ma. Although as mentioned previously the Lu-Hf rim age from AB07-08 is not very radiogenic and depends on the effect from the zircon inclusions so should be used with caution, the age from AB07-11 is meaningful. The garnets from AB07-11 are syn-kinematic and could potentially date movement on the Moine Thrust Zone. This contrasts with an age of 431.1 ± 1.2 Ma from the Loch Borrolan early suite which is syn-kinematic and an age of 429.2 ± 0.5 Ma from the Loch Borrolan Late suite which is post-kinematic (Goodenough et al. 2010). However, it is unlikely that these ages date the main phase of movement as the deformation within the Loch Borrolan early suite is not large; it is more likely that this is movement ceased, or relates to a later small pulse. Thus the ~ 460 Ma ages from close to the Moine Thrust could date early movement, suggesting that there was perhaps as much as 30 Myr of movement on the Thrust Zone. These ages also suggest that the Morar Group was affected by the Grampian event.

The Dava Succession and the Grampian terrane

The mineral ages obtained for the Mid-Ordovician event in the Northern Highland terrane are similar to the published ages for the Grampian event in the Dalradian Supergroup east of the Great Glen Fault (Figure 5-7). Within the Dalradian rocks of NE Scotland, the Grampian event is constrained by a U-Pb zircon age of 472 ± 3 Ma

for the syn-D₂ Portsoy gabbro (Oliver et al. 2000) and a U–Pb monazite age of 470 ± 1 Ma for the syn-to-post tectonic Aberdeen granite (Kneller & Aftalion 1987). Both are within error of a Sm–Nd age of 472.9 ± 2.9 Ma obtained from syn-tectonic garnets in Glen Clova (Baxter et al. 2002). The Grampian orogenic event in western Ireland also occurred at c. 470 Ma as indicated by U–Pb zircon ages obtained from the syn-tectonic Currywongaun (475 ± 1 Ma) and Cashel (470 ± 1 Ma) gabbros in Connemara (Friedrich et al. 1999). The Lu–Hf ages obtained from the Leven Schist (AB07-27) and the Dava Amphibolite (AB07-23) are in good agreement with the previously published dates. This shows that the Grampian event was shared by much of the Moine Supergroup. These ages could also indicate that there is no systematic effect from zircon inclusions, as both the Lu–Hf and Sm–Nd ages agree with each other and with U–Pb ages.

5.7.2 Implications of Late Ordovician garnet growth

Lu–Hf ages of 449.3 ± 1.2 Ma and 448.0 ± 1.7 Ma were obtained from garnets in the Talmine Pelite (AB07-15) and a Ben Hope Sill suite amphibolite (AB07-17). The Talmine Pelite (AB07-15) also gives a Sm–Nd three point isochron age of 456.2 ± 7.5 Ma. Within error of these ages is a Lu–Hf age from the Mull Amphibolite (AB07-30) of the Glenfinnan Group below the Sgurr Beag Thrust (gave an age of 449.7 ± 2.3 Ma). These ages provide evidence for a hitherto unrecognised Late Ordovician metamorphic event within the Moine Supergroup, underlying the Sgurr Beag Thrust. This event postdates peak Grampian metamorphism in the Naver nappe by c. 17 Ma, and predates Scandian nappe stacking and associated deformation within the Moine nappe by at least 13 Ma. The following discussion centres on the likely geotectonic significance of this metamorphic event and its expression within the Morar Group and other parts of the Moine Supergroup.

It might be argued that the Late Ordovician metamorphism is the result of a Grampian event that was rather more prolonged than currently thought. However, all the evidence from the Dalradian Supergroup indicates that the Grampian event was relatively short-lived (<7–8 Ma?) and followed rapidly by a change from oceanward to continent-directed subduction and development during the Arenig of an accretionary prism in the Southern Upland terrane (Figure 5-1 ; Dewey & Ryan 1990). The continuous record of sedimentation within the accretionary prism

through into the Wenlock precludes any further accretionary event along this part of the Laurentian margin until the collision with Avalonia in the Silurian-Devonian (Soper & Woodcock 1990). General considerations also support the notion that arc-continent collisions tend to be relatively short-lived events (Dewey 2006). Accordingly, it seems unlikely that these Late Ordovician ages can be attributed to the Grampian arc-continent collision. The possibility that they represent cooling following the Grampian event is highly unlikely due to the similarity of the Lu-Hf and Sm-Nd ages from the Talmine pelite. It is also unlikely that they represent influence from inclusions as all the samples are within error. In addition, two of the samples are amphibolites (the Ben Hope Sill and the Mull Amphibolite) and two are garnet mica schists (the Talmine Pelite and the Basal Pelite), thus have extremely different zircon and monazite inclusion populations and Zr and Nd contents, showing that the shared age is unlikely to be from influence from inclusions. The commonly observed differences between Lu-Hf and Sm-Nd ages is interpreted to reflect differences in closure temperature between the two systems (Ganguly & Tirone 1999; Ganguly et al. 1998; Lapen et al. 2003), as the ages from the Talmine pelite are within error this suggest that the garnet went through closure of both systems in a relatively short time.

The Scandian event is associated with northwesterly-directed displacement of the migmatites on the Naver Thrust, accompanied by widespread deformation of the underlying Morar Group as far south as Loch Duich and lower parts of the Naver nappe. The deformation is thought to be accompanied by amphibolite facies metamorphism (Strachan & Holdsworth 1988; Holdsworth 1989; Holdsworth et al. 2001; Strachan, unpublished data), estimated to have occurred at 5-6 kbar and 600-650°C (Friend et al. 2000), dated at 435-420 Ma (Kinny et al. 2003). The Mid-Ordovician garnet growth ages show that the Scandian, if present, is unlikely to have reached 600°C throughout the whole of the Moine Nappe as these garnets record ~448 Ma ages instead of 435-420 Ma ages associated with the Scandian. ~448 Ma ages have been recorded in the Moine Nappe of north Sutherland, close to the Moine Thrust in the SW Moine and in the Glenfinnan Group on Mull where the Sgurr Beag thrust is absent.

A correlation can be drawn between the northern Morar Group and the Laurentian-derived Uppermost Allochthon in west Norway, which contains evidence for a complex series of Ordovician accretionary events which occurred over a much longer time span than the Grampian event but significantly predated the final Scandian collision of Baltica and Laurentia (Roberts 2003, 2007). These events culminated in eclogite facies metamorphism at c. 450 Ma (Corfu et al. 2003), followed by rapid exhumation and development of a Late Ordovician to Silurian successor basin in the northern part of the Uppermost Allochthon (Roberts et al. 2003). The ages that Corfu et al. (2003) obtained from zircons and titanites from an eclogite within the Uppermost Allochthon are within error of the Late Ordovician metamorphic event now recognised in the Moine Supergroup, thus suggesting that the Northern Highland terrane appears to record a Caledonian history that has more in common with the Laurentian-derived rocks of Baltica than with the Grampian terrane of Scotland.

5.7.3 Scandian garnet growth

Within this study only one sample yielded a convincing Scandian age, the Strathy Complex Amphibolite. The Vaich Pelite gave two Lu-Hf ages which appear Scandian, the core age was 422.0 ± 5.2 Ma and from the rim the age was 443.1 ± 6.0 Ma. However, as mentioned earlier the garnets from this sample were not overly radiogenic and the ages should be used with caution. They show that there was some garnet growth related to the Caledonian but whether the growth relates to Grampian, ~448 Ma or Scandian metamorphism is impossible to tell.

5.7.4 Textural relations within the Moine Supergroup

The S_2 and L_2 fabrics developed throughout the Morar Group in north Sutherland are assigned to the Scandian orogenic event on the basis that they are present within syn- D_2 metagranites that have yielded Silurian U-Pb zircon ages of c. 435-420 Ma (Kinny et al. 2003a; Alsop et al 2010). However the errors on these ages are significant and in two of the three samples analysed large enough to include ~448 Ma ages, which could suggest that the Late Ordovician event is the cause for the S_2 and L_2 fabrics within the Moine Nappe. Another possibility is that it resulted in the D_1 folds and S_1 schistosity. Contrasting these scenarios is a preliminary U-Pb zircon

Neoproterozoic age (~575 Ma) from an undeformed metagabbro that intrudes the Morar Group of the Moine nappe east of the Kyle of Tongue (Kinny & Strachan pers comm., quoted in Strachan et al. 2010b). In this light, D₁ is probably assignable to the mid-Neoproterozoic Knoydartian orogenic event that has been documented elsewhere within the southern part of the Morar Group in northern Scotland (Rogers et al. 1998; Vance et al. 1998). An alternative solution that deserves consideration is that the D₂ folds within the Morar Group are composite in origin. These structures may have initially developed as tight to open structures during the Late Ordovician event, and were later strongly modified into their present tight-to-isoclinal, sheath-like geometry during intense shear associated with Scandian nappe stacking. Further structural and textural analysis is needed to resolve this question.

Recognition of Late Ordovician metamorphism within the Morar Group in north Sutherland prompts the re-examination of published isotopic data from elsewhere in the Moine Supergroup. Swarms of variably deformed trondjhemitic pegmatites intrude the high-grade Moine rocks of the Glenfinnan Group in Inverness-shire and Ross-shire. These were once thought to be linked to regional migmatisation but it now seems clear on structural grounds that the migmatites and the pegmatites are of quite different ages. Regional migmatisation most probably occurred during the Neoproterozoic (Knoydartian) and the pegmatites cut folds and fabrics that plausibly formed during either the Knoydartian or Grampian events (Cutts et al. 2010). Two pegmatites near Glenfinnan have yielded ages of 445 ± 10 Ma (Rb-Sr muscovite) and 450 ± 10 Ma (monazite bulk fractions) (van Breemen et al. 1974), however these results are imprecise and could record typical Grampian or Scandian ages. A more precise age comes from the Glen Dessary syenite pluton which was intruded into the Moine rocks of Inverness-shire at 447.9 ± 2.9 Ma (U-Pb zircon, Goodenough et al. 2010), which is within error of the Late Ordovician ages of this study. F₃ folds within the pluton have been dated at 442 ± 7 Ma by van Breemen et al. 1979. The wider significance of these intrusions has been difficult to understand in the context of a two-phase Grampian-Scandian tectonic model. However, it now seems entirely possible that they are genetically related to the Late Ordovician event, similar to the way that the Loch Loyal, Borrolan and Loch Ailsh syenites are interpreted to be related to the Scandian event.

Johnson & Strachan (2006) drew attention to the synchronicity of Scandian thrusting in Sutherland with Barrovian metamorphism to amphibolite facies. This is difficult to reconcile with theoretical studies that indicate that there would not have been sufficient time to generate the high metamorphic temperatures during a thrusting event that lasted no longer than 18 Ma and probably rather less. Accordingly, they suggested that a plausible explanation for the heat source was that it resulted from a 20-25 myr period of crustal heating in a back-arc setting between the Grampian and Scandian orogenic events. Thus most of the orogenic heat came from the pre-existing back-arc rather than the orogenic process itself. The new evidence reported here rather suggests a different conclusion: the Scandian metamorphic temperatures were in part 'inherited' from the Late Ordovician event.

5.7.5 Relationship between Northern Highland and Grampian terranes during the Silurian

There is no evidence within the Grampian terrane for regionally significant Silurian metamorphism and ductile deformation. This has prompted the suggestion that during the Silurian it was far removed from the location of the Scandian collision between Baltica and the sector of the Laurentian margin that contained the Northern Highland terrane (Coward 1990; Dallmeyer et al. 2001; Dewey & Strachan 2003; Kinny et al. 2003a). Thus Dewey & Strachan (2003) suggested that juxtaposition of the Grampian and Northern Highland terranes resulted from a late Silurian to early Devonian sinistral movement of 500-700 km along the Great Glen-Walls Boundary Fault. In contrast to this are the significantly more modest Great Glen Fault displacement estimates of <200 km implied by correlation of the 'Newer Granite' suite high Ba-Sr plutons across the Great Glen Fault (Thirlwall 1989) and from palaeomagnetic studies (Briden et al. 1984). If limited movement along the Great Glen Fault is correct, then the lack of Scandian deformation and metamorphism within the Grampian terrane could be explained by Scandian deformation diminishing southwards and a lower temperature for the Scandian event. The data presented here does not reflect the widespread 430-435 Ma high temperature Scandian event suggested within the literature, the only convincing Scandian garnet age within this study is from the Strathy Complex which has been faulted into the surrounding Moine, thus its relationship with the Moine is unresolved. This could

suggest that the Scandian event in the Northern Highland terrane was not characterised by temperatures high enough to reset the Lu-Hf and Sm-Nd systems within the garnets of either the Moine or Naver nappes, despite the latter being small garnets. The apparent restriction of the Late Ordovician garnet ages to the Northern Highland terrane could however reinforce the suggestion of a large displacement along the Great Glen Fault.

5.8 Conclusions

1. Within the Northern Highland terrane of the Scottish Caledonides, Lu-Hf ages of 466.0 ± 2.1 Ma and 453.9 ± 4.1 Ma have been obtained from prograde garnet in Moine gneisses of the Naver nappe in Sutherland. This confirms a Mid-Ordovician age for high-grade metamorphism and migmatization, and complements the previously published U-Pb zircon (SIMS) data (Kinny et al. 2003). The Glenfinnan Group migmatites at Drumnadrochit give Mid-Ordovician ages which are also interpreted to relate to migmatisation (Cutts et al. 2010). A similar age is also recorded further west in the Glenfinnan Group within the Loch Quoich Amphibolite (AB07-05).
2. The mineral ages obtained for the Mid-Ordovician event in the Northern Highland terrane are slightly younger than published datasets for arc-continent collision in the Grampian terrane east of the Great Glen Fault. This might indicate that the Northern Highland terrane was located further inboard from the arc-continent suture, or result from diachroneity of metamorphism along the strike of the Laurentian margin.
3. The Mid-Ordovician age that was obtained from syn-kinematic garnets from close to the Moine Thrust could date thrust movement, which suggests there may have been 30 Myr of movement with the U-Pb ages from the Loch Borrolan Complex marking the younger limit of movement (Goodenough et al. 2010). This age also demonstrates that the Grampian event affected the Morar Group.

4. Distinctively younger Lu-Hf ages have been obtained from prograde garnets within the structurally underlying Moine rocks of the Moine nappe and the Glenfinnan Group on Mull which has not been affected by the Sgurr Beag Thrust. Lu-Hf ages of 449.3 ± 1.2 Ma (Talmine Pelite), 447.2 ± 1.7 Ma (Ben Hope Sill amphibolite), 449.9 ± 5.4 Ma (Mull Amphibolite), the Sm-Nd core age of 449.7 ± 2.3 Ma (Basal Pelite) and the three point Sm-Nd age of 456.2 ± 7.5 Ma (Talmine) provide evidence for a hitherto unrecognised Late Ordovician regional metamorphic event. This event postdates peak metamorphism in the Naver nappe by c. 17 myr, and predates Silurian (Scandian) nappe stacking and associated deformation by at least 13 myr. The existing two-stage Grampian-Scandian model for Caledonian orogenesis in northern Scotland is thus overly-simplistic. The new Late Ordovician metamorphic ages also demonstrate that the Scandian did not reach mid to high amphibolite facies throughout the whole Moine Supergroup.
5. The apparent restriction of the Late Ordovician and Silurian events to the Northern Highland terrane could reinforce the suggestion that it was far removed from the Grampian terrane until the two were juxtaposed following major end-Caledonian sinistral displacement along the Great Glen Fault. The Laurentian-derived Uppermost Allochthons of Norway contain a very similar, protracted record of Ordovician accretion-related metamorphism that significantly predates Silurian continent-continent collision and closure of the Iapetus Ocean. The Caledonian history of the Northern Highland terrane thus has more in common with the Laurentian-derived rocks of Baltica than the Grampian terrane in Scotland.

6.1 Synopsis

This chapter demonstrates that the age of the migmatisation of the Yell Sound Group is between 469 Ma and 478 Ma, and is related to the Grampian orogeny. A significantly younger Lu-Hf age of 450.9 Ma from the rim of a garnet in the North Roe Schist, west of the Walls Boundary Fault, is within error of the Mid-Ordovician ages from the western part of the Moine Supergroup of the Scottish mainland. This could possibly be related to the formation of the Sand Voe Schuppen zone. Two ages from possible basement gneisses at Migga Ness within the Hascosay Slide of 857 Ma and 863 Ma show that these lithologies were affected by Neoproterozoic deformation and metamorphism. This suggests that that these units can be correlated in a broad sense with the lower parts of the Moine Supergroup (Morar Group) and the Krummedal Succession. The ages do not show whether Migga Ness is a part of the basement or more simply an intrusion, analyses of zircons would show definitively the age of the protolith.

6.2 Introduction

The pre-Devonian rocks in Shetland are the most northerly outcrops of the Caledonian orogen in the British Isles and have been correlated with the Moine and Dalradian supergroups of mainland Scotland (e.g Flinn et al. 1972; Flinn 1988). However, when compared to the Northern Highland and Grampian terranes and other parts of the north Atlantic Caledonides, Shetland has had relatively little geochronological work undertaken to attempt to ascertain the conditions of tectonism or deformation or evaluate the potential linkages with the Moine or Dalradian supergroups. This chapter reports the results of a preliminary geochronological study carried out on three samples from the metasedimentary rocks of the Yell Sound Group and one sample from potential basement in Shetland to determine the dominant phase of deformation and metamorphism.

6.3 Geological setting and previous geochronology

Within Shetland there are proposed equivalents of the Moine and Dalradian supergroups. Moine-like rocks are found on both sides of the Walls Boundary Fault (Figure 6-1), on the east of the fault, the Moine rocks make up most of Yell and part of Lunna Ness. They are known as the Yell Sound Group (formerly Yell Sound Division, Flinn 1988; Flinn 2007) and are dominated by psammitic gneisses with basement inliers. The basement inliers have been broadly correlated with the Lewisian Gneisses of the Caledonian Foreland and are thought to represent parts of the basement to the Yell Sound Group (Flinn 1988). The Yell Sound Group is the proposed equivalent of the Glenfinnan Group of the Northern Highlands as the psammitic gneisses contain layers of metapelites with garnet, kyanite and staurolite, indicating a higher grade metamorphism than the Morar or Loch Eil groups. There are also no signs of any preserved cross bedding, unlike the Morar or Loch Eil groups. The sequence is disrupted by the Nesting Fault which gives rise to some repetition of the Yell Sound Group sequence, and bound to the east by the Boundary Zone. The Boundary Zone is a tectonically complex zone which separates the Yell Sound Group from the Dalradian Supergroup; it outcrops on the eastern edge of Yell, and the western edges of Unst and Fetlar. Within the Boundary Zone are a series of gneissic, ultramafic rocks and marbles which are known as the Westing Group. Zircon and monazite from two metasediments samples within the Westing Group have been dated using LA ICPMS U-Pb and gave ages of 938 ± 8 Ma and 925 ± 10 Ma which date amphibolite facies metamorphism at temperatures of 650°C and pressures of 7 kbar (Cutts et al. 2009). This suggests that the Westing Group can be correlated with the Krummedal Succession of East Greenland and the Morar Group of the Moine Supergroup (Cutts et al. 2009; Chapter 5). Within the Boundary Zone of Yell is the Hascosay Slide which is made up of hornblendic gneisses which are thought to be similar to the Lewisian Gneisses. The Hascosay Slide is thought to be a thrust structure (Flinn 1988). Immediately to the west of the Hascosay Slide in north east Yell is the Valyre Gneiss, which is a microcline augen gneiss. The Valyre Gneiss represents a zone of intense shearing as it has a blastomylonitic texture; there are several more of these zones throughout Shetland.

Recent U-Pb monazite dating by Cutts et al. (in press) has yielded one age from within the Dalradian Supergroup equivalents of 470 ± 5 Ma and one age from the Yell Sound Group on Yell of 451 ± 4 Ma and three ages from the Yell Sound Group on Mainland of 458 ± 3 Ma, 459 ± 4 Ma and 447 ± 8 Ma. The ages from the Yell Sound Group are similar to the Mid-Ordovician ages quoted in Chapter 5. The age from the Dalradian comes from close to the base of the Unst ophiolite. Pressure and temperature estimates varied from 550°C and 7.5 kbar from the Dalradian to 775°C and 10 kbar on Mainland. On Yell, conventional thermobarometry from metapelitic assemblages and interlayered garnet-bearing mafic rocks gives estimates between $620\text{--}680^{\circ}\text{C}$ and 7-10 kbar (Flinn, 1994).

West of the Walls Boundary Fault, Moine-like rocks are found close to North Roe and consist of psammitic metasediments with pelites and quartzites which are interleaved with tectonically banded slices of basement gneisses, these gneisses are referred to as the Eastern Gneisses (Flinn 1988). The psammities are bound to the west by basement gneisses which Flinn (1988) referred to as the Western Gneisses. The Western Gneisses have been dated using K-Ar and Ar-Ar and yielded ages between 2500-2900 Ma (Flinn et al. 1979). The Moine-like psammities are bound to the east by the Virdibreck Shear Zone; on the eastern side lie rocks that have been correlated with the Dalradian Supergroup (Queyfirth Group), which have given Ar-Ar ages of 420-440 Ma (Flinn 1988). Together the psammities, Lewisian inliers and garnet mica schist comprise the generally east-dipping, NNE-striking Sand Voe Schuppen Zone, which is bound to the west by the Wester Keolka shear. The Wester Keolka shear is the western limit of Caledonian deformation within Shetland and because of this has been correlated with the Moine Thrust. Isolated occurrences of the Sand Voe Schuppen Zone form Hillswick Ness and two other isolated and tectonically bounded slivers lying immediately to the west of the Walls Boundary Fault (Flinn 1988). Slivers of the Western Gneisses within the Schuppen Zone have been dated using K-Ar and Ar-Ar and have given ages of between 1000-2300 Ma (Flinn et al. 1979; Flinn 1988). The Moine equivalents within this area are thought to correlate with the Morar Group of the Northern Highlands as they are dominantly psammities or garnet-mica schists, with preserved cross-bedding.

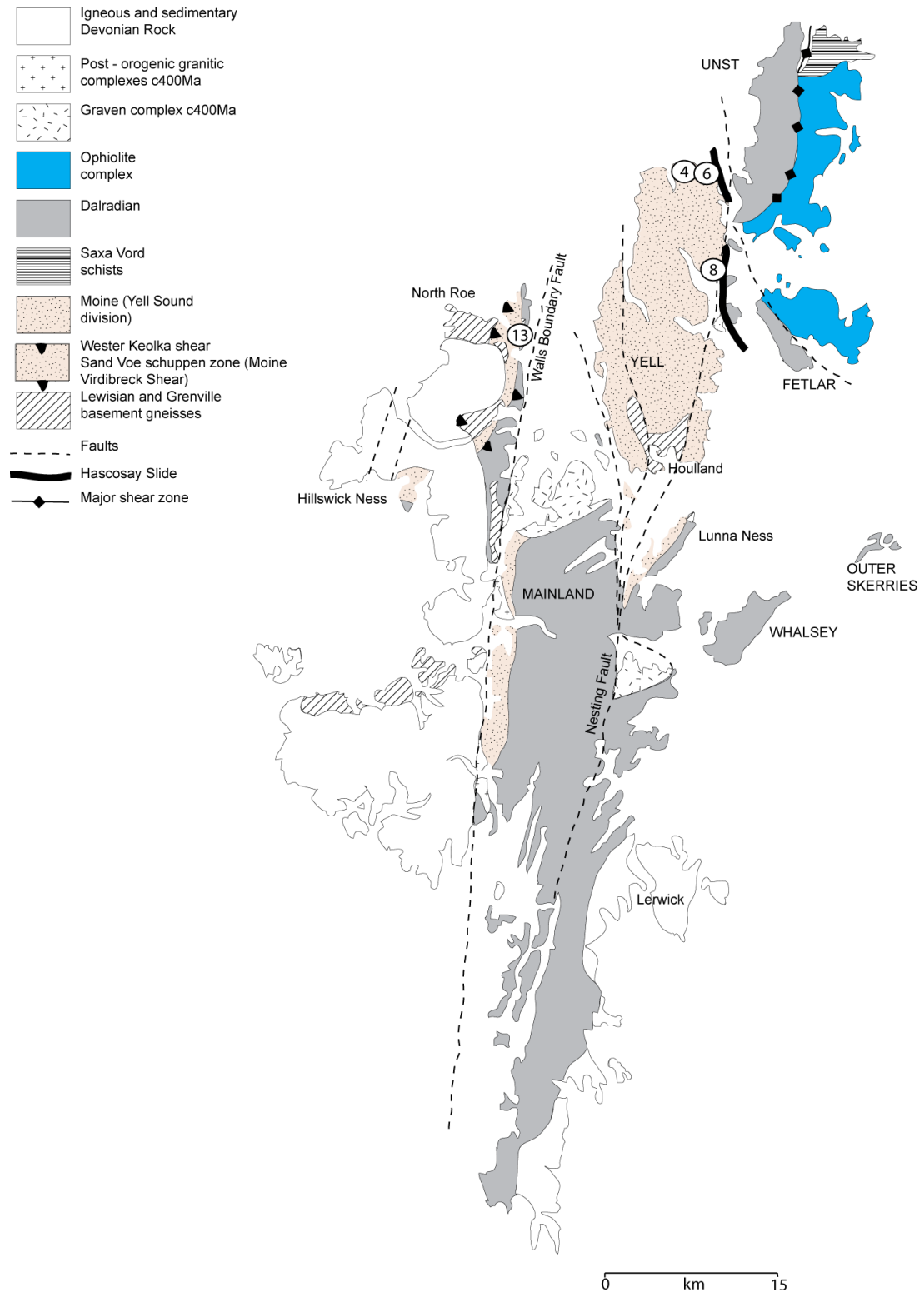


Figure 6-1, simplified geological map of Shetland showing the main units, faults and thrusts, adapted from Flinn (1988).

Dalradian Supergroup equivalent units make up much of Mainland and Whalsey, and on Unst and Fetlar they form the footwall to the Shetland Ophiolite (Figure 6-1). The ophiolite was derived from an intra-continental, ocean-floored basin that opened at ~600 Ma and was thrust onto the Laurentian margin during the Caledonian Orogeny, deforming and metamorphosing the Dalradian (Flinn et al. 1979; Flinn & Oglethorpe 2005). Most of the geochronology from Shetland has come from the ophiolite. A ^{40}Ar - ^{39}Ar hornblende age of 498 ± 2 Ma obtained from a hornblende schist from the obduction thrust is thought to date obduction (Flinn et al. 1991), a series of K-Ar ages of 465 ± 6 Ma to 479 ± 6 Ma also from the ophiolite sole could date obduction suggesting slightly younger thrusting. However, these ages are interpreted to have been affected by Ar loss (Spray 1988; Flinn et al. 1991). A U-Pb zircon age of 492 ± 3 Ma was yielded by a plagiogranite vein cross-cutting the sheeted dykes (Spray & Dunning 1991) which is almost within error of the date given by with Flinn et al. (1991). This suggests that the ophiolite was obducted at around 500 Ma. Cutts et al. (in press) suggest that the total thickness of the ophiolite on Unst is insufficient to produce the overburden required by the metamorphic data (described above), instead they suggest that the basal thrust is either an out-of-sequence thrust that has cross-cut metamorphic isograds or an extensional fault that has excised at least 10 km of crustal section. Pressure and temperature estimates using conventional methods of garnet-pyroxene thermobarometry from the ophiolitic sole gave estimates of 750°C and an estimated pressure of 3 kbars (Spray, 1988). Following ophiolite obduction and metamorphism of the Dalradian sediments was the final collision of Laurentia and Baltica during the Silurian (Dewey & Shackleton 1984; Flinn 1988; Dewey & Strachan 2003), and then the intrusion of a series of granites and finally the Old Red Sandstone was deposited on the eroded metamorphic complexes.

A major geological feature of Shetland is the Walls Boundary Fault, which has been correlated with the Great Glen Fault (Flinn 1992; Watts et al. 2007). As discussed in Chapter 5, this fault system has been interpreted by some authors (e.g. Dewey & Strachan 2003; Kinny et al. 2003) to have had 500-700 km of sinistral displacement along its length. Flinn (1992) suggest that there was 65 km of movement along the

Walls Boundary Fault in Jurassic times, prior to this there was at least 100 km of sinistral displacement.

6.4 Sample Descriptions

AB08-04 – Yell Sound Group Pelitic Gneiss

This sample was collected from Yell next to the Brekon granite gneiss at the Sands of Brekon, at HP 52751 05341 (Figure 6-1). The sample is a pelitic gneiss which has been migmatised and sheared, the vertically-dipping fabric is shown in Figure 6-2a. The shear direction is hard to determine, but Strachan (pers. comm.) suspects dextral shear towards the NNE. The granite gneiss shares the same shear fabric but the fabric apparently decreases towards the west, where the fabric becomes steeper and undulates. The granite gneiss was intruded into the Yell Sound Group country rock and then the whole rock parcel was deformed. Towards the end of the shearing pegmatite dykes were intruded (Figure 6-2b).



Figure 6-2, a – photograph of AB08-04 in the field prior to sampling showing the main fabric; b – shows folded pegmatites cutting through AB08-04; c thin section photograph of AB08-04 in plane polarised light showing the main foliation defined by the biotites and the plentiful small garnets; d showing the same view as c in cross-polars.

The Brekon granitic gneiss has been dated using zircons and gave a U-Pb ~965 Ma protolith age (Kinny & Strachan pers comm.). The rationale for sample AB08-04 was to determine the age of the main metamorphic overprint.

In thin section (Figure 6-2c & d) the sample consists of garnet, biotite, plagioclase, white mica and quartz with accessory zircon, rutile, sphene and opaques. Staurolite appears rarely and kyanite is seen to be reacting in. The garnets are small, only up to 2 mm in size, in the field they often appeared surrounded by melt which was thought to relate to the migmatisation event. They are subhedral with clean edges and large inclusions of quartz and biotite. The fabric is defined by white mica and biotite and does not surround the garnets.

AB08-06 – Migga Ness

This sample was also collected from the Hascosay Slide (Flinn 1988), at HP 53974 05230, Figure 6-1. Flinn (1988) described the Hascosay Slide as a tectonic melange of hornblendic gneisses and banded gneisses that may be Lewisian in origin. It is perhaps better defined as strain zone that is around 0.25 km in width and dips towards the west. There are no meta-sediments within the high strain zone; all the rocks are either amphibolites or felsic gneisses. The amphibolite sampled for this study had been boudinaged and the surrounding fabric appeared to be undulating around these large boudins (Figure 6-3b). In hand specimen the fabric suggests that this sample has been highly strained. The rationale for this sample was to establish whether it is truly part of the basement if these meta-igneous rocks instead intruded the Yell Sound Group.

In thin section it consists of garnet, clinopyroxene, amphibole and plagioclase, with accessory sphene and opaques. The sample is coarse-grained with garnets up to 25 mm in size with large inclusions of amphibole, pyroxene and opaques. The clinopyroxene is green and is surrounded by reaction rims of amphibole, indicating retrogression. Many of the plagioclase are symplectitic, perhaps suggesting interaction with fluid or retrogression textures. Due to the coarseness of the sample, study of the fabric in thin section is difficult, however there is a fabric made up of quartz and amphibole which appears to be migmatitic-like and is metamorphically segregated.

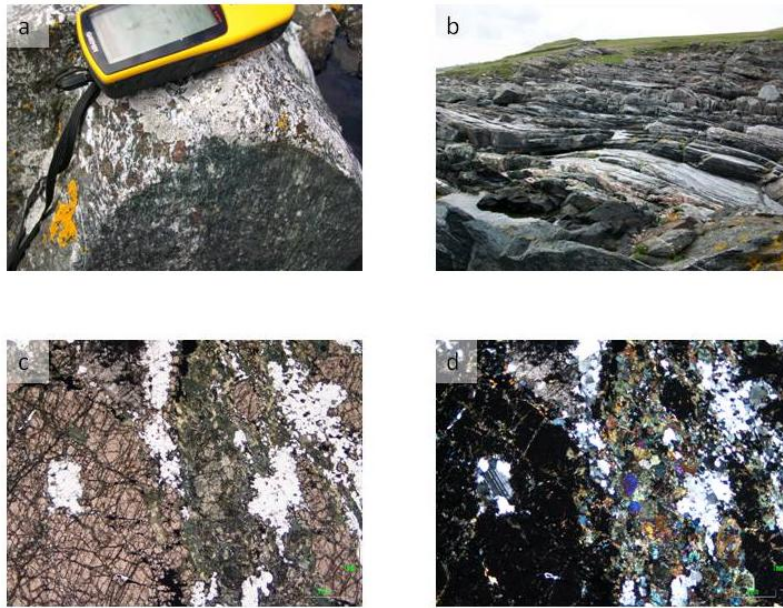


Figure 6-3, a – photograph of AB08-06 in the field prior to sampling showing the main fabric; b – shows the undulating fabric caused by the large boudins; c thin section photograph of AB08-06 in plane polarised light showing mineral relations, especially pyroxene surrounded by amphiboles; d showing the same view as c in cross polars.

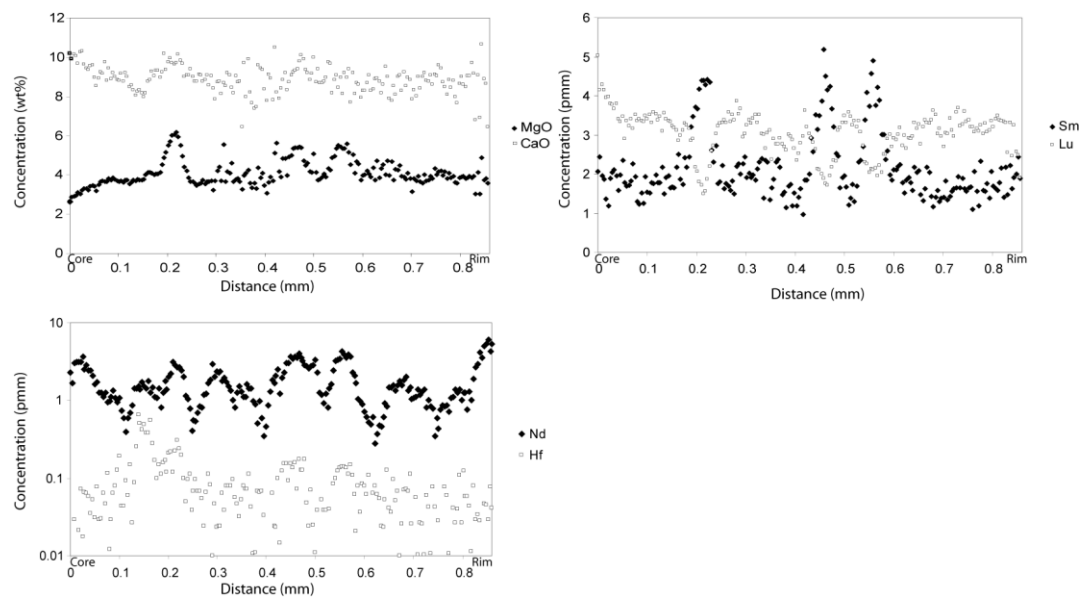


Figure 6-4, LA ICPMS profile for AB08-06 using a SiO_2 value of 37.1%

Migga Ness (AB08-06) was the only sample within this chapter to be subjected to LA ICPMS; the traces are shown in Figure 6-4. All the profiles are fairly homogeneous with a slight change towards the garnet core; MgO shows peaks which

are also seen in the Sm profile, which correlate to TiO_2 peaks (Appendix 2) which suggests that these represent inclusions of rutile or magnetite. The peaks seen in the Sm profile correspond to peaks in the CaO and Nd profiles, suggesting that some of them may be phosphate inclusions. There is one peak in the Hf profile which most likely relates to a zircon inclusion. The Lu, MgO and CaO show a very slight indication of zoning towards the core, which could suggest that the ages obtained from this sample will reflect prograde garnet growth.

AB08-08 – Kirkrabister Amphibolite

This sample was collected at HU 54004 95401 (Figure 6-1) it was a garnet amphibolite which had intruded the surrounding pelitic gneiss. In the field it was a narrow (>1 m) body with large garnets, shown in Figure 6-5a & b. The garnets were larger at the edges of the intrusion which may suggest that there has been fluid flow along the edges of the body.



Figure 6-5, a and b – photographs of AB08-08 in the field prior to sampling showing the amphibolite body; c – thin section photograph showing the large garnets wrapped by the amphibole-rich fabric in plane polarised light; d showing the same view as c in cross polars

In thin section it comprises garnet, amphibole, feldspar, quartz, opaques and zircon (Figure 6-5c & d). The fabric is dominated by amphibole which wraps the garnets. The garnets are up to 6 mm and euhedral with slightly curved inclusion trails. The

inclusions are made up of quartz, rutile and hornblende. The feldspar looks particularly chaotic, perhaps suggesting an interaction with fluid.

AB08-13 – North Roe Schist

The sample was collected on the west side of the Walls Boundary Fault near North Roe at HU 37410 89054, Figure 6-1. Flinn (1988) defined this area as the Sand Voe Schuppen Zone, which is a packet of slices of gneisses and meta-sedimentary rocks separated by faults. The sample is a garnet mica schist. In the field (Figure 6-6a & b) the fabric was steeping dipping and wraps the garnets, often with pressure shadows.



Figure 6-6 a and b– photograph of AB08-13 in the field prior to sampling showing the amphibolite body; c – shows the large garnets wrapped by the fabric; d showing the same view as c in cross polars

In thin section the sample consists of garnet, white mica, quartz, chlorite, titanite and chloritoid, (Figure 6-6c & d). The fabric is dominated by white mica and quartz and wraps the garnets. The garnets are euhedral to subhedral and are up to 8 mm in diameter. They are inclusion-rich with inclusions of quartz, chloritoid and opaques. Several of the garnets have large pressure shadows made up of quartz. It is difficult to distinguish the garnet cores from the rims in thin section. The garnet cores are

inclusion-rich and the inclusion trails are oblique to the surrounding fabric, the garnet rims have fewer inclusions.

6.5 Results and interpretation

The Lu-Hf and Sm-Nd results are summarised in Table 6-1 and Table 6-2. The garnet rim from the North Roe Schist (AB08-13) yielded a Lu-Hf two point garnet-whole rock age of 450.9 ± 4.1 Ma, this fraction gave a $^{176}\text{Lu}/^{177}\text{Hf}$ ratio of 0.509 indicating that this age should be reliable. The Hf concentration from this sample was 1.039 ppm, suggesting that there may have been some influence from zircon inclusions. The garnet core fraction from AB08-13 gave a Lu-Hf two point garnet-whole rock age of 559 ± 18 Ma. This fraction was very unradiogenic as it had a very low $^{176}\text{Lu}/^{177}\text{Hf}$ ratio of 0.056, this was most likely due to the high Hf content (4.548 ppm) indicating an influence from zircon inclusions, thus this age does not mean anything and should be discounted. The North Roe Schist (AB08-13) gave two Sm-Nd two point garnet-whole rock isochron ages of 473 ± 8 Ma for the core and 359 ± 160 Ma for the rim. The age from the garnet rim is not reliable as it has very low $^{147}\text{Sm}/^{144}\text{Nd}$ and $^{143}\text{Nd}/^{144}\text{Nd}$ ratios, this is most likely due to the extremely high Nd concentration of 22.439 ppm from this fraction suggesting a large influence from Nd-rich inclusions. The core gives an age of 472.6 ± 7.7 Ma and a three point isochron can be constructed which gives an age of 469.0 ± 6.0 Ma with an MSWD of 1.8, however this uses the unradiogenic fraction, thus the most accurate age from this sample is the two point core and whole rock age (472.6 Ma).

No Lu-Hf ages were yielded from AB08-04 as there was a problem during the chemistry which affected this sample. A Sm-Nd two point garnet-whole age was obtained from the sample of 467.5 ± 1.4 Ma. The garnet fraction gave a high $^{147}\text{Sm}/^{144}\text{Nd}$ ratio showing that this age is reliable. It also gave a low Nd concentration of 0.546 ppm, suggesting little or no influence from Nd-rich inclusions.

The Lu-Hf two point garnet-whole rock isochron ages from the Kirkrabister Amphibolite (AB08-08) are not all that meaningful as the $^{176}\text{Hf}/^{177}\text{Hf}$ and $^{176}\text{Lu}/^{177}\text{Hf}$ ratios for the garnet fractions are lower than the whole rock value, this is most likely due to the low Lu concentrations of the garnet fractions (1.121 ppm and 1.083 ppm),

thus these ages should be ignored. The Kirkrabister Amphibolite (AB08-08) gave a good Sm-Nd three point two garnet fractions-whole rock isochron age of 478.2 ± 2.3 Ma with an MSWD of 0.5. This age had had little or no effect from Nd-rich inclusions as the Nd concentrations for each fraction are 0.490 ppm and 0.583 ppm, confirming the reliability of this age.

Migga Ness (AB08-06) gave a Lu-Hf two point garnet-whole rock age of 856.7 ± 2.6 Ma. This sample had an extremely high $^{176}\text{Lu}/^{177}\text{Hf}$ ratio of 8.274 suggesting that this age is reliable. This is complemented by the low Hf concentration of 0.097 ppm which is similar to the pure garnet value estimated from the LA ICPMS trace from this sample of 0.086 ppm. Migga Ness (AB08-06) gave a Sm-Nd two point garnet-whole rock age of 863.1 ± 3.6 Ma which is within error of the Lu-Hf age for the same sample. This sample gave a reasonably high $^{147}\text{Sm}/^{144}\text{Nd}$ ratio of 0.989 suggesting that the age is meaningful, however it gave a Nd concentration of 1.743 ppm which is higher than the pure garnet Nd concentration of 0.87 ppm estimated from the LA ICPMS suggesting some influence from Nd-rich inclusions.

Table 6-1 Lu-Hf garnet results from Shetland samples. Ages marked with an * are interpreted to be not geologically meaningful.

Sample fraction	Lu ppm	Hf ppm	$^{176}\text{Hf}/^{177}\text{Hf}$	2σ	$^{176}\text{Lu}/^{177}\text{Hf}$	Initial	Lu-Hf Age (Ma)
AB08-04 Gt	-	-	-	-	-	-	-
AB08-04 WR	-	-	-	-	-	-	-
AB08-06 Gt	5.551	0.097	0.416717	0.000080	8.274	0.283458	856.7 ± 2.6
AB08-06 WR	0.791	0.401	0.287950	0.000037	0.279		
AB08/08 Gt Core	1.121	0.912	0.284156	0.000010	0.174	0.282641	$465.7 \pm 13^*$
AB08/08 Gt Rim	1.083	0.995	0.284017	0.000009	0.154	0.282716	$451.4 \pm 11^*$
AB08/08 WR	0.851	0.431	0.285073	0.000023	0.279		
AB08-13 Gt Rim	3.742	1.039	0.285909	0.000015	0.509	0.282231	450.9 ± 4.1
AB08-13 Gt Core	1.793	4.548	0.282743	0.000015	0.0557	0.282159	$555.2 \pm 34^*$
AB08-13 WR	0.429	2.672	0.282399	0.000015	0.0227		

Table 6-2 Sm-Nd garnet results from Shetland samples. Ages marked with an * are interpreted to be not geologically meaningful.

Sample fraction	Sm ppm	Nd ppm	$^{143}\text{Nd}/^{144}\text{Nd}$	2σ	$^{147}\text{Sm}/^{144}\text{Nd}$	Initial	Sm-Nd Age (Ma)	MSWD
AB08-04 Gt	2.485	0.546	0.519907	0.000021	2.755		467.5 ± 1.4	
AB08-04 WR	4.376	21.828	0.511841	0.000009	0.121			
AB08-06 Gt	2.849	1.743	0.517320	0.000013	0.989	0.511721	863.1 ± 3.6	
AB08-06 WR	3.256	9.754	0.512864	0.000012	0.202			
AB08/08 Gt Core	1.282	0.490	0.516872	0.000015	1.584			
AB08/08 Gt Rim	1.489	0.583	0.516766	0.000017	1.547			
AB08/08 WR	2.521	4.735	0.512924	0.000015	0.322	0.511916	478.2 ± 2.3	0.5

AB08-13 Gt Rim	4.563	22.439	0.511748	0.000009	0.123	0.511459	359.1 ± 160*	
AB08-13 Gt Core	1.890	2.753	0.512643	0.000009	0.415	0.511358	472.6 ± 7.7	
AB08-13 WR	4.019	17.869	0.511779	0.000011	0.136	0.511361	469.0 ± 6.0	1.8

6.6 Discussion

Ages of 856.7 Ma (Lu-Hf) and 863.1 Ma (Sm-Nd) show that AB08-06 (Migga Ness) was affected by Neoproterozoic deformation and metamorphism. The fabric suggests that the sample has been highly strained, most likely during the shearing event which pulled the amphibolite into boudins. As both of these ages are within error it is unlikely that either age could be recording partial resetting of old ~930 Ma garnet by a Caledonian ~470 Ma event. This demonstrates that Shetland, like the Moine Supergroup of Scotland, has been affected by several Neoproterozoic metamorphic events, an early event of 930 Ma recorded in the Westing Group which is similar to ages from the Renlandian and a younger ~860 Ma event which is similar to ages from Mull and the south west Moine (Chapter 4). This suggests that both the Westing Group and the units within the Hascosay Slide can be correlated broadly with the lower parts of the Moine Supergroup and the Krummedal Succession. The rationale behind dating this sample was to establish if Migga Ness was part of the basement or more simply an intrusion, the ages obtained do not show definitively demonstrate whether this sample is part of the basement or younger garnet growth relating to Knoydartian metamorphism. To establish the relationship between Migga Ness and the surrounding Yell Sound Group U-Pb analyses of zircons would give a protolith age which would determine this association.

The main migmatization event of the Yell Sound Group occurred at ~470 Ma shown by the Sm-Nd age from AB08-04 of 470.5 ± 1.4 Ma, and the Sm-Nd age from AB08-08 of 478.2 ± 2.3 Ma. The inclusion trails within garnets from AB08-08 are slightly curved, suggesting that these garnets could partially be syn-kinematic; suggesting that the ages from these samples is recording the dominant phase of deformation. These ages are similar to the age of 470 ± 5 Ma from the Dalradian equivalents on Unst directly below the ophiolite (Cutts et al. in press); this age was interpreted to date peak metamorphism as the peak temperature recorded by this sample was 550°C which is close to the U-Pb closure temperature of a matrix monazite. The younger monazite ages (459-447 Ma) from the Yell Sound Group are

interpreted to date cooling from a hotter peak metamorphic temperature somewhere in the region of 750-850°C (Cutts et al., in press). The garnets in this study are large enough not to have been affected by diffusion at these temperatures, thus the ages recorded should reflect peak metamorphism (Dutch & Hand 2010).

The Ordovician ages obtained within the Yell Sound Group and the Dalradian Supergroup on Shetland are very similar to ages from the Dalradian Supergroup within the Grampian Terrane of mainland Scotland. The ages from mainland Scotland include Rb-Sr muscovite, biotite and hornblende dates between 468 Ma and 484 Ma (Dempster et al. (1984), Sm-Nd garnet ages between 467-472 Ma (Oliver et al. 2000; Baxter et al. 2002), a Lu-Hf garnet age of 470.8 Ma from the Leven Schist (Chapter 5) and ages for granitic and gabbro intrusions between 467-489 Ma (Pankhurst et al. 1969; Fettes 1970; van Breemen & Boyde 1972; Pidgeon & Aftalion 1978; Kneller & Aftalion 1987; Friedrich et al. 1999; Oliver et al. 2000; Dempster et al. 2002). Mid-Ordovician ages are also seen with the Northern Highlands, Lu-Hf garnet ages of 466 Ma, 475 Ma and 465 Ma from the Naver Nappe, the Glenfinnan Group and the Morar Group respectively (Chapter 5). Sm-Nd garnet analyses give ages between 469 Ma and 502 Ma (Chapter 5). These ages are also seen in Ireland, based on U-Pb zircon ages of ~468 Ma (Friedrich et al. 1999) and in the Appalachians (Karabinos et al. 1998). Baxter et al. (2002) estimated pressures and temperatures of garnet growth of a sample from Glen Clova within the Grampian Terrane and obtained temperatures of 550-650°C and pressures of 7.2-9.2 kbar, Cutts et al. (2010) estimated pressure and temperature during mid-Ordovician garnet growth from the Glenfinnan Group and obtained values of 650°C and ~7 kbar. Both of these samples give similar pressures and temperatures to the values estimated from the Dalradian equivalents on Unst (Cutts et al. in press). Thus the results of this study add to the evidence that Shetland shares the same Ordovician event as the Northern Highlands, the Grampians, Ireland and the Appalachians.

It has been suggested that the metasediments in North Roe were affected by two major phases of deformation (Mykura 1976). The first produced the West Keolka Shear Zone and was responsible for the pervading schistosity. The second deformation produced easterly dipping shear belts and folds within the metasediments (Pringle 1970; Mykura 1976). The ages from this study suggest that

the first phase of deformation was 473 Ma, suggested by the Sm-Nd core age from the North Roe Schist (AB08-13) the later phase was perhaps 451 Ma indicated by the Lu-Hf age from the rim. The younger phase of deformation could be related to the formation of the Sand Voe Schuppen Zone. This would suggest that movement on the West Keolka Shear is 470 Ma in age and is more likely to be related to a Mid-Ordovician aged event than a Silurian aged event. These ages are similar to the Caledonian ages obtained from garnets in the Northern Highland Terrane in Chapter 4 of this study, which suggests that at least some parts of Shetland share a similar Caledonian history to the western Moine Supergroup of the Northern Highland Terrane.

6.7 Conclusions

1. The age of the migmatisation event within the Yell Sound Group is between 469.0 Ma and 478.2 Ma. This is related to the Grampian event and ophiolite emplacement.
2. The younger age of 450.9 Ma from the rim of the North Roe Schist is possibly related to the formation of the Sand Voe Schuppen zone and is within error of the Late-Ordovician ages from the western Moine Supergroup of the Northern Highland terrane. This suggests that at least some parts of Shetland share a similar Caledonian history to the western Moine Supergroup.
3. The ages from Migga Ness of 856.7 Ma and 863.1 Ma show that the Hascosay Slide, like the Westing Group was affected by Neoproterozoic deformation and metamorphism. This suggests that that these units can be correlated with the lower parts of the Moine Supergroup. The ages do not show whether Migga Ness is a part of the basement or more simply an intrusion, analyses of zircons would show definitively the age of the protolith.

7.1 Synopsis

This chapter provides new white mica and biotite Rb-Sr ages for ten samples from the Moine Supergroup and one sample from the Dalradian Supergroup. The white mica and biotite ages clearly show a systematic variation from south to north through the Moine Supergroup, with the southern localities yielding older ages and larger differences between the white mica and biotite ages. The white mica ages from almost all of the samples partially reflect Knoydartian metamorphism. These same samples also gave Neoproterozoic garnet growth ages, suggesting that in these areas Caledonian metamorphism was not hot or prolonged enough to have entirely reset the Rb-Sr system. This suggests that in many parts of the Moine Supergroup neither the Grampian or Scandian events reached amphibolite facies grade.

7.2 Introduction

Micas from slowly cooled medium-high grade metamorphic rocks generally give Rb-Sr ages that are younger than the time of peak metamorphism; this is thought to be due to the lower closure temperature (T_C) of the Rb-Sr system in micas than the peak metamorphic temperature of the rock (e.g. Dempster et al., 1985). This has led to Rb-Sr analyses on white micas, biotites and feldspars having been undertaken on many metamorphic terranes in order to establish uplift, cooling or the timing of peak metamorphism in low grade areas. Ar-Ar analyses are often carried out alongside as the T_C of Ar-Ar in white micas, hornblendes, biotites and feldspars are similar to that of Rb-Sr, (325 - 375°C, 450 - 525°C, 260 - 350°C, and 125 - 350°C respectively) (Spear 1993). Rb-Sr T_C estimates for white micas and biotites are 500°C and 300°C respectively (Armstrong et al., 1966; Jäger 1979). It should be noted, however, that T_C for Rb-Sr in micas depends on grain size, rock type, and Rb and Sr diffusion coefficients; thus the estimates mentioned above may not reflect the true T_C for the samples analysed here.

Rb-Sr analyses were undertaken on white micas and biotites from ten samples from the Moine Supergroup and one sample from the Appin Group of the Dalradian Supergroup. The majority of the analyses were undertaken by Kathryn McDermott as part of a six

week Nuffield undergraduate bursary at Royal Holloway. According to the results outlined in Chapters 4 and 5, the Moine Supergroup samples should have all been affected by Neoproterozoic Knoydartian and Caledonian metamorphism. The Appin Group sample might be anticipated to have only undergone Caledonian metamorphism. Metamorphism associated with the Caledonian Orogeny is thought to have occurred in two distinct events, the Grampian (475-460 Ma) and the Scandian (435-420 Ma). As discussed in Chapter 5, the Scandian event was thought to be of amphibolite-facies (e.g. Strachan et al., 2002; Kinny et al., 2003), thus should have been of a high enough temperature (>550 - 600°C) to reset Rb-Sr systems in white micas and biotites within the Moine Nappe (Morar group) and throughout the Northern Highland Steep Belt where Scandian deformation is strong. This would suggest that the Rb-Sr ages yielded from the samples within the Moine Supergroup ought to reflect cooling from the Scandian event and so should be younger than 435 Ma.

7.3 Previous Geochronology

There have been several previous studies that have used geochronological techniques that could be used to constrain the late uplift of the Moine Supergroup. The earliest of these was by Giletti et al. (1961) who undertook Rb-Sr and K-Ar on biotites and white micas and achieved ages in the range of 740-405 Ma. They concluded that there was regional metamorphism at 420 ± 15 Ma as the biotite ages were in close agreement. 740-655 Ma ages were recorded from white mica books found within the pegmatites of the Knoydart mica mine. The white mica books are up to 30.5 cm in diameter and 7.6 cm thick (Giletti et al., 1961) and apparently had not been affected by later heating associated with the Caledonian orogeny. The previous geochronology is summarised in Table 7-1.

Table 7-1 summary of all published Rb-Sr, Ar-Ar and K-Ar dates from the Moine Supergroup and inliers.

Date	Error	Sample Nr	Area	Lithology	System	Mineral	Reference
740.0	15.0	31	Knoydart mica mine	Pegmatite	Rb-Sr	Mu	Giletti et al 1961
740.0	25.0	31	Knoydart mica mine	Pegmatite	Rb-Sr	Mu	Giletti et al 1961
740.0	15.0	32	Knoydart mica mine	Pegmatite	Rb-Sr	Mu	Giletti et al 1961
725.0	15.0	32	Knoydart mica mine	Pegmatite	Rb-Sr	Mu	Giletti et al 1961
665.0	15.0	34	Sgurr Breac	Pegmatite	Rb-Sr	Mu	Giletti et al 1961
488.3	5.3	4	Moine Thrust Zone, Sutherland	Mylonite	Ar-Ar	Mu	Dallmeyer et al 2001
470.6	5.3	5A	Basement inlier	Amphibolite	Ar-Ar	Hbl	Dallmeyer et al 2001

461.5	5.3	3	Moine Thrust Zone, Sutherland	Mylonite	Ar-Ar	Mu	Dallmeyer et al 2001
458.1	5.2	2	Moine Thrust Zone, Sutherland	Mylonite	Ar-Ar	Mu	Dallmeyer et al 2002
451.8	5.2	10	Moine Nappe, Sutherland	Pelite	Ar-Ar	Mu	Dallmeyer et al 2001
449.0	13.5	D4	Dundonnell	Mylonite	K-Ar		Freeman et al 1998
446.0	5.3	6	Basement inlier, Sutherland	Hbl Gneiss	Ar-Ar	Hbl	Dallmeyer et al 2001
442.0	4.0	5B	Moine Nappe, Sutherland	Pelite	Rb-Sr	Mu	Dallmeyer et al 2001
441.0	13.0	kn1	Knockan	Mylonite	K-Ar		Freeman et al 1998
440.1	5.3	8	Basement inlier, Sutherland	Hbl Gneiss	Ar-Ar	Hbl	Dallmeyer et al 2001
437.0	5.8	kn5	Knockan	Mylonite	Rb-Sr	Mu	Freeman et al 1998
436.0	6.0	9	Moine Nappe, Sutherland	Psammite	Rb-Sr	Mu	Dallmeyer et al 2001
435.0	10.0	25	Inverbroom	Pelite	Rb-Sr	Bt	Giletti et al 1961
433.0	4.0	10	Moine Nappe, Sutherland	Pelite	Rb-Sr	Mu	Dallmeyer et al 2001
431.0	5.2	14	Naver Nappe	Amphibolite	Ar-Ar	Hbl	Dallmeyer et al 2001
430.0	5.2	9	Moine Nappe, Sutherland	Psammite	Ar-Ar	Mu	Dallmeyer et al 2001
430.0	5.9	kn1	Knockan	Mylonite	Rb-Sr	Mu	Freeman et al 1998
430.0	10.0	29	Morar	Psammite	Rb-Sr	Bt	Giletti et al 1961
429.0	5.7	D7	Dundonnell	Mylonite	Rb-Sr	Mu	Freeman et al 1998
428.0	7.0	3	Moine Thrust Zone, Sutherland	Mylonite	Rb-Sr	Mu	Dallmeyer et al 2001
428.0	5.7	D8	Dundonnell	Mylonite	Rb-Sr	Mu	Freeman et al 1998
425.0	9.0	23	Bettyhill	Pelite	Rb-Sr	Bt	Giletti et al 1961
425.0	5.5	kn3	Knockan	Mylonite	Rb-Sr	Mu	Freeman et al 1998
423.0	5.2	17	Naver Nappe	Semi-pelitic Gneiss	Ar-Ar	Mu	Dallmeyer et al 2001
421.6	5.3	7	Basement inlier, Sutherland	Hbl Gneiss	Ar-Ar	Hbl	Dallmeyer et al 2001
421.4	5.4	13	Naver Nappe, basement	Amphibolite	Ar-Ar	Hbl	Dallmeyer et al 2001
421.0	27.0	2	Moine Thrust Zone, Sutherland	Mylonite	Rb-Sr	Mu	Dallmeyer et al 2002
420.0	50.0	27	Glenelg Inlier	Acid Gneiss	Rb-Sr	Bt	Giletti et al 1961
420.0	12.0	28	Knoydart	Pelite	Rb-Sr	Bt	Giletti et al 1961
419.8	5.2	12	Moine Nappe, Sutherland	Pelite	Ar-Ar	Mu	Dallmeyer et al 2001
419.3	5.2	16	Naver Nappe	Semi-pelitic Gneiss	Ar-Ar	Mu	Dallmeyer et al 2001
418.3	5.2	20	Kirtomy Nappe	Migmatitic Gneiss	Ar-Ar	Mu	Dallmeyer et al 2001
418.0	5.2	11	Moine Nappe, Sutherland	Pelite	Ar-Ar	Mu	Dallmeyer et al 2001
417.9	5.2	15	Naver Nappe	Semi-pelitic Gneiss	Ar-Ar	Mu	Dallmeyer et al 2001
417.0	5.2	D4	Dundonnell	Mylonite	Rb-Sr	Mu	Freeman et al 1998
416.9	5.5	14	Naver Nappe	Amphibolite	Ar-Ar	Mu	Dallmeyer et al 2001
416.4	5.2	5B	Moine Nappe, Sutherland	Pelite	Ar-Ar	Mu	Dallmeyer et al 2001
415.0	4.0	15	Naver Nappe	Semi-pelitic Gneiss	Rb-Sr	Mu	Dallmeyer et al 2001
415.0	9.0	24	Carn Chuinneag	Fld gneiss	Rb-Sr	Fld	Giletti et al 1961
415.0	11.0	29	Morar	Psammite	Rb-Sr	Bt	Giletti et al 1961
414.5	5.3	18	Kirtomy Nappe	Amphibolite	Ar-Ar	Hbl	Dallmeyer et al 2001
413.0	5.0	4	Moine Thrust Zone	Mylonite	Rb-Sr	Mu	Dallmeyer et al 2001
412.8	5.5	21	Strathy Complex	Amphibolite	Ar-Ar	Hbl	Dallmeyer et al 2001
410.2	5.5	22	Strathy Complex	Amphibolite	Ar-Ar	Hbl	Dallmeyer et al 2001
408.0	5.9	D1	Dundonnell	Mylonite	Rb-Sr	Mu	Freeman et al 1998
405.0	10.0	26	Monar Lodge	Pelite	Rb-Sr	Bt	Giletti et al 1961
405.0	10.0	30	Strontian	Pegmatite	Rb-Sr	Bt	Giletti et al 1961
404.2	5.4	19	Kirtomy Nappe	Amphibolite	Ar-Ar	Hbl	Dallmeyer et al 2001
396.0	4.0	20	Kirtomy Nappe	Migmatitic Gneiss	Rb-Sr	Mu	Dallmeyer et al 2001
390.0	19.5	23	Bettyhill	Pelite	K-Ar		Giletti et al 1961

White micas from Moine mylonites at Knockan and Dundonnell were dated using a Rb-Sr white mica-feldspar two point isochron and gave ages in the range of 437-408 Ma (Freeman et al., 1998). K-Ar analysis was carried out on many of the same fractions and gave ages between 449-417 Ma. The K-Ar ages that were older than the Rb-Sr ages from the same fraction (449 ± 13.5 Ma and 441 ± 13 Ma) were discounted, as the Rb-Sr system is expected to give older ages in white micas due to a higher T_C , although one of these ages was within error of the Rb-Sr white mica ages suggesting that perhaps it is a meaningful age, these ages are detailed in Table 7-1. It was supposed that these samples had been affected by excess Ar due to fluid flow through the Moine Thrust shear zone thus the relevance of the ^{40}Ar - ^{39}Ar ages from this region is suspect (Freeman et al., 1998; Dallmeyer et al., 2001). The Rb-Sr ages were, however, thought to relate to shearing during movement on the Moine Thrust. Dallmeyer et al. (2001) used Ar-Ar and Rb-Sr techniques to date white micas and hornblendes in north Sutherland (Table 7-1). The Moine Thrust Zone mylonites gave three Ar-Ar white mica ages in the range of 488-458 Ma, which are older than the Rb-Sr ages obtained from the same separates (427-413 Ma), thus the significance of the Ar-Ar ages from this region is questionable. The Moine Nappe yielded three Rb-Sr white mica ages of 442-433 Ma and three Ar-Ar ages that were between 451-416 Ma, again one of the samples gave an older Ar-Ar age than Rb-Sr. Basement inliers within the Moine Nappe were also dated and gave Ar-Ar hornblende ages from 470-421 Ma. A semi-pelitic gneiss from the Naver Nappe gave one Rb-Sr age of 415 ± 4 Ma and three Ar-Ar white mica ages of 417-423 Ma and two Ar-Ar hornblende ages of 419 Ma and 431 Ma. The Strathy Complex gave two Ar-Ar hornblende ages of 412 Ma and 410 Ma. The Kirtomy nappe gave two Ar-Ar hornblende ages of 414 Ma and 404 Ma and an Ar-Ar white mica age of 418 Ma. One Rb-Sr analysis from the Kirtomy nappe gave an age of 396 Ma which is younger than the other ages obtained which was attributed to the sample not being very radiogenic. The majority of these ages are thought to relate to regional thrusting during the Late Silurian and cooling during and following amphibolite-facies metamorphism. The 470 ± 5 Ma obtained from the basement inlier within the Moine Nappe cannot reflect cooling post-Silurian/ Scandian cooling, it may demonstrate that part of the Moine Nappe region did not undergo mid- to high temperature deformation at this time (Dallmeyer et al., 2001). Dallmeyer et al. (2001) suggest that the 470 Ma age is related

to the Grampian event already recorded in the Naver Nappe, this would suggest that the Ar-Ar hornblende age recorded peak metamorphism.

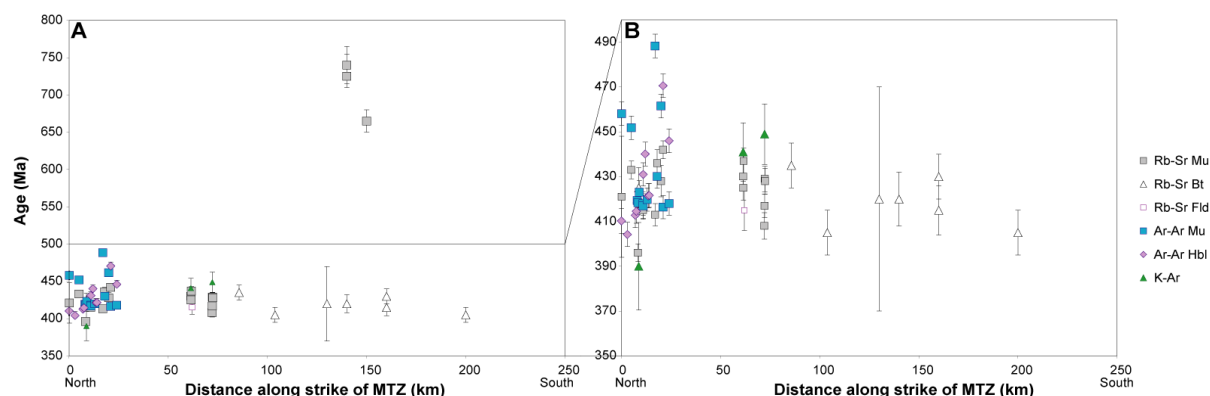


Figure 7-1, previously published Rb-Sr, Ar-Ar and K-Ar ages plotted against distance along strike of the Moine Thrust Zone, a shows all the data and b shows just the data between 500 – 350 Ma. Data from Giletti et al., 1961; Freeman et al., 1998; and Dallmeyer et al., 2001.

Figure 7-1A shows the published data plotted along strike of the Moine Thrust Zone, a shows all the previously published data including the three Neoproterozoic ages from Giletti et al., (1961). Graph B shows just the data between 500 Ma and 350 Ma to analyse cooling related to the Caledonian Orogeny, superficially the ages seem to decrease from north to south. However the only dates from the southern Moine are biotite Rb-Sr ages which have lower a closure temperature so are expected to record younger ages.

7.4 Sample descriptions

Samples were selected based on their white mica and biotite content, thus all the pelites collected from the 2007 field season were analysed and sample locations are shown in Figure 7-2. Detailed sample and thin section descriptions are found in the previous chapters, however some information about the quality and size of the white micas and biotites are included here.

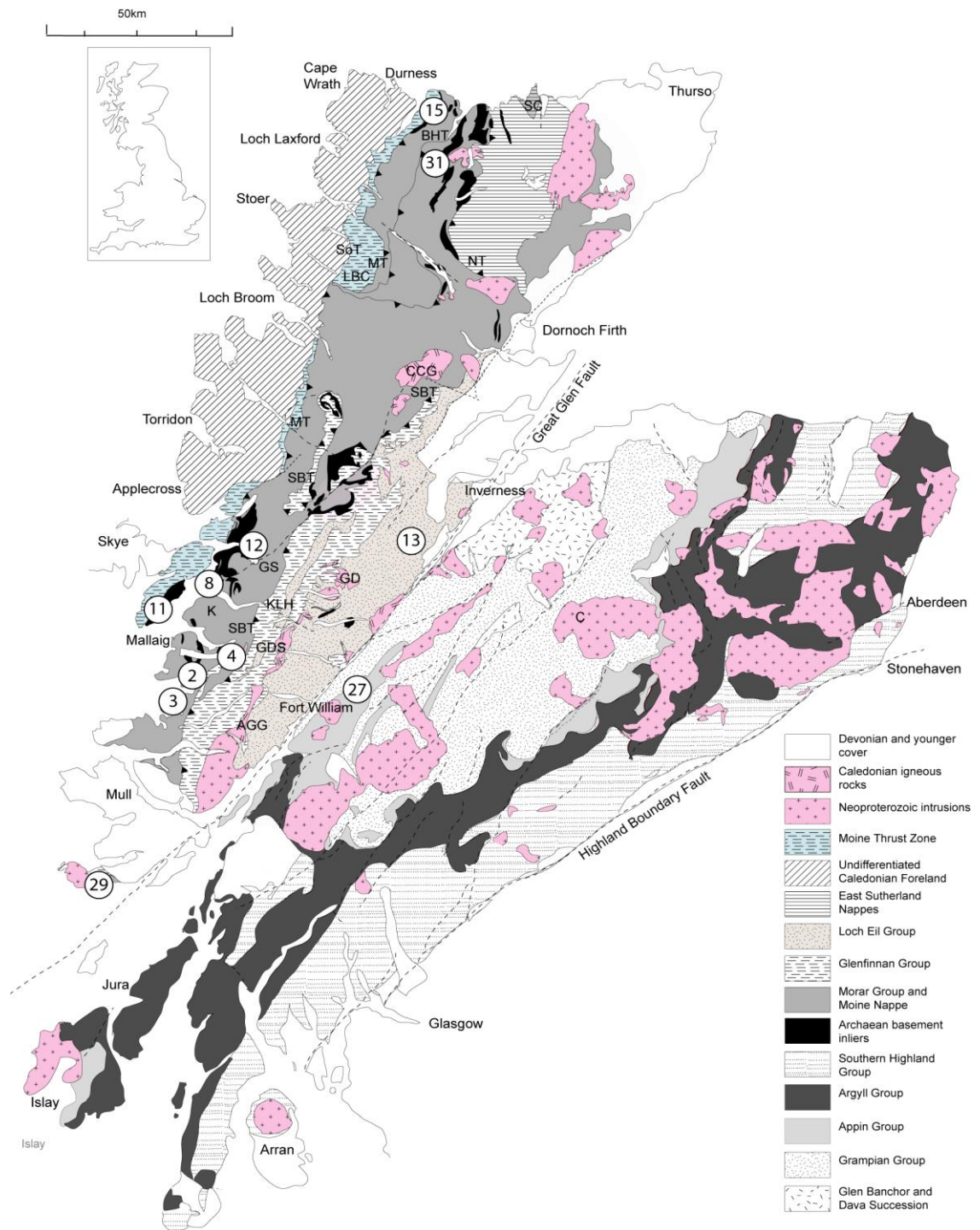


Figure 7-2 abbreviations; 2 – AB07-02; 3 – AB07-03; 4 – AB07-04; 8 – AB07-08; 11 – AB07-11; 12 – AB07-12; 13 – AB07-13; 15 – AB07-15; 27 – AB07-27; 29 – AB07-29; 31 – AB07-31; BHT – Ben Hope Thrust; K – Knoydart mica mine; MT – Moine Thrust; SBc – Sgurr Breac; SBT – Sgurr Beag Thrust; SoT – Sole Thrust.

AB07-02 – Polish Pelite [NM 7445 8392]

The Polish Pelite is part of the Morar Group and is a garnet mica schist. It was sampled within 10 metres of the sampling site of Vance et al. (1998) and gave an age of 822.7 ± 4.6 Ma from the garnet core and an age of 788.3 ± 4.4 Ma from the garnet rims using Sm-Nd two point isochrons. This study has yielded Lu-Hf garnet core and rim ages of 860.7 ± 2.7 Ma and 828.8 ± 3.5 Ma respectively and Sm-Nd ages of 795.9 ± 2.9 Ma and 772.6 ± 2.4 Ma for the core and the rims. Chapter 4 discusses the merit of these ages in detail; the mixing diagrams show that there has been no physical mixing and no partial resetting which would look like mixing on the diagrams. These ages demonstrate that the Polish Pelite records Neoproterozoic garnet growth and any later metamorphism was not at a sufficiently high enough temperature to wholly reset the Lu-Hf or Sm-Nd isotopic systems.

The white mica crystals in this sample are up to 1 mm in size and the biotite crystals are slightly smaller, together they form the main fabric, which wrap the garnets, along with quartz and plagioclase, Figure 7-3. The fabric is layered with mica-rich layers and quartz-rich layers. The white micas have many inclusions of an opaque mineral; the biotites have fewer inclusions of the opaque mineral but also have zircon inclusions with pleochroic halos.

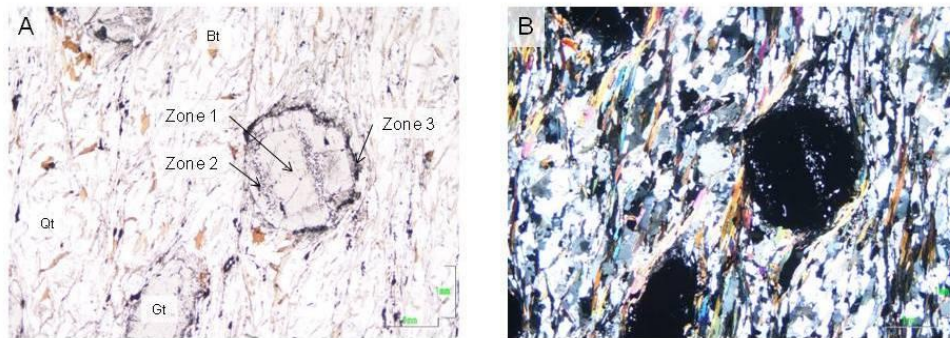


Figure 7-3 AB07-02 in thin section showing the white mica and biotite-dominated matrix wrapping the garnets.

AB07-03 – Glenuig Pelite [NM 6707 7756]

The Glenuig Pelite, from the Morar Group, is a garnet mica schist and was sampled within 10 metres of the sampling site of Vance et al. (1998). Vance et al. (1998) obtained one garnet-whole rock ages of 815 ± 21 Ma. This study has yielded Lu-Hf

garnet core and rim ages of 903 ± 2.9 Ma and 843.4 ± 3.3 Ma, and Sm-Nd core and rim ages of 756.7 ± 14.0 and 682.8 ± 38.0 Ma. Like the Polish Pelite these ages record Neoproterozoic metamorphism and show that any later Caledonian metamorphism was not of a high enough temperature to wholly reset Lu-Hf and Sm-Nd. Unlike the Polish Pelite there was no LA ICPMS data for garnets from this sample, thus mixing diagrams cannot be constructed. However it is very similar to the Polish Pelite and the ages obtained are not dissimilar, suggesting that partial resetting has not affected this sample.

The fabric in this sample wraps the garnets (Figure 7-4) and has been obviously crenulated with white micas and some biotites making up the P domains and quartz, plagioclase and the rest of the biotite making up the Q domains. The biotite in the Q domain is oblique to the micas in the P domain. Both the white micas and the biotites are up to 1 mm. The white micas have inclusions of an opaque mineral and the biotites have zircon inclusions with pleochroic halos.

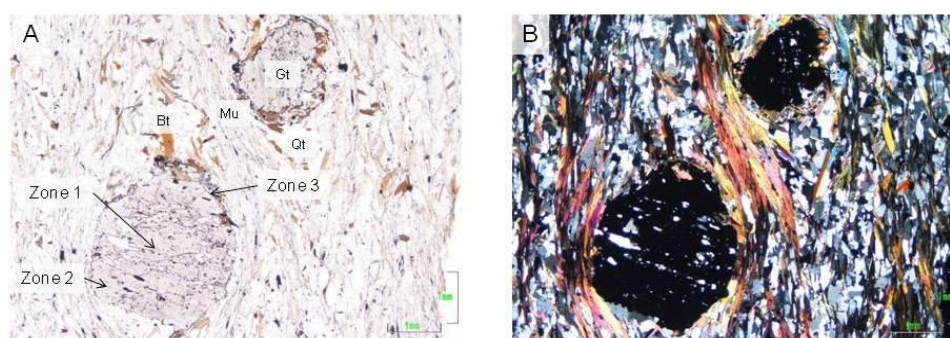


Figure 7-4 AB07-03 in thin section showing the crenulated matrix dominated by white mica and biotite with quartz-rich layers.

AB07-04 – Loch Eilt Semi-pelitic Gneiss [NM 8511 8174]

This sample is a semi-pelitic gneiss from east of Loch Eilt within the Glenfinnan Group. It has yielded Lu-Hf garnet core and rim ages of 739.5 ± 2.5 Ma and 697.7 ± 3.1 Ma. The Sm-Nd ages from this study are substantially younger and appear to be partially reset by later Caledonian metamorphism; the age obtained from the core is 539.6 ± 3.2 Ma and 497.6 ± 2 Ma from the garnet rim. Similar to the samples from the Morar Pelite, this sample records Neoproterozoic metamorphism. Later Caledonian metamorphism was not of a high enough temperature to affect the Lu-Hf system, however, temperatures were high enough to partially reset Sm-Nd.

This sample is of a higher grade than the samples described previously, it is a staurolite-garnet gneiss with some kyanite, rutile, apatite and zircon, Figure 7-5. The white micas and biotites are up to 3 mm in length and define the planar fabric. The biotites have zircon inclusions with pleochroic halos and both the white micas and biotites have inclusions of an opaque mineral.

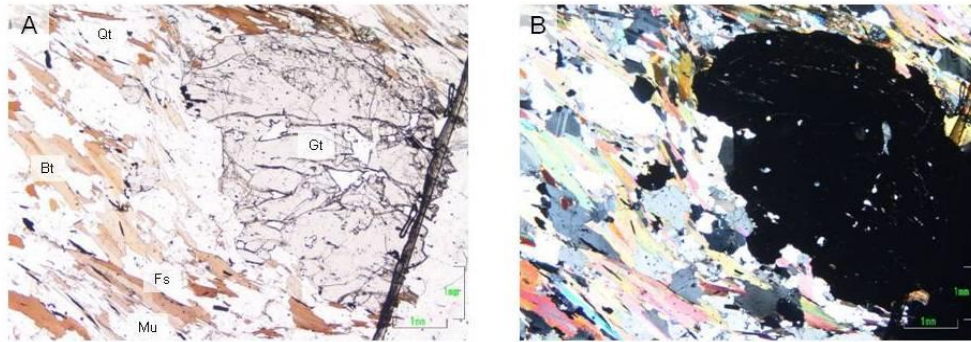


Figure 7-5 AB07-04 in thin section showing the coarser nature of this sample compared with AB07-02 and AB07-03. The thin section also shows plentiful biotite.

AB07-08 - Basal Pelite [NG 7689 1491]

The sample is a garnet-mica schist from the Basal Pelite of the Morar Group close to Sandaig. The garnets from this sample have yielded one robust Lu-Hf age from the garnet rim of 458.7 ± 2.8 Ma and one robust Sm-Nd age from the garnet core of 449.7 ± 2.3 Ma.

The ages from the garnets within this sample indicate that this sample has been affected by the Caledonian orogeny. The fabric of this sample is fine-grained and consists of white mica, quartz, biotite and feldspar which are all very inclusion-rich (Figure 7-6). The inclusions are predominantly opaque minerals. Also within this sample are large biotite porphyroblasts (up to 4 mm) which are very rich in zircon inclusions and often have a mica fish appearance.

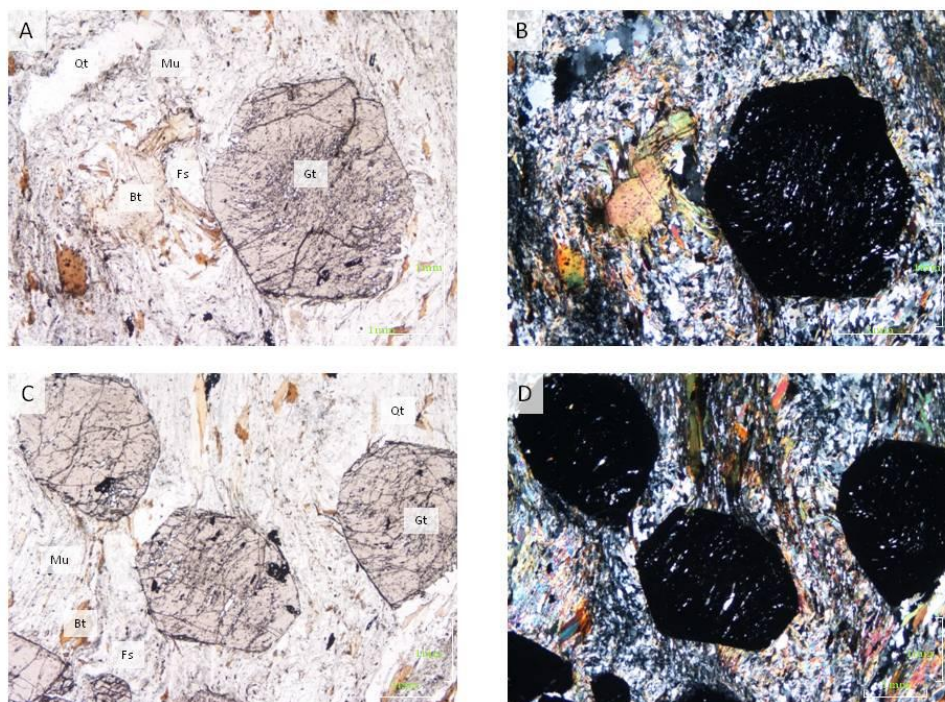


Figure 7-6 AB07-08 in thin section showing large biotite porphyroblasts with a fine-grained matrix surrounding them consisting of quartz, biotite and white mica.

AB07-11 – Armadale Pelite [NG 6409 0353]

The Armadale Pelite is a mylonitic pelite from the Morar Group within 4 km of the Moine Thrust Zone. The sample is a garnet-mica schist. This sample yielded one meaningful Lu-Hf age of 464.9 ± 2.4 Ma. This age shows that main phase of garnet growth recorded within this sample was during the Mid-Ordovician and was likely related to the Grampian event.

The white mica and most of the biotite make P domains in the crenulated fabric with some biotite present in the Q domains (Figure 7-7). The biotites are larger than the white micas reaching up to 1.5 mm while the white micas only reach 0.5 mm in size. The white micas are fairly free of inclusions and the biotites have zircon inclusions and are sometimes altered to retrogressive chlorite.

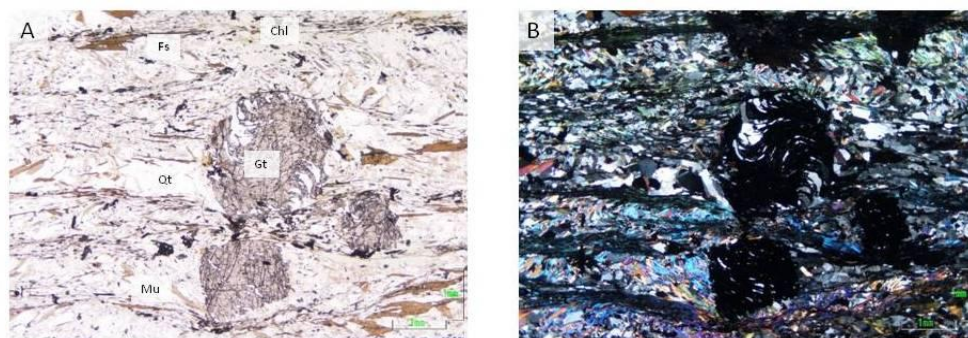


Figure 7-7 AB07-11 in thin section showing the crenulated matrix with quartz-rich and mica-rich domains.

AB07-12 – Eastern Unit Pelite [NG 9049 2330]

This sample is a garnet-kyanite-pelite from the metasedimentary rock series of the Eastern Unit of the Glenelg-Attadale basement inliers. The white mica in this sample has been studied by Rawson (2002) who found them to be phengitic in composition, indicating that they may be relicts of the eclogite facies metamorphism. This study has obtained a Lu-Hf age of 1669.6 ± 28.0 Ma and a Sm-Nd age of 912.5 ± 2.0 Ma from the garnets, this younger age probably reflects resetting during the Neoproterozoic metamorphic events. These ages suggest that the Caledonian event in this area was not of a high enough temperature to reset the Lu-Hf and Sm-Nd systems in garnet.

Biotite, white mica, plagioclase and quartz define the fabric which wraps the garnets, Figure 7-8. Kyanite is found with the plagioclase. Biotite is far more plentiful than white mica and the biotites are larger reaching up to 1 mm in size and they also have zircon inclusions. The white micas are up to 0.75 mm in length and have few inclusions of an opaque mineral.

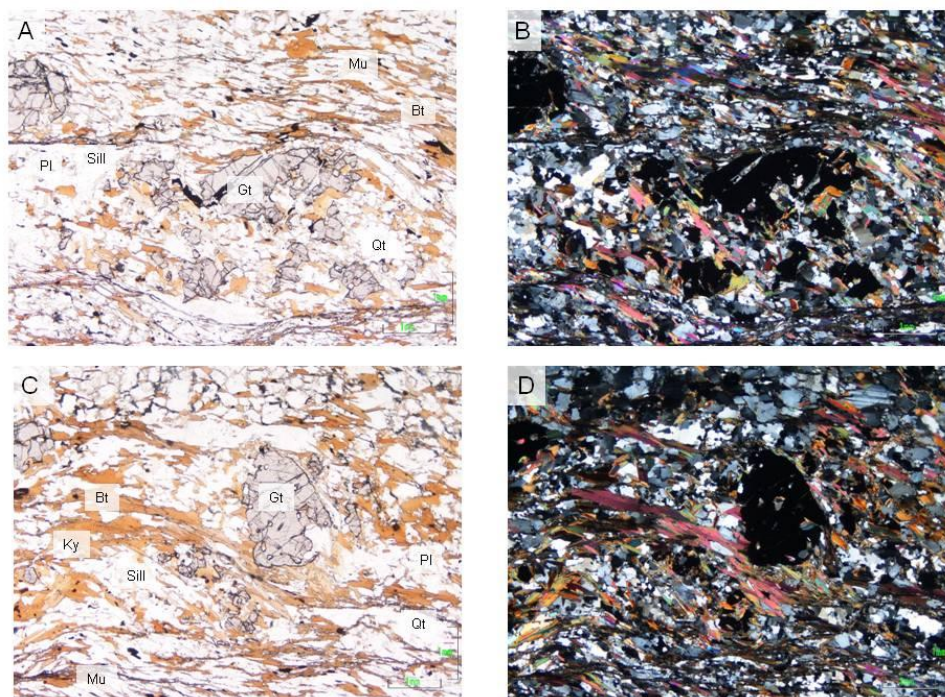


Figure 7-8 AB07-12 in thin section showing the plentiful biotite wrapping the garnets with white mica and opaque minerals.

AB07-13 – Drumnadrochit Migmatite [NH 4888 3233]

This sample is from the Glenfinnan Group migmatites exposed near Drumnadrochit. It is close to where Cutts et al. (2010) obtained their sample for monazite and zircon geochronology which showed three zones within one large garnet. The garnet core had inclusions which gave U-Pb monazite ages in the range of 825-780 Ma, the middle zone contained ~725 Ma inclusions and the outer zone (rim) ~465 Ma inclusions. This study obtained a two point isochron core age of 501.7 ± 3.4 Ma and a two point isochron rim age of 491.9 ± 3.5 Ma were also obtained. These ages show that this area has been subjected to Neoproterozoic and Caledonian metamorphism and all the events have been recorded so that the Sm-Nd ages are mixtures of all the metamorphic events.

The gneissic fabric is defined by biotite, white mica, plagioclase and quartz with rutile and kyanite present also present (Figure 7-9). The kyanite is always associated with a fine-grained white mica indicating that it is not in equilibrium. The biotites are up to 0.5 mm in size and have zircon inclusions. The white micas are up to 1 mm in size and

have few opaque inclusions and are often associated with the fine-grained mica that is reacting with kyanite.

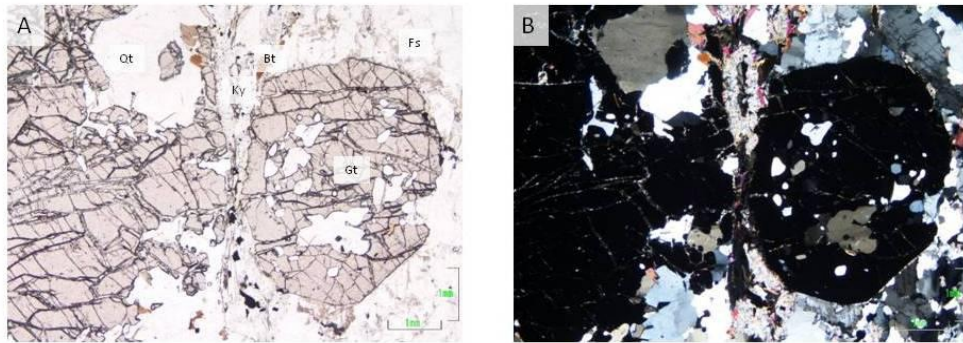


Figure 7-9 AB07-13 in thin section showing kyanite surrounded by fine-grained white mica and the gneissic fabric of the sample.

AB07-15 – Talmine Pelite [NC 5735 6324]

The Talmine Pelite is a biotite-white mica-garnet-albite-quartz schist from the Moine Nappe in north Sutherland. This study has obtained a Lu-Hf garnet age of 449.3 ± 1.2 Ma and a Sm-Nd age of 455.8 ± 7.5 Ma, which shows that garnet growth occurred during the Caledonian orogeny.

The fabric is dominated by white mica and biotite which is locally crenulated, Figure 7-10. The biotites are up to 1 mm and have zircon inclusions with pleochroic halos. Some of the biotites appear to be cross-cutting the main fabric indicating that some biotite growth occurred after the main phase of deformation. White mica is found mainly in P domains of the crenulated cleavage and is up to 1.5 mm.

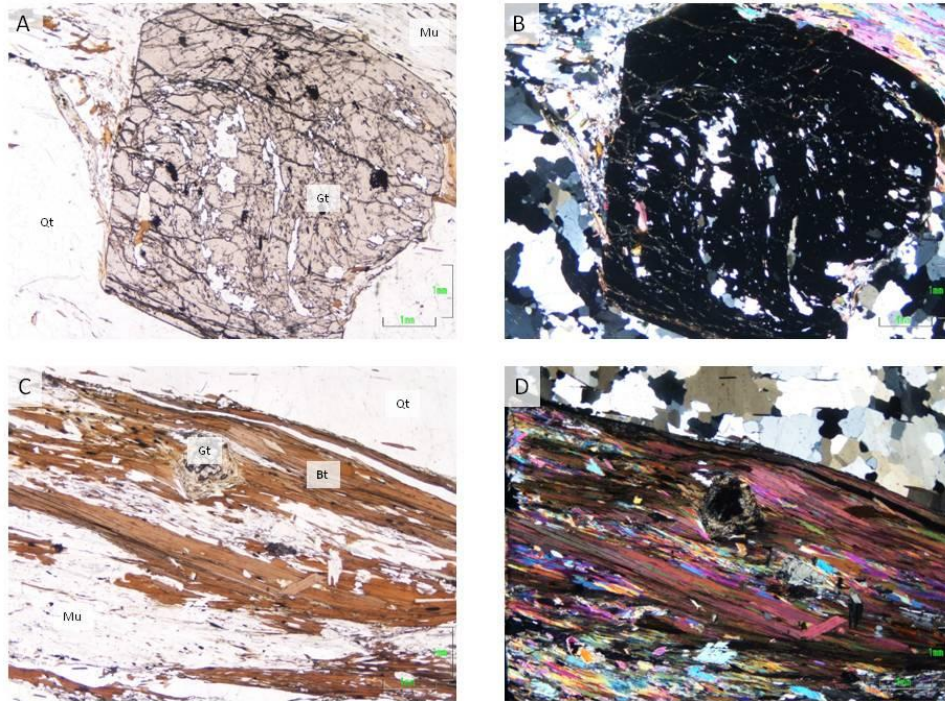


Figure 7-10 AB07-15 in thin section showing large garnets wrapped by the mica and quartz-rich fabric. C and D show the biotite and quartz-dominated layers.

AB07-27 – Leven Schist [NN 2611 8032]

The sample is from part of the Leven Schist which is part of the Appin Group within the Dalradian Supergroup. It is a biotite-garnet-mica schist with large (up to 5 mm) garnet and biotite porphyroblasts. It yielded a Lu-Hf garnet age of 470.8 ± 2.2 Ma which correlates well with previously published garnet ages from the Dalradian Supergroup (e.g. Oliver et al., 2000; Baxter et al., 2003) and indicates that this sample has been affected by the Grampian event.

The matrix is fine-grained (0.1 mm) with a weakly developed S_2 crenulation and is made up of white mica, quartz and biotite with accessory apatite, zircon and opaques, Figure 7-11. The matrix biotite has mainly been converted to chlorite. There are larger biotite porphyroblasts which are up to 2 mm in size which have zircon inclusions that are weakly curved with pleochroic halos and chlorite rims. Similar to the garnets the biotite poikiloblasts are post- D_1 .

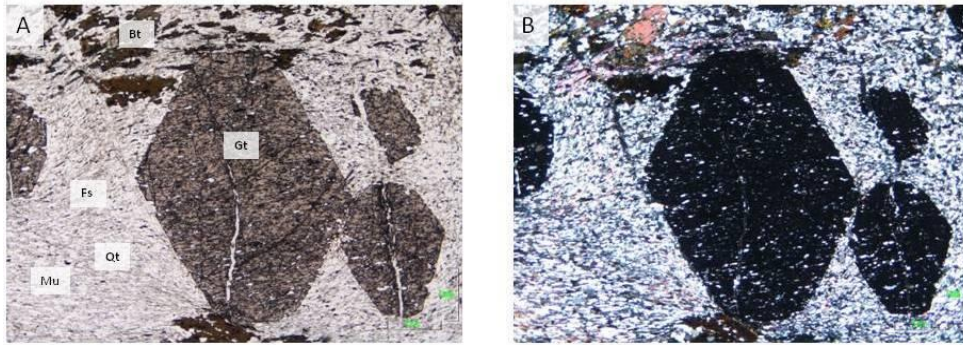


Figure 7-11 AB07-27 in thin section showing the crenulated fine-grained matrix consisting of quartz, white mica and biotite.

AB07-29 – Shiaba Pelite [NM 4438 1890]

The sample is from the Shiaba Pelite of the Morar Group on the Ross of Mull. It is a garnet-mica schist, although it contains evidence that it may have once had kyanite or staurolite, seen by fine-grained mica-filled pseudomorphs. It has yielded a Lu-Hf core age of 877.8 ± 3.5 Ma and a rim age of 831.8 ± 3.2 Ma. It only gave one meaningful Sm-Nd age of 665.2 ± 9.5 Ma from the garnet rim. The sample was affected by Neoproterozoic metamorphism and later metamorphism was not of high enough grade to reset Lu-Hf in garnet. It is possible that Sm-Nd may have been partially reset during Caledonian metamorphism but, as there is no LA ICPMS for this sample, it is difficult to ascertain whether or not this has occurred.

The matrix is crenulated and consists of Q and P domains (Figure 7-12). The white micas are up to 1 mm in length and have inclusions of an opaque mineral. The biotites are finer (up to 0.5 mm with zircon inclusions). The biotites also replace a high relief elongate mineral which is likely to have been kyanite or staurolite.

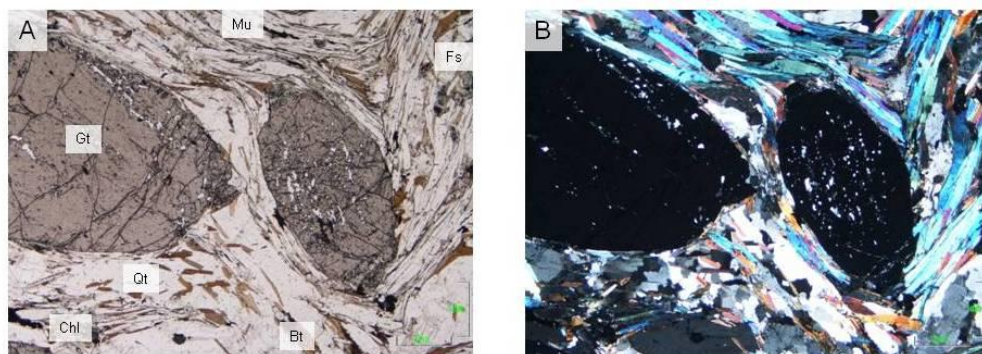


Figure 7-12 AB07-29 in thin section showing the strongly crenulated cleavage made up of white mica and biotite.

AB07-31 – Meadie Pelite [NC 5231 4022]

AB07-31 is the Meadie Pelite in central Sutherland, which was assigned to the basement by Moorhouse & Moorhouse (1988), but now is attributed to the Morar Group. This study has given Sm-Nd core ages of 841.3 ± 8.6 Ma and 950.9 ± 34.0 Ma and rim ages of 701.7 ± 9.7 Ma and 772.5 ± 26.0 Ma. Lu-Hf core and rim ages of 947.0 ± 4.2 Ma and 942.1 ± 3.7 Ma have also been obtained. These ages show that the main phase of metamorphism that this sample has recorded was in the Neoproterozoic.

This sample is a garnet-staurolite-kyanite schist, the matrix consists quartz, K feldspar, white mica and chlorite (Figure 7-13). Much of the biotite has been converted to chlorite and has inclusions of zircon. The white mica often has a dusty appearance and has inclusions of an opaque mineral. Both the white micas and biotites reach up to 1 mm in size. The fabric is continuous with the inclusion trails within the garnet, suggesting that the garnets are post-kinematic.

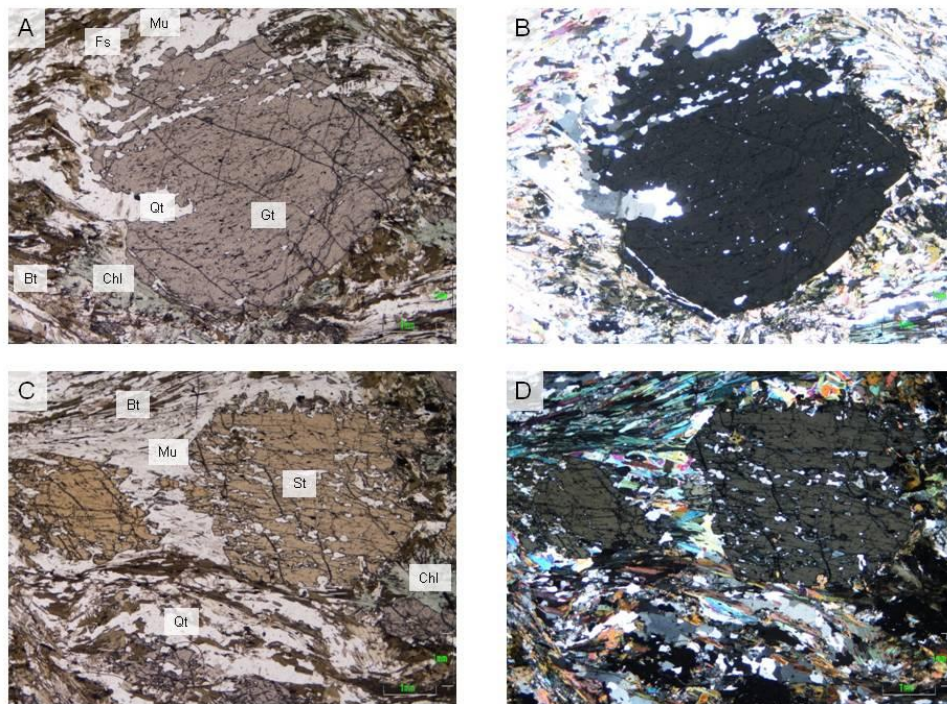


Figure 7-13 AB07-31 in thin section showing biotite that has been converted to chlorite with white mica which make up the fabric that joins up with inclusions in the garnet porphyroblasts.

7.5 Results and interpretation

The Rb-Sr analyses provide eleven two-point white mica-whole rock isochrons, shown in Table 7-2, and eleven two-point biotite-whole rock isochrons. The Morar Group in the south-west Moine gives three two point white mica-whole rock isochrons in the range of 472-546 Ma. AB07-02 (Polnish Pelite) gave a two point white mica age of 472.3 ± 1.6 Ma; the error is larger on this age than the other samples analysed due to the similarity of the $^{87}\text{Sr}/^{86}\text{Sr}$ white mica ratio to the whole rock ratio. However as the $^{87}\text{Rb}/^{86}\text{Sr}$ white mica ratio is double the whole rock the sample is radiogenic. AB07-03 (Glenuig Pelite) gave a white mica age of 486.2 ± 0.84 Ma which is a good age with a small error, as both of its ratios are significantly different from the whole rock ratios. AB07-29 (Shiaba Pelite) gave a white mica age of 545.7 ± 1.3 Ma, similar to AB07-02 the larger error is most likely due to the similarity of the $^{87}\text{Sr}/^{86}\text{Sr}$ white mica ratio to that of the whole rock, however as the $^{87}\text{Rb}/^{86}\text{Sr}$ ratio is 3.307 the age should be reliable. AB07-11 (Armadale Pelite) close to the Moine Thrust Zone gave a white mica-whole rock age of 428 ± 5 Ma, the white mica from this sample was not very radiogenic, only giving a $^{87}\text{Rb}/^{86}\text{Sr}$ ratio of 1.899 which is quite similar to the whole rock. AB07-08 (Basal Pelite) yielded a white mica age of 239.4 ± 6 Ma, this sample had $^{87}\text{Rb}/^{86}\text{Sr}$ and $^{87}\text{Sr}/^{86}\text{Sr}$ ratios that were lower than the whole rock values; this is most likely due to the high Sr content relative to Rb content of the white mica which has made the sample unradiogenic. AB07-15 (Talmine Pelite) gave a white mica age of 356.8 ± 1 Ma, the $^{87}\text{Rb}/^{86}\text{Sr}$ and $^{87}\text{Sr}/^{86}\text{Sr}$ ratios from the white mica were lower than the whole rock ratios and similarly to AB07-08 it is most likely because of the high Sr content of the white mica relative to the Rb content. The same conclusion applies for AB07-27 (Leven Schist) which gave a white mica age of 382 ± 6 Ma and also had a white mica $^{87}\text{Rb}/^{86}\text{Sr}$ ratio lower than the whole rock. AB07-31 (Meadie Pelite) gave an age of -4.6 ± 0.56 Ma which is due to the high $^{87}\text{Rb}/^{86}\text{Sr}$ of 7.248 seen in the whole rock; this is probably due to the very low Sr content relative to the Rb content of the whole rock fraction.

AB07-13 (Drumnadrochit Migmatite) from the Glenfinnan Group give a white mica-whole rock age of 483.0 ± 1.2 Ma, the larger error seen here is due to the similarity of the $^{87}\text{Sr}/^{86}\text{Sr}$ white mica ratio to the whole rock. AB07-04 (Loch Eilt Pelitic Gneiss) gave a white mica age of 444.4 ± 1.9 Ma which is a reliable age as both its $^{87}\text{Rb}/^{86}\text{Sr}$ and $^{86}\text{Sr}/^{86}\text{Sr}$ ratios are larger than the whole rock.

AB07-12 (Eastern Unit Pelite) from the Glenelg-Attadale basement inlier gave a two point white mica-whole rock age of 1025.4 ± 9.6 Ma, which is reliable as the $^{87}\text{Rb}/^{87}\text{Sr}$ and $^{87}\text{Sr}/^{86}\text{Sr}$ ratios from the white mica fraction are higher than the whole rock.

The Rb-Sr analyses gave eleven biotite-whole rock isochrons, shown in Table 7-2, in the range of 395-436 Ma. The biotite analyses were all radiogenic with the lowest $^{87}\text{Rb}/^{86}\text{Sr}$ ratio being 24-730. The youngest biotite date was from AB07-15 (Talmine Pelite) which gave an age of 394.1 ± 0.6 Ma and the oldest biotite date was 435.7 ± 0.4 Ma from the Leven Schist (AB07-27) of the Dalradian Supergroup. The oldest biotite date from within the Moine Supergroup was 428.3 ± 0.5 Ma from AB07-03 (Glenug Pelite).

Table 7-2; Rb-Sr Mica Analyses Results, (Bird & McDermott, Nuffield bursary, RHUL). The dates marked with an asterisk are samples that were not radiogenic enough to provide a meaningful age.

Sample Fraction	Rb ppm	Sr ppm	$^{87}\text{Sr}/^{86}\text{Sr}$	2se	$^{87}\text{Rb}/^{86}\text{Sr}$	Initial $^{87}\text{Sr}/^{86}\text{Sr}$	Rb-Sr Age (Ma)
AB07-02 WR	107.1900	300.6700	0.72352	0.00001	1.0294		
AB07-02 Mu	176.1000	251.4400	0.73021	0.00001	2.0236	0.71659	472.3 ± 1.6
AB07-02 Bt	370.6900	29.6266	0.93590	0.00002	36.8774	0.71742	416.0 ± 0.4
AB07-03 WR	144.9300	227.6900	0.72961	0.00001	1.8390		
AB07-03 Mu	221.3200	119.7300	0.75395	0.00002	5.3533	0.71687	486.2 ± 0.8
AB07-03 Bt	360.4700	44.5711	0.86278	0.00001	23.6698	0.71839	428.3 ± 0.5
AB07-04 WR	185.4500	103.4600	0.74333	0.00002	2.0526		
AB07-04 Mu	261.0600	261.3800	0.77670	0.00003	7.3237	0.73034	$444.4 \pm 1.9^*$
AB07-04 Bt	670.4400	3.7700	5.04000	0.020000	729.9903	0.73121	414.4 ± 3.9
AB07-08 WR	134.5984	201.2600	0.73418	0.00001	1.9331		
AB07-08 Mu	150.8158	254.3100	0.73344	0.00001	1.7140	0.72760	$239.4 \pm 6.0^*$
AB07-08 Bt	388.0960	14.8487	1.19249	0.00002	78.9255	0.72268	418.0 ± 0.4
AB07-11 WR	114.9645	256.1200	0.72660	0.00001	1.2965		
AB07-11 Mu	177.2073	269.5900	0.73027	0.00004	1.8992	0.71869	428.1 ± 5.0
AB07-11 Bt	374.1603	14.8179	1.17062	0.00003	76.0939	0.71890	416.8 ± 0.4
AB07-12 WR	128.8142	192.9100	0.74818	0.00001	1.9327		
AB07-12 Mu	194.6888	248.9500	0.75305	0.00001	2.2646	0.71983	1025.4 ± 9.6
AB07-12 Bt	296.1998	8.9906	1.32793	0.00003	100.7439	0.71890	412.0 ± 0.4
AB07-13 WR	83.5971	205.0000	0.72850	0.00001	1.1780		
AB07-13 Mu	151.6187	159.4200	0.73932	0.00001	2.7504	0.72039	483.0 ± 1.2
AB07-13 Bt	340.9705	3.8799	2.44790	0.00002	296.4955	0.72164	408.8 ± 0.4
AB07-15 WR	162.0181	120.0181	0.77611	0.00002	3.9179		
AB07-15 Mu	159.8365	360.9895	0.76273	0.00003	1.2834	0.75621	$356.8 \pm 1.0^*$

AB07-15 Bt	441.3075	8.8421	1.63599	0.00005	156.9559	0.75409	394.6 ± 0.4
AB07-27 WR	188.0092	211.0000	0.75281	0.00001	2.5802		
AB07-27 Mu	170.6310	219.5500	0.75102	0.00001	2.2501	0.73877	382.1 ± 5.5*
AB07-27 Bt	747.8691	20.7272	1.42784	0.00005	111.3508	0.73680	435.7 ± 0.4
AB07-29 WR	119.4959	232.1500	0.73127	0.00001	1.4874		
AB07-29 Mu	196.7660	172.1600	0.74542	0.00001	3.3072	0.71970	545.7 ± 1.3
AB07-29 Bt	410.6313	9.3603	1.54040	0.00001	136.7782	0.72237	419.9 ± 0.4
AB07-31 WR	162.5686	65.2360	0.79665	0.00001	7.2480		
AB07-31 Mu	215.8024	125.5600	0.79680	0.00001	4.9982	0.79712	-4.57 ± 0.6*
AB07-31 Bt	405.7732	12.0309	1.34889	0.00005	103.3355	0.75500	403.6 ± 0.4

7.6 Discussion

It has been suggested by several authors (Holdsworth 1989; Coward et al., 1990; Dallmeyer et al., 2001; Strachan et al., 2002; Kinny et al., 2003; Holdsworth et al., 2006, 2007) that the youngest of the Caledonian events in the Northern Highlands, the Scandian (440-420 Ma) probably reached amphibolite facies throughout the Moine Supergroup. This would suggest that it would have overprinted earlier Grampian (470-460 Ma) and Knoydartian (840-700 Ma) deformation and that the Rb-Sr white mica and biotite ages would reflect cooling from it. Previous geochronology has supported this in that the only Neoproterozoic ages from white micas came from very large mica books which would be extremely difficult to reset.

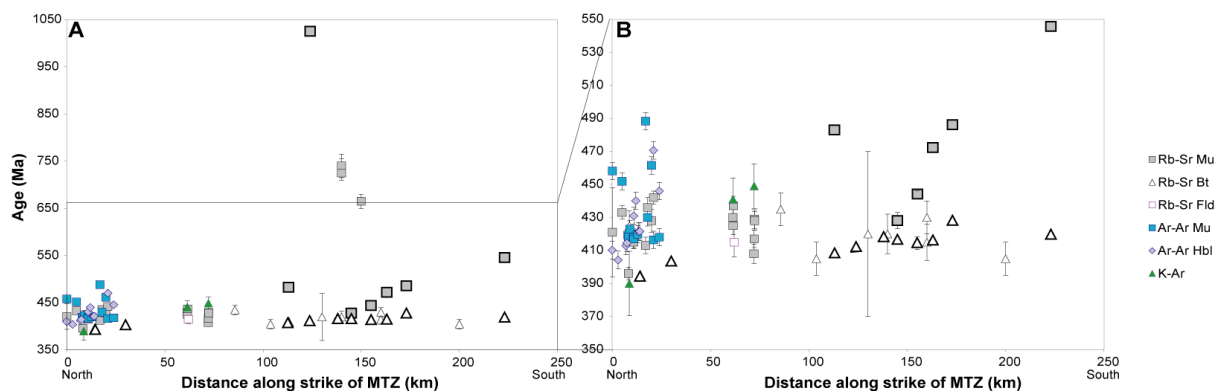


Figure 7-14, data from this study plotted with all previously published ages against distance along the Moine Thrust Zone, a shows all the dates and b shows the ages between 550 – 350 Ma. These graphs exclude sample AB07-27 (Leven Schist) as it is not part of the Moine Supergroup but part of the Dalradian Supergroup. Samples analysed for this study are marked in bold.

Figure 7-14A shows all the Rb-Sr ages from this study plotted with the previously published data along strike of the Moine Thrust Zone. The symbols with the heavy black outlines are the results from this study. There are several outliers, including the

Neoproterozoic ages from Giletti et al. (1961) and one Mesoproterozoic white mica age from AB07-12 (Eastern Unit Pelite) which is from the Glenelg-Attadale basement inlier. The white mica from AB0-12 is radiogenic and the age is interpreted to either reflect cooling from an earlier event which affected the basement or partial resetting of an older age by Knoydartian and/ or Caledonian metamorphism. Figure 7-14B shows the data between 550 Ma and 350 Ma to look closely at cooling related to the Caledonian orogeny.

Samples AB07-29 (Shiaba Pelite), AB07-03 (Glenuig Pelite), AB07-13 (Drumnadrochit Migmatite) and AB07-02 (Polnish Pelite) give white mica ages too old to be related to cooling from the Scandian or Grampian events. These ages are likely to represent partial resetting of Neoproterozoic ages by Caledonian heating. This is consistent with the Neoproterozoic ages obtained from the garnets from AB07-29, AB07-03 and AB07-02. As the white micas from these samples were not large (<1.5 mm), these ages suggest that in many parts of the Northern Highlands Caledonian deformation did not exceed 500°C , or did not exceed 500°C for very long, otherwise the white micas would have been completely reset and would give ages <460 Ma. Cutts et al. (2010) dated monazite inclusions within a garnet close to where AB07-13 was sampled and obtained 780 Ma ages from the core and 464 Ma from monazite inclusions within the garnet rim. Pressure and temperature estimates associated with this later phase of garnet growth are ~ 7 kbar and 650°C , which shows that during the Grampian event temperatures were high enough to grow garnet. The white mica from this sample gave an age of 483.0 ± 2.3 Ma which suggests that the Grampian event had not succeeded in completely resetting the Rb-Sr system within the white micas, although most of the white mica could have grown during the Grampian. AB07-11 (Armada Pelite) is the only sample which gives a white mica ages that can be related to cooling from the Caledonian orogeny of 428.1 ± 5 Ma. The garnet from this sample gave a Mid-Ordovician age which is likely to be related to peak metamorphism of this sample relates to the Grampian event. The white mica age could either to relate to cooling from the Grampian event or dating the shear fabric which wraps the garnet.

The data show a general increase in Rb-Sr biotite ages towards the southern parts of the Moine Supergroup; this is also seen in the new Rb-Sr white mica ages. The oldest Rb-Sr biotite age is from AB07-27 (Leven Schist) of 435.7 ± 0.4 Ma and relates to cooling

from the Grampian event within the Dalradian Supergroup. Within the Moine Supergroup the oldest ages are from AB07-03 (Glenuig Pelite) of 428.3 ± 0.5 Ma which could easily relate to cooling from the Grampian but not from the Scandian. The rest of the Rb-Sr biotite ages obtained fall between 419.9 ± 0.4 Ma (AB07-29), 418.0 ± 0.4 Ma (AB07-08) and 394.6 ± 0.4 Ma (AB07-15). These ages could be perceived as either cooling from the Scandian or the Grampian events. An alternative is that the biotite ages relate to peak metamorphism at lower temperatures than previously published. The biotite Rb-Sr data obtained in this study on its own shows an increase in age from the north to the south. This suggests that the northern parts of the Moine Supergroup were at $\sim 300^\circ\text{C}$ more recently than the south. It is difficult to see this in the previously published data as no one technique has been used throughout the Moine Supergroup, although it could be said that the Rb-Sr biotite and the K-Ar data support this.

The pairs of mineral analyses that are available for many of the samples might allow an evaluation of relative rates of cooling through contrasting T_C . The sample with the largest difference between white mica age and biotite age is AB07-12 (Eastern Unit Pelite); however, it is unlikely that the difference in these ages represents cooling from a metamorphic event, as it would suggest ~ 600 Ma of cooling. The sample with the largest difference between its white mica and biotite ages that could possibly be explained by cooling is AB07-29 (Shiaba Pelite). Assuming a T_C of Rb-Sr in white mica of 500°C and biotite of 300°C (Armstrong et al., 1966; Jäger 1979), AB07-29 gives cooling of $1.6^\circ\text{C}/\text{Ma}$ which is the slowest cooling rate within this study. However, as mentioned earlier the white mica ages from this sample (and AB07-02, AB07-03 and AB07-13) are likely to represent partial resetting of earlier Knoydartian ages, thus cooling rate calculations for these samples are difficult and may not mean very much. AB07-04 (Loch Eilt Pelitic Gneiss) gives a cooling rate of $6.7^\circ\text{C}/\text{Ma}$ which is similar to the uplift rate of parts of the Dalradian Supergroup (Dempster 1985) and faster than the northern Moine of Sutherland (Dallmeyer et al., 2001). The fastest cooling rate is from AB07-11 (Armadale Pelite) of $17.7^\circ\text{C}/\text{Ma}$, this sample is from close to the Moine Thrust Zone which suggests thrust movement lead to fast exhumation and rapid cooling.

7.7 Conclusions

1. The white mica and biotite ages clearly show a systematic variation from south to north with the southern localities yielding older ages and larger differences between the white mica and biotite ages.
2. The white mica ages from all the samples apart from AB07-11 (Armadale Pelite) partially reflect Knoydartian metamorphism; therefore this is the only sample which can give information on post-Caledonian uplift. AB07-11 (Armadale Pelite) is from close to the Moine Thrust Zone and has a fast cooling rate suggesting that uplift close to the thrust was more rapid than elsewhere in the Moine Supergroup. This is complemented by the significantly slower cooling rate from AB07-04 which is from the Glenfinnan Group.

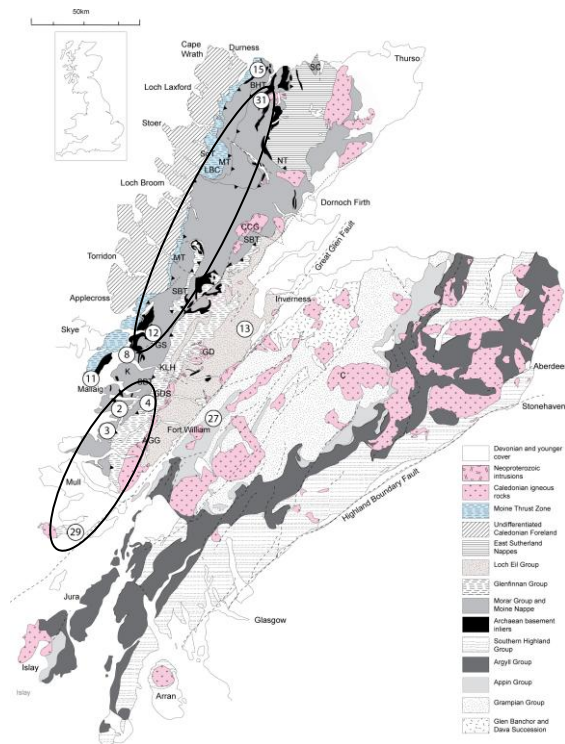


Figure 7-15 a simplified geological map of the Northern Highlands. The samples that do not give Caledonian garnet or white mica ages are circled.

3. A correlation can be drawn between the ages obtained from the garnets and the Rb-Sr white mica ages. In samples which record Neoproterozoic metamorphism (AB07-02, AB07-03, AB07-29) the white mica Rb-Sr ages are typically older than the Caledonian Orogeny, these samples are circled in Figure 7-15. The data from these samples suggest that in these areas Caledonian metamorphism

was not hot ($\sim 500^{\circ}\text{C}$) enough to have completely reset the Rb-Sr system. This suggests that in many parts of the Moine Supergroup neither the Grampian or Scandian events reached amphibolite facies grade.

4. The data from Cutts et al. (2010) for AB07-13 (Drumnadrochit Migmatite) shows that, while in parts of the Moine Supergroup the Caledonian Orogeny was not hot enough to grow garnet or to completely reset Rb-Sr in white mica, in other parts it gave estimated pressures and temperatures of ~ 7 kbar and 650°C . Caledonian garnets have also grown in several places in the samples that are not circled in Figure 7-15.

8.1 Introduction

The previous chapters have detailed new ages for the many phases of metamorphism that the Moine Supergroup has undergone. This chapter discusses the data as a whole to give more detail on the merits of the data set and to give a detailed geological history of the Moine Supergroup.

8.2 Garnet size and age

Several of the previous chapters have touched briefly on garnet size and the effect that it may have on the ages obtained. Larger garnets could potentially give older Sm-Nd and Lu-Hf ages as their larger size would make it more difficult for Hf or Nd to diffuse out of the garnet, thus would effectively give the larger garnet a higher closure temperature (T_C). Conversely it could be expected that smaller garnets would be more easily reset by later metamorphic events than larger garnets. Using this information it might be expected that larger garnets should yield older ages than smaller garnets. Figure 8-1 shows the size of all the garnets analysed within this study with their corresponding Lu-Hf and Sm-Nd age.

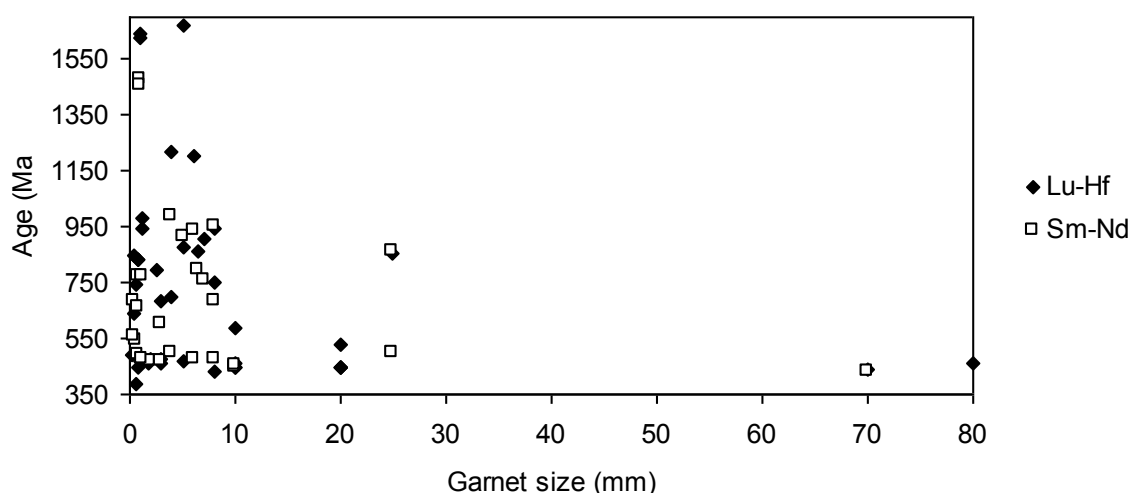


Figure 8-1 garnet size versus Lu-Hf and Sm-Nd age.

The garnet size used in Figure 8-1 is the average diameter in mm of the garnet using the thin section from the corresponding sample. In instances where it was felt that the thin section was not representative of the garnets throughout the same, a hand specimen was also used. Where garnet cores and rims were dated, the core was the full diameter of the garnet, including the rim, whereas the rim was just measured as the outer rim of the garnet. The reason for this was that it was assumed that Lu, Hf, Sm and Nd in the garnet core would have to diffuse through the garnet rim to escape. The figure shows no obvious correlation between garnet size and the age obtained, which suggests that all of the ages should reflect garnet growth or cooling from peak metamorphism.

8.3 Difference between Lu-Hf and Sm-Nd ages

This study has used both Lu-Hf and Sm-Nd to date the same garnet fractions, this data has been plotted in Figure 8-2. It can be seen that there is a general correlation between the Lu-Hf and Sm-Nd ages with the Sm-Nd ages usually being between 10-25% younger than the Lu-Hf ages.

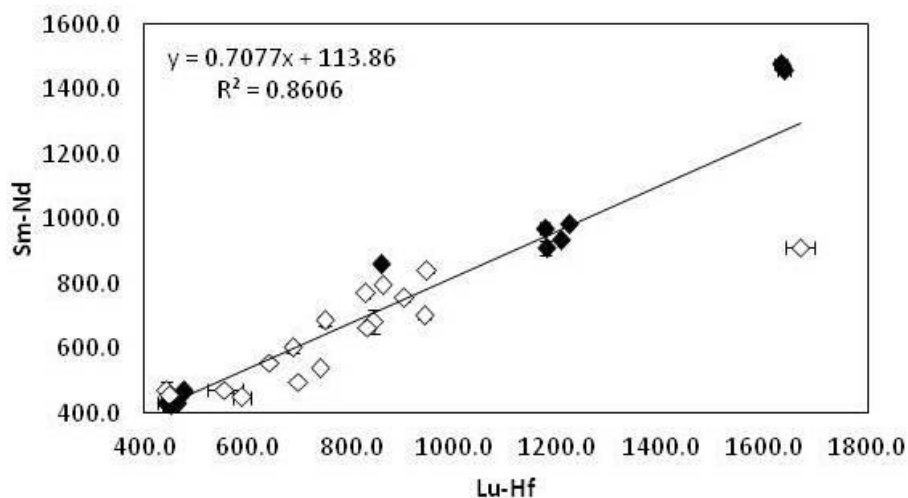


Figure 8-2 graph showing Lu-Hf ages versus Sm-Nd ages on all garnets which gave reliable ages. The empty symbols give ages from pelites and the filled symbols give ages from eclogites, amphibolites and granulites.

There are some exceptions, for example, the Grampian ages from the Drumnadrochit Amphibolite (AB07-14) are within error for both systems, these ages are seen in the bottom left-hand side of the graph. The Sm-Nd age from the Eastern Unit Pelite is

~45% younger than the Lu-Hf age; this is the right-hand most point which lies below the trend line. Another interesting observation is the spread of pelites along the trend (open symbol) when compared with the samples which have igneous protoliths (closed symbols), this could partly be due to the number of pelites sampled compared with amphibolites, eclogites etc. but it is something that requires more study.

8.4 Summary of conclusions from the previous chapters

The locations of all of the samples that were analysed from the Scottish mainland are shown in Figure 8-3; some of the sample names have been abbreviated and are detailed in the figure caption.

8.4.1 The basement inliers

The earliest phase of metamorphism recorded within the Moine Supergroup was dated at ~1670 Ma and ~1640 Ma from the Borgie Inlier and the metasediments from the Eastern Unit of the Glenelg-Attadale Inlier. These ages are within error of 1750-1640 Ma metamorphism reported from the Western Unit of the Glenelg-Attadale inlier by Storey et al. (2010). This event possibly could correlate with the later Laxfordian events recorded on the Caledonian foreland in Scotland (Kinny et al. 2005; Wheeler et al. 2010), which from a broader perspective most likely link with Labradorian (NE Laurentia) and Gothian (Baltica) events (Park 1995; Buchan et al. 2000).

The next phase of peak metamorphism recorded within the Northern Highland terrane was late Mesoproterozoic eclogite-facies metamorphism at ~1200 Ma within the Eastern Unit of the Glenelg-Attadale inlier. The timing of this eclogite-facies event is significantly older than that proposed by Sanders et al. (1984), and younger than the eclogite-facies event recorded within the WU. It is suggested here that this event corresponds to the Elzevirian phase of the Grenville orogeny in NE Laurentia (Karlstrom et al. 1999; 2001).

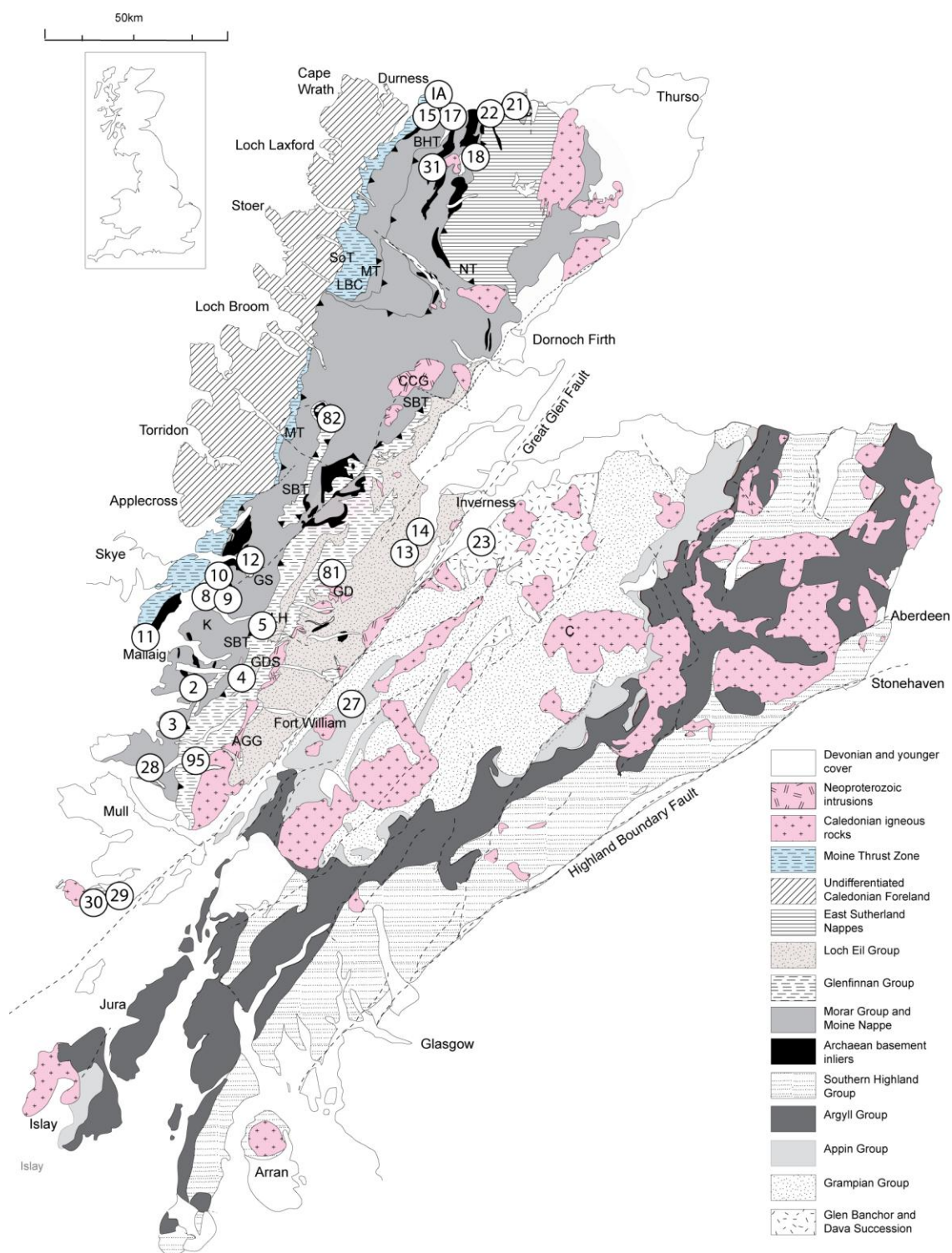


Figure 8-3, simplified geological map of the Northern Highland and Grampian terranes, Abbreviations are; AGG – Ardgorr Granitic Gneiss; BHT – Ben Hope Thrust; C – Cairngorms; CCG – Carn Chuinneag Granite; GD – Glen Doe; GS – Glen Shiel; K – Knoydart; KLH – Kinlochourn; LBC – Loch Borrolan Complex; MT – Moine Thrust; NT – Naver Thrust; SBT – Sgurr Beag Thrust; SC – Strathy Complex; SoT – Sole Thrust. Sample numbers are 2 – AB07-02; 3 – AB07-03; 4 – AB07-04; 5 – AB07-05; 8 – AB07-08; 9 – AB07-09; 10 – AB07-10; 11 – AB07-11; 12 – AB07-12; 13 – AB07-13; 14 – AB07-14; 15 – AB07-15; 17 – AB07-17; 18 – AB07-18; 21 – AB07-21; 22 – AB07-22; 23 – AB07-23; 27 – AB07-27; 28 – AB07-28; 29 – AB07-29; 31 – AB07-31; 81 – AB08-01; 82 – AB08-02; 95 – AB09-05; 1A – 1A1.

Both units within the Glenelg-Attadale inlier also gave ages that ranged between 1020 Ma and 912 Ma (this study; Sanders et al. (1984); Storey et al. (2010); Brewer et al. 2003), which have been interpreted to reflect thermal reworking during a younger metamorphic event. In the past, this younger phase of deformation has been assigned to the Ottawan phase of the Grenville orogeny. However, Lu-Hf ages obtained from the Morar Group show that there was an early garnet growth event at ~950 Ma to 900 Ma, so early Neoproterozoic events were not restricted to the basement inliers. These younger ages recorded from within the Glenelg-Attadale inliers may therefore result from variable to complete degrees of isotopic resetting during the garnet growth event recorded by the Morar Group. According to Figure 8-4 it would be easier to correlate the 1025-900 Ma events recorded by the inliers to Renlandian-related partial resetting than the Grenville.

8.4.2 Neoproterozoic garnet growth

The early garnet growth event (~950 Ma) recorded within the Morar Group was followed by another garnet core growth event at 880-860 Ma, then a garnet rim growth event at 840-830 Ma. All of these early garnet growth events were recorded using Lu-Hf dating as the LA ICPMS traces from these samples show that the Lu trace retains prograde zoning, thus these ages relate to garnet growth and are not cooling ages. Pressure and temperature estimates from these samples or from samples close by (Vance et al. 1998; Cutts et al. 2009; 2010; Cutts et al. unpublished) suggest that the garnets have not been through a high enough temperature for the Lu-Hf ages to reflect cooling from peak metamorphism. The early (>900 Ma) ages from the Morar Group have more in common with 'Renlandian' than 'Knöydartian' events which shows that the Renlandian was recorded as far south as the Scottish Highlands (Figure 8-4). Ages of 857 Ma (Lu-Hf) and 863 Ma (Sm-Nd) which are within the garnet core growth range of the Morar Group were obtained from possible basement at Migga Ness within the Hascosay Slide in Shetland, units within this slide (the Westing Group) also record metamorphism at ~930 Ma. This suggests that units within the Hascosay Slide can be correlated broadly with the lower parts of the Moine Supergroup (Morar Group) and the Krummedal Succession of East Greenland.

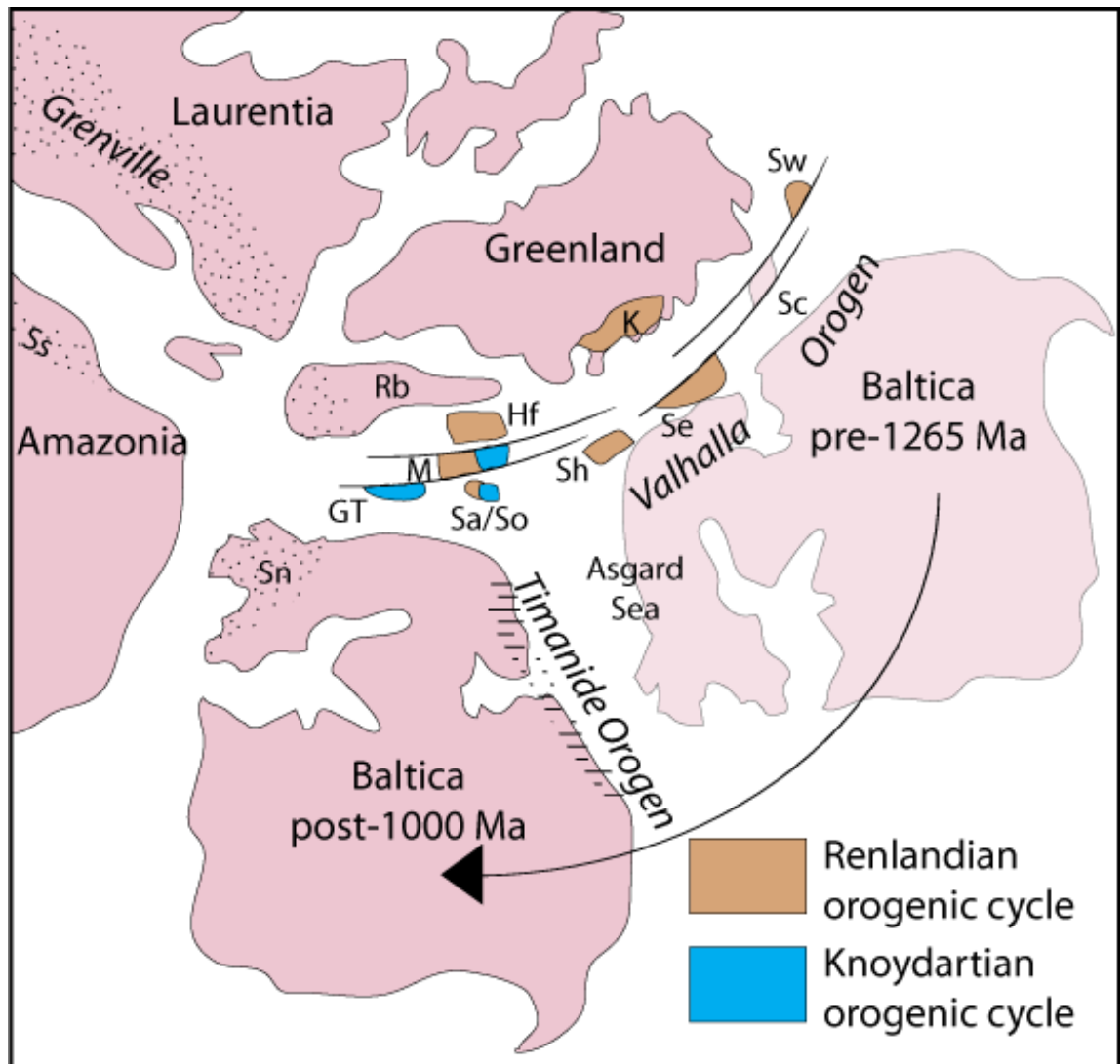


Figure 8-4, from Cawood et al. (2010) showing the Neoproterozoic reconstruction of eastern Laurentia, Baltica and northern Amazonia. Baltica is shown in pre and post 1265 Ma position. The rotation of Baltica opened the Asgard Sea. Brown blocks correlate to units associated with the Renlandian orogenic cycle and blue blocks relate to Knoydartian influenced units. The abbreviations are; GT – Grampian Terrane; M – Moine Supergroup; Hf – Hebridean Foreland; K – Krummedal succession; Rb – Rockall Bank; Sa/So – Sværholt and Sørøy successions; Sh – Shetland; Sn – Sveconorwegian orogeny; Ss – Sunsas orogen; Se – Eastern terrane of Svalbard; Sc – Central terrane of Svalbard; Sw – Western terrane of Svalbard.

The early Lu-Hf ages recorded from the Morar Group indicate that deposition of the Morar Group/ Moine Nappe must have ceased prior to ~950 Ma. The youngest published precise zircon age is 980 ± 4 Ma (Cawood et al. 2007) which gives approximately 30 Ma during which the Morar Group was deposited. Deposition of the Glenfinnan Group and the Loch Eil Group could have continued to at least ~870 Ma when the Ardour Granitic Gneiss and the Glen Doe metagabbro were emplaced into

the sediments (Millar 1999; Friend et al. 1997). The early metamorphic events recorded in the Morar Group are different from the Neoproterozoic garnet growth events recorded within the Glenfinnan Group which suggests that the Glenfinnan and the Morar groups were tectonically separate until at least 740 Ma. This study has shown that the Glenfinnan Group records three phases of garnet growth at 740 Ma, 700-680 Ma and 640 Ma. Cutts et al. (2010) also dated monazite inclusions within a garnet from close to where the Drumnadrochit Migmatite (AB07-13) was sampled and obtained ages that range from 840-780 Ma from the garnet core, suggesting that there was also an older phase of Neoproterozoic garnet growth.

8.4.3 Ordovician garnet growth

This study has confirmed the widespread existence of a Mid-Ordovician Grampian event which has been recorded within the Yell Sound Group dating the main migmatisation event. The Naver nappe in Sutherland also gave a Mid-Ordovician age which complements the previously published U-Pb zircon (SIMS) data (Kinny et al. 2003). A Mid-Ordovician age was also obtained from syn-kinematic garnets within the Morar Group from close to the Moine Thrust, which could date thrust movement. This could suggest that there may have been ~30 Myr of movement on the thrust with the U-Pb ages from the Loch Borrolan Complex marking the younger limit of movement (Goodenough et al. 2010). The migmatites within the Glenfinnan Group, close to the Great Glen Fault also give Mid-Ordovician ages which are interpreted to relate to migmatisation (Cutts et al. 2010). Further west, in the Glenfinnan Group the Loch Quioch Amphibolite (AB07-05) also yields a Mid-Ordovician age.

New Late-Ordovician data reported within this study show that the existing two-stage model for Caledonian orogenesis in northern Scotland is over-simplistic which has implication for regional tectonic models. This is demonstrated by new Late-Ordovician Lu-Hf and Sm-Nd ages that have been obtained from prograde garnets within the Moine nappe of North Sutherland and the SW Moine nappe and the Glenfinnan Group on Mull. Lu-Hf ages of 449.3 ± 1.2 Ma (Talmine Pelite, AB07-15), 447.2 ± 1.7 Ma (Ben Hope Sill amphibolite, AB07-17), 450 ± 5 Ma (Mull Amphibolite, AB07-30) and an Sm-Nd core age of 450 ± 2 Ma (Basal Pelite, Morar Group, AB07-08) provide evidence for a hitherto unrecognised Late Ordovician regional metamorphic event. These ages are within error of a Sm-Nd age of 456 ± 8 Ma also obtained from the Talmine Pelite

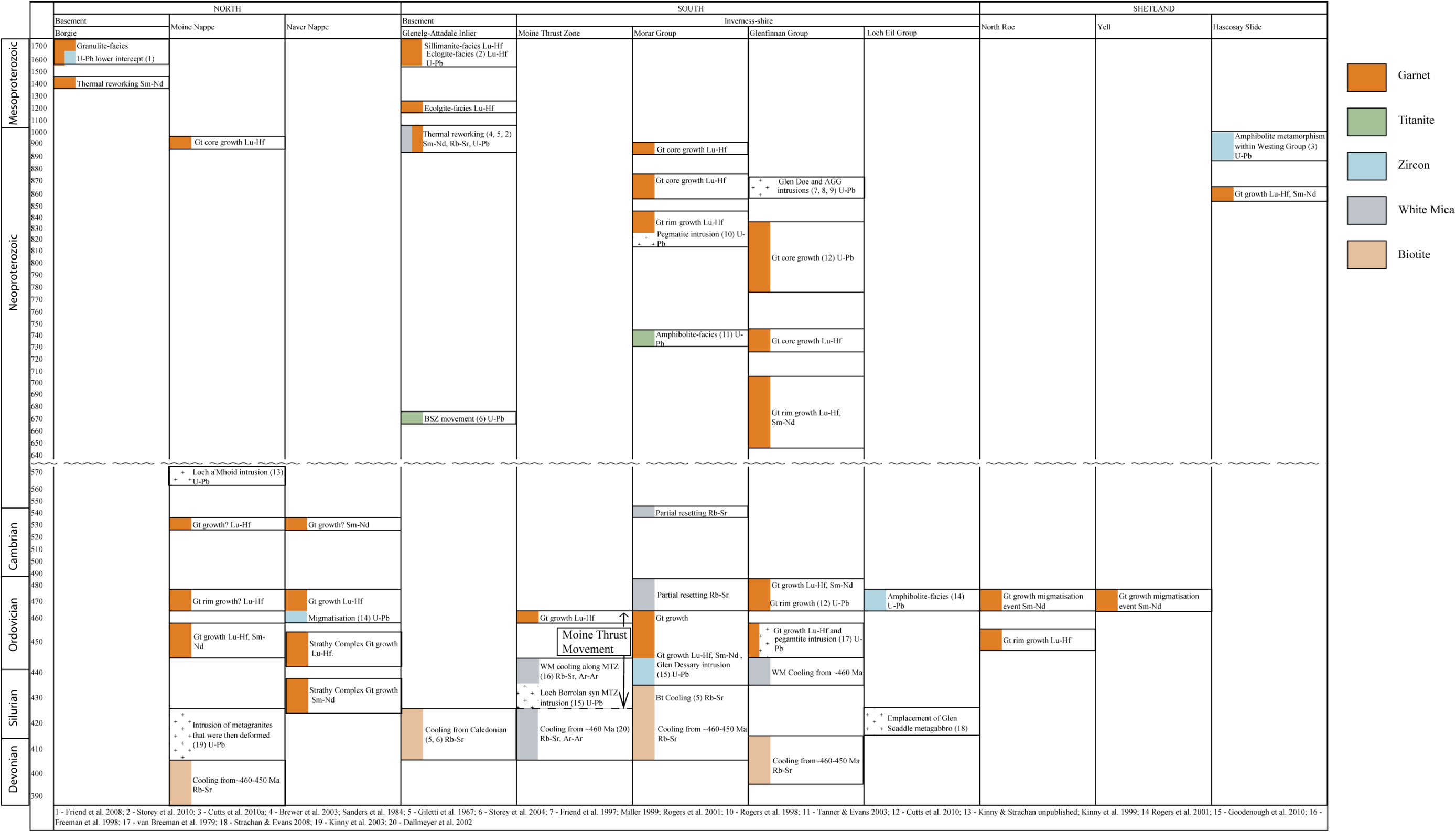
(AB07-15) garnets. This study suggests that the Caledonian history of the Northern Highland terrane has more in common with the Laurentian-derived rocks of Baltica than with the Grampian terrane of Scotland, due to the presence of late-Ordovician metamorphism.

One significantly younger Lu-Hf age of 390.3 Ma from the rim of a garnet the North Roe Schist of Shetland, which is west of the Walls Boundary Fault is possibly related to the formation of the Sand Voe Schuppen zone. More samples from this area need to be dated in order to clearly establish the events recorded in this area.

8.4.4 Summary Table

The metamorphic ages detailed above have been outlined in Table 8-1 along with many of the previously published ages. Previously published ages that have been superseded by dates within this study have been excluded from the table, for example the Sm-Nd garnet ages from Vance et al. (1998). In many instances only the Lu-Hf garnet age has been included as it was considered a better representation of peak metamorphism.

Table 8-1, summary of deformational events the Moine Supergroup has been subjected to. References used for the published ages are set out in the bottom of the table.



8.5 Future work

This project has shown that there have been several garnet growth phases within the Moine Supergroup, often recorded within the same garnet. These growth phases could be dated in more detail using microsampling techniques which could provide an age for each growth zone. Ideally this technique would be applied to several samples across the Moine Supergroup to establish the timing(s) of these garnet growth events; this would be particularly useful for the Neoproterozoic garnet ages which suggest several pulses of garnet growth. This information could then be coupled with detailed pressure and temperature information, using a method like THERMOCALC, which will allow modelling of the actual garnet zone compositions in pressure and temperature space, giving a detailed history of the conditions the various garnet zone grew under.

The effects of inclusions on the ages obtained from the garnets within this study have not been accurately quantified, in-situ analysis of the zircon and Nd-rich inclusions (monazite etc.) would allow for this effect to be modelled. This would particularly useful for many of the pelites which have plentiful zircon and monazite inclusions.

Another area of future work is looking at the closure temperature of Lu-Hf and Sm-Nd, Figure 8-2 shows that there may be a systematic relationship between the two systems. For this study it was difficult because the samples had been metamorphosed more than once, but in an area that had a range of metamorphic conditions and had only been metamorphosed once (e.g. Barrovian type metamorphism of the Dalradian) it would be possible to date several garnets to determine the closure temperature for each system.

The stratigraphy of the Ross of Mull has not been studied in detail since 1987, thus it would be extremely interesting to undertake detailed mapping to establish the nature of the Morar/ Glenfinnan Group contact. It would also be useful to determine whether the finely bedded sandstones and mudstones that lie above the Morar Group are truly Glenfinnan Group or a lateral equivalent.

REFERENCES

A

- Aftalion, M. & Van Breemen, O. 1980. U-Pb zircon, monazite and Rb-Sr whole rock systematics of granitic gneiss and psammitic to semipelitic host gneiss from Glenfinnan, northwestern Scotland. *Contributions to Mineralogy and Petrology*, 72, pp.87-98.
- Alsop, G.I., Holdsworth, R.E. & Strachan, R.A. 1996. Transport-parallel cross folds within a mid-crustal Caledonian thrust stack, northern Scotland. *Journal of Structural Geology*, 18, pp.783–790.
- Alsop, G.I. & Holdsworth, R.E. 1999. Vergence and facing patterns in large-scale sheath folds. *Journal of Structural Geology*, 21, pp.1335-1349.
- Alsop, G.I. & Holdsworth, R.E. 2002. The geometry and kinematics of flow perturbation folds. *Tectonophysics*, 350, pp.99-125.
- Alsop, G.I. & Holdsworth, R.E. 2004a. The geometry and topology of natural sheath folds: a new tool for structural analysis. *Journal of Structural Geology*, 26, pp.1561-1589.
- Alsop, G.I. & Holdsworth, R.E. 2004b. Shear zone folds: records of flow perturbation or structural inheritance? *In*: Alsop, G.I., Holdsworth, R.E., McCaffrey, K.J.W. & Hand, M. (eds) *Flow Processes in Faults and Shear Zones*. Geological Society, Special Publications, 224, pp.177-199.
- Alsop, G.I. & Holdsworth, R.E. 2005. Discussion on non-plane strain flattening along the Moine Thrust, Loch Strath nan Aisinnin, North-West Scotland. *Journal of Structural Geology*, 27, pp.781-784.
- Alsop, G.I. & Holdsworth, R.E. 2006. Sheath folds as discriminators of bulk strain type. *Journal of Structural Geology*, 28, pp.1588-1606.
- Alsop, G.I. & Holdsworth, R.E. 2007. Flow perturbation folding in shear zones. *In*: Ries, A.C., Bulter, R.W.H. & Graham, R.H. (eds) *Deformation of the Continental Crust: the Legacy of Mike Coward*. Geological Society, London, Special Publications, 272, pp.77-103.

Alsop, G.I., Holdsworth, R.E. & McCaffrey, K.J.W. 2007. Scale invariant sheath folds in salt, sediments and shear zones. *Journal of Structural Geology*, 29, pp.1585-1604.

Anczkiewicz, R. & Thirlwall, M. F. 2003. Improving precision of Sm-Nd garnet dating by H₂SO₄ leaching: a simple solution to the phosphate inclusion problem. *In*: Vance, D., Müller, W. & Villa, I. M. (eds) *Geochronology: Linking the Isotopic Record with Petrology and Textures*. Geological Society, London, Special Publications, 220, pp.83-91

Anderton, R. 1985. Sedimentation and tectonics in the Scottish Dalradian. *Scottish Journal of Geology*, 21, 407–436.

Arnold, J.R., 1954. Energy levels in ¹⁷⁶Lu and ¹⁷⁶Hf. *Physical Review*, 93, pp.743–745.

B

Bailey, E.B. 1910. Recumbent folds in the schists of the Scottish Highlands. *Quarterly Journal of the Geological Society of London*, 66, pp.586-620.

Banks, C.J., 2007. Exceptional preservation of sedimentary structures in metamorphic rocks: an example from the upper Grampian Group, Creag Stalcair, Perthshire. *Scottish Journal of Geology*, 43(1), pp.9-14.

Banks, C.J. & Winchester, J. A, 2004. Sedimentology and stratigraphic affinities of Neoproterozoic coarse clastic successions, Glenshirra Group, Inverness-shire, Scotland. *Scottish Journal of Geology*, 40(2), pp.159-174.

Barber, A.J. 1965. The history of the Moine Thrust zone, Lochcarron and Lochalsh, Scotland. *Proceedings of the Geologists' Association*, 76, pp.215-242.

Barber, A.J. & May, F. 1975. The history of the western Lewisian in the Glenelg inlier, Lochalsh, northern Highlands. *Scottish Journal of Geology*, 12, pp.35–50.

Barr, D. 1985. Migmatites in the Moine. *In*: Ashworth, J.R. (ed) *Migmatites*. Blackie, Glasgow & London, pp.226-264.

Barr, D., Roberts, A.M., Highton, A.J., Parson, L.M. & Harris, A.L. 1985. Structural setting and geochronological significance of the West Highland Granitic Gneiss, a deformed early granite within the Proterozoic, Moine rocks of NW Scotland. *Journal of the Geological Society, London*, 142, pp.663-675.

- Barr, D., Holdsworth, R.E. & Roberts, A.M. 1986. Caledonian ductile thrusting in a Precambrian metamorphic complex: the Moine of north-western Scotland. *Geological Society of America Bulletin*, 97, pp.754-764.
- Baxter, E.F., Ague, J.J. & DePaolo, D.J. 2002. Prograde temperature-time evolution in the Barrovian type-locality constrained by Sm/Nd garnet ages from Glen Clova, Scotland. *Journal of the Geological Society, London*, 159, pp.71-82.
- Becker H. 1997 Sm–Nd garnet ages and cooling history of high-temperature garnet peridotite massifs and high-pressure granulites from lower Austria. *Contributions to Mineralogy and Petrology* 127, 224–236.
- Bell, K. 1968. Age relations and provenance of the Dalradian Series of Scotland. *Bulletin of the Geological Society of America*, 79, 1167-1194.
- Blichert-Toft, J. & Albarede, F., 1997. The Lu-Hf isotope geochemistry of chondrites and the evolution of the mantle-crust system. *Earth and Planetary Science Letters*, 148(1-2), pp.243-258.
- Bonsor, H.C. & Prave, A.R. 2008. The Upper Morar Psammite of the Moine Supergroup, Ardnamurchan Peninsular, Scotland: depositional setting, tectonic implications. *Scottish Journal of Geology*.
- Boudin, A. & Deutsch, S., 1970. Geochronology: recent development in the lutetium-176/hafnium-176 dating method. *Science* 168, pp.1219–1220.
- Bowes, D.R. 1968. The absolute time scale and the subdivision of Precambrian rocks in Scotland. *Geologiska Föreningens i Stockholm Förhandlingar*, 90, pp.175-188.
- Bowring, S.A., Grotzinger, J., Condon, D.J., Ramezani, J. & Newall, M. 2007. Geochronologic constraints on the chronostratigraphic framework of the Neoproterozoic Huqf Supergroup, Sultanate of Oman. *American Journal of Earth Science*, 307, 1097–1145.
- Brewer, M.S., Brook, M. & Powell, D. 1979. Dating of the tectonometamorphic history of the southwestern Moine, Scotland. In: Harris, A.L., Holland, C.H. & Leake, B.E. (eds) *The Caledonides of the British Isles—Reviewed*. Geological Society, London, Special Publications, 8, 129–137.

- Brewer, T.S., Storey, C.D., Parrish, R.R., Temperley, S. & Windley, B.F. 2003. Grenvillian age decompression of eclogites in the Glenelg-Attadale Inlier, NW Scotland. *Journal of the Geological Society*, 160(4), pp.565-574.
- Briden, J.C., Turnell, H.B. & Watts, D.R. 1984. British palaeomagnetism, Iapetus Ocean, and the Great Glen Fault. *Geology*, 12, pp.428-431.
- Brinkman, G.A., Aten Jr., A.H.W. & Veenboer, J.Th., 1965. Natural radioactivity of K-40, Rb-87 and Lu-176. *Physica (Amsterdam)* 31, pp.1305-1319.
- Brook, M., Powell, D. & Brewer, M.S. 1976. Grenville age for rocks in the Moine of north-western Scotland. *Nature, London*, 260, pp.515-517.
- Brook, M., Powell, D. & Brewer, M.S. 1977. Grenville events in Moine rocks of the Northern Highlands, Scotland. *Journal of the Geological Society, London*, 133, pp.489-496.
- Brown, P.E., Miller, J.A., Grasty, R.L. & Fraser, W.E. 1965. Potassium-argon ages of some Aberdeenshire granites and gabbros. *Nature*, 201, pp.1287-1288.
- Brown, R.L., Dalziel, I.W.D. & Johnson, M.R.W. 1970. A review of the structure and stratigraphy of the Moinian of Ardgour, Moidart and Sunart, Argyll- and Inverness-shire. *Scottish Journal of Geology*, 6, pp.309-335.
- Buchan, K.L., Mertanen, S., Park, R.G., Pesonen, L.J., Elming, S.-A, Abrahamsen, N. & Bylund, G., 2000. Comparing the drift of Laurentia and Baltica in the Proterozoic: the importance of key paleomagnetic poles. *Tectonophysics* 319, pp.167-198.
- Buick, I., Hermann, J. Williams, I.S., Gibson, R.L. & Rubatto, D. 2006. A SHRIMP U-Pb and LA-ICP-MS trace element study of the petrogenesis of garnet-cordierite-orthoamphibole gneisses from the Central Zone of the Limpopo Belt, South Africa. *Lithos*, 88(1-4), pp.150-172.
- Burns, I.M. 1994. *Tectonothermal evolution and petrogenesis of the Naver and Kirtomy nappes, North Sutherland, Scotland*. PhD thesis, Oxford Brookes University.
- Burns, I.M. Fowler, M., Strachan, R.A. & Greenwood, P.B. 2004. Geochemistry, petrogenesis and structural setting of the meta-igneous Strathy Complex: a unique basement block within the Scottish Caledonides? *Geological Magazine*, 141, pp.209-223.

- Burton, K., Kohn, M.J., Cohen, A.S. & O'Nions, R.K. 1995. The relative diffusion of Pb, Nd, Sr and O in garnet. *Earth and Planetary Science Letters*, 133(1-2), pp.199-211.
- Butler, R.W.H. 1986. Structural evolution in the Moine of northwest Scotland: a Caledonian linked thrust system? *Geological Magazine*, 123, pp.1-11.
- Butler, R.W.H. & Coward, M.P. 1984. Geological constraints, structural evolution and the deep geology of the NW Scottish Caledonides. *Tectonics*, 3, pp.347-365.

C

- Cannat, M., 1989. Late Caledonian northeastward ophiolite thrusting in the Shetland Islands, U.K. *Tectonophysics*, 169, 257-270.
- Cawood, P.A., McCausland, P.J.A. & Dunning, G.R. 2001. Opening Iapetus: constraints from the Laurentian margin in Newfoundland. *Geological Society of America Bulletin*, 113, pp.443-453.
- Cawood, P.A., Nemchin, A.A., Smith, M. & Loewy, S. 2003. Source of the Dalradian Supergroup constrained by U-Pb dating of detrital zircon and implications for the East Laurentian margin. *Journal of the Geological Society, London*, 160, pp.231-246.
- Cawood, P.A., Nemchin, A.A., Strachan, R.A., Kinny, P.D. & Loewy, S. 2004. Laurentian provenance and tectonic setting for the upper Moine Supergroup, Scotland, constrained by detrital zircons from the Loch Eil and Glen Urquhart successions. *Journal of the Geological Society, London*, 161, pp.863-874.
- Cawood, P.A. & Pisarevsky, S.A. 2006. Was Baltica right-way up or upside down in the Neoproterozoic? *Journal of the Geological Society, London*, 163, pp.753-759.
- Cawood, P.A., Nemchin, A.A., & Strachan, R. 2007. Provenance record of Laurentian passive margin strata in northern Caledonides: implications for paleodrainage and paleogeography. *Geological Society of America, Bulletin*, 119, pp.993-1003.
- Cawood, P.A., Menchin, A.A., Strachan, R.A., Prave, A.R. & Krabbendam, M. 2007a. Sedimentary basin and detrital zircon record along East Laurentia and Baltica during assembly and breakup of Rodinia. *Journal of the Geological Society, London*, 164, pp.257-275.

- Cawood, P.A., Strachan, R.A., Cutts, K.A., Kinny, P.D., Hand, M. & Pisarevsky, S. 2010. Neoproterozoic orogeny along the margin of Rodinia: Valhalla orogen, North Atlantic. *Geology*, 38, pp.99-102.
- Clifford, P. 1960. The geological structure of the Loch Luichart area, Ross-shire. *Quarterly Journal of the Geological Society of London*, 115, pp.365-388.
- Clifford, T.N. 1957. The stratigraphy and structure of part of the Kintail district of southern Ross-shire – its relationship to the Northern Highlands. *Quarterly Journal of the Geological Society of London*, 113, pp.57-92.
- Chew, D.M., Daly, J.S., Page, L.M. & Kennedy, M.J. 2003. Grampian orogenesis and the development of blueschist-facies metamorphism in western Ireland. *Journal of the Geological Society, London*, 160, pp.911-924.
- Chew, D.M., Daly, J.S., Magna, T., Page, L.M., Kirkland, C.L., Whitehouse, M.J. & Lam, R. 2010. Timing of ophiolite obduction in the Grampian Orogen. *Geological Society of America Bulletin*, in press.
- Christensen, J.N., Rosenfeld, J.L. & DePaolo, D.J., 1989. Rates of tectonometamorphic processes from rubidium and strontium isotopes in garnet. *Science* 244 (4911), pp.1465–1469.
- Corfu, F., Ravna, E.J.K. & Kullerud, K. 2003. A Late Ordovician U-Pb age for the Tromsø Nappe eclogites, Uppermost Allochthon of the Scandinavian Caledonides. *Contributions to Mineralogy and Petrology*, 145, pp.502-513.
- Coward, M.P. 1990. The Precambrian, Caledonian and Variscan framework to NW Europe. In: Hardman, R.F.P. & Brooks, J. (eds) *Tectonic Events Responsible for Britain's Oil and Gas Reserves*. Geological Society, London, Special Publications, 55, pp.1-34.
- Cutts, K.A., Hand, M., Kelsey, D.E. & Strachan, R.A. 2009. Orogenic versus extensional settings for regional metamorphism: Knoydartian events in the Moine Supergroup revisited. *Journal of the Geological Society, London*, 166, pp. 201-204.
- Cutts, K. A., Hand, M., Kelsey, D.E., Wade, B., Strachan., R.A., Clark., C. & Netting, A. 2009a. Evidence for 930 Ma metamorphism in the Shetland Islands, Scottish

Caledonides: implications for Neoproterozoic tectonics in the Laurentia-Baltica sector of Rodinia. *Journal of the Geological Society*, 166(6), pp.1033-1047.

Cutts, K.A., Kinny, P.D., Strachan, R.A., Hand, M., Kelsey, D.E., Emery, M., Friend, C.R.L. & Leslie, A.G. 2010. Three metamorphic events recorded in a single garnet: Integrated phase modelling, *in situ* LA-ICPMS and SIMS geochronology from the Moine Supergroup, Scotland. *Journal of Metamorphic Geology*, 28, pp.249-267.

Cutts, K., Hand, M., Kelsey, D. & Strachan, R. 2011. P-T constraints and timing of Barrovian metamorphism in the Shetland Islands, Scottish Caledonides: implications for regional tectonic models. *Journal of Metamorphic Geology*, in press.

D

Dallmeyer, R.D., Strachan, R.A., Rogers, G., Watt, G.R. & Friend, C.R.L. 2001. Dating deformation and cooling in the Caledonian thrust nappes of north Sutherland, Scotland: insights from $^{40}\text{Ar}/^{39}\text{Ar}$ and Rb-Sr chronology. *Journal of the Geological Society, London*, 158, pp.501-512.

Dalmaso, J., Barci-Funel, G. & Ardisson, G.J., 1992. Reinvestigation of the decay of the long-lived odd-odd ^{176}Lu nucleus. *Applied Radiation and Isotopes*, 43, pp.69-76.

Daly, J.S., Aitchison, S.J., Cliff, R.A., Gayer, R.A. & Rice, A.H.N., 1991. Geochronological evidence from discordant plutons for a late Proterozoic orogen in the Caledonides of Finnmark, northern Norway. *Journal of the Geological Society, London*, 148, pp.29-40.

Dalziel, I.W.D. 1966. A structural study of the granitic gneiss of western Ardgour, Argyll and Inverness-shire. *Scottish Journal of Geology*, 2, pp.125-152.

Dalziel, I.W.D. 1992. On the organization of American plates during the Neoproterozoic and the breakout of Laurentia. *GSA Today*, 2, pp. 240-241.

Dalziel, I.W.D. 1997. Neoproterozoic-Palaeozoic geography and tectonics: review, hypothesis, environmental speculation. *Geological Society of America Bulletin*, 109, pp.16-42.

Dalziel, I.W.D. 2001. A global perspective on the Scottish Caledonides. *Transactions of the Royal Society of Edinburgh: Earth Sciences*, 91, pp.405-420.

- Dalziel, I.W.D. & Soper, N.J. 2001. Neoproterozoic extension on the Scottish promontory of Laurentia: paleogeographic and tectonic implications. *Journal of Geology*, 109, pp.299-317.
- Dempster, T.J., 1985. Uplift patterns and orogenic evolution in the Scottish Dalradian. *Journal of the Geological Society*, 142(1), pp.111-128.
- Dempster, T.J., Hudson, N.F.C. & Rogers, G. 1995. Metamorphism and cooling of the NE Dalradian. *Journal of the Geological Society*, 152, pp.383-390.
- Dempster, T.J., Rogers, G., Tanner, P.W.G., Bluck, B.J., Muir, R.J., Redwood, S.D., Ireland, T.R. & Paterson, B.A. 2002. Timing of deposition, orogenesis and glaciation within the Dalradian rocks of Scotland: constraints from U-Pb zircon ages. *Journal of the Geological Society*, 159(1), pp.83-94.
- Deer, W. A., Howie, R. A., & Zussman, J., 1992. An introduction to rock forming minerals. Second edition, Pearson Education Limited.
- Dewey, J.F. 1969. Evolution of the Appalachian-Caledonian Orogen. *Nature, London*, 222, pp.124-129.
- Dewey, J.F. 2006. Orogeny can be very short. *Proceedings of the National Academy of Sciences*, 102, pp.15286-15293.
- Dewey, J.F. & Shackleton, R.J. 1984. A model for the evolution of the Grampian tract in the early Caledonides and Appalachians. *Nature*, 312, pp.115-120.
- Dewey, J.F. & Ryan, P.D. 1990. The Ordovician evolution of the South Mayo Trough, western Ireland. *Tectonics*, 9, pp.887-903.
- Dewey, J.F. & Mange, M. 1999. Petrography of Ordovician and Silurian sediments in the western Irish Caledonides: tracers of a short-lived Ordovician continent—arc collision orogeny and the evolution of the Laurentian Appalachian—Caledonian margin. In: MacNiocaill, C. & Ryan, P.D. (eds) *Continental Tectonics*. Geological Society, London, Special Publications, 164, pp.55-107.
- Dewey, J.F. & Strachan, R.A. 2003. Changing Silurian-Devonian relative plate motion in the Caledonides: sinistral transpression to sinistral transtension. *Journal of the Geological Society, London*, 160, pp.219-229.

- Dixon, D., McNair, A. & Curran, S.C., 1954. The natural radioactivity of lutetium. *Philosophical Magazine*, 45, pp.683–694.
- Dodson, M.H. 1973. Closure temperature in cooling geochronological and petrological systems, *Contributions to Mineralogy and Petrology*, 40 pp. 259–264.
- Donhoffer, D. 1964. Bestimmung der halbwertszeiten der in der nature vorkommenden radioaktiven nuclide ^{146}Sm and ^{176}Lu mittels flüssiger szintillatoren. *Nuclear Physics*, 50, pp.489-496.
- Duchene, S., Blichert-Toft, J., Luais, B., Télouk, P., Lardeaux, J.M. & Albare`de, F. 1997 The Lu–Hf dating of garnets and the ages of the Alpine high-pressure metamorphism. *Nature* 387, pp.586–589
- Dutch, R. & Hand, M. 2009. Retention of Sm-Nd isotopic ages in garnets subjected to high-grade thermal reworking: implications for diffusion rates of major and rare earth elements and the Sm-Nd closure temperature in garnet. *Contributions to Mineralogy and Petrology*, 159, pp.93-112
- E*
- Emery, M. 2005. *Poly-orogenic history of the Moine rocks of the Glen Urquhart area, eastern Inverness-shire*. PhD thesis, University of Portsmouth, UK.
- F*
- Finlay, C.A. & Kerr, A. 1979. Garnet growth in a metapelite from the Moinian rocks of northern Sutherland, Scotland. *Contributions to Mineralogy and Petrology*, 71, pp.185-191.
- Fettes, D.J. 1970. The structural and metamorphic state of the Dalradian rocks and their bearing on the age of emplacement of the basic sheet. *Scottish Journal of Geology*, 6, 108-118.
- Flett, J.S. 1905. *On the petrographic characters of the inliers of Lewisian rocks among the Moine gneisses of the north of Scotland*. Memoirs of the Geological Survey, Summary of Progress for 1905, pp.155-167.
- Fleuty, M.J. 1961. The three fold-systems in the metamorphic rocks of Glen Orrin, Ross-shire, and Inverness-shire. *Quarterly Journal of the Geological Society of London*, 116, pp.447-479.

- Flinn, D. 1988. The Moine rocks of Shetland. In: Winchester, J.A. (ed) Late Proterozoic stratigraphy of the Northern Atlantic region. Blackie & Sons, Glasgow, pp.74-85.
- Flinn, D., 1992. The history of the Walls Boundary fault. *Journal of the Geological Society, London*, 149, 721-726.
- Flinn, D., 1994. Geology of Yell and some neighbouring islands in Shetland. *Memoir of the British Geological Survey*, Sheet 130 (Scotland).
- Flinn, D. 2007. The Dalradian rocks of Shetland and their implications for the plate tectonics of the northern Iapetus. *Scottish Journal of Geology*, 43, 125-142.
- Flinn, D., May, F., Roberts, J.L. & Treagus, J.L. 1972. A review of the stratigraphic succession of the East Mainland of Shetland. *Scottish Journal of Geology*, 8, pp.335-343.
- Flinn, D., Frank, P.L., Brook, M. & Pringle, I.R. 1979. Basement cover relations in Shetland. In: Harris, A.L. & Leake, B.E. (eds). *The Caledonides of the British Isles Reviewed*. Geological Society, London Special Publication, 8, pp.109-115.
- Flinn, D., Miller, J.A. & Roddom, D., 1991. The age of the Norwick hornblendic schists of Unst and Fetlar and the obduction of the Shetland Ophiolite. *Scottish Journal of Geology*, 27, pp.11-19.
- Flinn, D. & Oglethorpe, R.J.D., 2005. A history of the Shetland Ophiolite Complex. *Scottish Journal of Geology*, 41, 141-148.
- Flowerdew, M.J., Daly, J.S., Guise, P.G. & Rex, D.C. 2000. Isotopic dating of overthrusting, collapse and granitoid intrusion within the Grampian orogenic belt NW Ireland. *Geological Magazine*, 137, pp.419-435.
- Flowerdew, M.J., Daly, J.S. & Whitehouse, M.J. 2005. 470 Ma granitoid magmatism associated with the Grampian Orogeny in the Sliswood Division, NW Ireland. *Journal of the Geological Society, London*, 162, pp.563-575.
- Fraser, J.E., Searle, M.P., Parrish, R.R. & Noble, S.R. 2001. Chronology of deformation, metamorphism and magmatism in the southern Karakoram Mountains. *Geological Society of America Bulletin*, 113, pp.1443-1455.

- Freeman, S.R., Butler, R.W., Cliff, R.A. & Rex, D.C. 1998. Direct dating of mylonite evolution: a multi-disciplinary geochronological study from the Moine Thrust Zone, NW Scotland. *Journal of the Geological Society*, 155(5), pp.745-758.
- Friedrich, A.M., Hodges, K.V., Bowring, S.A. & Martin, M.W. 1999. Geochronological constraints on the magmatic, metamorphic and thermal evolution of the Connemara Caledonides, western Ireland. *Journal of the Geological Society, London*, 156, pp.1217-1230.
- Friend, C.R.L., Kinny, P.D., Rogers, G., Strachan, R.A. & Paterson, B.A. 1997. U-Pb zircon geochronological evidence for Neoproterozoic events in the Glenfinnan Group (Moine Supergroup): the formation of the Ardgour granite gneiss, north-west Scotland. *Contributions to Mineralogy and Petrology*, 128, pp.101-113.
- Friend, C.R., Strachan, R.A., Kinny, P.D. & Watt, G.R. 2003. Provenance of the Moine Supergroup of NW Scotland: evidence from geochronology of detrital and inherited zircons from sediments, granites and migmatites. *Journal of the Geological Society, London*, 160, pp.247-257.
- Friend, C.R.L. & Kinny, P.D. 1995. New evidence for the protolith ages of Lewisian granulites, northwest Scotland. *Geology*, 23, pp.1027-1030.
- Friend, C.R.L. & Kinny, P.D. 2001. A reappraisal of the Lewisian Gneiss Complex: geochronological evidence for tectonic assembly of disparate terranes in the Proterozoic. *Contributions to Mineralogy and Petrology*, 142, pp.198-218.
- Friend, C.R.L., Jones, K.A. & Burns, I.M. 2000. New high-pressure granulite facies event in the Moine Supergroup, northern Scotland: implications for Taconic (early Caledonian) crustal evolution. *Geology*, 28, pp.543-546.

G

- Ganguly, J. & Tirone, M. 1999. Diffusion closure temperature and age of a mineral with arbitrary extent of diffusion: theoretical formulation and applications. *Earth and Planetary Letters*, 170, pp.131-140.
- Ganguly, J., Tirone, M. & Hervig, R.L. 1998. Diffusion kinetics of Samarium and Neodymium in garnet, and a method for determining cooling rates of rocks. *Science*, 281, pp.805.

- Gee, D.G. 1975. A tectonic model for the central part of the Scandinavian Caledonides. *American Journal of Science*, 275-A, pp.468-515.
- Gehrke, R.J., Casey, C. & Murray, R.K., 1990. Half-life of ^{176}Lu . *Physical Review*, C 41, pp.2878–2882.
- Geikie, A. 1888. Report on the recent work of the Geological Survey in the North- West Highlands of Scotland. *Quarterly Journal of the Geological Society of London*, 44, pp.378-441.
- Gibbons, W. & Harris, A.L. (eds) 1994. A Revised Correlation of Precambrian Rocks in the British Isles. Geological Society, London, Special Report No. 22.
- Gibbons, W. & Gayer, R.A. 1985. British Caledonian Terranes. *In*: Gayer, R.A. (ed), *The tectonic evolution of the Caledonian-Appalachian Orogen*, Viewseg, Brunswick, pp.3-16.
- Giletti, B.J., Moorbath, S. & Lambert, R.St.J. 1961. A geochronological study of the metamorphic complexes of the Scottish Highlands. *Quarterly Journal of the Geological Society of London*, 117, pp.233-272.
- Glendinning, N.R.W. 1988. Sedimentary structures and sequences within a late Proterozoic tidal shelf deposit: the Upper Morar Psammite Formation of northwestern Scotland. *In*: Winchester, J.A. (ed.) *Later Proterozoic Stratigraphy of the Northern Atlantic Regions*. Blackie, Glasgow, pp.14-31.
- Glover, B.W. & McKie, T., 1996. A sequence stratigraphical approach to the understanding of basin history in orogenic Neoproterozoic successions: an example from the central Highlands of Scotland. *Geological Society, London, Special Publications*, 103(1), pp.257-269.
- Glover, R.N. & Watt, D.E., 1957. A search for electron capture in ^{176}Lu . *Philosophical Magazine*, 2, pp.699–702.
- Goodenough, K.M., Millar, I.L., Strachan, R.A., Krabbendam, M. & Evans, J.A. 2011. Timing of regional deformation and development of the Moine Thrust Zone in the Scottish Caledonides: constraints from the U-Pb geochronology of alkaline intrusions. *Journal of the Geological Society, London*, 168, pp.99-114.

Grant, C.J. & Harris, A.L. 2000. The kinematic and metamorphic history of the Sgurr Beag Thrust, Ross-shire, NW Scotland. *Journal of Structural Geology*, 22, pp.191–205.

Grinyer, G.F., Waddington, J.C., Svensson, C.E., Austin, R.A.E., Ball, G.C., Hackman, G., O'Meara, J.M., Osborne, C., Sarazin, F., Scraggs, H.C. & Stöver, H.D.H. 2003. Half-life of ^{176}Lu . *Physical Review*, C 67, pp.014302.

H

Halliday, A.N., Graham, C.M., Aftalion, M. & Dymoke, P. 1989. Short Paper: The depositional age of the Dalradian Supergroup: U-Pb and Sm-Nd isotopic studies of the Tayvallich Volcanics, Scotland. *Journal of the Geological Society*, 146(1), pp.3-6

Harris, A.L. 1995. The nature and timing of orogenesis in the Scottish Highlands and the role of the Great Glen Fault. *In*: Hibbard, J., van Staal, C.R. & Cawood, P.A. (eds) *Current Perspectives in the Appalachian-Caledonian Orogen*. Geological Association of Canada, Special Paper, 41, pp.65-79.

Harris, A.L., Baldwin, C.T., Bradbury, H.J., Johnson, H.D. & Smith, R.A. 1978. Ensialic sedimentation: the Dalradian Supergroup. *In*: Bowes, D.R. & Leake, B.E. (eds) *Crustal Evolution in Northwest Britain and Adjacent Regions*. Geological Society, London, *Special Reports*, 6, 52–75.

Harris, A.L. & Johnson, M.R.W. 1991. A.L. Harris and M.R.W. Johnson *In*: C.Y. Craig, Editor, *Moine Geology of Scotland*, Geological Society, London, pp.87-148.

Harris, A.L., Haselock, P.J., Kennedy, M. & Mendum, J.R. 1994. The Dalradian Supergroup in Scotland, Shetland and Ireland. *In*: Gibbons, W. & Harris, A.L. (eds) *A Revised Correlation of Precambrian Rocks in British Isles*. Geological Society, London, *Special Reports*, 22, 33–53.

Harris, A.L., Baldwin, C.T., Bradbury, H.J., Johnson, H.D. & Smith, R.A. 1978. Ensialic basin sedimentation: the Dalradian Supergroup: *In*: Bowes, D.R. & Leake, B.E. (eds) *Crustal evolution in Northwestern Britain and adjacent regions*. Geological Journal Special Issue, 10, pp.115-138.

Herr, E. Merz, P. Eberhardt & P. Signer, 1958. zur Bestimmung der Halbwertszeit des Lu-176 durch den Nachweis von radiogenem Hf-176, *Z. Naturforsch.* 13a, pp.268–273.

- Hickman, A. H. 1975. The stratigraphy of late Precambrian metasediments between Glen Roy and Lismore. *Scottish Journal of Geology*, 11, 117-42.
- Higgins, A.K., 1988, The Krummedal supracrustal sequence in East Greenland. In: Winchester, J.A. (ed.) *Later Proterozoic stratigraphy of the northern Atlantic regions*: Blackie, Glasgow, pp.86-96.
- Higgins, A.K. & Phillips, W.E.A. 1979. East Greenland Caledonides – an extension of the British Caledonides. *Geological Society, London, Special Publications*, 8, pp.19-32.
- Higgins, A.K., Elvevold, S., Escher, J.C., Frederiksen, K.S., Gilotti, J.A., Henriksen, N., Jepsen, H.F., Jones, K. A., Kalsbeek, F., Kinny, P.D., Leslie, A.G., Smith, M.P., Thrane, K. & Watt, G.R., 2004, The foreland-propagating thrust architecture of the East Greenland Caledonides 72° - 75°N: *Journal of the Geological Society, London*, 161, pp.1009-1026.
- Highton, A.J., Hyslop, E.K. & Noble, S.R. 1999. U-Pb zircon geochronology of migmatization in the northern Central Highlands: evidence for pre-Caledonian (Neoproterozoic) tectonometamorphism in the Grampian Block, Scotland. *Journal of the Geological Society, London*, 156, pp.1195-1204.
- Hoffman, P.F. 1991. Did the breakout of Laurentia turn Gondwanaland inside-out? *Science*, 252, pp.1409-1412.
- Holdsworth, R.E. 1988. The stereographic analysis of facing. *Journal of Structural Geology*, 10, pp.219-223.
- Holdsworth, R.E. 1989. The geology and structural evolution of a Caledonian fold and ductile thrust zone, Kyle of Tongue region, Sutherland, northern Scotland. *Journal of the Geological Society, London*, 146, pp.809-823.
- Holdsworth, R.E. 1989a. Late brittle deformation in a Caledonian ductile thrust wedge: new evidence for gravitational collapse in the Moine Thrust sheet, Sutherland, Scotland. *Tectonophysics*, 170, pp.17–28.
- Holdsworth, R.E. 1990. Progressive deformation structures associated with ductile thrusts in the Moine Nappe, Sutherland, N. Scotland. *Journal of Structural Geology*, 12, pp.443-452.

- Holdsworth, R.E. & Roberts, A.M. 1984. A study of early curvilinear fold structures and strain in the Moine of the Glen Garry region, Inverness-shire. *Journal of the Geological Society, London*, 141, pp.327-338.
- Holdsworth, R.E., Harris, A.L. & Roberts, A.M. 1987. The stratigraphy, structure and regional significance of the Moine rocks of Mull, Argyllshire, W Scotland. *Geological Journal*, 22, pp.83-107.
- Holdsworth, R.E. & Strachan, R.A. 1988. The structural age and possible origin of the Vagastie Bridge granite and associated intrusions, central Sutherland. *Geological Magazine*, 125, pp.613-620.
- Holdsworth, R.E. & Grant, C.J. 1990. Convergence-related 'dynamic spreading' in a mid-crustal ductile thrust zone: a possible orogenic wedge model. *In*: Knipe, R.J. & Rutter, E.H. (eds) *Deformation Mechanisms, Rheology and Tectonics*. Geological Society, London, Special Publications, 54, pp.491-500.
- Holdsworth, R.E., Strachan, R.A. & Harris, A.L. 1994. Precambrian rocks in northern Scotland east of the Moine Thrust: the Moine Supergroup. *In*: Gibbons, W. & Harris, A.L. (eds) *A revised correlation of Precambrian rocks in the British Isles*. Geological Society, London, Special Report, 22, pp.23-32.
- Holdsworth, R.E., Strachan, R.A. & Alsop, G.I. 2001. *Geology of the Tongue District*. Memoir of the British Geological Survey, HMSO.
- Holdsworth, R.E., Strachan, R.A., Alsop, G.I., Grant, C.J. & Wilson, R.W. 2006. Thrust sequences and the significance of low-angle, out-of-sequence faults in the northernmost Moine Nappe and Moine Thrust Zone, NW Scotland. *Journal of the Geological Society, London*, 163, pp.801-814.
- Holdsworth, R.E., Alsop, G.I. & Strachan, R.A. 2007. Tectonic stratigraphy and structural continuity of the northernmost Moine Thrust Zone and Moine Nappe, Scottish Caledonides. *In*: Ries, A.C., Butler, R.W.H. & Graham, R.H. (eds) *Deformation of the Continental Crust: the Legacy of Mike Coward*. Geological Society, London, Special Publications, 272, pp.121-142.
- Hollister, L.S. 1966. Garnet zoning: an interpretation based on the Rayleigh fractionation model. *Science*, 154, pp.1647-1651

Howarth, R.J. & Leake, B.E. 2002. *The Life of Frank Coles Phillips (1902-1982) and the Structural Geology of the Moine Petrofabric Controversy*. Geological Society, London, Memoirs, 23.

Hyslop, E.K. 1992. *Strain-induced metamorphism and pegmatite development in the Moine rocks of Scotland*. PhD thesis, University of Hull.

J

Jagoutz, E., 1988. Nd and Sr systematics in an eclogite xenolith from Tanzania: Evidence for frozen mineral equilibria in the continental lithosphere. *Geochimica et Cosmochimica Acta*, 52(5), pp.1285-1293.

Johnstone, G.S., Smith, D. I. & Harris, A.L. 1969. The Moinian Assemblage of Scotland. In: Kay, M (ed) North Atlantic Geology and Continental Drift, a Symposium, *Memoirs of the Association of Petroleum Geologists*, 12, pp.159-180

Johnson, M.R.W. & Strachan, R.A. 2006. A discussion of possible heat sources during nappe stacking: the origin of Barrovian metamorphism within the Caledonian thrust sheets of NW Scotland. *Journal of the Geological Society, London*, 163, pp.579-583.

Jones, K. & Blake, S. 2003. Arc-continent collision: the Grampian phase of the Caledonian Orogeny. In: Jones, K. & Blake, S. *Mountain building in Scotland*, pp.47-72.

K

Karabinos, P., Samson, S., Hepburn, J. & Stoll, H., 1998. Taconic orogeny in the New England Appalachians: Collision between Laurentia and the Shelburne Falls arc. *Geology*, 26, 215-218.

Karlstrom, K.E., Harlan, S.S., Williams, M.L., McLelland, J., Geissman, J.W., & Ahall, K.-I., 1999. Refining Rodinia: geologic evidence for the Australian–western US connection in the Proterozoic. *GSA Today* 9, pp.1–7.

Karlstrom, K.E., Ahall, K.-I., Harlan, S.S., Williams, M.L., McLelland, J. & Geissman, J.W. 2001. Long-lived (1.8-1.0 Ga) convergent orogen in southern Laurentia, its extensions to Australia and Baltica, and implications for refining Rodinia. *Precambrian Research*, 11, pp.5-30.

- Kelley, S. 1988. The relationship between K-Ar mineral ages, mica grainsizes and movement on the Moine Thrust Zone, NW Highlands, Scotland. *Journal of the Geological Society, London*, 145, pp.1–10.
- Kelley, S.P. & Powell, D. 1985. Relationships between marginal thrusting and movement on major, internal shear zones in the N. Highland Caledonides, Scotland. *Journal of Structural Geology*, 7, pp.43-56.
- Kennedy, W.Q. 1955. The tectonics of the Morar anticline and the problems of the north-west Caledonian front. *Quarterly Journal of the Geological Society of London*, 110, pp.375-390.
- Kinny, P.D., Friend, C.R.L., Strachan, R.A., Watt, G.R. & Burns, I.M. 1999. U-Pb geochronology of regional migmatites, East Sutherland, Scotland: evidence for crustal melting during the Caledonian orogeny. *Journal of the Geological Society, London*, 156, pp.1143-1152.
- Kinny, P.D., Strachan, R.A., Rogers, G.R., Friend, C.R.L. & Kocks, H. 2003. U-Pb geochronology of deformed meta-granites in central Sutherland, Scotland: evidence for widespread Silurian metamorphism and ductile deformation of the Moine Supergroup during the Caledonian orogeny. *Journal of the Geological Society, London*, 160, pp.259-269.
- Kinny, P.D., Strachan, R.A., Kocks, H. & Friend, C.R.L. 2003a. U-Pb geochronology of late Neoproterozoic augen granites in the Moine Supergroup, NW Scotland: dating of rift-related, felsic magmatism during supercontinent break-up? *Journal of the Geological Society of London*, 160, pp.925-934.
- Kirkland, C.L., Daly, J.S. & Whitehouse, M.J. 2005. Early Silurian magmatism and the Scandian evolution of the Kalak Nappe Complex, Finnmark, Arctic Norway. *Journal of the Geological Society, London*, 162, pp.985-1003.
- Kirkland, C.L., Daly, J.S. & Whitehouse, M.J. 2006. Granitic magmatism of Grenvillian and late Neoproterozoic age in Finnmark, Arctic Norway – Constraining pre-Scandian deformation in the Kalak Nappe Complex. *Precambrian Research*, 145, pp.24-52.

- Kirkland, C.L., Daly, J.S. & Whitehouse, M.J. 2007. Provenance and terrane evolution of the Kalak Nappe complex, Norwegian Caledonides: implications for Neoproterozoic palaeogeography and tectonics. *Journal of Geology*, 115, pp.21-41.
- Kirkland, C.L., Strachan, R.A. & Prave, A.R. 2008. Detrital zircon signature of the Moine Supergroup, Scotland: Contrasts and comparisons with other Neoproterozoic successions within the circum-North Atlantic region. *Precambrian Research*, 163, pp.332-350.
- Kneller, B.C. & Aftalion, M. 1987. The isotopic and structural age of the Aberdeen granite. *Journal of the Geological Society, London*, 144, pp.717-722.
- Kocks, H. 2002. *Structural setting and petrogenesis of Silurian granites in the Caledonides of northern Scotland*. PhD thesis, Oxford Brookes University.
- Kocks, H., Strachan, R.A. & Evans, J.A. 2006. Heterogeneous reworking of Grampian metamorphic complexes during Scandian thrusting in the Scottish Caledonides: insights from the structural setting and U-Pb geochronology of the Strath Halladale Granite. *Journal of the Geological Society, London*, 163, pp.525-538.
- Komura, K., Sakamoto, K. & Tanaka, S., 1972. The half-life of long-lived ^{176}Lu . *Nuclear Physics, A* 198, pp.73–80.
- Krabbendam, M., Prave, A.R. & Cheer, D. 2008. A fluvial origin for the Neoproterozoic Morar Group, NW Scotland: implications for Torridon-Morar group correlation and the Grenville Orogen Foreland Basin. *Journal of the Geological Society, London*, 165, pp.379-394.
- Kretz, R., 1983. Symbols for rock forming minerals. *American Mineralogist*, 68, pp.277-279.

L

- Lambert, R.St.J. 1969. Isotopic studies relating to the Pre-Cambrian history of the Moinian of Scotland. *Proceedings of the Geological Society, London*, 1652, pp.243-245.
- Lambert, R.St.J. & Poole, A.B. 1964. The relationship of the Moine schists and Lewisian gneisses near Mallaigmore, Inverness-shire. *Proceedings of the Geologists' Association*, 75, pp.1-14.

- Lambert, R.St.J. & McKerrow, W.S. 1976. The Grampian Orogeny. *Scottish Journal of Geology*, 12, pp.271-292.
- Lambert, R.St.J., Winchester, J.A. & Holland, J.G. 1979. Time, space and intensity relationships of the Precambrian and Lower Palaeozoic metamorphisms of the Scottish Highlands. *In*: Harris, A.L., Holland, C.H. & Leake, B.E. (eds) *The Caledonides of the British Isles — Reviewed*. Geological Society, London, Special Publications, 8, pp.363-367.
- Lapen, T. J., Johnson, C. M., Baumgartner, L. P., Mahlen, N. J., Beard, B. L. & Amato, J. M. 2003. Burial rates during prograde metamorphism of an ultra-high-pressure terrane: an example from Lago di Cignana, western Alps, Italy. *Earth and Planetary Science Letters*, 215, pp.57-72
- Lapworth, C. 1885. The Highland Controversy in British geology: its causes, course and consequence. *Nature*, 32, pp.558-559.
- Leslie, A.G. & Nutman, A.P., 2003, Evidence for Neoproterozoic orogenesis and early high temperature Scandian deformation events in the southern East Greenland Caledonides: *Geological Magazine*, 140, pp.309-333.
- Leslie, A.G, Smith, M, & Soper, N.J. 2008 Laurentian margin evolution and the Caledonian Orogeny : a template for Scotland and East Greenland. *In*: Higgins, A.K.; Gilotti, J.A.; Smith, M.P., (eds.) *The Greenland Caledonides : evolution of the northwest margin of Laurentia*. Geological Society of America, 307-343. (Memoir (Geological Society of America), 202).
- Li, Z.X., Bogdanova, S.V., Collins, A.S., Davidson, A., De Waele, B., Ernst, R.E., Fitzsimons, I.C.W., Fuck, R.A., Gladkochub, D.P., Jacobs, J., Karlstom, K.E., Lu, S., Natapov, L.M., Pease, V., Pisarevsky, S.A., Thrane, K. & Vernikovsky, V. 2008. Assembly, configuration, and break-up history of Rodinia: A synthesis. *Precambrian Research*, 160, pp.179-210.
- Libby, W.F. 1939. Natural Radioactivity of Lutecium. *Physical Review*, 56, 21-23.
- Long, L.E. & Lambert, R.St.J. 1963. Rb-Sr isotopic ages from the Moine series. *In*: Johnson, M.R.W. & Stewart, F.H. (eds) *The British Caledonides*. Oliver & Boyd, Edinburgh, pp.217-246.

Ludwig, K.R. 2001. User's manual for Isoplot/Ex v. 2.47: a geochronological toolkit for Microsoft Excel. BGC Special Publication.

Ludwig, K.R. 2010. Isoplot/Ex 3.00. National Science Foundation.

Luo, J. & Kong, K. 2006. Half-life of ^{176}Lu . *Applied Radiation and Isotopes*, 64, pp.588-590.

M

MacQueen, J.A. & Powell, D. 1977. Relationships between deformation and garnet growth in Moine (Precambrian) rocks of western Scotland. *Geological Society of America Bulletin*, 88, pp.235-240.

May, F., Peacock, J.D., Smith, D.I. & Barber, A.J. 1993. Geology of the Kintail District. Memoir of the British Geological Survey.

Mawby J., Hand M., Foden J., Kelly S. P., Kinny P. & McDougall I. 1998 U-Pb, Sm-Nd, ^{40}Ar - ^{39}Ar and K-Ar constraints on thermal history of the Alice Springs Orogeny in the Harts Range, southeastern Arunta Inlier, central Australia. *Australian Geological Society Abstracts*, 49 295.

McCourt, W.J. 1980. The geology of the Strath Hallade-Altnabreac district: Institute of Geological Sciences Environmental Protection Unit Report no. 80-1.

McIntyre, D.B. 1952. The tectonics of the Beinn Dronaig area, Attadale. *Transactions of the Edinburgh Geological Society*, 15, pp.258-264.

McNair, A., 1961. The half-life of long-lived lutetium-176. *Philosophical Magazine*, 6, pp.851-856.

Millar, I.L. 1999. Neoproterozoic extensional basic magmatism associated with emplacement of the West Highland granite gneiss in the Moine Supergroup of NW Scotland. *Journal of the Geological Society, London*, 156, pp.1153-1162.

Mittlefehldt D. W., McCoy T. J., Goodrich C. A. & Kracher A. 1998. Non-chondritic meteorites from asteroidal bodies. In: *Planetary materials*, edited by Papike J. J. Washington, D. C.: *Mineralogical Society of America*. pp. 4-1-4-195.

Molyneux, S.G., 1998. An upper Dalradian microfossil reassessed. *Journal of the Geological Society*, 155(5), pp.741-743.

- Moorhouse, S.J. 1976. The geochemistry of the Lewisian and the Moinian of the Borgie area, north Sutherland. *Scottish Journal of Geology*, 12, pp.159-167.
- Moorhouse, S.J. 1977. *The geology and geochemistry of Central Sutherland*. PhD thesis, University of Hull, UK.
- Moorhouse, S.J. & Moorhouse, V.E. 1979. The Moine amphibolite suites of central and northern Sutherland. *Mineralogical Magazine*, 43, pp.211-225.
- Moorhouse, S.J. & Moorhouse, S.J. 1988. The Moine Assemblage in Sutherland. In: Winchester, J.A. (ed) *Later Proterozoic Stratigraphy of the Northern Atlantic Regions*. Blackie & Sons, Glasgow, pp.54-73.
- Moorhouse, S.J., Moorhouse, V.E. & Holdsworth, R.E. 1988. Excursion 12. North Sutherland, in: Allison, I., May, F. & Strachan, R.A. (eds) *An Excursion Guide to the Moine Geology of the Scottish Highlands*. Scottish Academic Press, Edinburgh, pp.216-248.
- Murchison, R.I. & Geikie, A. 1861. On the altered rocks of the western islands of Scotland, and the north-western and central Highlands. *Quarterly Journal of the Geological Society of London*, 17, pp.171-229.
- Müller, W., Shelley, M., Miller, P., & Broude, S. 2009. Initial performance metrics of a new custom-designed ArF excimer LA-ICPMS system coupled to a two-volumn laser-ablation cell. *Journal of Analytical Atomic Spectrometry*, 24, pp.209-214.
- Mykura, W. 1976. British Regional Geology Orkney and Shetland, Institute of Geological Sciences, pp.16-39.
- N*
- Nir-El, Y. & Haquin, G., 2003. Half-life of ^{176}Lu . *Physical Review*, C 68, 067301.
- Nir-El, Y. & Lavi, N., 1998. Measurement of the half-life of ^{176}Lu . *Applied Radiation and Isotopes*, 49, pp.1653–1655.
- Noble, S.R., Hyslop, E.K. & Highton, A.J. 1996. High-precision U-Pb monazite geochronology of the c. 806 Ma Grampian Shear Zone and the implications for the evolution of the Central Highlands of Scotland. *Journal of the Geological Society, London*, 153, pp.511-514.

Norman, E.B., 1980. Half-life of ^{176}Lu . *Physical Review*, C 21, pp.1109–1110.

O

Oliver, G.J.H., Chen, F., Buchwaldt, R. & Hegner, E. 2000. Fast tectonometamorphism and exhumation in the type area of the Barrovian and Buchan zones. *Geology*, 28, pp.459-462.

Oliver, G.J.H., Wilde, S.A. & Wan, Y. 2008. Geochronology and dynamics of Scottish granitoids from the late Neoproterozoic break-up of Rodinia to Palaeozoic collision. *Journal of the Geological Society, London*, 165, pp.661-674.

Otamendi, J. E., de la Rosa, J. D., Patiño Douce, A.E. & Castro, A. 2002. Rayleigh fractionation of heavy rare earths and yttrium during metamorphic garnet growth. *Geological Society of America*, 30, pp.159-162

P

Pankhurst, R.J. 1970. Geochronology of the basic complexes. *Scottish Journal of Geology*, 6, pp.83-107.

Pankhurst, R.J. 1974. Rb-Sr whole-rock chronology of Caledonian events in northeast Scotland. *Bulletin of the Geological Society of America*, 85, pp.345-350.

Park, R.G. 1969. Structural correlation in metamorphic belts. *Tectonophysics*, 7, pp.323-338.

Park, R.G., 1995. Paleoproterozoic Laurentia–Baltica relationships: a view from the Lewisian. In: Coward, M.P., Ries, A.C. (Eds.), *Early Precambrian Processes*. *Geological Society, London Special Publication*, 95, pp.211–224.

Patchett, P.J. & Tatsumoto, M., 1980. Lu–Hf total-rock isochron for the eucrite meteorites. *Nature*, 288, pp.571–574.

Patchett, P., White, W.M., Feldmann, H., Kielinczuk, S. & Hofmann, A.W. 1984. Hafnium/rare earth element fractionation in the sedimentary system and crustal recycling into the Earth's mantle. *Earth and Planetary Science Letters*, 69(2), pp.365-378

Peach, B.N. & Horne, J. 1930. *Chapters on the Geology of Scotland*. Oxford University Press, London. Peach, B.N., Horne, J., Gunn, W., Clough, C.T. & Hinxman, L.W. 1907.

The Geological Structure of the Northwest Highlands of Scotland. Memoirs of the Geological Survey of Great Britain.

Peach, B.N., Horne, J., Woodward, H.B., Clough, C.T., Harker, A. & Wedd, C.D. 1910. *The Geology of Glenelg, Lochalsh and south-east part of Skye.* Memoirs of the Geological Survey of Great Britain.

Peach, B.N., Gunn, W., Clough, C.T., Hinxman, L.W., Crampton, C.B., Anderson, E.M. & Flett, J.S. 1912. *The Geology of Ben Wyvis, Carn Chuinneag, Inchbae and the surrounding country.* Memoirs of the Geological Survey of Great Britain.

Peach, B.N., Horne, J., Hinxman, I.W., Crampton, C.B., Anderson, F.M. & Carruthers, R.G. 1913. *The geology of central Ross-shire.* Memoirs of the Geological Survey of Great Britain.

Pearce, J.A., & Cann, J R., 1973. Tectonic setting of basic volcanic rocks determined using trace element analyses. *Earth and Planetary Science Letters* 19, pp.290-300.

Peters, D. 2001. *A geochemical and geochronological assessment of the Great Glen Fault as a terrane boundary.* PhD thesis, University of Keele, UK.

Phillips, F.C. 1937. A fabric study of some Moine schists and associated rocks. *Quarterly Journal of the Geological Society of London*, 93, pp.581-616.

Phillips, E.R., Highton, A.J., Hyslop, E.K. & Smith, M. 1999. The timing and P-T conditions of regional metamorphism in the Central Highlands, Scotland. *Journal of the Geological Society, London*, 156, pp.1175-1193.

Piasecki, M.A.J. 1980. New light on the Moine rocks of the Central Highlands of Scotland. *Journal of the Geological Society, London*, 137, pp.47-59.

Piasecki, M.A.J. 1984. Ductile thrusts as time markers in orogenic evolution: an example from the Scottish Caledonides. *In: Galson, D. & Mueller, S.E. (eds) First European Geotraverse Workshop: the northeastern segment.* Publication of the European Science Foundation, Strasbourg, pp.109-114.

Piasecki, M.A.J. & van Breemen, O. 1979. A Moravian age for the 'younger Moines' of central and western Scotland. *Nature*, 78, pp.734-736.

Piasecki, M.A.J. & van Breemen, O. 1983. Field and isotopic evidence for a c. 750 Ma tectonothermal event in the Moine rocks of the central Highland region of the Scottish

- Caledonides. *Transactions of the Royal Society of Edinburgh, Earth Sciences*, 73, pp.119-134.
- Piasecki, M.A.J., van Breemen, O. & Wright, A.E. 1981. Late Precambrian geology of Scotland, England and Wales. *In*: Kerr, J.W. & Fergusson, A.J. (eds) *Geology of the North Atlantic Borderlands*. Memoir of the Canadian Society of Petroleum Geologists, 7, pp.57-94.
- Pickering, K.T., Bassett, M.G. & Siveter, D.J. 1988. Late Ordovician-Early Silurian destruction of the Iapetus Ocean: Newfoundland, British Isles and Scandinavia – a discussion. *Transactions of the Royal Society of Edinburgh: Earth Sciences*, 79, pp.361-382.
- Pidgeon, R.T. & Aftalion, M. 1978. Cogenetic and inherited zircon U-Pb systems in granites: Palaeozoic granites of Scotland and England. *In*: Bowes, D.R. & Leake, B.E. (eds) *Crustal Evolution in Northwestern Britain and Adjacent Regions*, Geological Journal Special Issue, 10, pp.183-220.
- Pollington, A.D. & Baxter, E.F., 2011. High precision microsampling and preparation of zoned garnet porphyroblasts for Sm–Nd geochronology. *Chemical Geology*, 281(3-4), pp.270-282.
- Pollington, A.D. & Baxter, E.F., 2010. High resolution Sm–Nd garnet geochronology reveals the uneven pace of tectonometamorphic processes. *Earth and Planetary Science Letters*, 293(1-2), pp.63-71
- Powell, D. 1964. The stratigraphical succession of the Moine schists around Lochailort (Inverness-shire) and its regional significance. *Proceedings of the Geologists' Association*, 75, pp.223-250.
- Powell, D. 1966. The Structure of the South-Eastern Part of the Morar Antiform, Inverness-shire. *Proceedings of the Geologists' Association*, 77, pp.79-100.
- Powell, D. 1974. Stratigraphy and structure of the western Moine and the problem of Moine orogenesis. *Journal of the Geological Society, London*, 130, pp.575-593.
- Powell, D., Baird, A.W., Charnley, N.R. & Jordan, P.J. 1981. The metamorphic environment of the Sgurr Beag Slide: a major crustal displacement zone in Proterozoic, Moine rocks of Scotland. *Journal of the Geological Society, London*, 138, 661-673.

- Powell, D., Brook, M. & Baird, A.W. 1983. Structural dating of a Precambrian pegmatite in Moine rocks of northern Scotland and its bearing on the status of the 'Moravian Orogeny'. *Journal of the Geological Society, London*, 140, 813-823.
- Powell, D. & Phillips, W.E.A. 1985. Time of deformation in the Caledonide orogen of Britain and Ireland. *In*: Harris, A.L. (ed.) *The Nature and Timing of Orogenic Activity in the Caledonian Rocks of the British Isles*. Geological Society, London, Memoirs, 9, 17-39.
- Powell, D. & Glendinning, R. 1988. Excursion 4: Glenfinnan to Morar. *In*: Allison, I., May, F. & Strachan, R.A. (eds) *An Excursion Guide to the Moine Geology of the Scottish Highlands*. Scottish Academic Press, Edinburgh, 80-102.
- Powell, D., Andersen, T.B., Drake, A.A., Hall, L. & Keppie, J.D. 1988. The age and distribution of basement rocks in the Caledonide orogen of the N Atlantic. *In*: Harris, A.L. & Fettes, D.J. (eds) *The Caledonian-Appalachian Orogen*. Geological Society, London, Special Publications, 38, 63-74.
- Prave, A.R. 1999. The Neoproterozoic Dalradian Supergroup of Scotland: an alternative hypothesis. *Geological Magazine*, 136, pp.609-627.
- Prave, A.R., Fallick, A.E., Thomas, C.W. & Graham, C.M. 2009. A composite C-isotope profile for the Neoproterozoic Dalradian Supergroup of Scotland and Ireland. *Journal of the Geological Society, London*, 166, pp.845-857.
- Prince, C., 2000. Comparison of laser ablation ICP-MS and isotope dilution REE analyses — implications for Sm–Nd garnet geochronology. *Chemical Geology*, 168(3-4), pp.255-274.
- Pringle, J. 1940. The discovery of Cambrian trilobites in the Highland Border rocks near Callander, Perthshire (Scotland). *Advancement of Science*, 1, 252.
- Prodi, V., Flynn, F. & Glendenin, L.E., 1969. Half-life and beta spectrum of ^{176}Lu . *Physical Review*, 188, pp.1930–1933.
- Puchkov, V.N. 2009. The evolution of the Uralian orogen. *In*: Murphy, J.B., Keppie, J.D., & Hynes, A. (eds) *Ancient Orogens and Modern Analogues*. Geological Society, Special Publications, 327, 161-195.

R

- Rainbird, R.H., Hamilton, M.A. & Young, G.M. 2001. Detrital zircon geochronology and provenance of the Torridonian, NW Scotland. *Journal of the Geological Society, London*, 158, 15-27.
- Ramsay, J.G., 1958. Superimposed folding at Loch Monar, Inverness-shire and Ross-shire. *Quarterly Journal of the Geological Society of London*, 113, 271-307.
- Ramsay, J.G. 1958a. Moine-Lewisian relations at Glenelg, Inverness-shire. *Quarterly Journal of the Geological Society of London*, 113, 487-523.
- Ramsay, J.G. 1960. The deformation of early linear structures in areas of repeated folding. *Journal of Geology*, 68, 75-93.
- Ramsay, J.G. 1963. Structure and metamorphism of the Moine and Lewisian rocks of the North-West Caledonides. *In*: Johnson, M.R.W. & Stewart, F.H. (eds). *The British Caledonides*. Oliver & Boyd, Edinburgh, 143-170.
- Ramsay, J.G. 1967. Folding and fracturing of rocks. McGraw Hill Book Co. N. York.
- Ramsay, J.G. & Spring, J.S. 1962. Moine stratigraphy in the Western Highlands of Scotland. *Proceedings of the Geologists' Association*, 73, 295-322.
- Rathbone, P.A. & Harris, A.L. 1979. Basement-cover relationships at Lewisian inliers in the Moine rocks. *In*: Harris, A.L., Holland, C.H. & Leake, B.E. (eds) *The Caledonides of the British Isles – Reviewed*. Geological Society, London, Special Publications, 8, 101-107.
- Rathbone, P.A., Coward, M.P. & Harris, A.L. 1983. Cover and basement: A contrast in style and fabrics. *In*: Harris, L.D. & Williams, H. (eds) *Tectonics and Geophysics of Mountain Chains*. Geological Society of America Memoir, 158, 213-223.
- Read, H.H. 1931. *The Geology of Central Sutherland*. Memoir of the Geological Survey of Great Britain.
- Read, H.H. 1934. Age problems of the Moine Series of Scotland. *Geological Magazine*, 71, 302-317.
- Read, H.H. & Phemister, J. 1926. The geology of Strath Oykeell and Lower Loch Shin. Memoir of the Geological Survey, Scotland.

- Richey, J.E. & Kennedy, W.Q. 1939. The Moine and Sub-Moine Series of Morar, Inverness-shire. *Geological Survey of Great Britain Bulletin*, 2, 26-45.
- Roberts, A.M. & Harris, A.L. 1983. The Loch Quoich Line - a limit of early Palaeozoic crustal reworking in the Moine of the northern Highlands of Scotland. *Journal of the Geological Society, London*, 140, 883-892.
- Roberts, A.M., Smith, D.I. & Harris, A.L. 1984. The structural setting and tectonic significance of the Glen Dessary syenite, Inverness-shire. *Journal of the Geological Society, London*, 141, 1033-1042.
- Roberts, A.M., Strachan, R.A., Harris, A.L., Barr, D. & Holdsworth, R.E. 1987. The Sgurr Beag nappe: a reassessment of the northern Highland Moine. *Bulletin of the Geological Society of America*, 98, 497-506.
- Roberts, D., 2001. The Scandinavian Caledonides: a multiply deformed collage of Baltican, Laurentian, Iapetan and possible Siberia lithostructural elements. (Poster and extended abstract) *IGCP Project 453 Symposium, Sion, Switzerland*, September 2001, Abstract Volume.
- Roberts, D., Melezhik, V.M. & Haldal, T. 2002. Carbonate formations and early NW-directed thrusting in the highest allochthons of the Norwegian Caledonides: evidence of a Laurentian ancestry. *Journal of the Geological Society, London*, 159, pp.117-120.
- Roberts, D. 2003. The Scandinavian Caledonides: event chronology, palaeogeographic settings and likely modern analogues. *Tectonophysics*, 365, 283-299.
- Roberts, D. & Gee, D.G. 1985. An introduction to the structure of the Scandinavian Caledonides. In: Gee, D.G. & Sturt, B.A. (eds) *The Caledonide orogen – Scandinavia and related areas*. John Wiley & Sons, Chichester, 55–68.
- Roberts, D., Nordgulen, Ø. & Melezhik, V. 2007. The Uppermost Allochthon in the Scandinavian Caledonides: From a Laurentian ancestry through Taconian orogeny to Scandian crustal growth on Baltica. *Geological Society of America Memoirs*, 200, 357-377.
- Robertson, S. & Smith, M. 1999. The significance of the Geal Charn—Ossian Steep Belt in basin development in the Central Scottish Highlands. *Journal of the Geological Society, London*, 156, 1175-1182.

Rogers, G. & Pankhurst, R.J. 1993. Unravelling dates through the ages: geochronology of the Scottish metamorphic complexes. *Journal of the Geological Society, London*, 150, 447-464.

Rogers, G., Hyslop, E.K., Strachan, R.A., Paterson, B.A. & Holdsworth, R.E. 1998. The structural setting and U-Pb geochronology of Knoydartian pegmatites in W. Inverness-shire: evidence for Neoproterozoic tectonothermal events in the Moine of NW Scotland. *Journal of the Geological Society, London*, 155, 685-696.

Rogers, G., Kinny, P.D., Strachan, R.A., Friend, C.R.L. & Paterson, B.A. 2001. U—Pb geochronology of the Fort Augustus granite gneiss: constraints on the timing of Neoproterozoic and Palaeozoic tectonothermal events in the NW Highlands of Scotland. *Journal of the Geological Society, London*, 158, 7-14.

Rutledge, H. 1952. The structure of the Fannich Forest area. *Transactions of the Edinburgh Geological Society*, 15, 317-321.

S

Sakamoto, K., 1967. The half-lives of natural ^{176}Lu and ^{180}Ta . *Nuclear Physics*, A 103, pp.134–144.

Sato J. & Hirose T. (1981). Half-life of ^{138}La . *Radiochemical and Radioanalytical Letters*, 46, 145–52.

Sanders, I.S., Van Calsteren, P.W.C. & Hawkesworth, C.J. 1984. A Grenville Sm-Nd age for the Glenelg eclogite in north-west Scotland. *Nature*, 312, pp.439-440.

Scherer, E.E., Cameron, K.L. & Blichert-Toft, J., 2000. Lu–Hf garnet geochronology: closure temperature relative to the Sm–Nd system and the effects of trace mineral inclusions. *Geochimica et Cosmochimica Acta*, 64(19), pp.3413-3432.

Scherer, E., Münker, C. & Mezger, K. 2001. Calibration of the Lutetium-Hafnium Clock. *Science*, 293, pp.683-687.

Skora, S., Baumgartner, L.P., Mahlen, N.J., Johnson, C.M., Pilet, S. & Hellebrand, E., 2006. Diffusion-limited REE uptake by eclogite garnets and its consequences for Lu–Hf and Sm–Nd geochronology. *Contributions to Mineralogy and Petrology*, 152, pp.703–720.

- Skora, S., Baumgartner, L.P., Mahlen, N.J., Lapen, T.J., Johnson, C.M. & Bussy, F., 2008. Estimation of a maximum Lu diffusion rate in a natural eclogite garnet. *Swiss Journal of Geosciences*, 101, pp.637–650.
- Skora, S., Lapen, T.J., Baumgartner, L.P., Johnson, C.M., Hellebrand, E. & Mahlen, N.J. 2009. The duration of prograde garnet crystallization in the UHP eclogites at Lago di Cignana, Italy. *Earth and Planetary Science Letters*, 287(3-4), pp.402-411.
- Sguigna, A.P., Larabee, A.J. & Waddington, J.C., 1982. The half-life of ^{176}Lu by a γ - γ coincidence measurement. *Canadian Journal of Physics*, 60, pp.361–364.
- Smith, M., Robertson, S. & Rollin, K.E. 1999. Rift basin architecture and stratigraphical implications for basement-cover relationships in the Neoproterozoic Grampian Group of the Scottish Caledonides. *Journal of the Geological Society, London*, 156, 1163-1173.
- Söderlund, U., Patchett, P.J., Vervoort, J.D. & Isachsen, C.E. 2004. The ^{176}Lu decay constant determined by Lu-Hf and U-Pb isotope systematics of Precambrian intrusions. *Earth and Planetary Science Letters*, 219, pp.311-324.
- Sønderholm, M. and Tirsgaard, H., 1993, Lithostratigraphic framework of the Upper Proterozoic Eleonore Bay Supergroup of East and North-East Greenland: *Bulletin Grønlands Geologiske Undersøgelse*, 167, 38 pp.
- Soper, N.J. 1994. Was Scotland a Vendian RRR junction? *Journal of the Geological Society, London*, 151, 579-582.
- Soper, N.J. & Brown, P.E. 1971. Relationship between metamorphism and migmatization in the northern part of the Moine Nappe. *Scottish Journal of Geology*, 7, 305-325.
- Soper, N.J. & Wilkinson, P. 1975. The Moine Thrust and Moine Nappe at Loch Eriboll, Scotland. *Scottish Journal of Geology*, 11, 239-259.
- Soper, N.J. & Barber, A.J. 1982. A model for the deep structure of the Moine thrust zone. *Journal of the Geological Society, London*, 139, 127-138.
- Soper, N.J. & Hutton, D.H.W. 1984. Late Caledonian sinistral displacements in Britain: Implications for a three-plate model. *Tectonics*, 3, 781-794.
- Soper, N.J. & Woodcock, N.H. 1990. Silurian collision and sediment dispersal patterns in northern Britain. *Geological Magazine*, 127, 527-542.

- Soper, N.J., Strachan, R.A., Holdsworth, R.E., Gayer, R.A. & Greiling, R.O. 1992. Sinistral transpression and the Silurian closure of Iapetus. *Journal of the Geological Society, London*, 149, 871-880.
- Soper, N.J. & Harris, A.L. 1997. Report: Highland field workshops 1995-1996. *Scottish Journal of Geology*, 33, 187-190.
- Soper, N.J., Harris, A.L. & Strachan, R.A. 1998. Tectonostratigraphy of the Moine Supergroup: a synthesis. *Journal of the Geological Society, London*, 155, 13-24.
- Soper, N.J., Ryan, P.D. & Dewey, J.F. 1999. Age of the Grampian orogeny in Scotland and Ireland. *Journal of the Geological Society, London*, 156, 1231-1236.
- Spear, F.S., and Peacock, S.M. (1989) Metamorphic pressure-temperature-time paths. *American Geophysical Union Short Course in Geology*, 7, 102 p.
- Spray, J.G., 1988. Thrust-related metamorphism beneath the Shetland Islands oceanic fragment, northeast Scotland. *Canadian Journal of Earth Sciences*, 25, pp.1760-1776.
- Spray, J.G. & Dunning, G.R., 1991. A U/Pb age for the Shetland Islands oceanic fragment, Scottish Caledonides: evidence from anatectic plagiogranites in 'layer 3' shear zones. *Geological Magazine*, 128 (6), 667-671
- Storey, C., Brewer, T. & Parrish, R., 2004. Late-Proterozoic tectonics in northwest Scotland: one contractional orogeny or several? *Precambrian Research*, 134(3-4), pp.227-247.
- Storey, C.D., Brewer, T.S., Anczkiewicz, R., Parrish, R.R. & Thirlwall, M.F. 2010. Multiple high-pressure metamorphic events and crustal telescoping in the NW Highlands of Scotland. *Journal of the Geological Society*, 167(3), pp.455-468.
- Strachan R.A. 1985. The stratigraphy and structure of the Moine rocks of the Loch Eil area, western Inverness-shire. *Scottish Journal of Geology* 21:9-22.
- Strachan, R.A. 1986. Shallow marine sedimentation in the Proterozoic Moine succession, northern Scotland. *Precambrian Research*, 32, 17-33.
- Strachan, R.A. & Holdsworth, R.E. 1988. Basement-cover relationships and structure within the Moine rocks of central and southeast Sutherland. *Journal of the Geological Society, London*, 145, 23-36.

- Strachan, R.A., May, F. & Barr, D. 1988. The Glenfinnan and Loch Eil Divisions of the Moine Assemblage. *In*: Winchester, J.A. (ed.) *Later Proterozoic Stratigraphy of the Northern Atlantic Regions*. Blackie, Glasgow, 32-45.
- Strachan, R.A., Smith, M., Harris, A.L. & Fettes, D.J. 2002. The Northern Highland and Grampian terranes. *In*: Trewin, N. (ed) *Geology of Scotland* (4th edition). Geological Society, London, 81-147.
- Strachan, R.A. & Evans, J.A. 2008. Structural setting and U-Pb geochronology of the Glen Scaddle Metagabbro: evidence for polyphase Scandian ductile deformation in the Caledonides of northern Scotland. *Geological Magazine*, 145, pp. 361-371.
- Strachan, R.A., Holdsworth, R.E., Krabbendam, M. & Alsop, G.I. 2010. The Moine Supergroup of NW Scotland: insights into the analysis of polyorogenic supracrustal sequences. *In*: Law, R.D., Butler, R.W.H., Holdsworth, R.E., Krabbendam, M. & Strachan, R.A. (eds) *Continental Tectonics and Mountain Building: The Legacy of Peach and Horne*. Geological Society, Special Publications, 335, 231-252.
- Strachan, R.A., Holdsworth, R.E., Friend, C.R.L., Burns, I.M. & Alsop, G.I. 2010a. Excursion 13: North Sutherland. *In*: Strachan, R.A., Friend, C.R.L., Alsop, G.I. & Miller, S. (eds) *A Geological Excursion Guide to the Moine Geology, of the Northern Highlands of Scotland*. Scottish Academic Press, in press.
- Sutton, J. & Watson, J.V. 1953. The supposed Lewisian inlier of Scardroy, central Ross-shire and its relations with the surrounding Moine rocks. *Quarterly Journal of the Geological Society of London*, 108, 99-126.
- Sutton, J. & Watson, J.V. 1954. The structure and stratigraphical succession of the Moines of Fannich Forest and Strath Bran, Ross-shire. *Quarterly Journal of the Geological Society of London*, 109, 21-53.
- Sutton, J. & Watson, J.V. 1959. Structures in the Caledonides between Loch Duich and Glenelg, North-West Highlands. *Quarterly Journal of the Geological Society of London*, 114, 231-54.
- Sutton, J. & Watson, J.V. 1962. An interpretation of Moine-Lewisian relations in central Ross-shire. *Geological Magazine*, 99, 527-541.

T

- Tanner, P.W.G. 1970. The Sgurr Beag Slide - a major tectonic break within the Moinian of the western Highlands of Scotland. *Quarterly Journal of the Geological Society of London*, 126, 435-463.
- Tanner, P.W.G. 1976. Progressive regional metamorphism of thin calcareous bands from the Moinian rocks of N.W. Scotland. *Journal of Petrology*, 17, 100-134.
- Tanner, P.W.G. 1995. New evidence that the Lower Cambrian Leny Limestone at Callender, Perthshire, belongs to the Dalradian Supergroup, and a reassessment of the 'exotic' status of the Highland Border Complex. *Geological Magazine*, 132, 473-483.
- Tanner, P.W.G., Johnstone, G.S., Smith, D.I. & Harris, A.L. 1970. Moinian Stratigraphy and the problem of the Central Ross-shire Inliers. *Bulletin of the Geological Society of America*, 81, 299-306.
- Tanner, P.W.G. & Evans, J.A. 2003. Late Precambrian U-Pb titanite age for peak regional metamorphism and deformation (Knoydartian orogeny) in the western Moine, Scotland. *Journal of the Geological Society, London*, 160, 555-564.
- Tatsumoto, D., Unruh, M. & Patchett, P.J. 1981. U-Pb and Lu-Hf systematics of Antarctic meteorites, *Proc. 6th Symp. Antarctic meteorites.*, Natl. Inst. Polar Res, Tokyo, pp. 237-249.
- Thomas, C.W., Graham, C.M., Ellam, R.M. & Fallick, A.E. 2004. $^{87}\text{Sr}/^{86}\text{Sr}$ chemostratigraphy of Neoproterozoic Dalradian limestones of Scotland and Ireland: constraints on depositional ages and time scales. *Journal of the Geological Society, London*, 161, 229-242.
- Tobisch, O.T. 1966. Observations on primary deformed sedimentary structures in some metamorphic rocks from Scotland. *Journal of Sedimentary Petrology*, 35, 415-419.
- Tobisch, O.T. 1985. Discussion of the structural setting and tectonic significance of the Glen Dessary syenite, Inverness-shire. *Journal of the Geological Society, London*, 142, 716-717.
- Tobisch, O.T., Fleuty, M.J., Merh, S.S., Mukhopadhyay, D. & Ramsay, J.G. 1970. Deformational and metamorphic history of Moinian and Lewisian rocks between Strathconon and Glen Affric. *Scottish Journal of Geology*, 6, 243-265.

- Tohver, E., Bettencourt, J.S., Tosdal, R., Mezger, K., Leitel, W.B. & Pavolla, B.L. 2004. Terrane transfer during the Grenville orogeny: tracing the Amazonian ancestry of southern Appalachian basement through Pb and Nd isotopes. *Earth and Planetary Science Letters*, 228, 161-176.
- Torsvik, T.H. 2003. The Rodinia Jigsaw Puzzle. *Science*, 300, 1379-1381.
- Thirlwall, M. F. 1989. Short Paper: Movement on proposed terrane boundaries in northern Britain: constraints from Ordovician-Devonian igneous rocks. *Journal of the Geological Society*, 146, 373-376
- Thirlwall, M.F. 2001. Inappropriate tail corrections can cause large inaccuracy in isotope ratio determination by MC-ICP-MS. *Journal of Analytical Atomic Spectrometry*, 16, 1121-1125
- Thirlwall, M.F. & Anczkiewicz, R. 2004. Multidynamic isotope ratio analysis using MC-ICP-MS and the causes of secular drift in Hf, Nd and Pb isotope ratios. *International Journal of Mass Spectrometry*, 235, 59-81
- V
- van Breemen, O. & Boyd, R. 1972. A radiometric age for pegmatite cutting the Behelvie mafic intrusion, Aberdeenshire. *Scottish Journal of Geology*, 8, pp.115-120.
- van Breemen, O., Pidgeon, R.T. & Johnson, M.R.W. 1974. Precambrian and Palaeozoic pegmatites in the Moines of northern Scotland. *Journal of the Geological Society, London*, 130, 493-507.
- van Breemen, O., Halliday, A.N., Johnson, M.R.W. & Bowes, D.R. 1978. Crustal additions in late Precambrian times. *In*: Bowes, D.R. & Leake, B.E. (eds) *Crustal Evolution in Northwestern Britain and Adjacent Regions. Geological Journal Special Issue*, 10, 81-106.
- van Breemen, O., Aftalion, M. & Johnson, M.R.W. 1979. Age of the Loch Borrolan complex, Assynt, and late movements along the Moine Thrust zone. *Journal of the Geological Society, London*, 136, 489-496.
- Vance, D., Strachan, R.A. & Jones, K.A. 1998. Extensional versus compressional settings for metamorphism: garnet chronometry and pressure-temperature-time histories in the Moine Supergroup, northwest Scotland. *Geology*, 26, 927-930.

- Vance, D. & O'Nions, R., 1990. Isotopic chronometry of zoned garnets: growth kinetics and metamorphic histories. *Earth and Planetary Science Letters*, 97(3-4), pp.227-240.
- van Staal, C.R., Dewey, J.F., McKerrow, W.S. & MacNiocaill, C. 1999. The Cambrian-Silurian tectonic evolution of the northern Appalachians and British Caledonides: history of a complex, southwest Pacific type segment of Iapetus. *In*: Blundell, D. & Scott, A.C. (eds) *Lyell: the Present is the Key to the Past*. Geological Society, Special Publications, 143, 199-242.
- van Staal, C.R., Whalen, J.B., Valverde-Vaquero, P., Zagorski, A. & Rogers, N. 2009. Pre-Carboniferous, episodic accretion-related, orogenesis along the Laurentian margin of the northern Appalachians. *In*: Murphy, J.B., Keppie, J.D., & Hynes, A. (eds) *Ancient Orogens and Modern Analogues*. Geological Society, Special Publications, 327, 271-316.
- W*
- Watt, G.R., Kinny, P.D. and Friderichsen, J.D., 2000, U-Pb geochronology of Neoproterozoic and Caledonian tectonothermal events in the East Greenland Caledonides: *Journal of the Geological Society, London*, v. 157, pp.1031-1048.
- Wheeler, J., Park, R.G., Rollinson, H.R. & Beach, A. 2010. The Lewisian Complex: insights into deep crustal evolution. *Geological Society, London, Special Publications*, 335(1), pp.51-79.
- Whitehouse, M.J., Claesson, S., Sunde, T. & Vestin, J. 1997. Ion microprobe U-Pb zircon geochronology and correlation of Archaean gneisses from the Lewisian Complex of Gruinard Bay, northwestern Scotland. *Geochimica et Cosmo*, 61, 4429-4438.
- Whitehouse, M.J., Fowler, M.B. & Friend, C.R.L. 1996. Conflicting mineral and whole-rock isochron ages from the Late-Archaean Lewisian Complex of northwestern Scotland: implications for geochronology in polymetamorphic high-grade terrains. *Geochimica et Cosmochimica Acta*, 60, 3085-3102.
- Wilson, D. & Shepherd, J. 1979. The Carn Chuinneag granite and its aureole. *In*: Harris, A.L., Holland, C.H. & Leake, B.E. (eds) *The Caledonides of the British Isles — Reviewed*. Geological Society, London, Special Publications, 8, 669-675.

- Wilson, G.V. 1953. Mullions and rodding structures in the Moine Series of Scotland. *Proceedings of the Geologists' Association*, 64, 118-151.
- Wilson, G.V., Watson, J. & Sutton, J. 1953. Current-bedding in the Moine series of Northwestern Scotland. *Geological Magazine*, 90, 377-387.
- Winchester, J.A. 1971. Some geochemical distinctions between Moinian and Lewisian rocks and their use in establishing the identity of supposed inliers in the Moinian. *Scottish Journal of Geology*, 7, 327-344.
- Winchester, J.A. 1974. The zonal pattern of regional metamorphism in the Scottish Caledonides. *Journal of the Geological Society, London*, 130, 509–524.
- Winchester, J.A. & Lambert, R.St.J. 1970. Geochemical distinctions between the Lewisian of Cassley, Durcha and Loch Shin, Sutherland and the surrounding Moinian. *Proceedings of the Geologists' Association*, 81, 275-301.

APPENDIX 1: XRF DATA

	AB07/2	AB07/3	AB07/4	AB07/5	AB07/8	AB07/9	AB07/10
SiO ₂	56.54	58.64	57.95	46.81	62.81	49.65	40.85
Al ₂ O ₃	19.97	19.53	20.08	13.58	17.87	14.58	13.20
Fe ₂ O ₃	10.19	8.62	8.57	15.44	7.82	13.16	19.88
MgO	2.48	2.03	2.21	6.27	2.46	8.02	8.70
CaO	2.24	2.43	2.22	10.40	1.86	11.07	9.01
Na ₂ O	2.30	2.26	3.32	1.03	1.59	1.96	1.75
K ₂ O	3.52	4.49	3.46	1.36	4.16	0.092	0.34
TiO ₂	1.06	0.92	1.08	3.58	0.95	1.20	4.62
MnO	0.19	0.16	0.12	0.28	0.11	0.204	0.28
P ₂ O ₅	0.38	0.31	0.32	0.52	0.28	0.095	0.46
Total	98.86	99.38	99.32	99.27	99.89	100.03	99.09
Total	99.17	99.66	99.56	99.51	100.17	100.21	99.48
Mg#	0.33	0.32	0.34	0.45	0.38	0.55	0.46
LOI	2.14	2.00	1.63	0.79	1.82	0.10	0.79
Ni	42.6	38.0	35.2	48.7	47.1	118.4	173.2
Cr	92.9	72.4	74.7	220.8	88.0	286.9	91.0
V	152.4	120.8	125.9	463.7	130.2	306.2	733.5
Sc	21.4	18.6	19.3	54.5	17.2	43.2	47.9
Cu	65.5	35.1	23.6	80.3	46.7	99.3	54.6
Zn	132.4	122.8	122.0	130.8	147.7	102.2	124.2
Cl	-93	-107	-94	-123	-60	62	1059
Ga	27.0	24.3	26.6	20.1	24.2	17.3	22.7
Pb	21.0	20.0	22.8	4.1	17.0	1.3	2.7
Sr	304.0	293.2	284.9	56.1	200.9	104.8	372.4
Rb	109.1	147.5	195.0	53.1	138.2	0.6	1.6
Ba	1070	967	522	114	1020	20	43
Zr	187.4	176.3	211.9	372.3	214.3	57.7	92.1
Nb	16.6	17.7	24.0	6.0	16.8	4.2	17.9
Th	12.6	13.7	18.3	1.7	14.1	-0.1	1.4
Y	43.4	46.8	49.0	84.6	41.3	21.3	47.1
La	65	66	52	10	59	2	15
Ce	131.4	134.5	107.0	38.8	119.8	11.5	53.6
Nd	62.1	62.4	48.8	30.2	53.6	6.8	37.0
Calc Sm	12.4	12.5	9.8	6.0	10.7	1.4	7.4
Calc Lu	0.7	0.8	0.8	1.4	0.7	0.4	0.8
Calc Hf	4.2	3.9	4.7	8.3	4.8	1.3	2.0
data on pellets							
TiO ₂ Rh	1.11	0.98	1.11	3.54	0.91	1.28	4.74
CaO-W	2.31	2.53	2.43	10.62	1.63	11.05	9.56
TiO ₂ -W	1.09	0.98	1.10	3.51	0.91	1.29	4.64

Appendix 1: XRF Data

	AB07/11	AB07/12	AB07/13	AB07/14	AB07/15	AB07/17	AB07/18
SiO2	62.90	57.71	62.79	48.53	59.98	48.35	49.78
Al2O3	17.38	17.70	18.18	15.06	19.27	13.82	12.46
Fe2O3	7.33	9.82	7.86	15.58	9.21	15.18	15.04
MgO	2.21	5.28	2.77	7.40	3.43	6.17	6.88
CaO	2.06	1.92	1.76	8.26	1.13	10.42	10.55
Na2O	2.22	2.26	2.98	2.14	1.82	1.68	2.00
K2O	3.77	3.85	2.40	0.33	3.53	1.44	0.23
TiO2	0.99	1.10	1.13	2.75	0.83	1.53	2.01
MnO	0.13	0.086	0.12	0.21	0.11	0.38	0.197
P2O5	0.26	0.094	0.19	0.296	0.13	0.14	0.099
Total	99.24	99.82	100.18	100.55	99.43	99.11	99.25
Total	99.52	100.18	100.42	100.79	99.67	99.35	99.47
Mg#	0.37	0.52	0.41	0.49	0.42	0.45	0.48
LOI	1.95	1.62	1.92	0.52	2.36	4.37	0.97
Ni	31.8	115.4	36.0	68.5	53.0	67.4	116.5
Cr	78.7	231.0	69.1	174.2	94.7	159.4	132.2
V	106.3	250.4	118.4	415.5	129.0	356.3	438.8
Sc	17.0	27.6	18.9	54.0	20.7	49.3	39.6
Cu	20.7	105.5	26.0	8.2	28.1	7.9	56.5
Zn	115.2	180.2	89.1	90.1	259.1	127.9	128.0
Cl	-20	413	-38	383	173	206	430
Ga	21.6	24.7	23.3	24.1	28.8	16.6	19.9
Pb	14.3	11.0	13.1	3.3	28.0	6.5	2.6
Sr	255.8	192.4	205.4	140.7	123.1	201.7	76.6
Rb	115.1	128.3	84.9	7.3	165.7	42.2	6.3
Ba	1037	816	564	28	526	415	44
Zr	244.7	158.3	361.8	192.8	191.7	90.3	75.9
Nb	15.4	13.8	22.0	6.3	14.2	5.8	5.4
Th	10.5	13.6	23.2	2.0	13.8	0.5	1.1
Y	36.3	28.3	69.8	65.4	30.8	30.6	16.5
La	81	45	64	4	14	5	-1
Ce	113.9	88.5	132.6	26.4	51.2	19.9	6.5
Nd	54.0	38.6	61.4	17.5	17.4	10.0	6.3
Calc Sm	10.8	7.7	12.3	3.5	3.5	2.0	1.3
Calc Lu	0.6	0.5	1.2	1.1	0.5	0.5	0.3
Calc Hf	5.4	3.5	8.0	4.3	4.3	2.0	1.7
TiO2Rh	1.006	1.099	1.13	2.84	0.87	1.496	2.12
CaO-W	2.08	1.96	1.89	8.58	0.93	12.21	10.42
TiO2-W	1.01	1.10	1.11	2.79	0.87	1.47	2.099

Appendix 1: XRF Data

	AB07/21	AB07/22	AB07/23	AB07/27	AB07/29	AB07/30	AB07/31
SiO2	52.74	67.11	47.15	61.92	60.58	47.21	59.20
Al2O3	15.29	8.26	14.98	18.58	18.83	14.71	20.88
Fe2O3	19.11	12.35	15.62	7.55	8.43	14.88	9.77
MgO	6.71	2.23	7.15	1.64	2.38	6.67	3.62
CaO	2.17	2.22	10.08	2.51	1.81	7.39	0.70
Na2O	1.86	0.54	1.56	2.99	2.45	2.19	0.84
K2O	0.704	3.11	0.31	3.006	3.25	1.697	4.093
TiO2	0.58	2.09	2.59	0.88	0.88	3.54	0.81
MnO	0.14	0.19	0.28	0.091	0.13	0.25	0.13
P2O5	0.077	0.56	0.203	0.15	0.29	0.57	0.17
Total	99.39	98.66	99.92	99.32	99.03	99.12	100.22
Total	99.55	99.06	100.09	99.54	99.27	99.40	100.45
Mg#	0.41	0.26	0.48	0.301	0.36	0.47	0.42
LOI	0.90	0.84	0.30	1.23	2.22	0.79	2.09
Ni	110.2	21.7	66.8	23.9	36.1	63.1	53.4
Cr	328.5	41.2	125.3	58.0	70.7	189.2	90.0
V	245.0	167.5	383.4	77.8	120.2	430.2	129.7
Sc	30.5	25.9	48.3	17.5	17.5	48.3	26.4
Cu	5.2	21.6	14.8	-0.6	33.3	12.7	50.2
Zn	47.6	142.1	127.2	113.6	125.6	144.6	152.1
Cl	155	75	-91	-143	-128	-36	30
Ga	18.7	16.1	22.3	26.8	24.0	21.9	30.6
Pb	3.3	6.1	4.4	18.4	24.5	8.4	23.0
Sr	31.7	46.1	126.6	198.0	229.9	287.2	66.1
Rb	20.7	165.1	6.3	171.2	119.0	83.5	161.9
Ba	70	928	14	561	842	178	621
Zr	43.2	1100.5	159.8	255.4	152.4	395.4	200.0
Nb	0.7	32.9	2.4	25.9	17.7	7.3	14.8
Th	1.0	40.6	1.1	24.6	13.3	3.4	16.3
Y	16.8	135.7	47.2	62.1	43.2	80.2	49.1
La	0	47	5	74	56	16	35
Ce	9.4	102.5	16.0	159.4	113.3	52.1	84.5
Nd	5.3	49.5	12.6	68.2	50.6	37.7	30.9
Calc Sm	1.1	9.9	2.5	13.6	10.1	7.5	6.2
Calc Lu	0.3	2.3	0.8	1.1	0.7	1.4	0.8
Calc Hf	1.0	24.5	3.6	5.7	3.4	8.8	4.4
TiO2Rh	0.61	2.15	2.35	0.90	0.95	3.54	0.91
CaO-W	2.23	2.30	10.12	2.56	1.87	7.79	0.68
TiO2-W	0.597	2.13	2.33	0.899	0.95	3.46	0.91

	AB08/1	AB08/4	AB08/6	AB08/8	AB08/13	AB08/22
Ag	1.900	0.300	1.300	0.800	1.100	0.100
As	-0.443	0.689	-1.010	1.161	-1.576	-1.482
Ba	626.320	769.214	33.406	93.364	779.062	804.551
Bi	-0.013	-0.013	1.134	1.020	0.102	-0.357
Br	0.504	1.068	0.692	1.727	0.692	0.127
CaO	1.228	1.033	5.748	3.202	0.315	0.632
Cd	-2.500	-2.100	-2.900	-3.100	-1.900	0.300
Ce	46.910	59.507	15.936	6.704	70.551	22.493
Co	70.300	50.600	62.200	64.800	29.300	42.000
Cr	98.679	72.673	4.507	114.637	93.360	47.160
Cs	13.259	3.860	2.347	5.353	3.736	0.911
Cu	24.092	0.534	40.571	17.436	15.535	24.303
Fe2O3	9.594	6.970	11.221	19.206	7.558	4.588
Ga	23.862	21.978	24.290	15.642	29.000	22.407
Ge	1.480	1.985	1.796	1.985	1.733	1.859
Hf	4.164	4.383	2.703	3.215	6.355	2.922
Hg	-3.300	-2.100	-1.800	-5.900	-1.100	-1.600
I	4.200	4.600	1.800	-0.200	1.200	2.700
La	19.460	23.904	7.640	6.573	25.149	10.750
Mn	0.079	0.101	0.194	0.541	0.320	0.065
Mo	0.953	0.254	0.154	0.054	0.054	1.053
Nb	18.810	13.449	3.233	4.143	25.790	15.675
Nd	25.578	23.777	18.557	12.077	19.727	9.287
Ni	87.906	34.448	26.371	41.563	26.564	15.218
Pb	16.184	11.039	2.133	1.935	23.408	23.309
Rb	158.398	112.153	3.412	15.048	115.965	100.015
Sb	1.484	1.949	2.556	3.990	1.826	0.802
Sc	12.700	14.700	27.000	58.600	11.800	9.000
Se	-0.300	-0.400	0.000	-0.600	-0.500	-0.200
Sm	7.000	0.400	3.700	-0.100	2.300	-1.200
Sn	2.899	4.348	-1.812	-0.996	2.718	2.355
Sr	185.134	339.363	181.234	12.674	154.229	262.053
Ta	-5.368	-1.345	-3.426	-3.010	-2.871	-1.345
Te	-0.900	-2.900	-4.400	-1.700	-1.700	-2.800
Th	4.601	10.637	0.049	1.336	14.497	9.351
TiO2	1.989	0.845	1.381	1.529	0.744	0.507
Tl	0.904	0.419	0.662	0.743	0.743	0.743
U	2.990	2.897	0.484	0.484	1.320	3.269
V	206.179	116.819	293.300	330.958	140.431	74.582
W	265.447	251.218	187.487	236.087	114.437	224.463
Y	19.347	34.755	37.192	44.330	26.572	23.177
Yb	1.600	4.700	4.100	7.100	2.300	3.800
Zn		196.526	64.352	78.136	96.300	107.437
Zr	162.299	187.901	45.629	90.408	209.157	138.304